การปรับปรุงความคงทนของตัวเร่งปฏิกิริยา Co/HZSM-5 ภายใต้สภาวะที่มีน้ำและอุณหภูมิสูง สำหรับปฏิกิริยารีดักชันแบบเลือกเกิดของแก๊สไนตริกออกไซด์ด้วยมีเทน

นางสาวพรสวรรค์ กาญจนวณิชย์กุล

วิทยานิพนธ์นี้เป็นส่วนหนึ่งของการศึกษาตามหลักสูตรปริญญาวิศวกรรมศาสตรดุษฎีบัณฑิต

สาขาวิชาวิศวกรรมเคมี ภาควิชาวิศวกรรมเคมี

คณะวิศวกรรมศาสตร์ จุฬาลงกรณ์มหาวิทยาลัย

ปีการศึกษา 2544

ISBN 974-03-1327-2

THE DURABILITY IMPROVEMENT OF Co/HZSM-5 CATALYST UNDER HYDROTHERMAL PRETREATMENT FOR SELECTIVE CATALYTIC REDUCTION OF NO BY METHANE

Miss Pornsawan Kanchanawanichkun

A Dissertation Submitted in Partial Fulfillment of the Requirements
for the Degree of Doctor of Engineering in Chemical Engineering
Department of Chemical Engineering
Faculty of Engineering
Chulalongkorn University
Academic Year 2001

ISBN 974-03-1327-2

Thesis Title	The durability improvement of Co/HZSM-5 catalyst under hydrothermal pretreatment for selective catalytic reduction of NO by methane
By	Miss Pornsawan Kanchanawanichkun
Field of study	Chemical Engineering
Thesis advisor	Professor Piyasan Praserthdam, Dr.Ing.
Thesis coadvisor	Associate Professor Tharathon Mongkhonsi, Ph.D.
	Dr. Nakarin Mongkolsiri, D.Eng

Accepted by the Faculty of Engineering, Chulalongkorn University in Partial Fulfillment of the Requirements for the Doctor's Degree

…….Dean of Faculty of Engineering
(Professor Somsak Panyakeow, D.Eng.)

Thesis Committee

……. Chairman
(Professor Wiwut Tanthapanichakoon, Ph.D.)

……. Thesis Advisor
(Professor Piyasan Praserthdam, Dr.Ing.)

……. Thesis coadvisor
(Associate Professor Tharathon Mongkhonsi, Ph.D.)

……. Thesis coadvisor
(Dr. Nakarin Mongkolsiri, D.Eng.)

……. Member
(Dr. Suphot Phatanasri, D.Eng.)

……. Member
(Assistant Professor Suttichai Assabumrungrat, Ph.D.)

……. Member
(Dr.Siripoln Kunatippapong, D.Eng.)

พรสวรรค์ กาญจนวณิชย์กุล: การปรับปรุงความคงทนของตัวเร่งปฏิกิริยา Co/HZSM-5 ภายใต้สภาวะที่มีน้ำและอุณหภูมิสูงสำหรับปฏิกิริยารีดักชันแบบเลือกเกิดของแก๊สไนตริกออกไซด์ด้วยมีเทน (THE DURABILITY IMPROVEMENT OF Co/HZSM-5 CATALYST UNDER HYDROTHERMAL PRETREATMENT FOR SELECTIVE CATALYTIC REDUCTION OF NO BY METHANE)
อ. ที่ปรึกษา: ศ.ดร. ปิยะสาร ประเสริฐธรรม, อาจารย์ที่ปรึกษาร่วม: รศ.ดร.ธราธร มงคลศรี และ ดร.นครินทร์ มงคลศิริ, 156 หน้า ISBN 974-03-1327-2.

งานวิจัยนี้ได้ศึกษาการปรับปรุงความคงทนของตัวเร่งปฏิกิริยา MFI ที่มีการแลกเปลี่ยนไอออนกับโคบอลต์ ภายใต้สภาวะที่มีน้ำและอุณหภูมิสูง สำหรับปฏิกิริยารีดักชันแบบเลือกเกิดของแก๊สไนตริกออกไซด์ด้วยมีเทน เนื่องจากภายใต้สภาวะนี้ตัวเร่งปฏิกิริยา MFI ที่มีการแลกเปลี่ยนไอออนกับโคบอลต์ไม่เสถียรและเกิดการเสื่อมพังทางโครงสร้าง ดังนั้นจึงมีการเติมโลหะตัวที่สองบนตัวเร่งปฏิกิริยา MFI ที่แลกเปลี่ยนไอออนกับโคบอลต์ เพื่อปรับปรุงความคงทนของตัวเร่งปฏิกิริยา พบว่าโลหะแพลเลเดียมและแคดเมียมช่วยเพิ่มความคงทนของตัวเร่งปฏิกิริยา MFI ที่แลกเปลี่ยนไอออนกับโคบอลต์ได้สูงกว่าโลหะตัวอื่น ๆ เนื่องจากแพลเลเดียมและแคดเมียมช่วยป้องกันการเสื่อมพังของโครงสร้างซีโอไลต์ และยังพบว่าปริมาณที่เหมาะสมในการปรับปรุงความคงทนของตัวเร่งปฏิกิริยา MFI ที่มีการแลกเปลี่ยนไอออนกับโคบอลต์ คือ ประมาณ 0.4 % โดยน้ำหนักของแพลเลเดียม นอกจากนี้ยังพบว่า การเตรียมตัวเร่งปฏิกิริยาขนาดผลึกต่าง ๆ กัน มีผลต่อความคงทนของตัวเร่งปฏิกิริยา MFI ที่แลกเปลี่ยนไอออนกับโคบอลต์ด้วย พบว่าตัวเร่งปฏิกิริยาที่มีผลึกขนาดเล็ก จะมีความคงทนต่อสภาวะที่มีน้ำและอุณหภูมิสูงได้ดีกว่า ตัวเร่งปฏิกิริยาที่มีผลึกขนาดใหญ่ ภายหลังจากสภาวะที่มีน้ำและอุณหภูมิสูงพบว่าตัวเร่งปฏิกิริยาที่มีผลึกขนาดเล็กจะมีความเป็นผลึกและปริมาณอลูมิเนียมในโครงสร้างลดลงเล็กน้อย ในขณะที่ตัวเร่งปฏิกิริยาที่มีผลึกขนาดใหญ่จะสูญเสียความเป็นผลึกและปริมาณอลูมิเนียมในโครงสร้างมากกว่า แสดงให้เห็นว่าเกิดการพังของโครงสร้างซีโอไลต์ในตัวเร่งปฏิกิริยาที่มีผลึกขนาดใหญ่มากกว่าตัวเร่งปฏิกิริยาที่มีผลึกขนาดเล็ก

ภาควิชา.....วิศวกรรมเคมี.....
สาขาวิชา.....วิศวกรรมเคมี.....
ปีการศึกษา.....2544.....

ลายมือชื่อนิสิต.....
ลายมือชื่ออาจารย์ที่ปรึกษา.....
ลายมือชื่ออาจารย์ที่ปรึกษาร่วม.....
ลายมือชื่ออาจารย์ที่ปรึกษาร่วม.....

#3971159521: MAJOR CHEMICAL ENGINEERING
KEY WORD: Co/HZSM-5 / durability / hydrothermal pretreatment / crystallinity/dealumination
PORNSAWAN KANCHANAWANICHKUN: THE DURABILITY IMPROVEMENT OF Co/HZSM-5 CATALYST UNDER HYDROTHERMAL PRETREATMENT FOR SELECTIVE CATALYTIC REDUCTION OF NO BY METHANE
THESIS ADVISOR: PROF. PIYASAN PRASERTHDAM, Dr.Ing.,
THESIS COADVISOR: ASSOCIATE PROF. THARATHON MONGKHONSI, Ph.D., and Dr.NAKARIN MONGKOLSIRI, D.Eng., 156 pp. ISBN 974-03-1327-2.

The durability improvement of Co/HZSM-5 catalysts under hydrothermal pretreatment for selective catalytic reduction of NO by methane was studied. Co/HZSM-5 catalyst is not durable under long steam aging in severe conditions. Therefore, the second metal was introduced into Co/HZSM-5 in order to improve the durability of Co/HZSM-5. It was found that Palladium and Cadmium increased the durability of Co/HZSM-5 more than the other metals because both metals prevent the framework dealumination of zeolite. In addition, the presence of Pd loading amount approximately 0.4 wt.% was appropriate for enhancing durability of Co/ZSM-5. Furthermore, The effect of crystal size on the durability of Co/HZSM-5 was investigated. It was found that the durability of small crystal sizes of Co/HZSM-5 was higher than that of large crystal sizes of Co/HZSM-5. After hydrothermal treatment, the small crystal size catalyst showed a slight decrease in crystallinity and tetrahedral aluminum while the large crystal size catalyst lost crystallinity and tetrahedral aluminum. This indicated that the occurrence of framework dealumination was higher in the large crystal size catalyst.

Department…..Chemical Engineering …. Student's signature……
Field of Study..Chemical Engineering….. Advisor's signature……...
Academic year……2001……...Co-advisor's signature……...
Co-advisor's signature….……..……

ACKNOWLEDGEMENTS

The author would like to give special recognition to Professor Piyasan Praserthdam, her advisor, for his invaluable suggestions and highly constructive comments. She is similarly grateful for the heartfelt assistance, encouragement and friendship that she has received from Associate Professor Tharathon Mongkhonsi and Dr. Nakarin Mongkolsiri her co-advisors. In particular, she also appreciated for their kind cooperation she has had with Professor Wiwut Tanthapanichakoon who was the chairman of the committee, Dr. Suphot Phatanasri, Dr. Suttichai Assabumrungrat and Dr. Siripoln Kunatippapong who were members of the committee.

Also, she gratefully acknowledges the generous financial support given by National Science and Technology Development Agency (NSTDA) and Thailand Research Fund (TRF).

Finally, she would like to manifest her greatest gratitude to her parents, her family, all Catalysis Laboratory members for their tremendous support and overwhelming encouragement which gradually embodied the completion of this dissertation.

CONTENTS

PAGE

CONTENTS(Cont.)

PAGE

LIST OF TABLES

TABLE **PAGE**

LIST OF FIGURES

FIGURE **PAGE**

LIST OF FIGURES(Cont.)

FIGURE **PAGE**

LIST OF FIGURES(Cont.)

FIGURE **PAGE**

LIST OF FIGURES(Cont.)

FIGURE **PAGE**

LIST OF FIGURES(Cont.)

FIGURE **PAGE**

LIST OF FIGURES(Cont.)

FIGURE **PAGE**

CHAPTER I

INTRODUCTION

The main pollutants in exhaust gas from vehicle engines include carbon dioxide, carbon monoxide, hydrocarbon, nitrogen oxide (NO_x), sulfur dioxide and particles. Presently, the most significant problem is the removal of nitrogen oxide which are known to contribute to the formation of acid rain, ground-level ozone (smog) and general atmospheric visibility degration. For these reasons, NO_x emission are control.

The catalytic methods for removing NO_x form engine exhaust gases are usually classified into (i) decomposition, (ii) non-selective reduction and (iii) selective reduction. The catalytic decomposition to elements without a reductant was deemed for a long time much too slow to be of practical use [1]. The three-way catalytic converters used for the purification of emissions from spark ignition engines are an example for non-selective reduction. The exhaust gases containing essential no excess oxygen, nitrogen oxide are non-selective reduced by hydrocarbon, carbon monoxide and/or hydrogen. However, the traditional three-way catalyst does not control NO_x emissions in oxygen-rich exhaust gas. The reduction of NO_x content under such conditions can be accomplished by using selective reducing agents which preferentially react with nitrogen oxides rather than with O_2.

The selective catalytic reduction (SCR) of nitric oxide by ammonia is the method for the clean-up of flue gas from stationary source over catalysts based on vanadium oxides [2]. Despite the general use of such a process, there are problems associated with NH_3 as reducing agent which include ammonia slip, equipment corrosion and high equipment costs. Therefore, an effective NO_x reduction process with an affordable, non-ammonia reductant is desirable. Hydrocarbons could offer an attractive alternative reductant to ammonia. The use of hydrocarbons as reducing agents for NO_x was reported in the 70's. Several groups reported interesting results on NO_x reduction in the presence of excess oxygen with non-methane hydrocarbon, e.g. propane, propene and ethylene. Iwamoto and Hamada [3] discuss the use of hydrocarbons as reductants for NO_x. Initial patent application suggested that methane

was also a suitable hydrocarbon, but this was not the case for many of zeolite later tested, especially for Cu-ZSM-5. Until recently, little progress has been made on the use of methane as the reductant. Given the plentiful supply of methane in the world and the wide spread use of methane as a fuel, the use of methane as a selective reductant would be desirable.

Since the late 1980s, it has been reported that NO_x can be selectively reduced by hydrocarbons in the presence of excess oxygen on copper ion exchanged MFI [4-8], H-form zeolite [9], γ-alumina [10] and Cobalt ion exchanged MFI [11-12]. Metal ion exchanged zeolite catalysts were shown to have higher activity for the selective catalytic reduction of NO_x by hydrocarbons than alumina-based catalysts or metal - free zeolite. Among them, copper ion-exchanged MFI was first reported as the most efficient catalyst. However, Cu-MFI tend to be easily deactivated under practical condition even at 500 °C due to agglomeration of Cu [13], the sintering of Cu into Cu oxide wet conditions lead to the deterioration of the catalytic activity and it is completely unselective for NO_x reduction using methane [14]. When methane is used as reductant, Co-loaded zeolite shows the highest NO_x conversion under practical condition.

The use of methane as reducting agent become particularly interesting pioneered by the work of Li and Armor [12]. They found that Co-ZSM-5 and Co-Ferrierite appear to be more active than other transition metal ions for the selective catalyst reduction of NO_x with methane [15]. The effect of water on the activity of the selective catalytic reduction of NO by methane over Co-ZSM-5 was investigated by Armor et al. [16]. They suggested that the water effect is kinetic phenomenon and concluded that Co-ZSM-5 was more stable in wet NO steam at high temperatures than Cu-ZSM-5. Howe and Budi [17] reported briefly that Co-ZSM-5 catalysts are not durable under long steam aging.

The extensive efforts have recently been made to improve both transition and noble metal catalysts including their NO reduction activity and selectivity, and more important still, their durability under real operation conditions. One of the avenues that many researchers have explored to achieve the above objective, is to create catalyst of high activity and selectivity the combination of catalytic site for NO oxidation and NO reduction. The addition of precious metal (Pt, Rh or Ir) to In/HZSM-5 was investigated by Kikuchi [18]. They reported that such solids are

highly selective for the reduction of NO with methane in feed stream containing up to 10% of water vapor. The role of the precious metal would be accelerate the NO reduction even in the presence of water vapor. The author compares a number of cobalt-exchange zeolite and found Co/ZSM-5 to be the most active one. However, it is well known that ZSM-5 catalysts have a disadvantage in thermal and hydrothermal stability; owing to both the sintering of the exchanged metal component and dislocation of the aluminum from the zeolite framework [19] and this are serious problems for the practical application.

In this study, we aim to develop the new catalysts to defeat these problems and investigate such potentials. This work was divided into two parts, for the first, the second metal was taken into Co/ZSM-5 catalyst in order to improve the durability against hydrothermal treatment. The other, the influence of crystal size on hydrothermal treatment was also studied. Moreover, the fresh and pretreated catalysts were observed in order to determine and compare the characteristics of these catalysts. The objectives and scope of this study will be describe as follows:

1.1 The Objectives of This Study

To improve the durability of Co/ZSM-5 catalysts under hydrothermal pretreatment for selective catalytic reduction of NO by methane

1.2 The Scope of This Study

1.2.1 Preparation of Co/HZSM-5 by ion-exchanging ZSM-5 commercial catalyst with Cobalt acetate. The second metal elements, i.e. Pd, Cd, Ba, Cu, La, Ni, Zn, Ag, Fe, Ce, and Mn were ion-exchanged into Me/Co/HZSM-5 in an appropriate procedure.

1.2.2 Prepare parent Na/ZSM-5 by rapid crystallization method and vary crystal sizes of ZSM-5.

1.2.3 Pretreatment of catalyst using hydrothermal treatment condition at 600 ^{o}C with 10 mole% water for 24 h.

1.2.4 Characterization of catalysts by following methods:

a) Structure and crystallinity of catalysts by X-ray diffractometer (XRD).
b) Morphology of catalyst by Scanning Electron Microscopy (SEM).
c) Quantitative analysis of substance in catalysts by Atomic Absorption Spectroscopy (AAS).
d) Specific surface area by N_2 adsorption based on BET method (BET).
e) State of cobalt by Electron Spin Resonance Spectrometer (ESR).
f) Quantitative analysis of tetrahedral aluminum in zeolite by Al-Nuclear Magnetic Resonance (^{27}Al-NMR).

1.2.5 Study the catalytic activity of catalyst for the selective reduction of NO by methane in excess oxygen using feed gas compositions of NO 1000 ppm, CH_4 1 vol% and O_2 10 vol% balance He at GHSV 10,000 h^{-1}. The reaction was carried out between 300 and 700 ^{o}C.

CHAPTER II

LITERATURE REVIEWS

The selective catalytic reduction (SCR) of NO with hydrocarbon in the presence of excess oxygen has recently attracted wide interest in light of growing environmental concerns over NO_x emissions from diesel and lean-burning gasoline engines and the desire for a practical alternative to the ammonia selective catalytic reduction process for stationary emission controls. Since 1990 Iwamoto et al. [20] and Held et al [21] reported that NO_x can be selectively reduced by hydrocarbon on Cu/HZSM-5 and brought this topic into worldwide study. Several reaction mechanisms have been proposed for the SCR of NO by hydrocarbon. The mechanism study will be summarized as follows.

The oxidation of NO to reactive NO_2 that reacts with hydrocarbon was proposed to be the mechanism by Hamada et al. [22]. Shelef et al. [23] also suggested that the oxidation of NO to NO_2 might be the first step of the SCR. NO_2 was then reduced by hydrocarbon to form N_2 and CO_2. Using Cu/ZSM-5 Petunchi and Hall [24] compared the reactions among hydrocarbons, NO and NO_2. They mentioned the critical role of NO_2 in the reaction mechanism. A FT-IR study of Beutel et al. [25] suggested that NO_y ($y \geq 2$) was able to abstract H atoms from hydrocarbon molecules. Charjar et al. [26] noticed that the reduction of NO_2 by propane could occur in absence of oxygen. Furthermore, The works of Yokoyama and Misono [27] and Guyon et al. [28] supported NO_2 formation as the first step in selective reduction of NO.

Nevertheless, Iwamoto et al. [29] suggested that the first step of the SCR reaction would be the partial oxidation of hydrocarbon with O_2 to form an oxygenated hydrocarbon which served as the intermediate in the reaction. NO would preferably interact with this intermediate rather than hydrocarbon to produce dinitrogen and CO_2 which are the final products of the NO removal process. Montreuil and Shelef. [30] observed that a partial oxidation specie could reduce NO in the absence of oxygen atmosphere. This strongly supported the important role of oxygenated hydrocarbon in the reduction of NO by hydrocarbon in an excess oxygen condition. In addition, the

study of Bennett et al. [31] which concerned the steady state kinetics of NO reduction over Cu/ZSM-5, indicated that the intermediate of the reduction might be a partial oxidation product of hydrocarbon. Kharas's study. [32] agreed with this mechanism as well.

However, Ansell et al. [33] proposed that carbonaceous deposits where a key intermediate of the lean NO_x reaction over Cu/ZSM-5. From their temporal-analysis-of-products (TAP) experiments, they suggested that the reduction is the interaction between coke which formed on the zeolite component and NO_2 type species which formed on the exchanged copper sites. Shelef [30] proposed that the Cu/ZSM-5 catalyst is bifunctional. He noticed that Brønsted acid sites on ZSM-5 activated hydrocarbons via oligomerization while copper sites activated NO to form NO_2.

On the other hand, the gas switching experiments of Burch and Millington [34] showed that the conversion of NO to N_2 reached steady state in a very short period of time. Therefore, the carbon deposition might not responsible for the NO reduction to N_2. They proposed instead that the reaction was a redox process in which decomposition of NO occurs and hydrocarbon removes adsorbed oxygen to maintain the active site in a suitable state. Cho [35] also supported this mechanism. He suggested that the reaction mechanism of NO reduction involved the NO decomposition which accompanied with hydrocarbon oxidation. The decomposition of NO was accomplished at Cu sites whereas hydrocarbon adsorbed on ZSM-5. The critical role of hydrocarbon adsorbed on ZSM-5 was scavenge oxygen from the active sites in the high temperature regime, regenerating these sites for NO decomposition.

Accordingly, it can be suggested that the mechanism depends on the type of catalysts and hydrocarbon used. In all these early reports, the presence of oxygen is essential for the NO reduction, demonstrating that hydrocarbons can be effective for the selective reduction of NO. However, the used of methane as a selective reducing agent for NO was never reported. The used of methane is normally restricted, because the activation of the strong C-H bond often necessitates high reaction temperature. On the other hand, methane is abundantly and readily available in many part of the world and , therefore, very desirable as a selective reducing agent. In 1992 Li and Armor announced [11] a new catalytic technology that uses methane to reduce

NO_x in the presence of excess levels of oxygen. Selected metal exchanged zeolites are effective catalyst for the novel, selective reduction of NO_x by methane in the presence of excess oxygen. A complete conversion of NO to nitrogen is obtained over a Co-ZSM-5 catalyst at 400 °C. This discovery provides a new, and perhaps an alternative approach for NO_x emission control for both stationary and mobile source. The properties, performance, and operation of these catalysts for the reduction of NO by methane will be described below.

The first reported on CH_4-SCR over Co-exchanged zeolites was by Li and Armor [12]. They discovered a Co-ZSM-5 (n_{Co}/n_{Al} = 0.7) that can effectively reduced NO_x with methane in the presence of excess oxygen and observed a reaction temperature of 400 °C increasing NO conversion into N_2 with increasing CH_4 concentration, reaching 95% conversion at C_{CH4}/ C_{NO} = 2.4, but at a gas hourly space velocity as low as 7500 h^{-1}. The NO conversion was enhanced by the presence of some oxygen and remained almost constant with increasing oxygen concentration. In contrast to Pt-containing catalysts, where the main reduction product was N_2O, on the Co-containing catalysts neither N_2O nor CO was detected. Instead of oxygen itself, N_2O could serve as an efficient source of oxygen, greatly enhancing the NO conversion in the absence of oxygen [36,37]. In contrast to these results Burch and Scire [38] reported that the NO reduction on Co/ZSM-5 with methane or ethane was higher in the absence of oxygen than in the presence of oxygen, even through at higher temperatures, suggesting the occurrence of different reaction paths with or without oxygen.

The maximum NO conversion decreased with increasing space velocity, and the temperature at which the maximum conversion was obtained shifted to higher value. At the maximum NO conversion, the CH_4 conversion was about 80%. The overall catalytic activity was proportional to the number of exchanged Co cations in the zeolite. Co/HZSM-5 was active at higher temperatures than Co/NaZSM-5. The NO conversion was proportional to the NO adsorption capacity of the catalyst at room temperature [39]. Co on the zeolites ZSM-5, ZSM-11, mordenite and beta was active, whereas the zeolites Y and L as well as Al_2O_3 were poor supports [40]. Co/ferrierite was even more active than the above mentioned Co/Zeolite, which was relate to its low activity for methane combustion [41,42]. However, this holds only in model exhaust gases without H_2O and SO_2.

Many papers were devoted to the role of NO_2: Hall and coworkers mainly studied the reduction of NO_x with methane on Co/ZSM-5 catalysts using model gases without water [43,44]. They compared the NO reduction and the NO_2 reduction with methane in an excess of oxygen with and without the catalyst. With catalyst, the obtained results were virtually the same in the two reactions and in the reaction of NO_2 with CH_4 in the absence of oxygen, as long as enough oxygen could be supplied by NO_2, indicating the pivotal role of NO_2 in the reaction. Oxygen was suggested not to participate directly in the methane oxidation, but to be important for the oxidation of NO into NO_2. Without catalyst, no N_2 was formed whereas methane combustion could be observed at somewhat higher temperatures [43]. It was proposed that the NO reduction and the CH_4 oxidation were coupled reactions and initiated by the reaction of CH_4 with NO_2, resulting in the formation of a CH_3 radical [44]. This was confirmed by Cant and coworkers who, when using CH_4 and/or CD_4, observed a strong deuterium kinetic isotope effect, suggesting that the rate-determining step was the breaking of a carbon-hydrogen bond [45]. Nitromethane could then be formed, and Sun et al. [46] indeed got indications from in situ DRIFT spectroscopy for the presence of nitromethane on the catalyst surface. Several other studies dealt with the reactions of nitromethane over Co/ZSM-5. By means of quantitative IR spectroscopy, NH_3, HCN, HNCO, N_2O, N_2 and CO_2 were detected as reaction products. This led to speculations about the reaction mechanism. However, a clear distinction between byproducts, spectator species and reaction intermediates could not be made [47-50].

Yan et al. found that the activity of a physical mixture of Co/Al_2O_3 and H-zeolites is much higher in CH_4-SCR that the sum of the activities of the individual components. This synergistic effect was tentatively explained by the generation of NO_2 on Co^{2+} ions and the subsequent reduction of NO_2 by CH_4 over the H^+ ions [50].

Chong and coworkers reported that the activity of Co/ZSM-5 for C_3H_8-SCR in a model gas without water increased with cobalt content up to $n_{Co}/n_{Al} = 0.5$. Exceeding this level favored the propane combustion resulting in decreased NO conversion [52]. Catalysts containing only cobalt in ion exchange positions were found to be inactive in NO_2 formation and to require higher temperatures for achieving considerable NO conversion. With increasing Co loading up to $n_{Co}/n_{Al} = 0.5$, cobalt oxide particles were partly formed, which turned out to be active in NO oxidation, thus strongly enhancing the NO reduction at lower temperatures. Whereas catalysts not active in the NO_2 formation became dark after the reaction, catalysts

active in NO_2 formation did not change their color, indicating that NO_2 could also serve as a scavenger for coke precursors. In addition, it was presumed that NO_2 activated hydrocarbons for the NO reduction [53]. On catalysts not active in NO_2 formation, the presence of oxygen promoted the NO reduction, which was tentatively ascribed to the formation of species like Co-O where NO was not that strongly adsorbed [54]. Catalysts prepared by incipient wetness impregnation were far more active at lower temperatures than catalysts prepared by ion exchange, which was suggested to be due to the presence of some cobalt oxide in the impregnated samples despite the low overall cobalt loading [55]. The introduction of Ca, Sr and especially Ba into the impregnated or ion-exchanged catalysts significantly increased the NO conversion, probably as a result of suppressed propane oxidation [52,55]. By contrast, Kawai and Sekizawa observed no considerable change of the activity of Co/H-ZSM-5 catalysts by pre-exchange with Ba^{2+} ions [56].

The results discussed so far are supplemented by the findings of Osaka Gas Co. that the formation of Co_3O_4 in excessively loaded Co/beta catalysts clogged the micropores and hence decreased the activity [57,58]. This refutes the assumptions that NO_2 plays a key role in the HC-SCR and that the presence of Co_3O_4 is important. It was indeed observed (in contrast to the other studies with feed streams containing 9 vol. % of H_2O) that the NO_x conversion was higher with NO as reactant than with NO_2, although the C_3H_8 conversion became higher with NO_2. This indicates that too much NO_2 in the gas phase decreases the selectivity for the NO_x reduction, since the hydrocarbon is consumed by the reduction of NO_2 to NO [59]. In samples with to $n_{Co}/n_{Al} \approx 0.5$, an additional Co species was observed in the Raman spectrum, which was supposed to be Co-O-Co species or a cluster with more than three Co atoms. Since these samples exhibited a higher NO_x reduction activity and selectivity than any other sample with lower or higher Co loading, it was suggested that this additional Co species were especially active. However, the NO oxidation activity of catalysts with $n_{Co}/n_{Al} \approx 0.5$ was low, which is another argument against a key role of NO_2 in the HC-SCR [60].

Again in a model gas without water, Campa et al. found that the catalytic activities of Co/H-ZSM-5 and Co/Na-ZSM-5 having similar Co contents were well comparable, thus excluding any important involvement of acid sites. Another intriguing observation was that the selectivity to N_2O reached values up to 30%, for

Co catalysts a high value which has nowhere else been reported [61]. On the other hand, Miller et al. examined the reduction of NO_2 by methane at 400°C over Co/H-mordenite and Co/Na-mordenite. They found that the activity of the acidic zeolite was much higher and, therefore, claimed that the formation of N_2 occurs on the acid sites of the support, whereas Co^{2+} ions non-selectively reduce NO_2 to NO [62]. This conclusion could be premature, because no temperature dependence was investigated, i.e. the maximum activity of Co/Na-mordenite and Co/H-mordenite could be the same at different temperatures. However, Montes de Correa and Luz Villa de P. concluded as well from studies of CH_4-SCR with NO_2 on Co/H-zeolites and H-zeolites that the reduction of NO_2 to N_2 occurred on the support rather than on the Co sites and appeared to be proportional to the zeolite acidity [63].

Many groups conducted IR studies of adsorbed species on Co catalysts: Iwamoto et al. observed that Co/ZSM-5 irreversibly adsorbed the largest amount of NO among various metal ion-exchanged zeolites [64,65]. The irreversibly adsorbed NO species were mainly attributed to two different dinitrosyl adsorbates according to two kinds of cobalt ions [66]. The weakly adsorbed dinitrosyl species desorbed via a transient formation of mononitrosyl species [67]. Li et al. [68] and Zhu et al. [69] reported also the existence of dinitrosyl and mononitrosyl species over Co/zeolites exposed to NO. At temperatures above 200°C in an oxygen-containing atmosphere, all adsorbed NO species were found to disappear and to be replaced by adsorbed NO_2 species. Bell and coworkers conducted in situ IR investigations during CH_4-SCR over Co/Na-ZSM-5 zeolite and observed, besides mono- and dinitrosyl species, Al^{3+}-NCO and Co^{2+}-CN species. They suggested that the cyanide species were reaction intermediates and preferentially reacted with NO_2, which was readily formed from NO and O_2 and was more strongly adsorbed than NO [70-72]. By contrast, Sachtler and coworkers presumed that the prevailing adsorption complex in Co/Na-ZSM-5 was the nitrito complex Co-ONO exchanging its nitrogen atom spontaneously with gaseous NO [73-75].

Sun et al. found by EPR and XPS that, regardless of the pretreatment, cobalt species in Co/Na-ZSM-5 were in the + II oxidation state stabilized in the zeolite matrix. Therefore, they suggested that electron transfer might not be necessary for achieving NO_x reduction [76].

Based on the possibility of an oxygenated reaction intermediate, Vassallo et al. used methanol as reducing agent in comparison with methane over Co/mordenite.

The NO conversion started to increase at similar temperatures for both reducing agents, the maximum conversion being more than twice as high with methanol. Without catalyst, no NO conversion was observed with CH_4, but 30% conversion with CH_3OH at 600^oC with or without oxygen in the feed stream. They concluded that CH_3OH could be an intermediate in CH_4SCR [77,78].

Gutierrez et al. observed that the addition of 0.5 wt.% of Pt to a Co/mordenite catalyst with 2.0 wt.% of Co led to a more than two-fold increase of the NO conversion in CH_4-SCR, if the catalyst was pretreated in hydrogen. This was explained by the fact that, as observed by temperature-programmed reduction, the presence of Pt facilitated partial reduction of Co [79].

Water inhibited the reaction, and did so much more on Co/H-ferrierite than on Co/ZSM-5 [80,81]. This inhibition was reversible upon eliminating water from the system and was more severe at low temperature. Temperature-programmed desorption studies on Co/Na/ZSM-5 suggested that the competitive adsorption between H_2O and NO was the reason for the inhibition by water [16]. Upon introduction of SO_2, the NO conversion on Co/HZSM-5 was slightly diminished at the reaction temperature of 500 °C, considerably increases at 550 °C and even doubled at 600 °C, which was proposed to result from SO_2 poisoning preferentially the site more active for CH_4 combustion. With the simultaneous presence of H_2O and SO_2, the NO conversion was decreased at lower temperature, but still slightly higher at 600 °C than without H_2O and SO_2. On the other hand, the NO conversion on Co-ferrierite was greatly diminished by the addition of SO_2, and even more so in the presence of both H_2O and SO_2. One the possible reason for this might be that the eight-ring channels of ferrierite were blocked by SO_2 molecule [81]. A role of the eight-ring channel was also invoked to explain the high activity of Co/ferrierite in the absence of H_2O and SO_2: Co^{2+} ions eight-ring were supposed to be more selective for the use of CH_4 than Co^{2+} ions in 10-rings where due to the enhanced CH_4 combustion, the CH_4 concentration for NO reduction was low. Correspondingly, the 10-ring zeolite ZSM-5 and even more so the 12-ring zeolite mordenite were less active supports than ferrierite [36].

Howe and coworkers tested the effect of a hydrothermal treatment (24 h at 800^oC in 15 vol.% H_2O in air) on the performance of Co/ZSM-5 and observed dealumination of the zeolite framework, causing loss of cation exchanged capacity

and residual Bronsted acidity with a concomitant decrease in the catalytic activity. Pre-exchange of the zeolite with La^{3+} ions stabilized the catalysts by inhibiting dealumination [17,82]. Corresponding, Park [83] reported that the activity of an amorphous La-Co-oxide perovskite phase incorporated into ZSM-5 zeolite was much higher in C_3H_6-SCR over a broad temperature range than that of Co/ZSM-5 and Co/ZSM-5. Pre-exchange of co/TSZ zeolite (similar to ZSM-5) with K^+ or Cs^+ ions likewise increased the durability of the catalysts during treatment with a model gas with 3 vol.% of water for 15 h at 800^{o}C [84].

Ogura et al. [85] observed that Pd-Co/H-ZSM-5 catalysts had a considerably higher activity in CH_4-SCR than the corresponding Pd/H-ZSM-5 and Co/H-ZSM-5 catalysts. Besides, the addition of 10 vol.% of water to the feed stream lowered the catalytic activity of Pd/H-ZSM-5 and even more so of Co/H-ZSM-5, whereas the performance of Pd-Co/H-ZSM-5 was hardly affected. The role of Co was attributed to the acceleration of the NO oxidation.

Several other studies focused on HC-SCR under more realistic conditions, i.e. using real exhaust gases and/or catalysts washcoated onto honeycombs. According to the foregoing results, Eshita et al. [86] observed that the additional incorporation of alkaline-earth metals and/or rare-earth metals into Co/H-ZSM-5 zeolites could inhibit coke formation and Co aggregation by forming perovskite type complex oxides with Co. A Co-La-Sr/H-ZSM-5 catalyst on a cordierite honeycomb maintained 93% of its initial NO_x conversion efficiency of 60% after exposure to lean-burn engine exhaust corresponding to a distance of 30,000 km. Ciambelli et al. [87] tested Co/H-ZSM-5 with n_{Co}/n_{Al} = 2.3 in the exhaust gas of a spark ignition heavy-duty engine using methane as fuel and achieved a maximum NO_x conversion of only 20% at 400^{o}C. However, the Co content of their catalyst might have been unfavorably high. Co/beta proved to be durable over a test period of 4000 h, converting about 65% of NO_x at 400^{o}C, a gas hourly space velocity of 15000 h^{-1}, C_{C3H8}/C_{NO} = 3.3 and 9 vol.% of H_2O as well as 0.3 vol. ppm of SO_2 in the feed. In the exhaust gas of a lean-burning gas engine without addition of a reducing agent, a NO_x conversion of about 30% was still reached at the same gas hourly space velocity [88]. Takeshima et al. [89] observed an increase in NO_x conversion over a Co/ZSM-5 catalyst in the exhaust of a lean-burn engine by sulfuruzing the catalyst via H_2S treatment, thereby reducing the oxidizing activity and enhancing the selectivity for NO_x reduction. Washing of the sulfurized catalyst with glycol further increased the catalytic activity, probably because pore

clogging cobalt sulfide (formed by H_2S treatment of cobalt oxide) was removed. Miyoshi [90] studied the performance of a Co/ZSM-5 honeycomb catalyst in simulated exhaust gas and found, upon heat treatment up to 800 °C, hardly any changein crystallinity, even though dealumination did occur. Rak and Veringa [91] examined the catalytic activity of Co/Na-ZSM-5 with an alumina binder on cordierite honeycombs. Unfortunately, they were using model exhaust gases without water and low gas hourly space velocity, therefore making a statement on the principle applicability of their catalysts unreasonable.

Zeolite catalysts have some advantages such as providing the site of ion-exchanged for highly dispersed and coordinately unsaturated cations, endowing acidic active sites, enrichment of reactants in zeolite pore, and so on. On the other hand, zeolite channel structure might have negative effects on catalytic performance. The most plausible negative effect may be seen in a diffusion-limited reaction, in which the rate of masss transfer in zeolite channels cannot keep up with the instrinsic reaction rate [92,93]. This is because the mass transfer in the intracrystalline space of zeolites is sometimes quite slow depending on the interactions between diffusion on the closeness of the size of molecules to that of the channels [94]. Thus the intracrystalline diffusion must be an important factor for the design of highly active zeolite catalysts and the understanding of the diffusion in zeolites should be necessary to the development of the zeolite catalytic process.

The most important fact worked out in these papers is the influence of the reducing agent: normally, CH_4-SCR was not influenced by intracrystalline diffusion, since the reaction rate was considerably lower than with propane, whereas in C_3H_8-SCR the NO_x conversion was found to be higher on catalysts with a smaller crystal size [95]. It was suggested that the superior activity of the large-pore zeolite Co/beta could be ascribed to the ease of diffusion of reactants, products and inhibitors such as water and SO_2 in its channels [96,97]. By contrast, the activity of Co/ferrierte was low in C_3H_8-SCR, probably because the diffusion in its small pores was hindered [97,98].

Corresponding results were reported by Shichi et al. [99] on Co/H-mordenite, they observed that intercrystalline diffusion did not affect the NO_x reduction, whereas intracrystalline diffusion had a significant effect: the reaction rate over large-crystallite Co/H-mordenite was lower than over the small-crystallite zeolite.

However, this effect was again only pronounced with propane as reducing agent, but not with methane.

In their studies (which occurred, in fact, some what earlier than the above-discussed work), Hall and coworkers went one step further: they examined the NO_x reduction on Co/Na-ZSM-5 in model gases containing NO, O_2 and various hydrocarbons including methane, propane, isobutane, n-pentane, 2,2-dimethylpropane (neopentane), 3,3-dimethylpentane, 2,2,4-trimethylpentane and 3,3-diethylpentane (neononane). The hydrocarbon concentrations were varied to maintain a constant flux of carbon, e.g. 0.8 vol.% of methane, but 0.2 vol.% of isobutane. The maxinum NO conversion as a function of the reducing agent followed the order isobutane > methane > neopentane ≈ n-pentane ≈ 2,2,4-trimethylpentane > propane ≈ 3,3-dimethylpentane >> neononane. Whereas the maxinum conversion was reached at a temperature of 400^{o}C with isobutane and propane and 450^{o}C with methane, n-pentane and 3,3-dimethylpentane, it was only achieved at 500^{o}C with neopentane and 550^{o}C with 2,2,4-trimethylpentane and neononane. For all hydrocarbons, the NO conversion was almost the same at a given degree of hydrocarbon conversion into CO_2 except for neononane, where it was much lower. As neononane is too bulky to enter the zeolite pores, it was expected to be particularly effective as a pore blocker, thus slowing down the NO reduction. It was concluded that the formation of nitrogen (or nitrogen dioxide which would then react at the external surface or in the gas phase) must occur in the intrazeolitic channels [100,101].

The selective reduction of NO with CH_4 in the presence of excess O_2 over HZSM-5 and H-mordenites was investigated by Satsuma et.al. [102], and the factors controlling catalytic activity were discussed. The activity for the reduction of NO into N_2 was independent of crystal size and pellet size, indicating that the diffusion in zeolite channel and macro-pore has negligible effect on the catalytic activity. The catalytic activity proportionally increased with the acid amount, which strongly indicates that, the acid amount in the controlling factor for this reaction. The activity was also dependent on the type of zeolites, which may be due to the difference in the acid strength, but not in the pore structure.

The influence of intracrystalline diffusion on the selective catalytic reduction of NO by hydrocarbons (propane. ethene) was investigated [103] by using Cu-MFI catalysts of different zeolite crystal sizes. The influence of hydrocarbon as a reductant on the diffusion process was also investigated, employing kinetic and

temperature-programmed desorption studies. It was concluded that the adsorption property of hydrocarbon on the Cu-MFI catalyst is revealed to play an important role in determining intracrystalline diffusivity and the diffusion influence on the selective reduction of NO over zeolite catalysts.

The adsorption of water in ZSM-5 has been used to study the crystal chemistry of the family of HZSM-5 materials. Several of the features discussed are generic in nature, applying to all high-silica zeolites. The strongest interaction of water is with the acidic protons associated with framework aluminum atoms. The quantity of water adsorbed is proportional to the framework aluminum content and this water adsorbs rapidly. Weaker adsorption occurs on external surface silanol groups and on centers ascribed to intracrystalline defects created as charge balancing centers for the charged template, tetrapropylam-monium (TPA) ions. An adsorption isotherm is presented for external surface adsorption. For a high-silica ZSM-5, adsorption ascribed to defect sites corresponds to four H_2O molecules per unit cell, equal in number to the number of TPA(+) ions and hence the number of these sites [104].

The influence of hydrocarbon molecular size on the HC-SCR activity was investigated over Cu-MFI zeolites having different crystal sizes. In the case of n-hexane as a reductant, the catalytic activity did not depend on the zeolite crystal size. In the case of 2,2-dimethylbutane, however, the observed reaction rate depended on the zeolite crystal size, indicating that the reaction was controlled by intracrystalline diffusivity. It was verified that the catalytic activity for the SCR of NO by a larger hydrocarbon over Cu-MFI zeolite was restricted by geometry-limited diffusion depending on the hydrocarbon molecular size and the zeolite pore size [105].

From many studied contributed to Co/ZSM-5 lists above, it can be understood that the utilization of Co/ZSM-5 appear to be the most appealing, especially since it can activate methane as the reducing agent. Unfortunately, Co/ZSM-5 bases catalysts suffer from deactivation in the presence of water. The second metal cations were tried to introduce in Co/ZSM-5 in order to examine its effect on the durability of Co/ZSM-5 catalyst. It is also well know that a small crystal size zeolite may provide high conversion because of the diffusion influence on the SCR of NO over zeolite catalysts [92-105]. However these studies have not been concerned with the durability of such catalysts. Thus, we also aims to investigate the effect of crystal zeolite size on the durability of Co/HZSM-5 under hydrothermal treatment.

CHAPTER III

THEORY

The stable gaseous oxide of nitrogen include N_2O (nitrous oxide), NO (nitric oxide), N_2O_3 (nitrogen trioxide), NO_2 (nitrogen dioxide) and N_2O_5 (nitrogen pentoxide). An unstable form, NO_3, also exists. Of these, the only ones present in the atmosphere in any significant amount are N_2O, NO and NO_2. Thus these three are potential contributor to air pollution. Nitrous oxide (N_2O) is an inert gas with anesthetic characteristics. Its ambient concentration is 0.50 ppm. Which is considerably below the threshold concentration for a biological effect. In addition, it has a balanced environmental cycle, which is independent of the other oxide of nitrogen.

Nitric oxide (NO) is a colorless gas and its ambient concentration is usually far less than 0.5 ppm. At these concentration its biological toxicity in terms of human health is significant. However, nitric oxide is a precursor to the formation of nitrogen dioxide and is an active compound in photochemical smog formation as well. Hence it initiates reactions that produce air pollutants. Consequently, the control of NO is an important factor in reducing air pollution. Nitrogen dioxide (NO_2) is a reddish brown gas and is quite visible in sufficient amounts. A concentration of 1 ppm of NO_2 probably would be detected by the eye. The toxicological and epidemiological effects of NO_2 on human being are not completely known. As far as we know, NO_2 is not a primary pollutant in the sense that it directly affects human health, unless the concentration is extremely high. In the past, the threshold limit in ambient air has been considered to be around 5 ppm for daily exposure. A threshold level for physiological derangement of approximately 1.5 ppm NO_2 has been suggested. The environmental hazard of nitrogen dioxide is primarily associated with the pulmonary (respiratory) effects of the pollutant. Healthy individuals exposed to concentration of NO_2 of from 0.7 to 5.0 ppm for 10 to 15 min have developed abnormalities in pulmonary airway resistance. Exposure to 15 ppm of NO_2 causes eye and nose irritation, and pulmonary discomfort is noted at 25 ppm for exposure of less than 1 hr. However these results are probably without medical significance with regard to present atmospheric concentrations, since they occurred only at nitrogen dioxide

levels of from 5 to 20 times that of ambient air. The significance of current atmospheric levels of NO_2 with regard to human health is inadequately know.

3.1 Sources and concentration of NO_x

Well over 90 percent of all the man-made nitrogen oxides that enter our atmosphere are produced by the combustion of various fuels. On a nation wide basis, roughly one-half of the NO_x is from stationary sources, while the remainder is from mobile sources such as spark-ignition and compression-ignition engines in automobiles and trucks

On a global basis, the man-made emission rate of NO_x is not grave concern at the present time. Nitrogen oxides are an essential part of the nitrogen cycle in nature. Nitrogen dioxide is hydrolyzed to nitric acid in the atmosphere, which in turn is precipitated out as nitrates. These return to the earth's surface as fertilizer for organic growth. Among the possible atmospheric reactions for the formation of nitric acid are:

$$O_3 + NO_2 \rightarrow NO_3 + O_2$$

$$NO_3 + NO_2 \leftrightarrow N_2O_5$$

$$N_2O_5 + H_2O \rightarrow 2HNO_3$$

$$OH + NO_2 \rightarrow HNO_3$$

Nitric acid is a major contributor to acid rain. The real danger posed by NO_x at the concentrations found in metropolitan area lies in its role in photochemical reactions leading to smog formation. These atmospheric reactions lead to the formation of chemical compounds that do have a direst adverse effect on human being and plants. In some situations, NO_x maybe present in a high enough concentration, yet no react to form smog because other necessary conditions for the reaction are absent. However, nearly every major city in any technologically advanced country at times now experiences the effects induced by the presence of NO_x.

Figure 3.1 illustrates the various chemical transformations of NO in our atmosphere that lead to air pollution problem. Note that NO is the key starting point for all of the other oxides of nitrogen. NO is not only produced by the burning of fossil fuels, but also by lightning, microbial decomposition of proteins in the soil and volcanic activity. One produce, NO is rapidly oxidized by ozone or OH to from the higher oxides of nitrogen, such as NO_2, HNO_2 and HO_2NO_2. Thus, if NO is

prevented from entering the atmosphere, most of the downstream effect of NO_x pollution can be eliminated.

At an emission source the concentration of oxides of nitrogen is much higher than ambient values. For example, the NO_x concentration in the flue gas from a gas-fried domestic water heater is 10 ppm or less, while the level in the flue gas from the steam boiler of a power plant may reach 500 to 1000 ppm. The actual quantities of NOx produced by any given industry can be quite large. From such combustion processes the NO_x is the exhaust stack gas would be 90% or more NO, and the rest NO_2. The type of fuel used can alter the emission rate significantly. Generally, the NO_x emission, base on the same energy released, increase in the order gas-oil-coal. This trend is illustrated in Table 3.1, which compares the fuels for different types of applications. In about 1970, nationwide data for stationary sources showed that coal and oil combustion each accounted for 35 to 45% of NO_x emission, while gas contributed about 15%. These values continue to change as specific fuel allocations are altered in the light of new energy and air pollution problems. Because of the difference in NO_x emissions from the combustion of coal, oil and gas, the standards of performance for new stationary sources promulgated by EPA are different for different fuels.

Table 3.1 Comparison of the effect of fuel type on NO_x emissions, expressed as lb $NO_x/10^9$ Btu released [106]

	Household and commercial	Industry	Electric utilities
Natural gas	110	205	375
Fuel oil	80-480	480	690
Coal	340	840	840

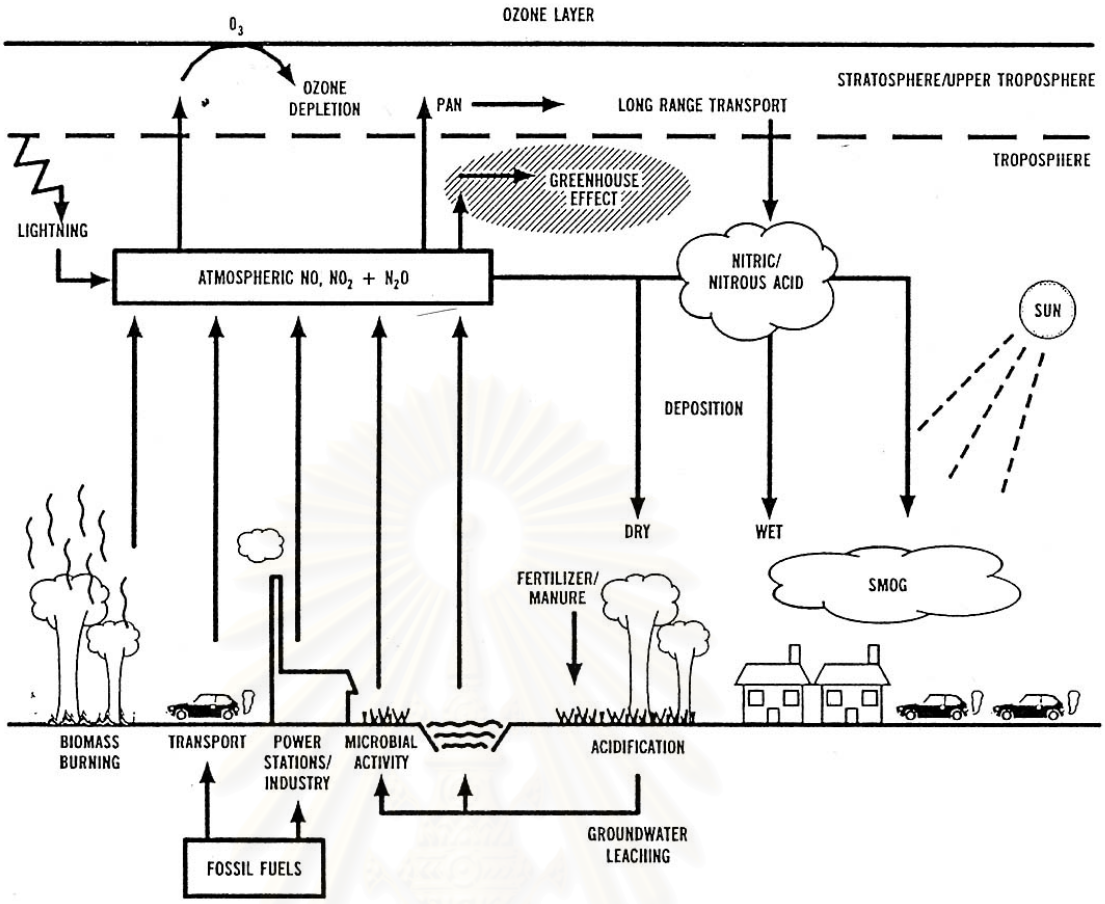

Figure 3.1 Cycling of nitrogen in the environment [107]

The quantity of NO_x dispersed into the atmosphere can be reduced two ways. The primary method is control over the reaction, which produces the pollutant. As a second possibility, the pollutant might be removed after it is formed. The control methods for NO_x emissions requires a general understanding of the basic chemistry, thermodynamics and kinetics of the formation reactions. The vast majority of NO_x emissions come from the burning of flues in stationary and mobil devices. The major noncombustion source of NO_x is in the manufacture and use of nitric acid.

3.2 Flue-gas control methods for NO_x

In some combustion processes it may not be feasible, for various reasons, to use direct combustion control to attain desirable level of NO_x emissions. In these case it will be necessary to remove the oxide of nitrogen from the cool flue gases before they are released to the atmosphere. A number of methods for NO_x removal are currently being investigated.

Control of NO_x emissions by flue-gas treatment is a formidable task. For the reason is that the volume rate of flue gas requiring treatment is enormous at any given installation. Among the possible removal techniques for oxides of nitrogen are catalytic decomposition, non-selective and selective catalytic reduction

3.3 Catalytic decomposition

The direct decomposition of NO into N_2 and O_2 would be highly desirable. Numerous data are available for a variety of catalysts. Even though the kinetics of the reaction mechanism is in dispute, data to date indicate the decomposition reaction to be extremely slow. No catalyst has been found which provides sufficient activity at reasonable temperatures. Removal of NO from flue gases by such a technique is not feasible at this time.

3.4 Nonselective catalytic reduction of NO_x

One of the earliest techniques used to abate NO_x emissions from engines and nitric acid plants was to deplete the oxygen by operating the engine near stoichiometric or by adding a hydrocarbon or purge gas to deplete the oxygen via a chemical reaction in the exhaust.

For stationary engine operation, the engine is normally operated near stoichiometric conditions, whereby the catalytic chemistry is very similar to automotive three-way catalyst technology. A typical response of engine emissions from a natural gas fired stationary engine is given in Figure 3.2

The main differences from this application relative to automotive exhaust control are in the operating conditions (temperature, steady-state operation, and so forth) and the aging phenomenon.

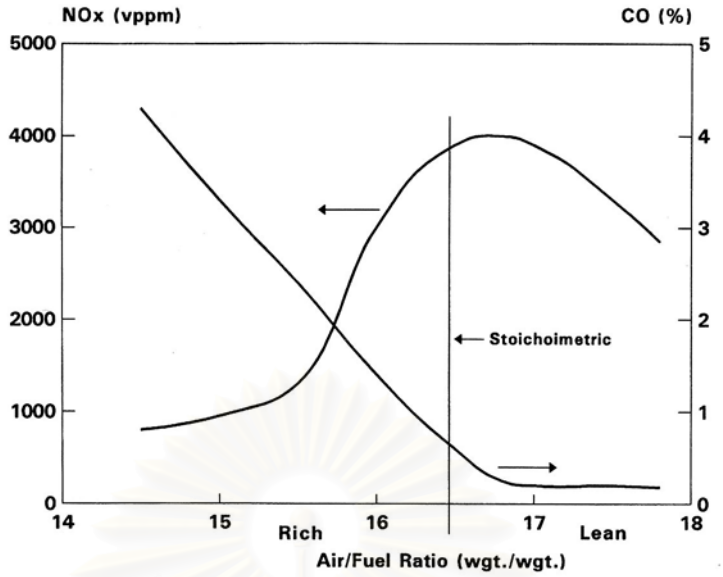

Figure 3.2 Emissions of natural gas fueled stationary engine as a function of air-to-fuel ratio[108]

The major reactions involved NSCR NO_x are as follows:

$$CO + 1/2O_2 \rightarrow CO_2$$
$$H_2 + 1/2O_2 \rightarrow H_2O$$
$$HC + O_2 \rightarrow CO_2 + H_2O$$
$$NO_x + CO \rightarrow CO_2 + N_2$$
$$NO_x + H_2 \rightarrow H_2O + N_2$$
$$NO_x + HC \rightarrow CO_2 + H_2O + N_2$$

3.5 Selective catalytic reduction of NO_x

Selective catalytic reduction (SCR) of NO_x using ammonia was first discovered in 1957. It was found that NH_3 could react selectively with NO_x, producing elemental N_2 over a Pt catalyst in excess of oxygen. The major desired reactions are:

$$4NH_3 + 4NO + O_2 \rightarrow 4N_2 + 6H_2O$$
$$4NH_3 + 2NO_2 + O_2 \rightarrow 3N_2 + 6H_2O$$

One undesirable product, N_2O, which given its strong infrared absorptivity, is considered to be a powerful greenhouse gas:

$$2NH_3 + 2O_2 \rightarrow 3N_2O + 3H_2O$$

At temperature about 100 - 200 °C, NH_3 can also react with the NO_2 present in the process gas producing explosive NH_4NO_3 as in the reaction below:

$$2NH_3 + 2NO_2 + H_2O \rightarrow NH_4NO_3 + NH_4NO_2$$

The reaction can be avoided by never allowing the temperature to fall below about 200 °C. The tendency for formation of NH_4NO_3 can also be minimized by metering into the gas stream less than the precise amount NH_3 necessary to react stoichiometrically with the NO_x (1 to 1 mole ratio) By doing so, there is little excess NH_3 that can slip out of the reactor

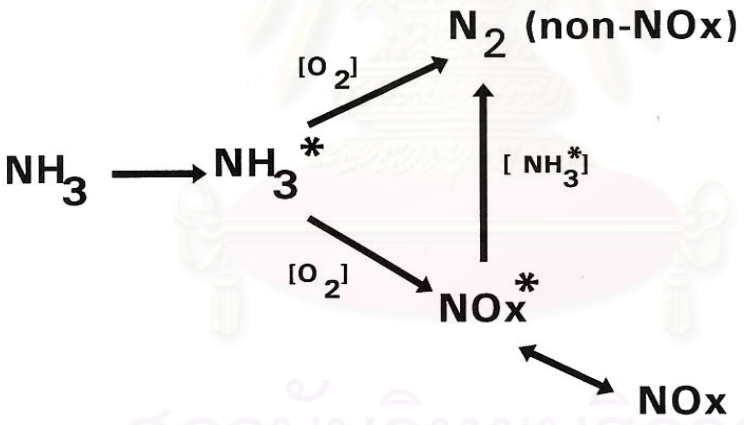

Figure 3.3 Reaction network-catalytic reaction scheme of NH_3 , NO_x and O_2 [108]

It is apparent that NH_3/NO_x ratios much greater that 1 result insignificant NH_3 slip. In all applications, there is always a specification on permit NH_3 slip. Frequently, this is < 5 - 10 ppm. The major reactions involved in SCR NO_x reduction are depicted schematically in Figure 3.3.

There is a great incentive to use natural gas or other hydrocarbons as a reductant in stationary SCR rather than NH_3.

$$CH_4+2NO+O_2 \rightarrow N_2+2H_2O+CO_2$$

For many new power plants, natural gas is commonly used as a fuel and is readily available. Secondly, NH_3 is more expensive, requires special handling and storage, and requires a sophisticated metering system to avoid NH_3 slip. Technology referred to as lean NO_x is in the early stage of development. The most promising material is a ZSM-5 zeolite ion exchanged with Cu. However, the activities, selectivities, and thermal stability are still not acceptable for commercial use. This catalyst dose not works well CH_4 and is most reactive with C_2 compounds. Recent studies have the possibility of using natural gas as a reductant with a Cobalt exchanged on ZSM-5 zeolite as the catalyst, but much work still needs to be done to bring this technology to the commercial world. Reaction rates are low, and their strong inhibition by H_2O.

There is a great deal of research in progress today to find a 'lean-NOx' catalyst that would function with a hydrocarbon reductant to eliminate the technological and safety issues associated with the use of ammonia. This is a particularly important issue for mobile sources such as lean-burn gas engine and diesel fueled vehicles for which ammonia would not be a suitable reductant. Unfortunately, Cu/ZSM-5 and Pt/ZSM-5 catalysts for SCR of NO_x with hydrocarbons are poisoned and deactivated by H_2O and SO_2 in the typical flue gas. Thus, at their present stage of development these catalysts are not sufficiently active or stable to be commercially viable, i.e. achieve high NO_x conversion.

Catalyst design includes consideration of: (1) active catalyst phase; (2) support surface area and porosity; (3) catalyst support geometry, i.e. channels per unit reaction cross-section and wall thickness; (4) density; and (5) crush strength. The attributes of the ideal SCR catalyst are follows:

- High NO reduction efficiency with minimal pressure variation:
  - low NH_3 slippage
  - low SO_3 formation
  - high selectivity for N_2.

- Maximum operation flexibility
  - broad temperature range
  - resistance to erosion/abrasion/spalling
  - resistance to contamination/poisons
  - minimal O_2 requirement.
- Good hydrothermal stability:
  - high temperature
  - low susceptibility to startup/shutdowns and thermal cycling.

It is difficult to design a catalyst that combines all of these attributes, because optimal design for one property may lead to less than optimal performance for another.

3.6 Molecular sieve and zeolite

Zeolite , or crystalline aluminosilicates having pore of molecular dimension, occur naturally in the vugs and vesicles of basaltic lava, in volcanic deposits from saline, alkaline lake and nonmarine tuff beds. These naturally occurring zeolites, the first known examples of molecular sieves, were studied scientifically as early as 1760, whereas their selective adsorption and ion-exchanged properties have been known for decades. Today, zeolites and other molecular sieves, the crown jewels of catalysis, promise to revolutionize chemicals manufacture, petroleum refining and coal and/or natural gas conversion processes through the concept of catalysis by molecular design.

3.6.1 Composition of molecular sieves

Strictly speaking, the term molecular sieve refers to a class of crystalline materials having a range of compositions that exhibit shape-selective adsorption and reaction properties, whereas the term zeolite refers to the shape-selective materials composed only of aluminosilicates. The range of materials that make up molecular sieves includes carbon, silica, aluminosilicates, aluminophosphates, metallosilicates (e.g. gallosilicates, chromosilicates, borosilicates, and ferrisilicates) and metalloaluminates (e.g. germinium aluminates). In fact, the list of cations that can be

incorporated into molecular sieve frameworks has been expanded to include 16 or more elements (Si, Al, Ga, Ge, Be, Li, Mg, Ti, Cr, Mn, Fe, Co, Zn, B, C, P etc.)

3.6.2 Composition and structure of zeolites.

Zeolites or aluminosilicates have the general formula $M_v(AlO_2)_x(SiO_2)_y.zH_2O$; the AlO_2 and SiO_2 species are the fundamental units that share oxygen ions to form tetrahedral AlO_4 and SiO_4 building blocks for the zeolite unit cell. Thus, the framework of a zeolite is made up of aluminum and silicon tetrahedral, while metal or hydrogen cations (M) occupy exchangeable cationic sites. Table 3.2 shows the unit cell composition for several important Na-exchanged zeolites along with aperture size (limiting pore size). Note that because the silicon ion has a charge of +4 and aluminium +3, the number of Na^+ ions required for charge equalization is equal to the number of aluminum ions.

Table 3.2 Composition and limiting pore diameters for common zeolites [109]

Type	Composition per unit cell				Aperature
	Na	AlO_2	SiO_2	H_2O	Size (Å)
A	12	12	12	27	4.2
Faujasite X	86	86	106	264	8.0
Faujasite Y	56	56	136	264	8.0
Erionite	4.5	9	27	27	4.4
Mordenite	8	8	40	24	6.6
Pentasil (ZSM-5)	9	9	87	16	5.5
Pentasil (Silicate)	0	0	96	16	5.5

The synthesis of zeolites from its basic building blocks is illustrated in Figure 3.4. A typical aluminosilicate is formed by polymerization of SiO_4 and AlO_4 tetrahedra to form sheet-like polyhedra (squares and hexagons) which in turn form cubes, hexagonal prisms and truncated octahedral (14-sided). These three-dimensional tertiary building blocks in turn are arranged regularly to form a superstructure inside

which exist pores and a supercage. Each supercage has a characteristic window size aperture which blocks entry of sufficiently large molecules, i.e. the sieve effect.

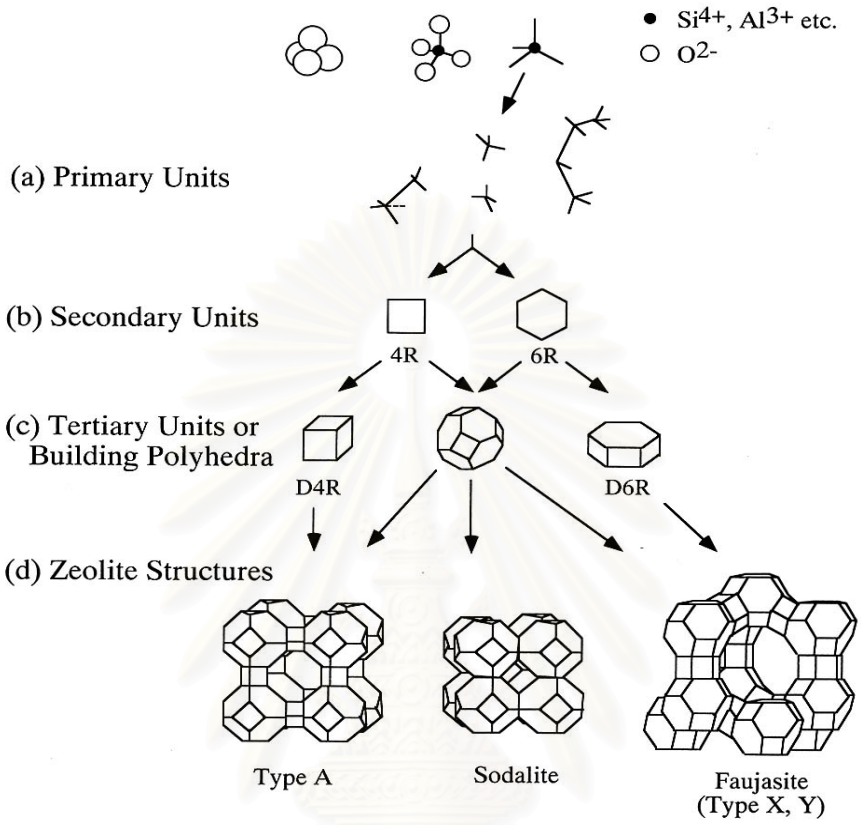

Figure 3.4 Formation of three common zeolites from primary SiO_4 and AlO_4 tetrahedral units through a combination of secondary ring units, and ultimately different mixes tertiary polyhedra [109]

3.6.3 Pore structure of molecular sieves.

The zeolites listed in Table 3.2 are just a few of the many possible molecular sieve structures. According to Vaughan [110]: ‘few fields of chemistry offer such chemical diversity; although only about 60 structures are known, tens of thousands of theoretical structures are possible.

Probably the simplest level of classifying molecular sieve structure is in terms of pore diameter and ring size. By convention, ring size is specified by the number of T atoms or TO_4 units where T = Si, Al, P or B. Pore diameters of aluminosilicate

molecular sieves (A, erionite, pensil, mordenite and faujasite) range from 3 to 8 Å, whereas ring sizes range from 8 Å for erionite to 12 Å for Y-Zeolite.

3.6.4 Exchangeability

Most zeolites are synthesized in the alkali cation form (mostly Na^+) in which the positively charged cations balance the negatively charged framework system. In aluminosilicates, these cations are readily exchanged by other mono-, di- and trivalent cations including NH_4^+, H^+, Ca^{2+}, and La^{3+}. Cations in ALPOs are not exchangeable. According to Ward [111] the rate and degree of cation exchange in zeolites depends on:

- the type of cation being exchanged, its diameter and charge;
- the nature of, size of and strength of cation coordination complex;
- ion exchange temperature;
- thermal treatment of the zeolite, before or after exchange;
- the structural properties of the zeolite and its Si:Al ratio;
- the locations of cations in the zeolite;
- the concentration of the cation exchange solution;
- any previous treatment of the zeolite.

H-sieves (hydrogen ion-exchanged sieves) are made by first ammonium ion exchange, followed by thermal decomposition.

3.6.5 Active sites

The complex crystalline structure of each zeolite leads to a multiplicity of cation positions in the pores and supercages.

3.6.6 Acidity

Acidity in zeolites increases with decreasing Si:Al ratio, since acid sites are associated with Al ions; acidity is also a function of cation. H-sieves are strong acids but often too unstable for commercial use. Nevertheless, zeolites exchanged with di- and trivalent ions are sufficiently acidic; for example, Ca^{2+} is thought to be present as $Ca(OH)^+$ plus H^+. ALPOs are mildly acidic relative to the aluminosilicates. The

Bronsted and Lewis acidities of zeolites play important roles in their abilities to catalyze various hydrocarbon reactions, e.g. cracking and isomerization.

3.6.7 Thermal stability

The thermal stability of zeolites increases with increasing silica content and by exchange with rare earth cations. Most sieves are uncharged by dehydrating to 400 ºC; high silica (ultrastabilized forms prepared by steam pre-treatment) and rare earth-exchanged sieves are stable to 700-800 ºC. Generally, extensive dehydration causes loss of Bronsted acidity due to the removal of OH or silanol surface groups.

Thermal treatment of zeolites in the presence of water normally leads to dealumination. In fact, it is one of the recommended methods for preparing ultrastable zeolites. Moderate dealumination generally increases catalytic activity or leaves it unchanged, whereas advanced dealumination leads to a decrease in activity due to a loss of active sites and ultimately collapse of the zeolite structure. For example, dealumination of mordenite significantly changes important chemical and physical properties such as crystal structure, thermal stability, sorption capacity and acidity, as well as catalytic properties. Maximum thermal stability is reached for an SiO_2:Al_2O_3 ratio of about 19. The sorption capacity towards water is highly reduced after dealumination because of the absence of strong polarizing cations which can dissociate water to strongly adsorbed hydroxy groups; accordingly, the number of Bronsted acid sites also decreases. Nevertheless, the hydrocarbon cracking activity of mordenite increases with increasing Si:Al ratio. For further details on zeolite stability, the reader is referred to the comprehensive review of McDaniel and Maher [112].

CHAPTER IV

EXPERIMENTAL

4.1 Catalysts preparation

In this study, five of ZSM-5 zeolite catalysts, having different crystal size but the same Si/Al ratio (Si/Al ≈ 23) and ZSM-5 commercial catalyst with Si/Al ratio of 23 in Na form supplied by ALSI-PENTA ZEOLITE SM-55 were also used. Co/HZSM-5 and Me/Co/HZSM-5 were prepared for the NO removal reaction. The preparations of Co/HZSM-5 and Me/Co/HZSM-5 were described as follows :

4.1.1 Preparation of NaZSM-5

The preparation procedure of ZSM-5 by rapid crystallization method was shown in Figure 4.1, while reagents were shown in Table 4.1. This method could advantageously and rapidly prepare the uniform and fine zeolite crystals with the following improvements: (i) the preparation of supernatant liquid was separated from that of gel, which was important to prepare the uniform crystals, (ii) the precipitated gel was milled before the hydrothermal treatment, which was essential to obtain the uniform and fine crystals, and (iii) the temperature under the hydrothermal treatment was programmed to minimize the time which was necessary for the crystallization. The detail preparation procedures of ZSM-5 were described below.

4.1.1.1 Preparation of Gel Precipitation and Decantation Solution

A supernatant liquid was separated from the gel, which is important for preparing the uniform crystals. A gel mixture was prepared by adding solution A-1 and solution B-1 into solution C-1 dropwise with vigorous stirring using a magnetic stirrer at room temperature. The pH of the mixed solution was maintained within the range 9-11 because it was expected that this pH range is suitable for precipitation. The gel mixture was separated from the supernatant liquid by a centrifuge. The precipitated gel mixture was milled for 1 h by a powder miller (Yamato-Notto, UT-

22). The milling procedure was as follows: milled 15 min → centrifuge (to remove the liquid out) → milled 15 min → centrifuge → milled 30 min. Milling the gel mixture before the hydrothermal treatment was essential to obtain the uniform, fine crystals.

A decantation solution was prepared by adding solution A-2 and solution B-2 into solution C-2 same as for the preparation of the gel mixture. During the time the supernatant liquid from A-2, B-2, and C-2 was mixing together. The pH of the solution was adjusted to between 9-11. H_2SO_4 (conc.) or 1 M NaOH solution were used to adjust pH of the decant mixture to an appropriate level if it was necessary. The colorless supernatant liquid was separated from the mixture by sedimentation and centrifugation.

4.1.1.2 Crystallization

The mixture of the milling precipitate and the supernatant of decant solution was charged in a 500 ml Pyrex glass container. The glass container was placed in a stainless steel autoclave. The atmosphere in the autoclave was replaced by nitrogen gas and pressurized up to 3 kg/cm^2 gauge. In order to vary the crystal sizes of ZSM-5, the mixture in the autoclave was heated from room temperature to 160 ^oC with various heating rates 0.4, 0.5, 0.9, 1.0, and 1.5 ^oC/min, and then up to 210 ^oC with a constant heating rate of 12 ^oC/h while being stirred at 60 rpm, followed by cooling of the hot mixture to room temperature in the autoclave overnight. The temperature was programmed to minimize the time necessary for the crystallization. The product crystals were washed with de-ionized water about 8 times using the centrifugal separator (about 15-20 min. for each time), to remove Cl^- from the crystals, and dried in an oven at 110 ^oC for at least 3 h.

4.1.1.3 Calcination

The dry crystals were calcined in an air stream at 540 ^oC for 3.5 h, by heating them from room temperature to 540 ^oC in 1 h , to burn off the organic template and leave the cavities and channels in the crystals. The calcined crystals were finally cooled to room temperature in a desiccater. The obtained Na-ZSM-5 is the parent

ZSM-5 zeolite which will be further transformed to the other appropriate forms for the experiments in this study.

Table 4.1 Reagents used for the preparation of Na-ZSM-5 :Si/Al = 25

Solution for the gel Preparation		Solution for decant-solution Preparation	
<u>Solution A1</u>		<u>Solution A2</u>	
$AlCl_3$	1.799 g	$AlCl_3$	1.799 g
TPABr	5.72 g	TPABr	7.53 g
NaCl	11.95 g	De-ionized water	60 ml
De-ionized water	60 ml	H_2SO_4(conc.)	3.4 ml
H_2SO_4 (conc.)	3.4 ml		
<u>Solution B1</u>		<u>Solution B2</u>	
Sodium silicate	69 g	Sodium silicate	69 g
De-ionized water	45 ml	De-ionized water	45 ml
<u>Solution C1</u>		<u>Solution C2</u>	
TPABr	2.16 g	NaCl	26.27 g
NaCl	40.59 g	De-ionized water	104 ml
NaOH	2.39 g		
De-ionized water	208 ml		
H_2SO_4(conc.)	1.55 ml		

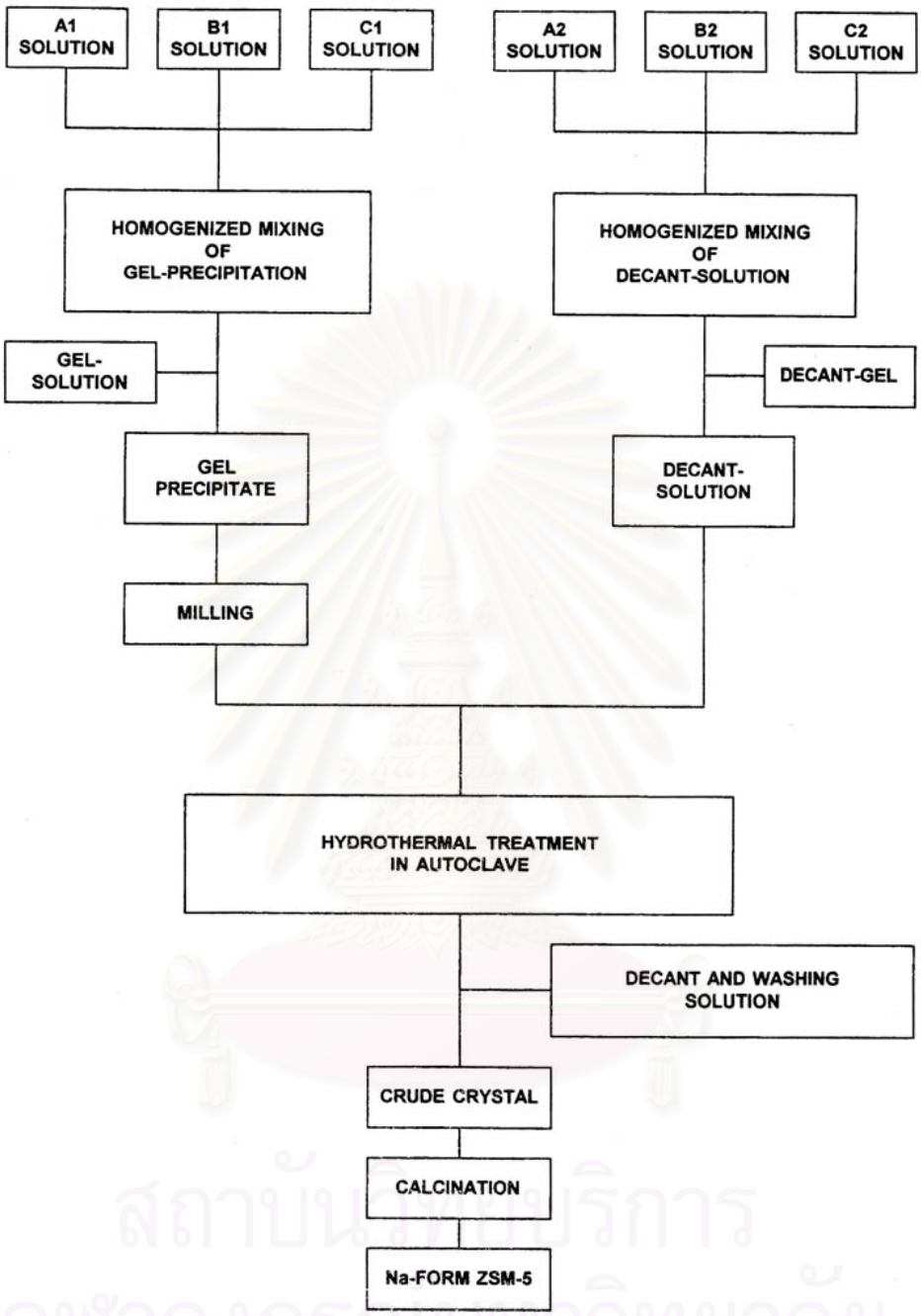

Figure 4.1 The preparation procedure of ZSM-5 by rapid crystallization method.

Moreover, the Na-ZSM-5 obtained form each batch was check by using the X-Ray Diffraction (XRD) analysis to confirm the ZSM-5 structural and crystallinity of sample. If, unfortunately, the XRD pattern could not be acceptable, the sample would be discarded and a new sample has to be made.

4.1.2 Ammonium ion-exchanged

To make NH_4-ZSM-5, the parent Na-ZSM-5 powder was firstly mixed with 1 M NH_4NO_3 solution at 30 ml per gram of catalyst. In the procedure, the catalyst amount did not exceed 5 grams to approach complete exchange. The slurry of zeolite and solution was then stirred and heated on a hot plate, maintained at 80 °C by reflux. After heating the mixture for about 1h, the mixture was cooled down to room temperature and centrifuged to remove the used solution. The remained crystals were mixed again with NH_4NO_3 solution in the same amount. The previous step was repeated. The exchanged catalyst was then washed twice with deionized water using centrifuge. Subsequently, the exchanged crystals were dried in an oven at 110-120 °C for at least 3 h. The dried catalyst obtained is the NH_4-form of ZSM-5. The NH_4-ZSM-5 was converted to H-form ZSM-5 by removing NH_3 species from the catalyst surface. NH_3 can be removed by thermal treatment of the NH_4-ZSM-5 zeolite. This was done by heating a sample in a furnace from ambient temperature to 540 °C in 1 h and holding the sample at 540 °C for 3.5 h. After the catalyst was cooled down, it was stored in a glass bottle in a desiccater for further use.

4.1.3 Cobalt loading by ion-exchanged

The suitable metal-exchanged technique comprises contacting the zeolite with a solution which contains the salt of the desired replacing cation. A preferred exchange solution is cobalt (II) acetate. Approximately 3 g of H-form catalyst was stirred with 150 ml of a dilute (0.01 M) cobalt (II) acetate solution. The metal exchange was typically carried out at 80 ^{o}C for 24 h. More repeats of ion-exchanged step were required upon the amount of cobalt needed. The wet cake obtained by separation from the solution was washed with de-ionized water and dried at 110 ^{o}C overnight.

4.1.4 The second metals loading by ion-exchanged

The second metals, ie Pd, Cd, Ba, Cu, La, Ni, Zn, Ag, Fe, Ce, and Mn were introduced individually to Co/HZSM-5 by ion exchanging in a nitrate or acetate solution of each cation. The amount of the second component on Co/HZSM-5 is ca. 0.4 wt%. Next, the ion-exchanged catalyst was washed twice with deionized water by using centifuge separation and dried at 110 ^{o}C overnight. The samples were calcined at 540 ^{o}C for 3.5 h in air.

4.2 Pretreatment condition

The pretreatment procedure used in this study concerns the hydrothermal treatment condition. The catalyst were pretreated in He while elevating the temperature from room temperature to 600 °C with heating rate 10 °C/min. The catalyst samples were then kept at 600 °C for 24 h while adding 10% mole of water vapor. The catalysts were then cooled down to room temperature in the He stream.

4.3 Nitric Oxide Reduction

4.3.1 Chemicals and Reagents

Nitric oxide (1%) in helium, Methane (10%) in helium, and oxygen of ultra high purity grade (99.999%) were provided by Thai Industrial Gases Limited.

4.3.2 Instruments and apparatus.

A flow diagram of the steady state nitric oxide reduction system is shown in Figure 4.2. The system consists of a reactor, an automation temperature controller, an electrical furnace, a gas control system and saturator. The instruments used in this system is listed and explained below:

1. Reactor: The NO reduction reactor was a conventional micro-reactor made from quartz tube with 0.6 cm inside diameter. The reaction was carried out under ordinary gas flow and atmospheric pressure. The effluent gas was sampled and analyzed by an on-line gas chromatograph.

2. Automation temperature controller: This unit consisted of a magnetic switch connected to a variable voltage transformer and a RKC temperature controller series REX-C900 connected to a thermocouple attached to the catalyst bed in reactor. A dial setting established a set point at any temperature within the range between 0 to 999 °C

3. Electrical furnace: The furnace supplied the required heating to the reactor for NO reduction reaction. The reactor could be operated from room temperature up to 600 °C at maximum voltage of 220 volts.

4. Gas controlling system: Nitric oxide, methane, oxygen and helium cylinders each was equipped with a pressure regulator (0-120 psig), and and on-off valve. Needle valves were used to adjust flow rate of gases. A gas sampling valve was used to take samples of effluent gas.

5. Gas Chromatography: Thermal conductivity detector (TCD) gas chromatograph. SHIMADZU GC8-ATP was used to analyze feed and effluent gas. Operating condition used was shown in Table 4.2

Table 4.2 Operating conditions of gas chromatograph

Gas chromatography	SHIMADZU GC-8APT	SHIMADZU GC-8AIT
Detector	TCD	TCD
Packed column	MS-5A	PORAPAK - Q
Carrier gas	He (99.999%)	He (99.99%)
Flow rate of carrier gas	30 ml/min	60 ml/min
Column temperature	70 ^{o}C	90 ^{o}C
Detector temperature	100 ^{o}C	110^{o}C
Injector temperature	100 ^{o}C	110 ^{o}C
Analyzed gas	O_2, N_2,CO,CH_4	CH_4, CO_2

4.3.3 Procedure

The catalytic test was carried out by using a conventional microreactor. The catalyst in powder form was tabletted with a tablet machine. It was crushed and sieved to 8-16 mesh to be used for the reaction. A 0.2 g portion of the catalyst was packed in the quartz tube reactor and the catalyst-bed length was about 13 mm. It was heated at room temperature to 500 °C for 1 h under He stream (35 ml/min), held at this temperature for 1 h, and then cooled down to room temperature. A gas mixture containing NO (1000 ppm), CH_4 (1 vol%), O_2 (10 vol%), and He balance was fed at a total flow rate of 50 ml/min (GHSV~10,000 h^{-1}). The samples of reaction and product gases were taken for the concentration measurement. The gas samples were analyzed by using gas chromatograph with Molecular Sieve-5A (For O_2, N_2, CH_4 and CO) columns. The gas chromatograph was equipped with Shimadzu C-R6A integrator. The concentration of CH_4 before and after the reaction were analyzed for CH_4 consumption. The conversion of NO was calculated based on the concentration of N_2 formed. Figure 4.2 illustrated the reaction scheme for NO reduction.

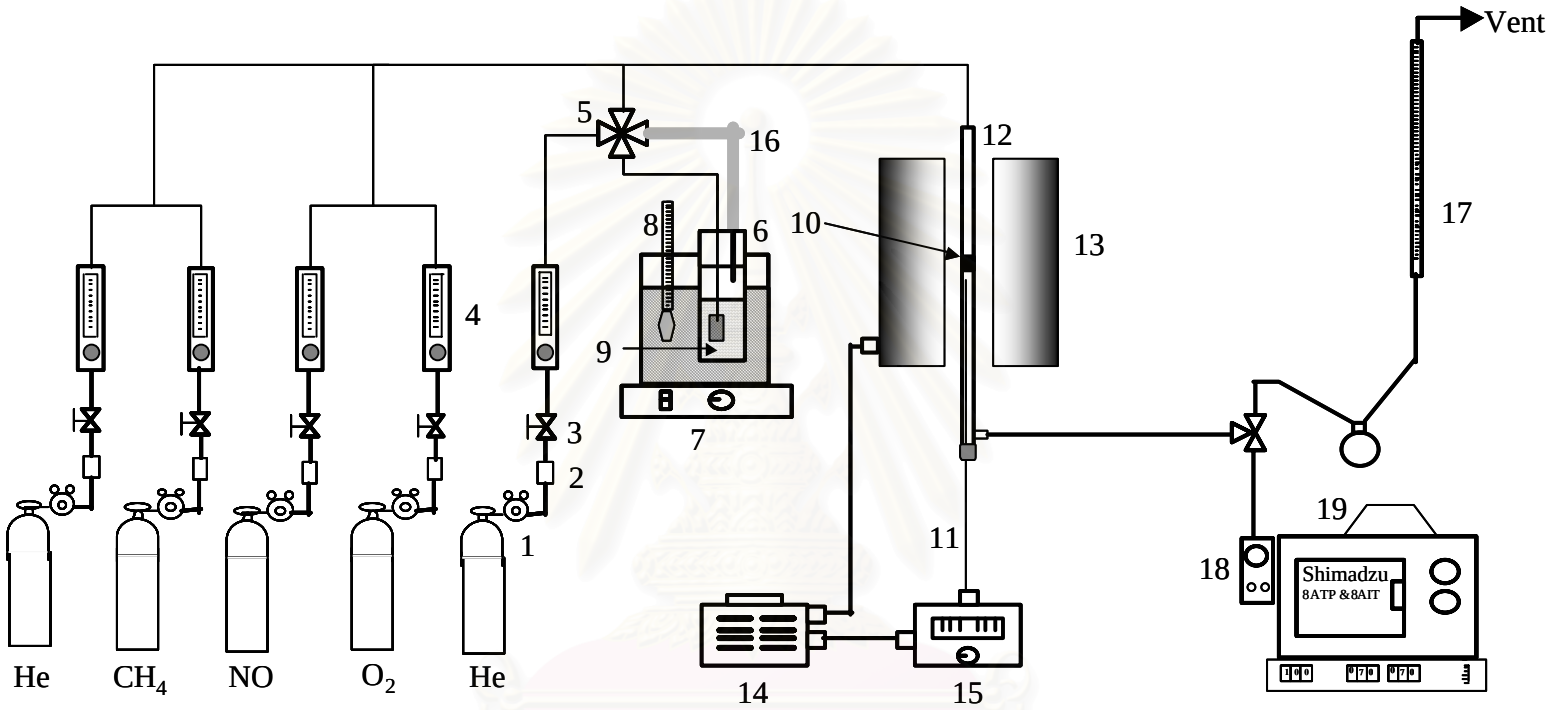

1. Pressure Regulator
2. Gas Filter
3. On - Off Valve
4. Flow meter
5. 4 - way Valve
6. Saturator
7. Magnetic Stirrer
8. Thermometer
9. Water
10. Catalyst Bed
11. Thermocouple
12. Reactor
13. Furnace
14. Variable Voltage Transformer
15. Temperature Controller
16. Heating Tape
17. Bubble Flow Meter
18. Sampling Valve
19. Gas Chromatography

Figure 4.2 Schematic diagram of the reaction line for NO and methane conve rsion analyzing by gas chromatograph consisting of molecular si eve-5A and Porapak Q columns

4.4 Characterization of the catalysts

4.4.1 X-Ray Diffraction analysis (XRD)

The Crystallinity and X-ray diffraction (XRD) patterns of the catalysts were performed by a X-ray diffractometer SEIMENS D5000 connected with a personal computer with Diffract AT version 3.3 program for fully control of the XRD analyzer. The experiments was carried out by using CuKα radiation with Ni filter and the operating condition of measurement are shown below:

2θ range of detection : 4 - 60°

Resolution : 0.04°

Number of Scan : 10

The functions of base line subtraction and smoothing were used in order to get the well formed XRD spectra.

4.4.2 Scanning Electron Microscope (SEM)

The shape and size of the crystal of the prepared catalysts were observed by using JEOL JSM-35 CF Scanning Electron Microscope (SEM) at the Scientific and Technological Research Equipment Centre, Chulalongkorn University.(STREC).

4.4.3 X-Ray Fluorescence analysis (XRF)

Quantities of Al, Si, and also Na in the samples were determined by using XRF analyzer at the Science Service Department, Rama VI Road, Bangkok. About 0.5 g of catalyst sample was used for one measurement.

4.4.4 Atomic Adsorption Spectrometry (AAS)

Metal content was analyzed by the atomic absorption spectrometry (AAS) method. The catalyst was digested into solution before analysis by AAS.

About 100 mg of catalyst was digested in a solution containing solution of 20 ml of conc. HCl, 10 ml of conc. HNO_3, and 10 ml of H_2O. The mixture was heated

until the color of the zeolite support changed to white. During the heating step, H_2O had to be added to the mixture to maintain the volume. Then, 5 drops of HF were added into the mixture in order to digest the support. The heating step was repeated until the solution became clear. Then the volume of the solution was made up to 50 ml by adding de-ionized water.

The concentration of cobalt in the prepared solution was analyzed by AAS. The unit is located at the Scientific and Technological Research Equipment Centre, Chulalongkorn University. The obtained concentration was converted to convenient % wt. of cobalt per weight of catalyst by applying the calculation shown in Appendix A-3.

4.4.5 BET Surface Area measurement

Surface area of the catalysts were measure by the BET method, with nitrogen as the adsorbate using a micrometritics model ASAP 2000 at liquid-nitrogen boiling point temperature at the Analysis Center of Department of Chemical Engineering, Faculty of Engineering, Chulalongkorn University. The operating condition are list as follows:

Sample weight:	0.3 g
Degas temperature	150 ^{o}C
Vacuum pressure	<10 μHg
Pressure table	30 points

4.4.6 ^{27}Al Magnetic Angle Spinning Nuclear Magnetic Resonance (^{27}Al MAS NMR)

Quantitative analysis of aluminum tetrahedral in zeolites was conformed by ^{27}Al- magnetic angle spinning nuclear magnetic resonance (^{27}Al MAS NMR, BRUKER DPX-300 spectroscopy operating at 78.2 MHz) at National Metal and Materials Technology Center (MTEC) Ramma VI Road, Bangkok. The signal of alumina tetrahedral could be detected at around 50 ppm.

4.4.7 Electron Spin Resonance (ESR)

Electron Spinning Resonance (ESR) analysis was chosen to study the presence of specie which has unpaired electron. Electron spin resonance spectrum of the catalyst was conducted by using JEOL JES-RE 2X Electron Spin Resonance Spectrometer at the Scientific and Technological Research Equipment Centre, Chulalongkorn University (STREC).

CHAPTER V

RESULTS AND DISCUSSION

In this research, improved catalysts were prepared and their activity on the selective NO reduction with methane in the presence of excess oxygen were investigated and compared to those of Co/HZSM-5, which receives interest due to its durability under hydrothermal pretreatment. The result and discussion in this chapter were separated into two main parts. For the first, effect of second metals on the durability improvement of Co/HZSM-5 under hydrothermal pretreatment for NO removal by methane was studied. The other, effect of crystal size on the durability of Co/HZSM-5 in the SCR of NO with methane was investigated.

5.1 Effect of the second metal on the durability improvement of Co/HZSM-5 under hydrothermal pretreatment for NO removal by methane

5.1.1 Characterization of the catalysts

The commercial catalysts used in this part were first characterized to overview the difference of their characteristics and properties. The structure and crystallinity of ZSM-5 catalyst were measured by XRD. The specific surface area and amount of Si, Al, Na and Co in catalysts were measured to consider their physical properties. The morphology was determine by SEM. The high spin Co^{2+} on the sample was investigated by ESR. Finally, ^{27}Al MAS NMR was tested to observe the structure of aluminum in the sample as solid form.

5.1.1.1 X-Ray Diffraction pattern

The structure and crystallinity of various second metals of before and after pretreatment Co/HZSM-5 catalysts were analyzed by X-ray diffraction (XRD). The XRD patterns of all Na-ZSM-5, H-ZSM-5, Co/HZSM-5 and Me/Co/HZSM-5 were the same as expected because all of catalyst used in this study were prepared from the same parent Na-ZSM-5 zeolite. Hence, the ZSM-5 crystal structure should not be

affected by cations exchanged. X-ray diffraction lines of H-ZSM-5, Co/HZSM-5 and Me/Co/HZSM-5 with and without hydrothermal treatment are depicted in Figures 5.1 to 5.13. No change of ZSM-5 structure was observed under ion exchange and hydrothermal treatment. However, from the comparison of XRD patterns between the fresh and pretreated catalysts, there were obvious losses of XRD intensities particularly in Co/HZSM-5 and Cu/Co/HZSM-5. In addition, the XRD pattern of both fresh and pretreated catalysts did not show the formation of detectable cobalt oxide crystallite ($2\theta = 31.30°$ and $36.88°$)[113]. These noticed that cobalt was well dispersed in all ZSM-5 samples used in this study.

5.1.1.2 Physical Properties

The physical properties of the before and after pretreatment catalysts were summarized in Table 5.1. The specific surface area estimated by BET and compositions of catalysts in this study were determined. BET surface area is reduced with the presence of second metal.

Table 5.1 showed the zeolite catalysts with Si/Al ratio 23 exchanging with different type of the second metals at the same level of metal content and Co loading. Crystallinity, as determined by XRD profiles, was calculated based on the area of main peak compared with that of HZSM-5 as a reference. No significant lost of crystallinity was observed on these catalysts except Co/HZSM-5 and Cu/Co/HZSM-5 catalysts.

5.1.1.3 Morphology

SEM photographs of the commercial catalyst are shown in Figure 5.14. As shown the shapes of the catalyst are uniform hexagonal crystal shape, which have an average crystal size diameter of 3 μm. After hydrothermal treatment at 600 ^{o}C in 10% water for 24 h, no significant change in morphology of the samples was observed.

Table 5.1 Physical properties of various the second metals on Co/HZSM-5 catalysts.

Catalyst	Metal (wt%)		BET surface area (m^2/g)		Crystallinity (%)		The relative area of tetrahedral ^{27}Al (%)	
	Co	Me	Fresh	pretreated	Fresh	pretreated	Fresh	pretreated
Co/HZSM-5	1.03	-	334	298	99	83	88	71
Pd/Co/HZSM-5	0.97	0.39	331	321	100	99	100	100
Cd/Co/HZSM-5	0.98	0.40	329	325	99	98	100	100
Ba/Co/HZSM-5	0.98	0.42	322	319	100	95	100	96
Cu/Co/HZSM-5	1.01	0.39	332	298	99	78	89	76
La/Co/HZSM-5	0.97	0.41	317	312	98	91	86	76
Ni/Co/HZSM-5	1.00	0.38	325	315	100	93	88	87
Zn/Co/HZSM-5	0.99	0.40	322	317	100	90	86	84
Ag/Co/HZSM-5	1.00	0.40	323	315	100	98	84	80
Fe/Co/HZSM-5	0.99	0.37	326	316	99	89	83	78
Ce/Co/HZSM-5	0.98	0.40	320	313	97	92	86	78
Mn/Co/HZSM-5	0.97	0.37	316	311	100	95	83	74

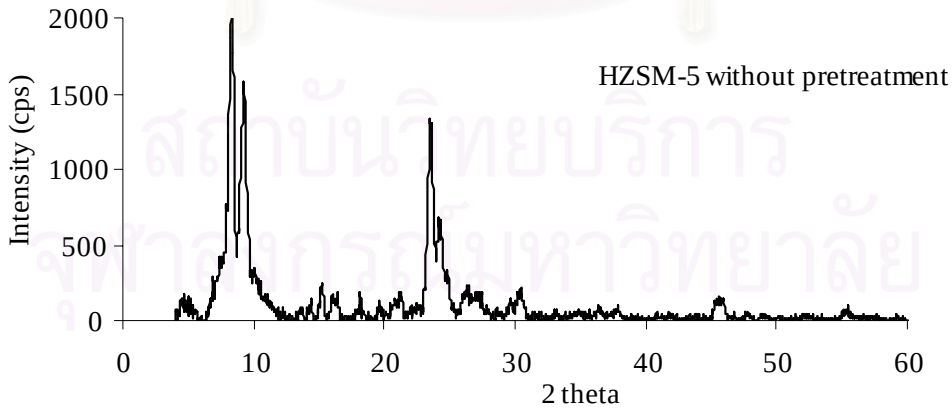

Figure 5.1 XRD patterns of HZSM-5 catalysts as a reference

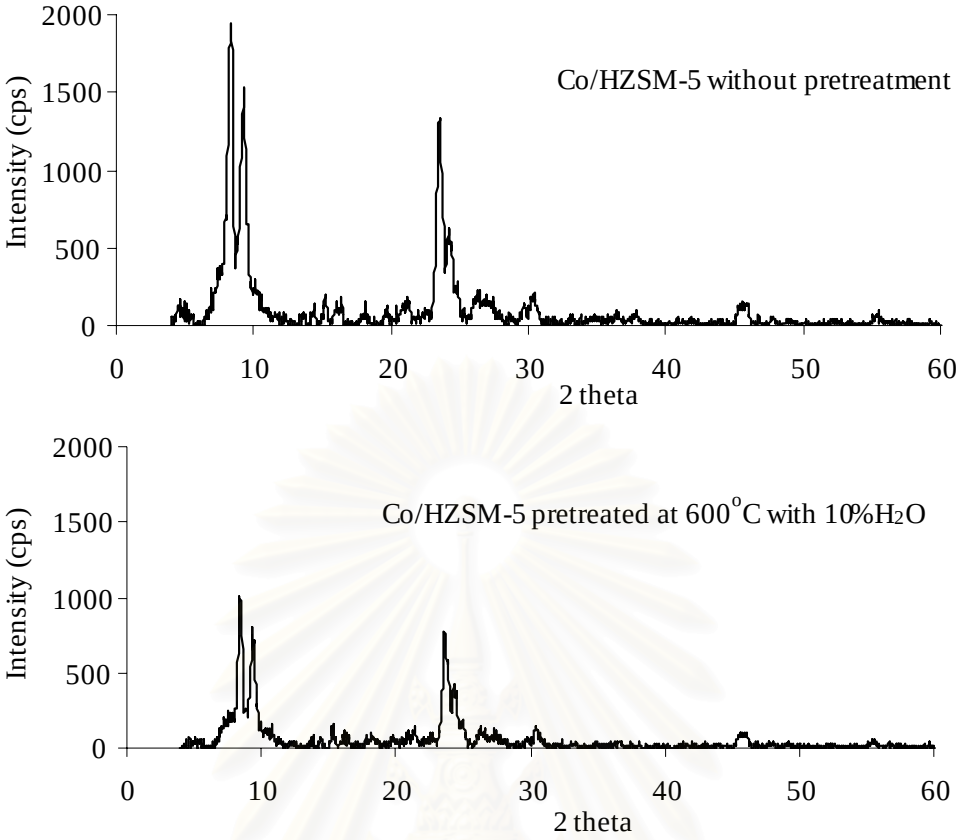

Figure 5.2 XRD patterns of Co/HZSM-5 catalysts

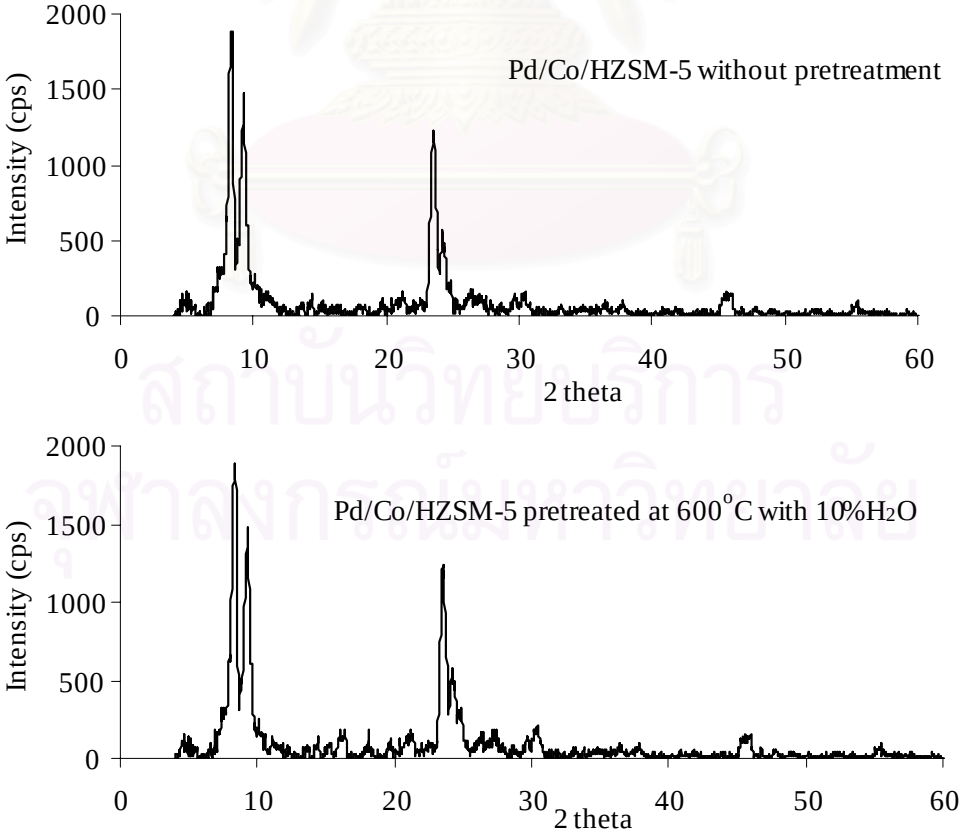

Figure 5.3 XRD patterns of Pd/Co/HZSM-5 catalysts

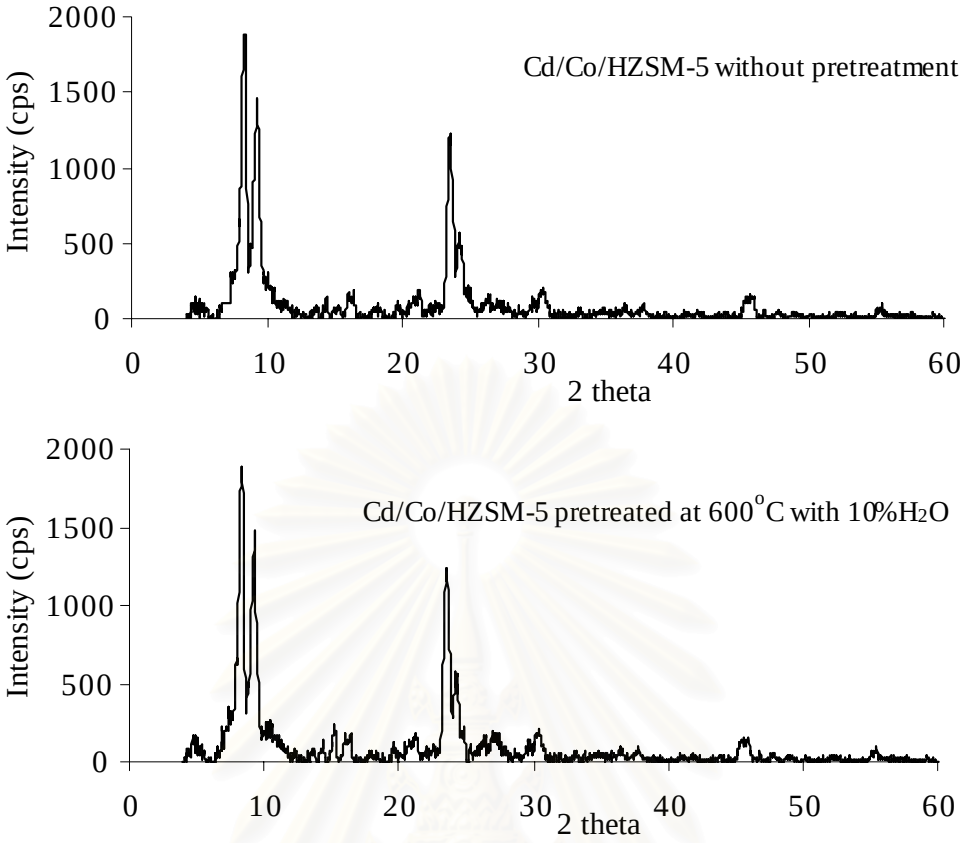

Figure 5.4 XRD patterns of Cd/Co/HZSM-5 catalysts

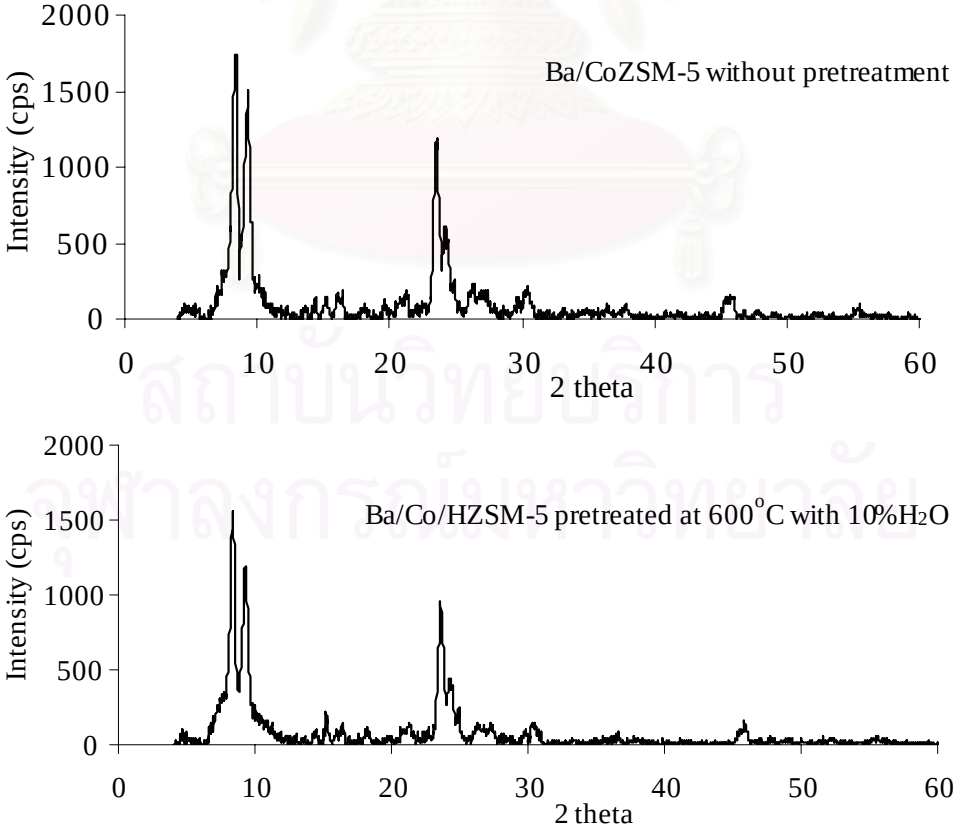

Figure 5.5 XRD patterns of Ba/Co/HZSM-5 catalysts

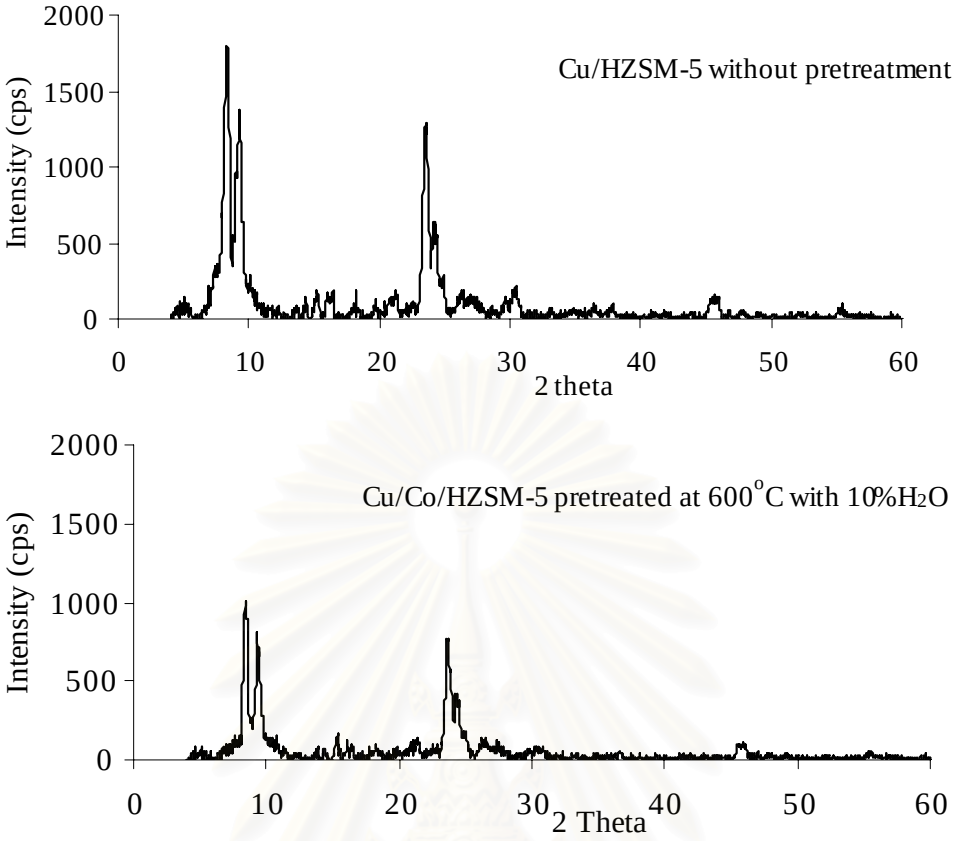

Figure 5.6 XRD patterns of Cu/Co/HZSM-5 catalysts

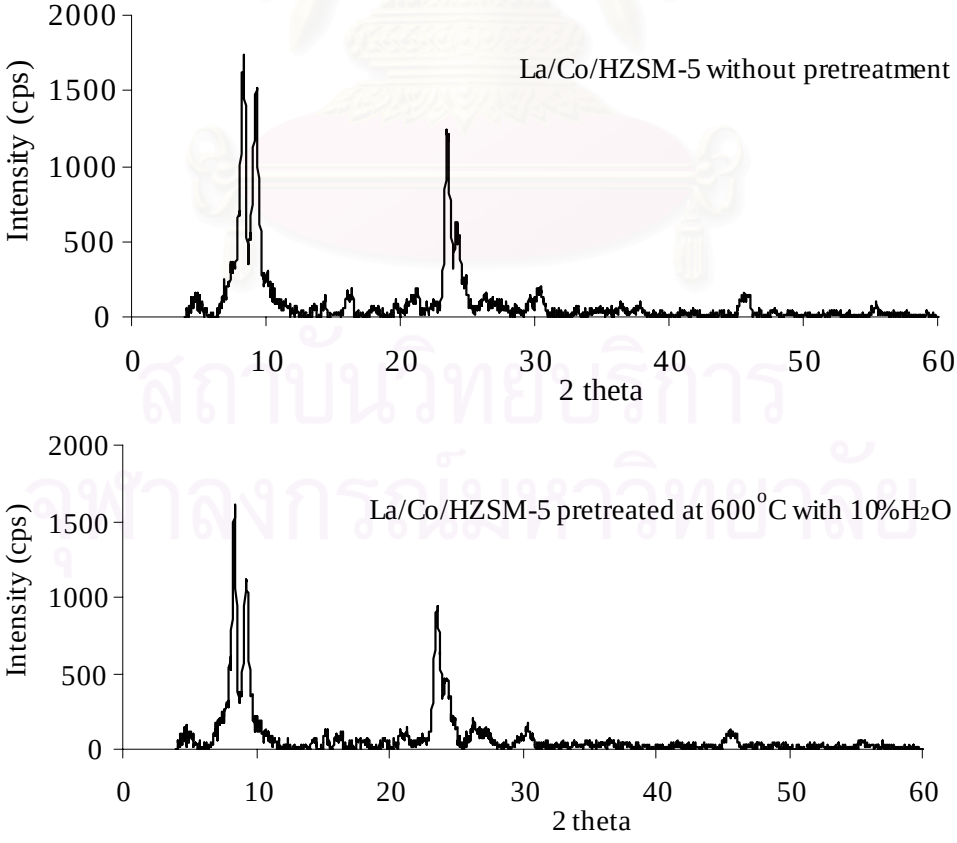

Figure 5.7 XRD patterns of La/Co/HZSM-5 catalysts

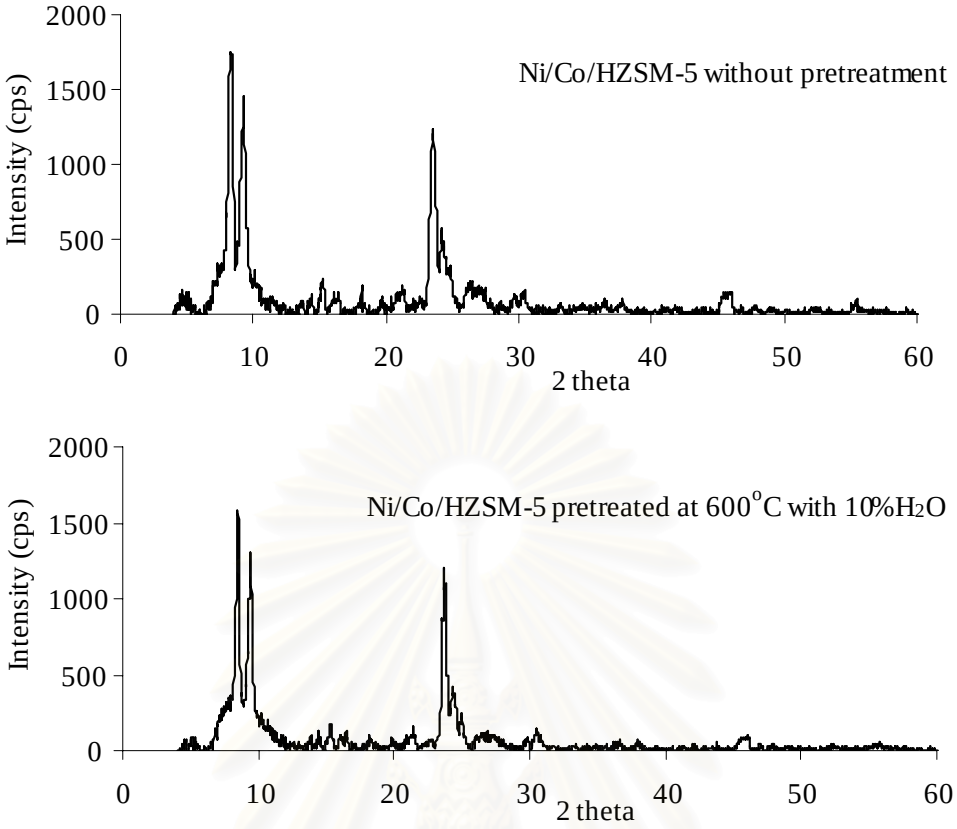

Figure 5.8 XRD patterns of Ni/Co/HZSM-5 catalysts

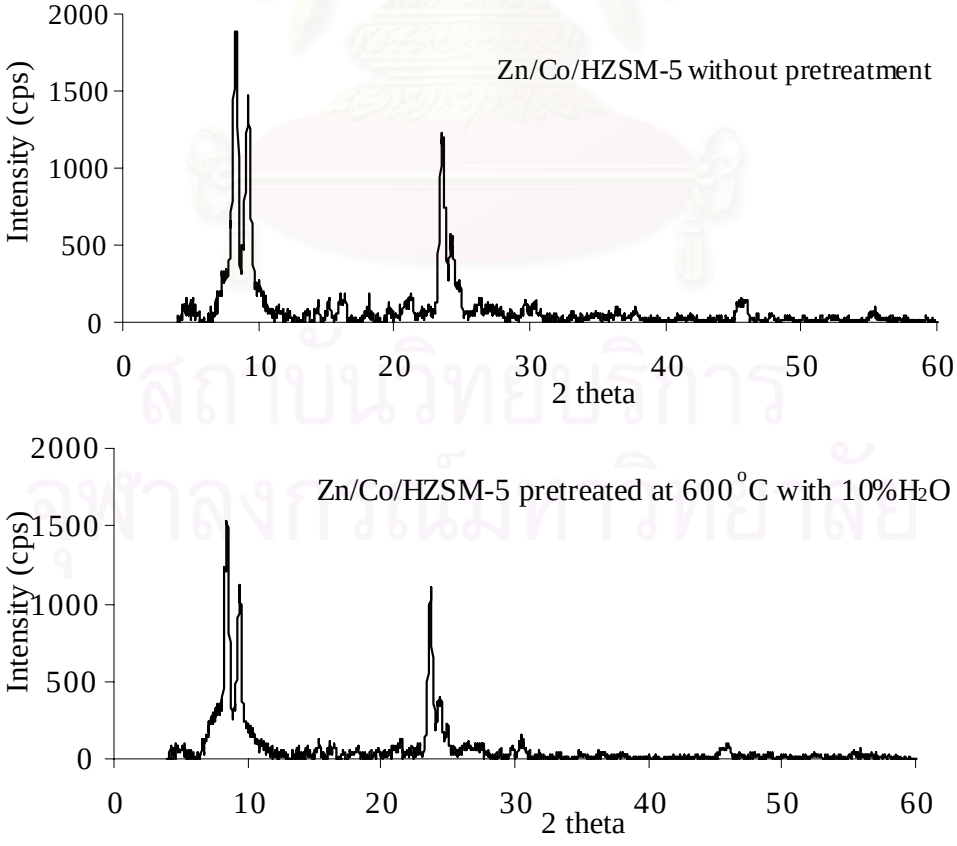

Figure 5.9 XRD patterns of Zn/Co/HZSM-5 catalysts

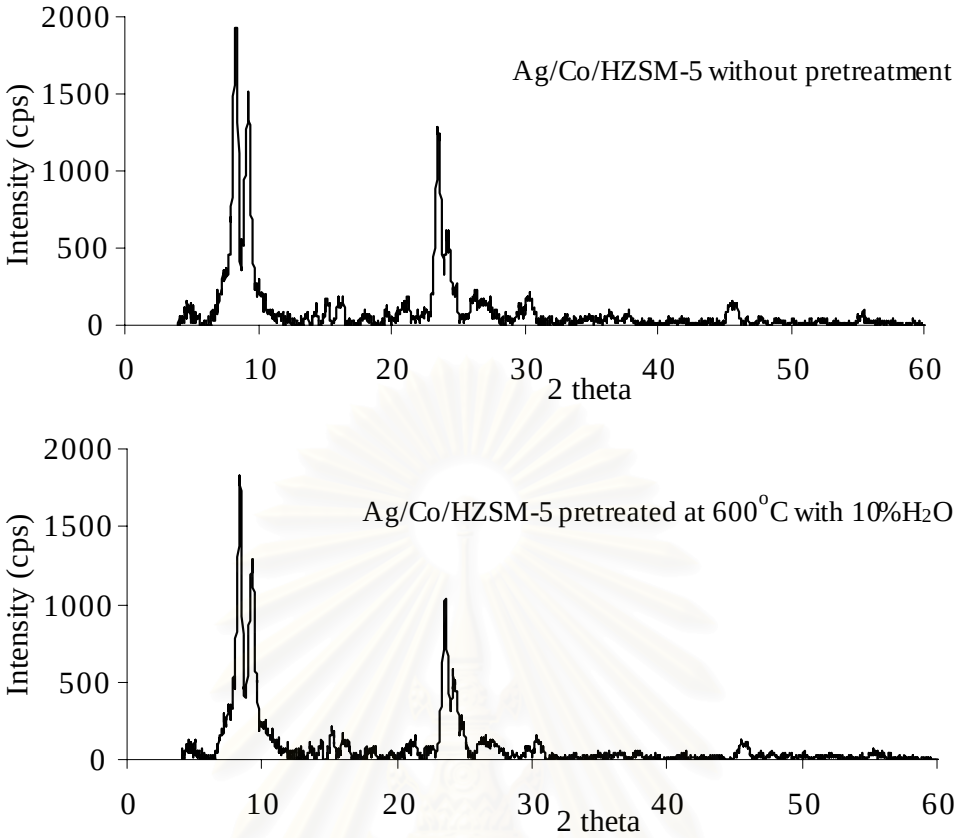

Figure 5.10 XRD patterns of Ag/Co/HZSM-5 catalysts

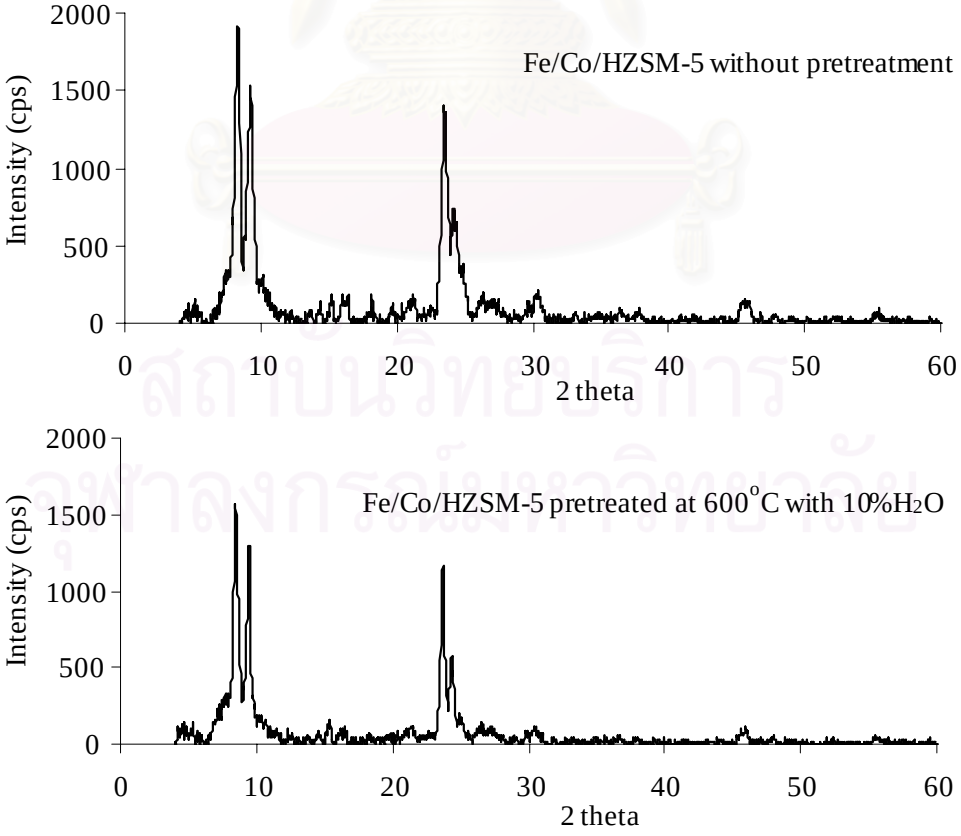

Figure 5.11 XRD patterns of Fe/Co/HZSM-5 catalysts

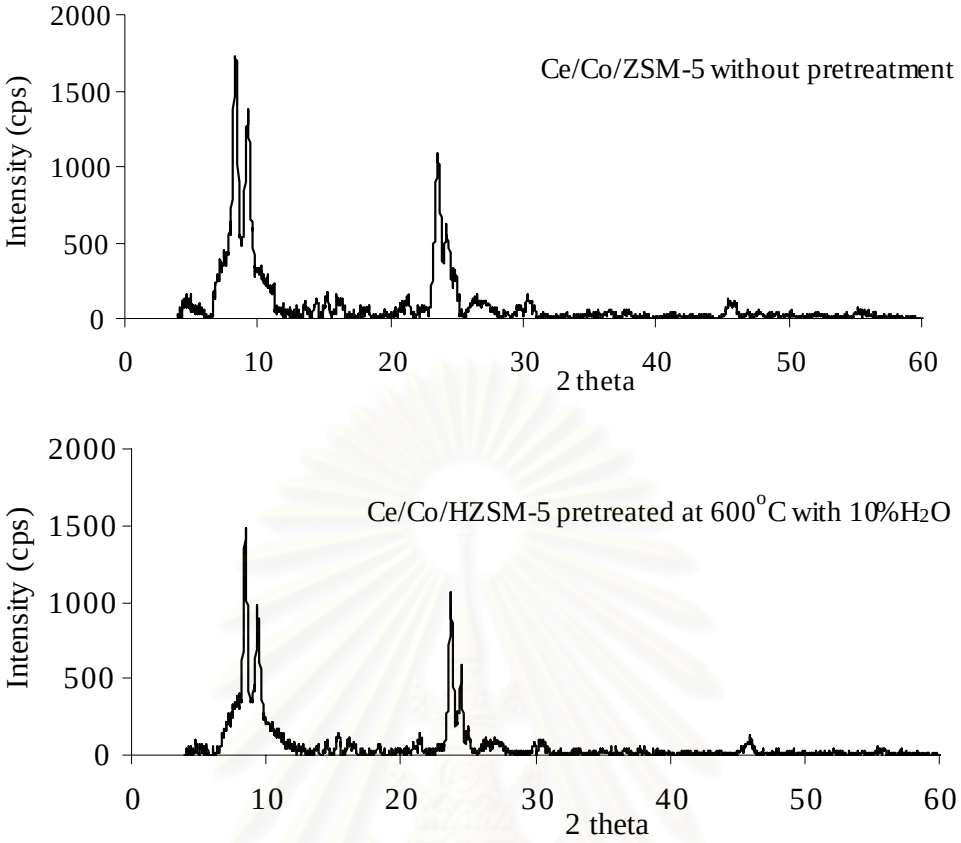

Figure 5.12 XRD patterns of Ce/Co/HZSM-5 catalysts

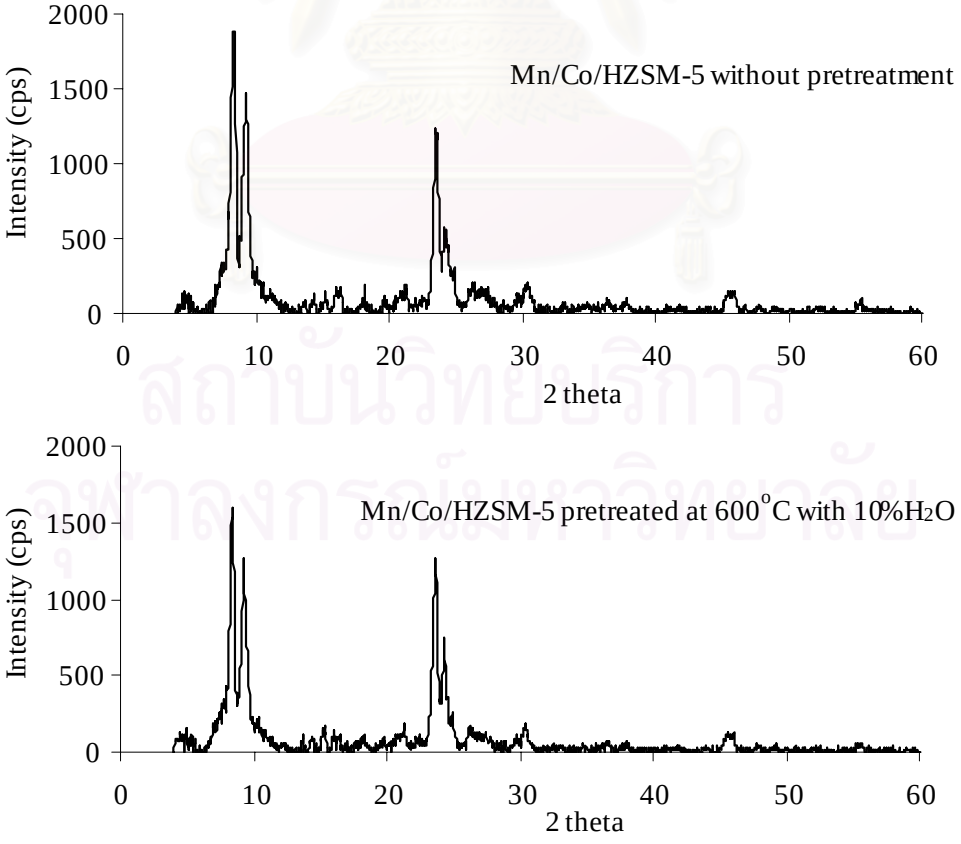

Figure 5.13 XRD patterns of Mn/Co/HZSM-5 catalysts

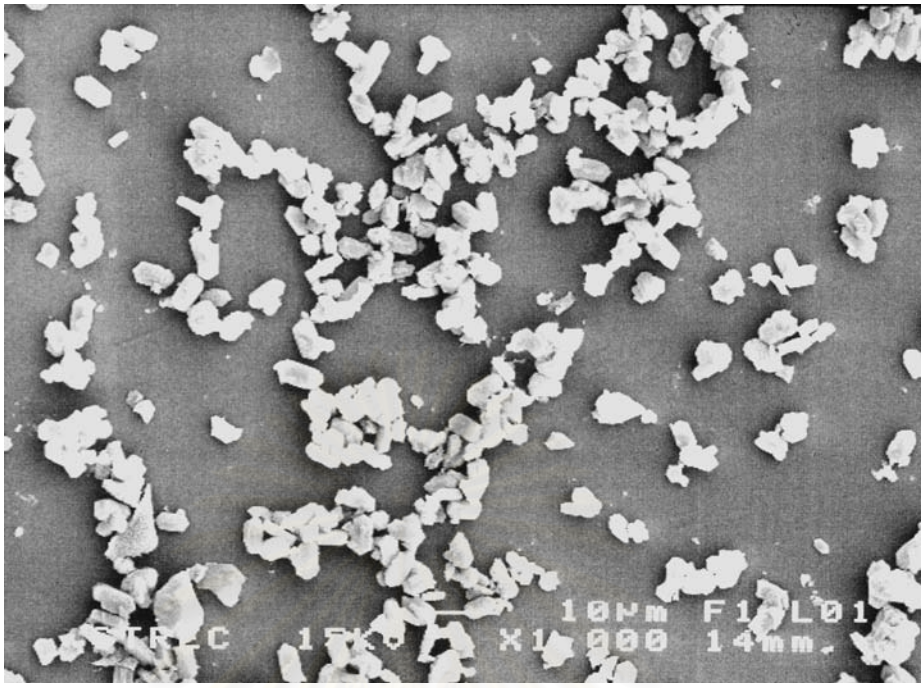

(a)

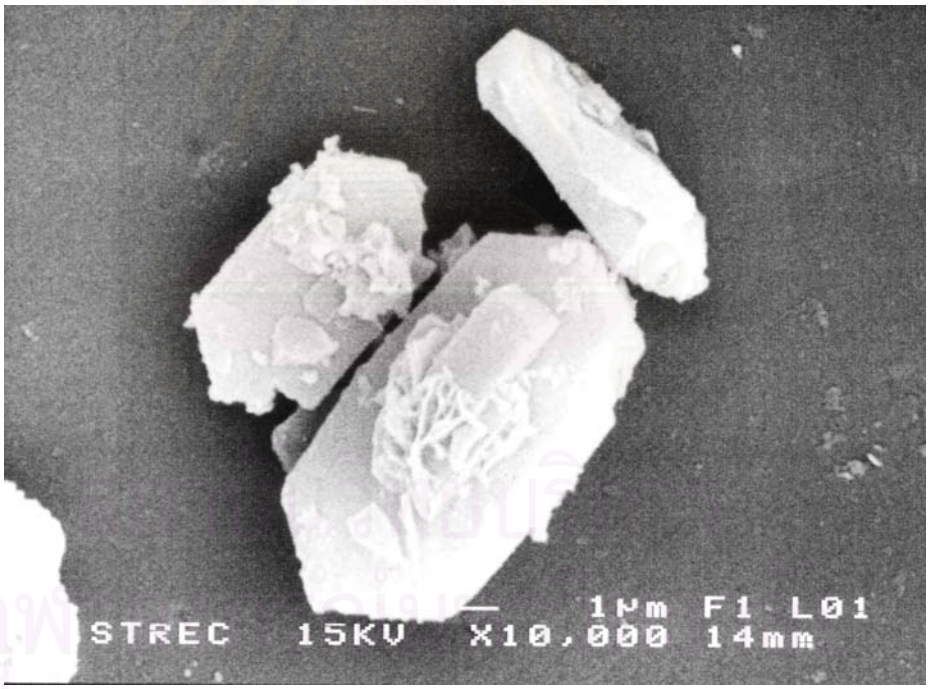

(b)

Figure 5.14 Scanning electron micrograph of catalyst (a) Co/HZSM-5×1,000, (b) Co/HZSM-5×10,000

5.1.1.4 Dealumination

Measuring ^{27}Al MAS NMR spectrum also provides information about the environment of the aluminum atoms in the zeolite samples. When aluminum atoms are tetrahedrally connected to the framework $Al(OSi)_4$, tetrahedral aluminum, a peak at a chemical shift of ~ 60 ppm is visible in the spectrum. Extra lattice framework aluminum species are usually octahedrally coordinated, octahedral aluminum, has a chemical shift of ~ 0 ppm. Quantitative analysis of tetrahedral aluminum in zeolites was conducted by ^{27}Al MAS NMR. The ^{27}Al MAS NMR spectrum comparison of before and after hydrothermal pretreatment catalysts is shown in Figure 5.15 to 5.26. It was found that the ^{27}Al MAS NMR spectrum of Co/HZSM-5, Cu/Co/HZSM-5, La/Co/HZSM-5, Fe/Co/HZSM-5, Ce/Co/HZSM-5 and Mn/Co/HZSM-5 catalysts clearly exhibits the difference between the fresh and the pretreated catalysts. On the other hand, The ^{27}Al MAS NMR spectrum of fresh and pretreated of Pd/Co/HZSM-5 catalysts does not have any difference, as well as Cd/Co/HZSM-5 catalyst. While, there some differences in the fresh and pretreated ^{27}Al MAS NMR spectra of Ba/Co/HZSM-5, Ni/Co/HZSM-5, Zn/Co/HZSM-5 and Ag/Co/HZSM-5.

Figure 5.15 shows the ^{27}Al MAS NMR spectra of fresh and pretreated Co/HZSM-5 catalysts. The spectra of Co/HZSM-5 catalyst show a loss of tetrahedral aluminum but increase in octahedral aluminum after hydrothermal treatment, due to the framework dealumination [82]. For hydrothermal pretreatment Pd/Co/HZSM-5 and Cd/Co/HZSM-5 catalysts, only one signal at around 60 ppm was observed and no peak relating to octahedral aluminum was noticed. However, the octahedral aluminum signal was shown in a small signal on the other second metals Co/HZSM-5 such as Fe/Co/HZSM-5. The relative area of tetrahedral aluminum is calculated from the area of tetrahedral aluminum per summation area of tetrahedral and octahedral aluminum and shown in Table 5.1. This suggests that the stabilization of the tetrahedral Al, after hydrothermal treatment, by the most effective additive Pd^{2+} and Cd^{2+}on Co/HZSM-5 and the other second cations, Ba^{2+}, Ag^{+}, La^{3+}, Zn^{2+}, Ni^{2+}, Fe^{2+}, Ce^{3+} and Mn^{2+} could stabilize the zeolite framework structure by preventing the occurrence of dealumination.

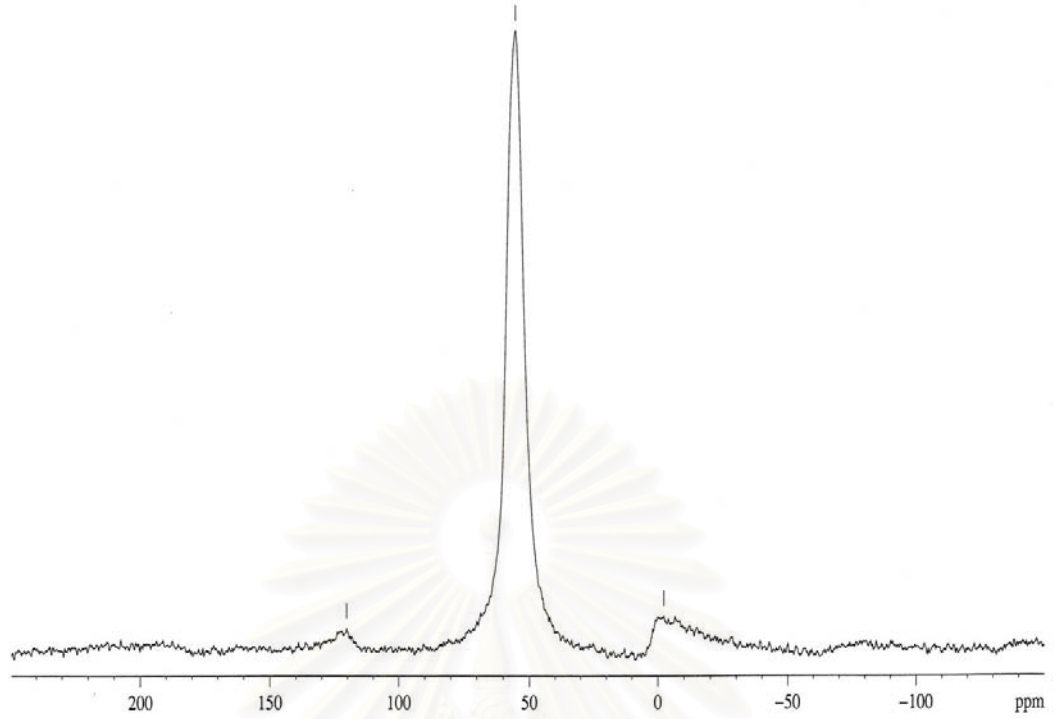

(a)

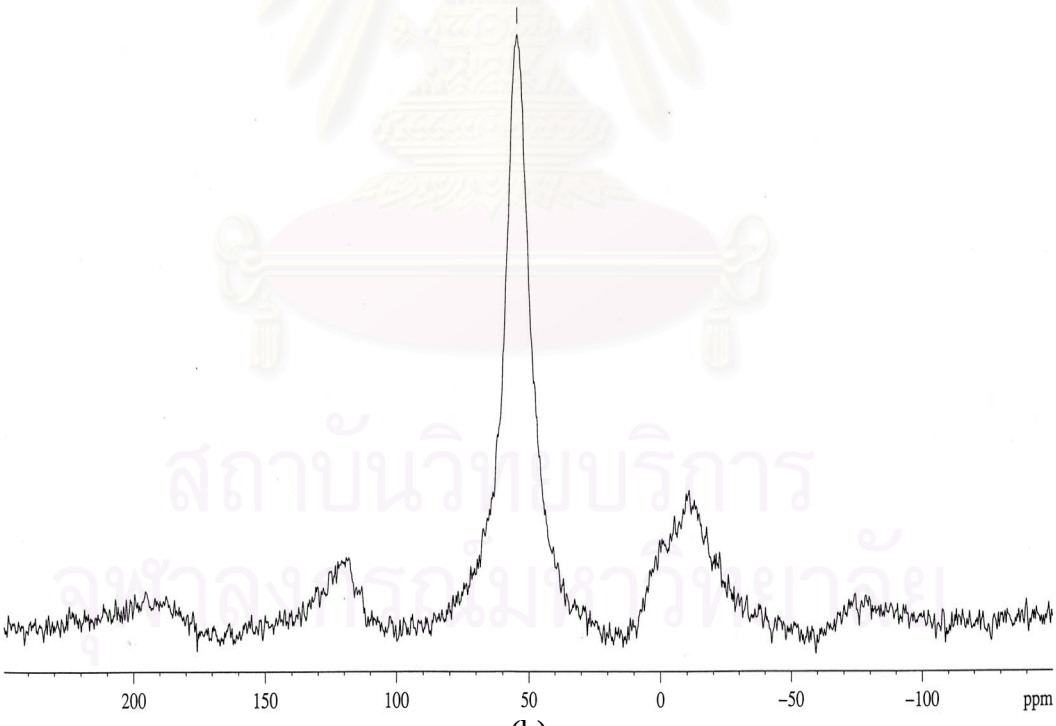

(b)

Figure 5.15 ^{27}Al MAS-NMR spectra of Co/HZSM-5 (a) fresh catalyst, (b) pretreated catalyst.

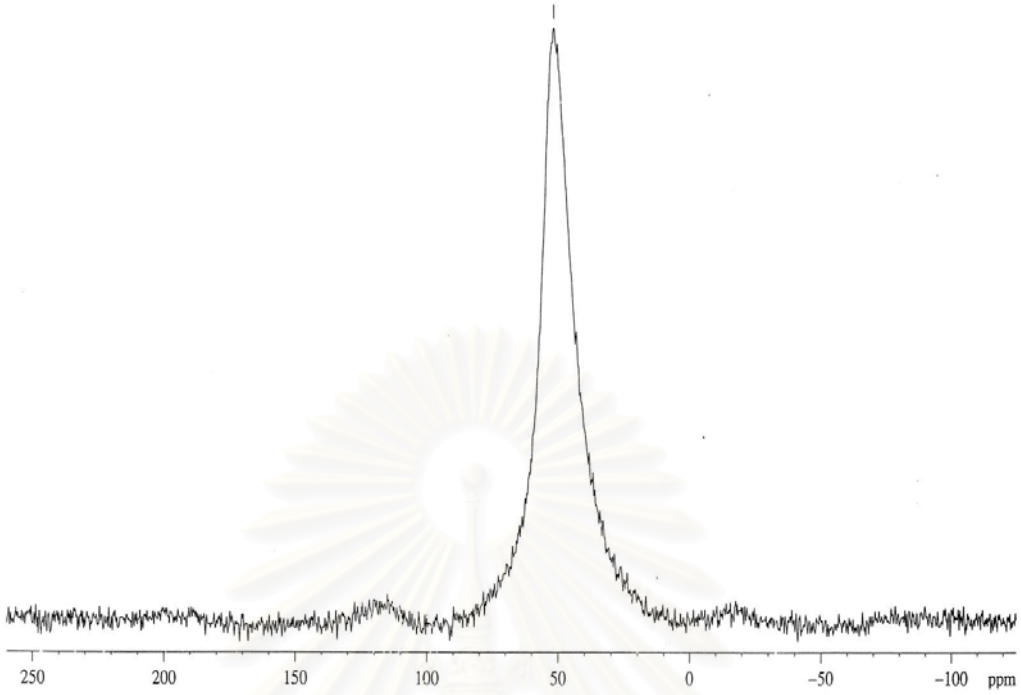

(a)

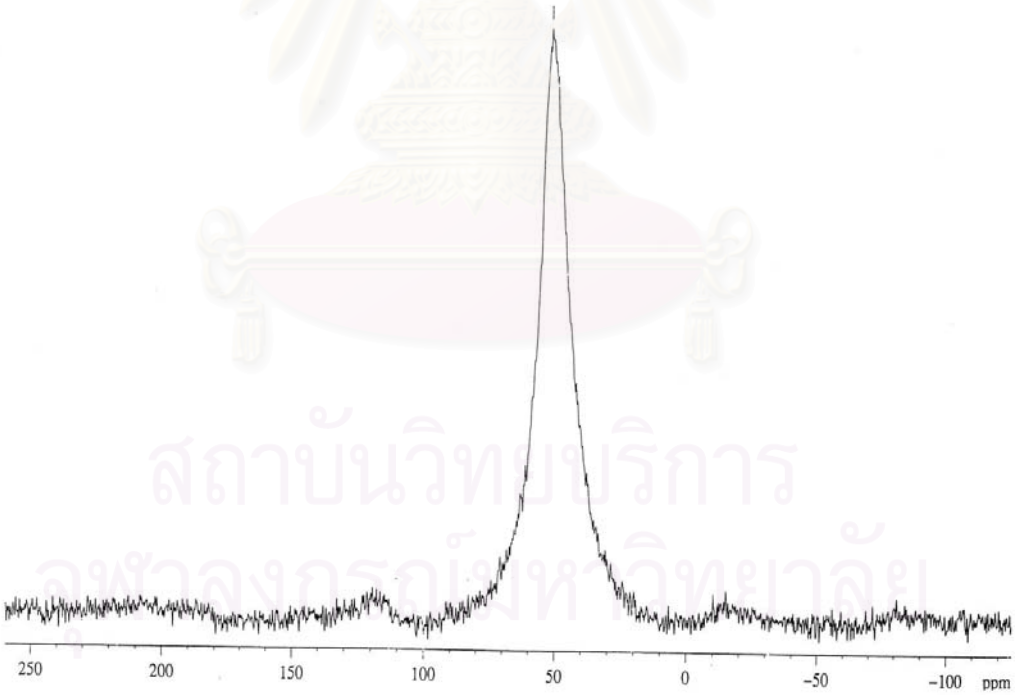

(b)

Figure 5.16 ^{27}Al MAS-NMR spectra of Pd/Co/HZSM-5 (a) fresh catalyst, (b) pretreated catalyst.

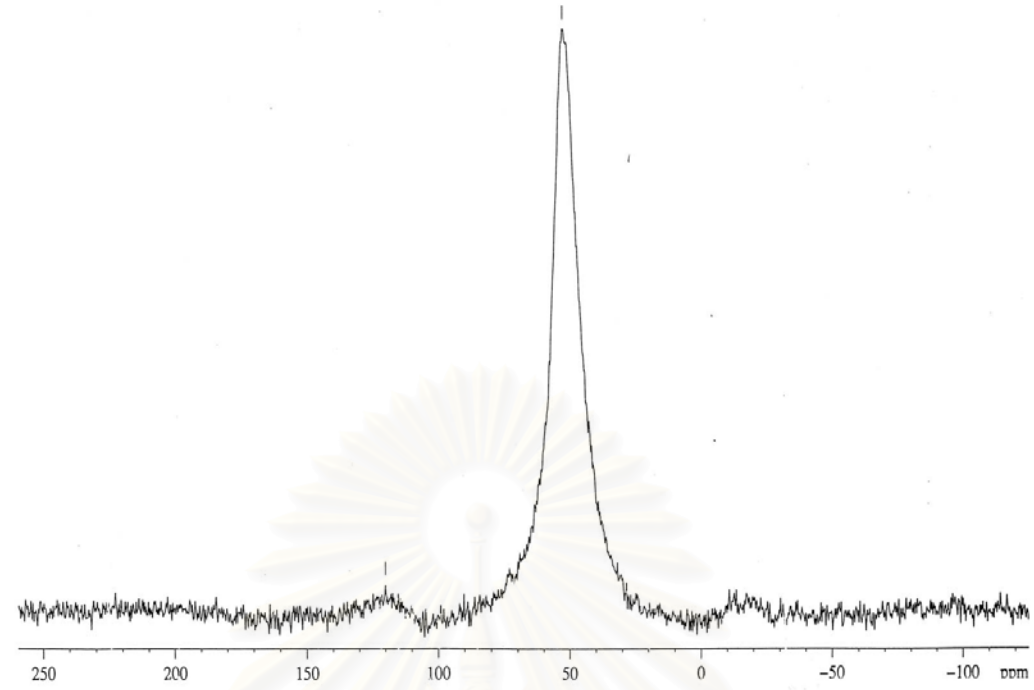

(a)

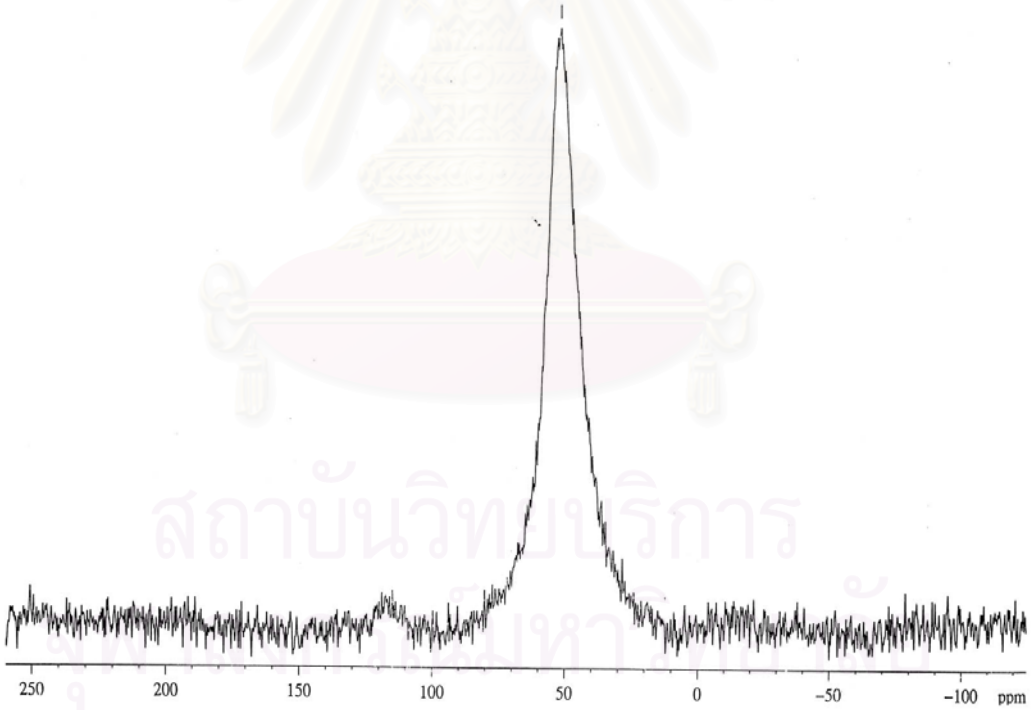

(b)

Figure 5.17 ^{27}Al MAS-NMR spectra of Cd/Co/HZSM-5 (a) fresh catalyst, (b) pretreated catalyst.

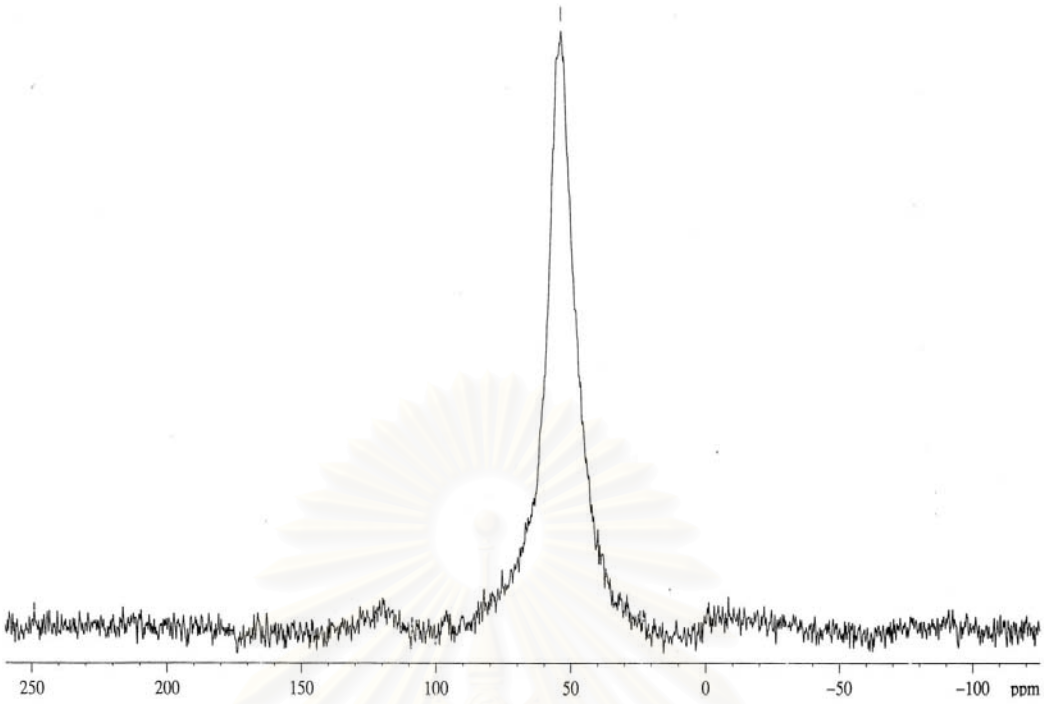

(a)

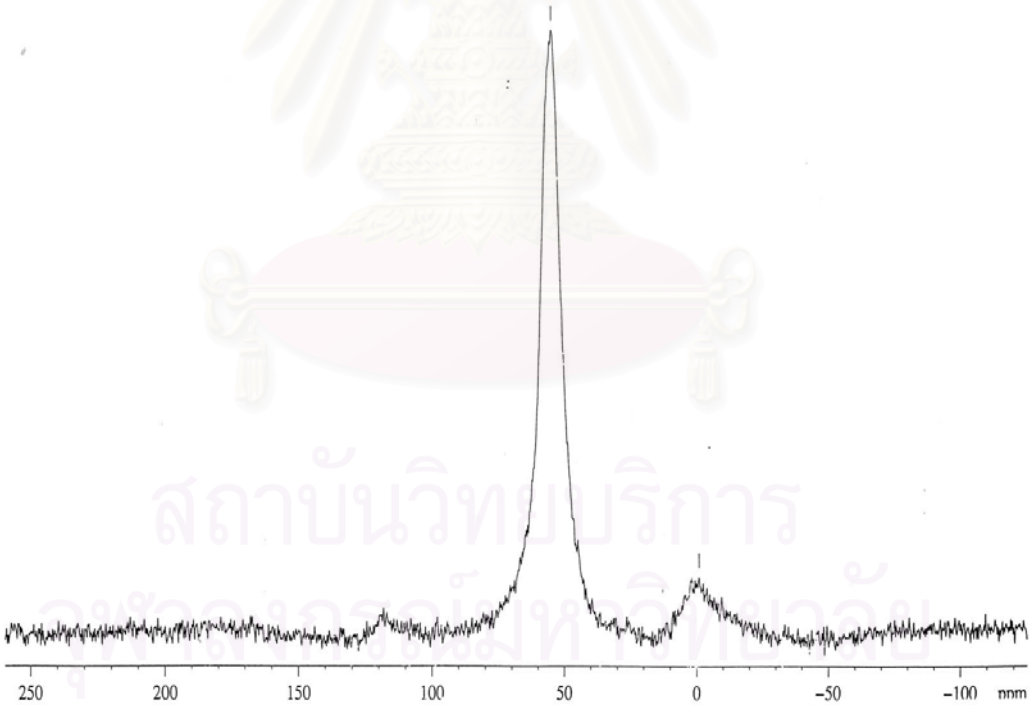

(b)

Figure 5.18 ^{27}Al MAS-NMR spectra of Ba/Co/HZSM-5 (a) fresh catalyst, (b) pretreated catalyst.

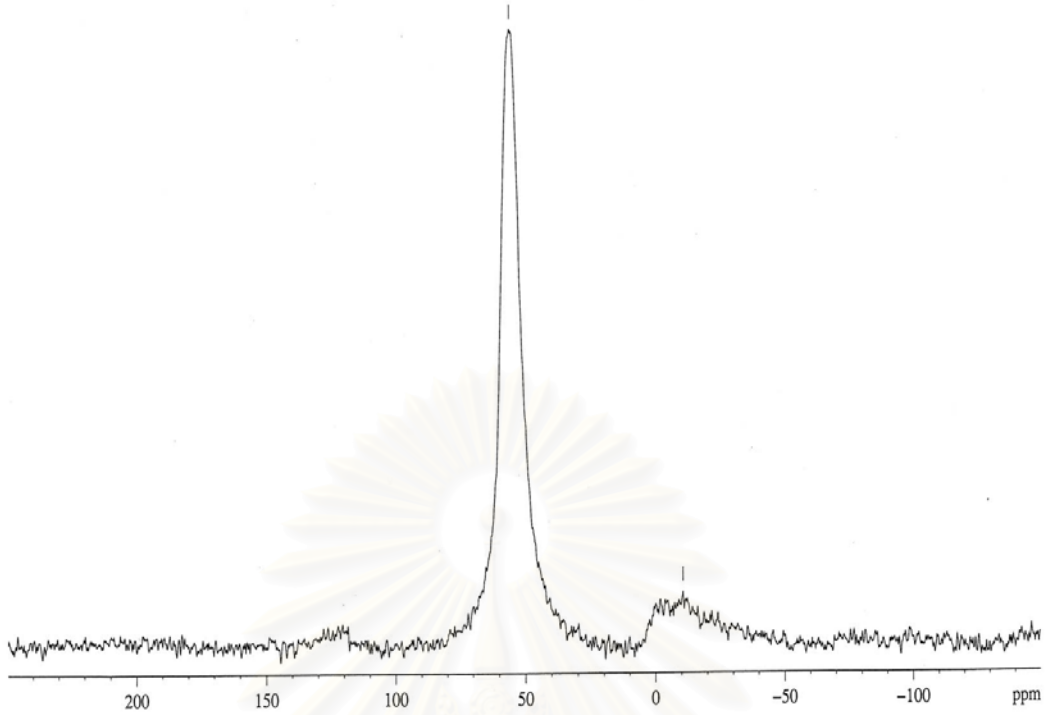

(a)

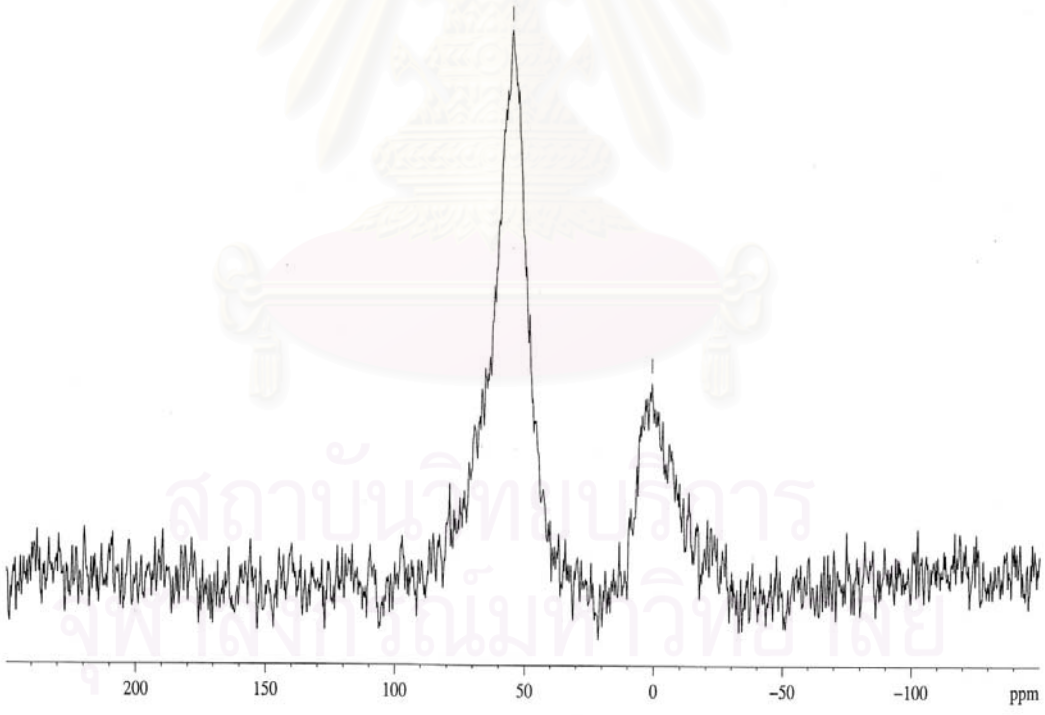

(b)

Figure 5.19 ^{27}Al MAS-NMR spectra of Cu/Co/HZSM-5 (a) fresh catalyst, (b) pretreated catalyst.

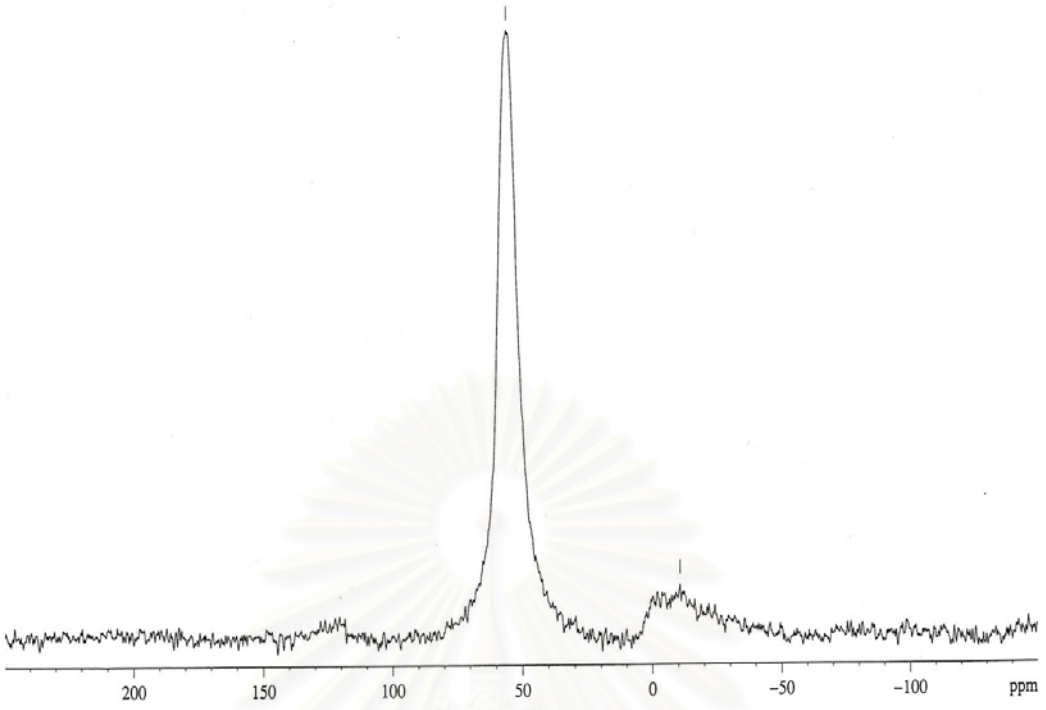

(a)

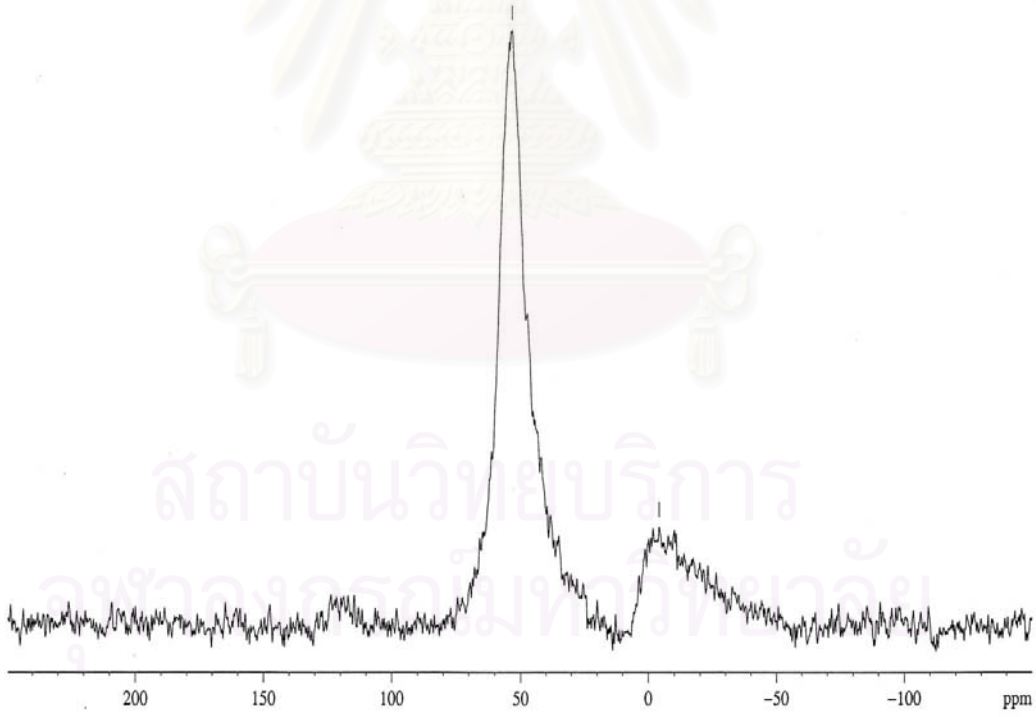

(b)

Figure 5.20 ^{27}Al MAS-NMR spectra of La/Co/HZSM-5 (a) fresh catalyst, (b) pretreated catalyst.

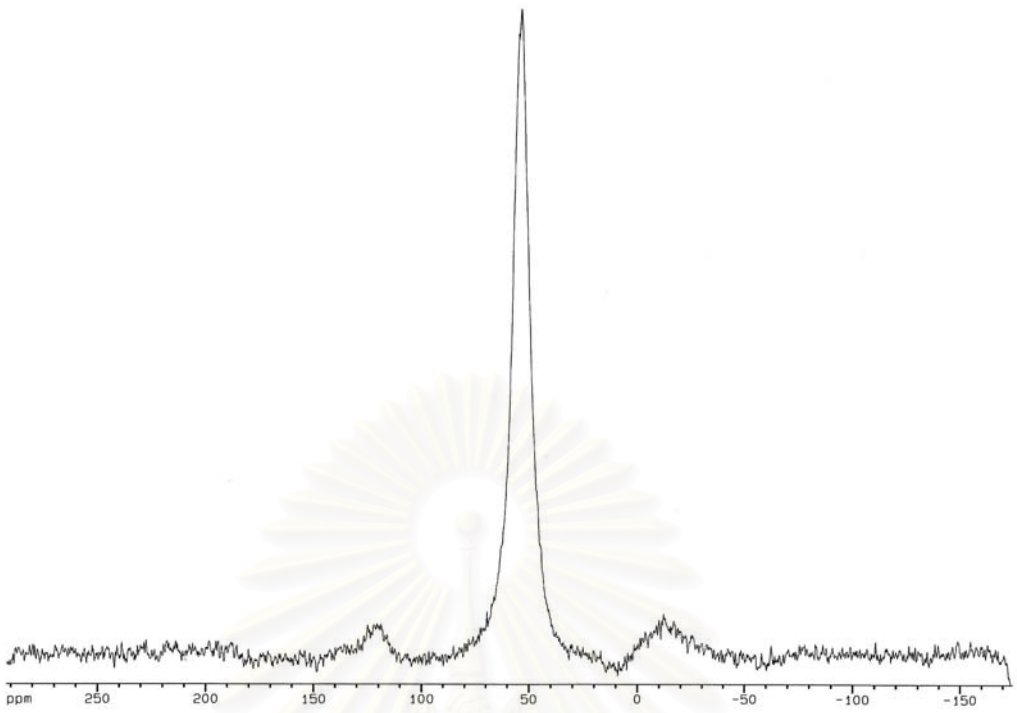

(a)

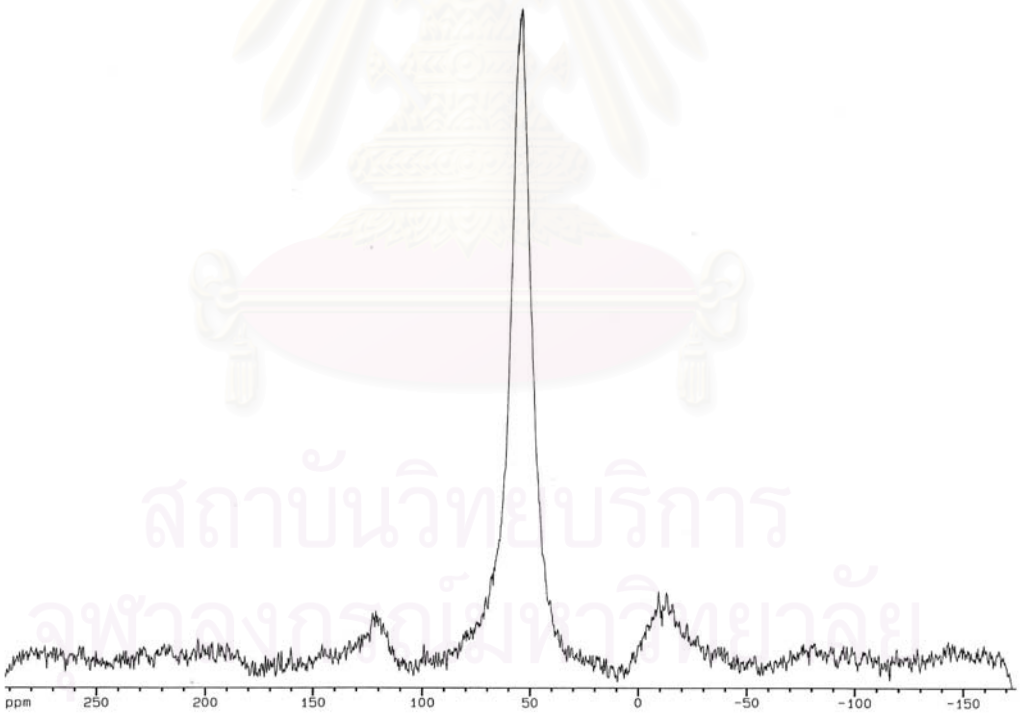

(b)

Figure 5.21 ^{27}Al MAS-NMR spectra of Ni/Co/HZSM-5 (a) fresh catalyst, (b) pretreated catalyst.

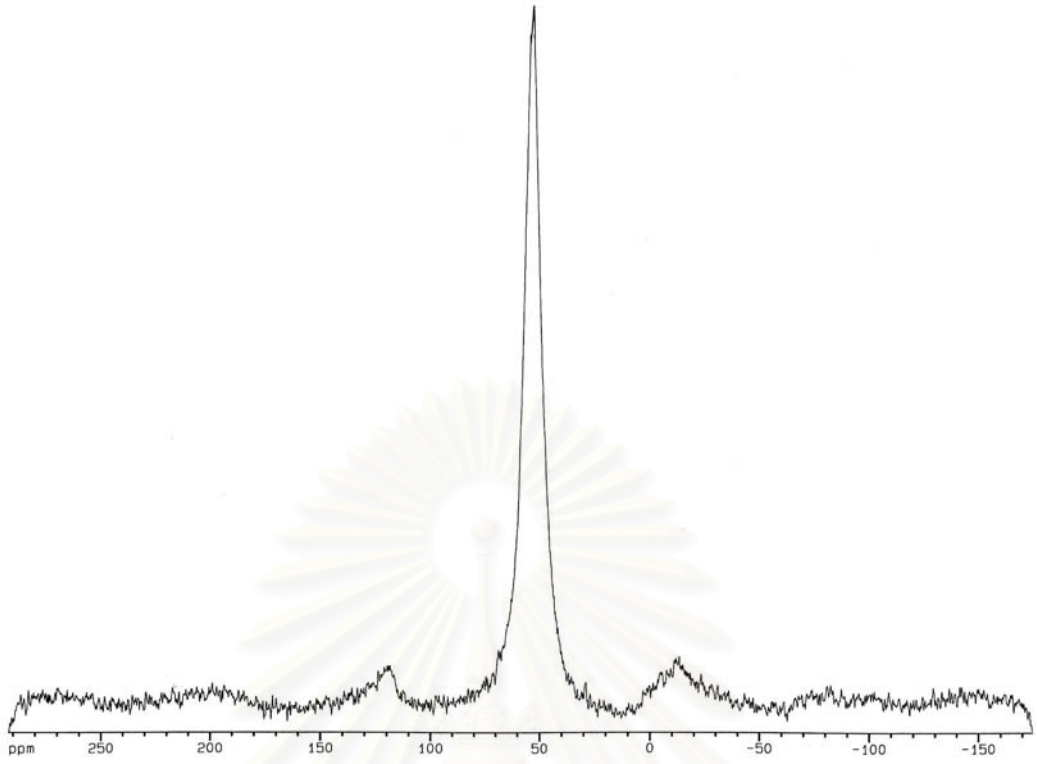

(a)

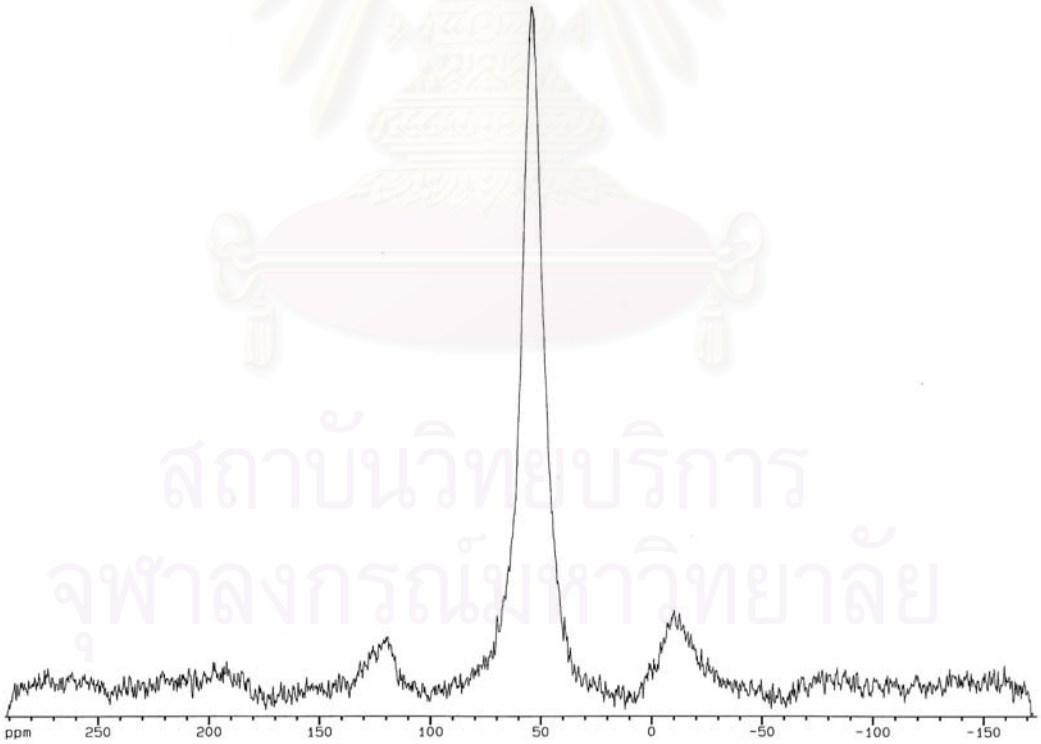

(b)

Figure 5.22 ^{27}Al MAS-NMR spectra of Zn/Co/HZSM-5 (a) fresh catalyst, (b) pretreated catalyst.

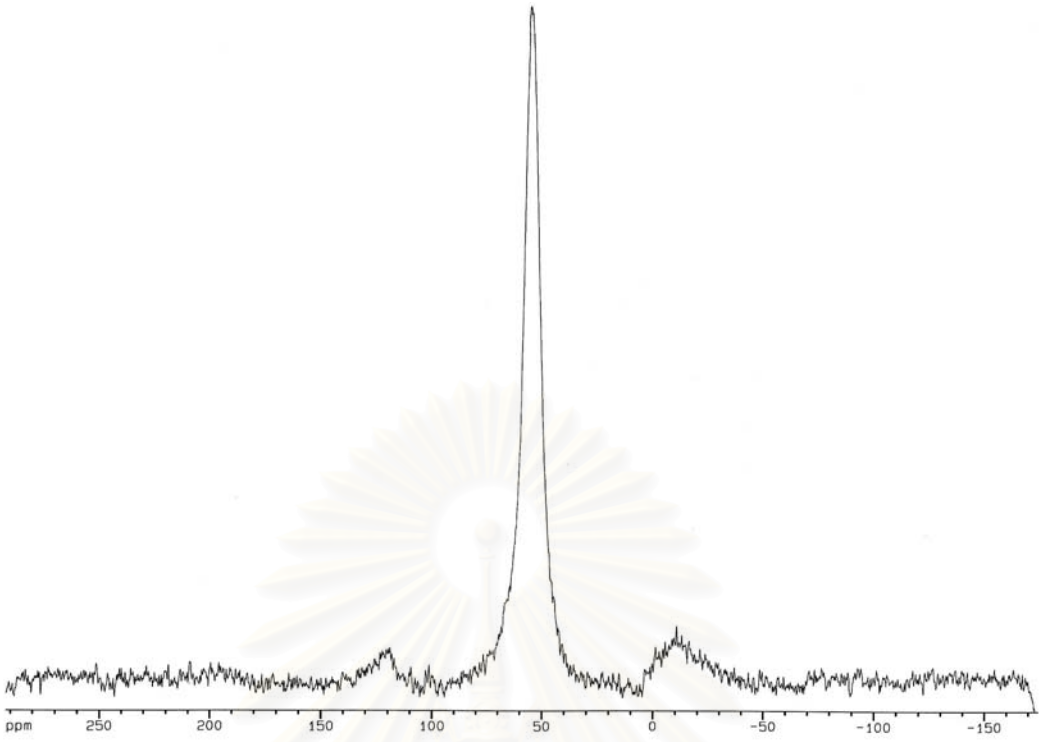

(a)

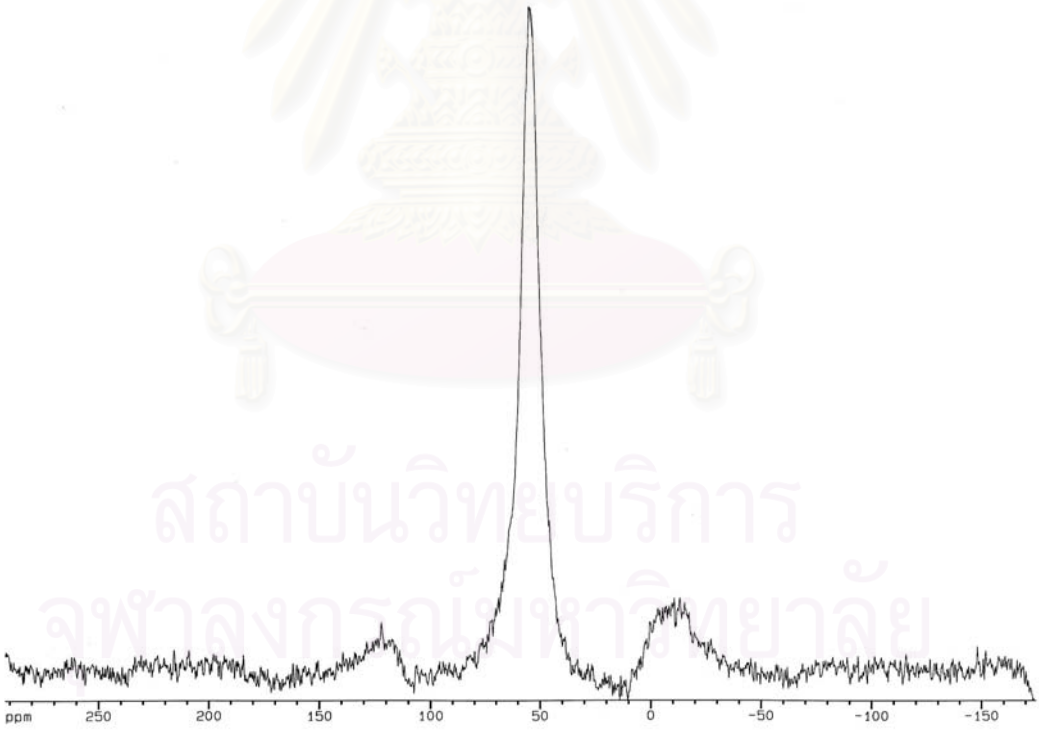

(b)

Figure 5.23 ^{27}Al MAS-NMR spectra of Ag/Co/HZSM-5 (a) fresh catalyst, (b) pretreated catalyst.

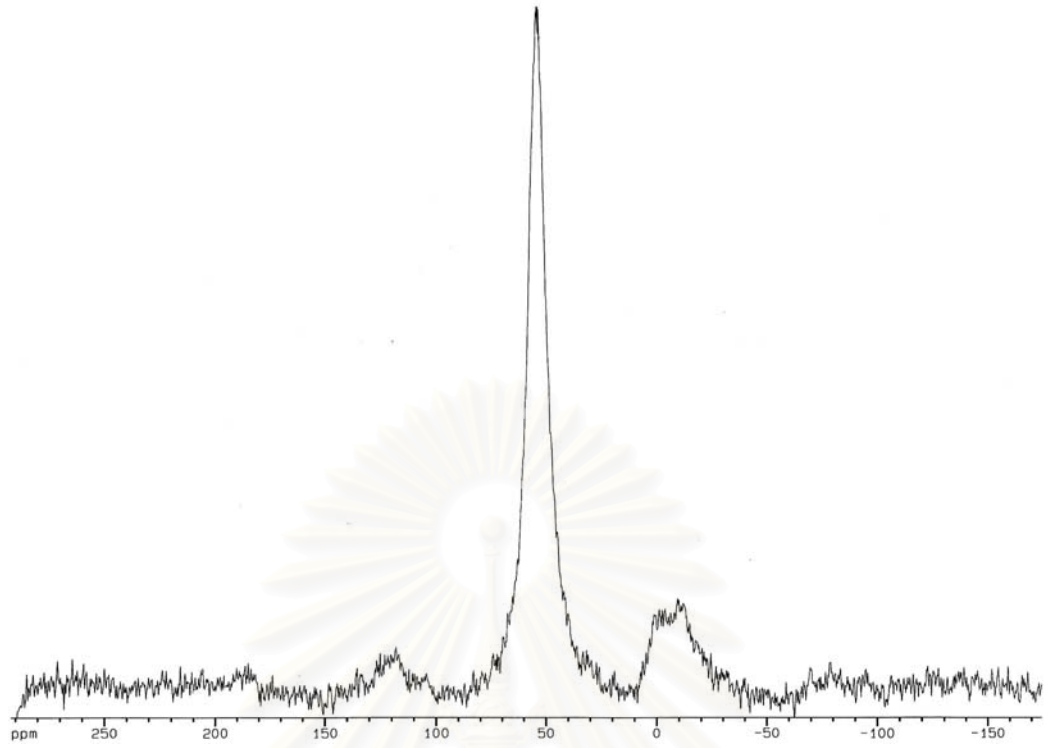

(a)

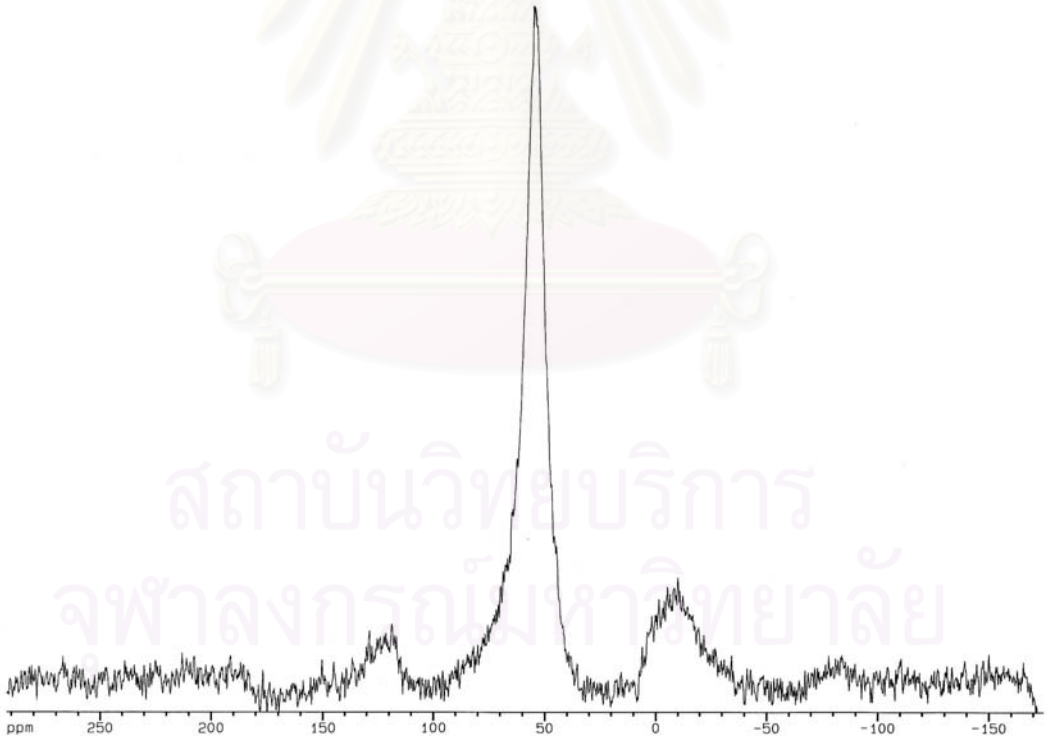

(b)

Figure 5.24 ^{27}Al MAS-NMR spectra of Fe/Co/HZSM-5 (a) fresh catalyst, (b) pretreated catalyst.

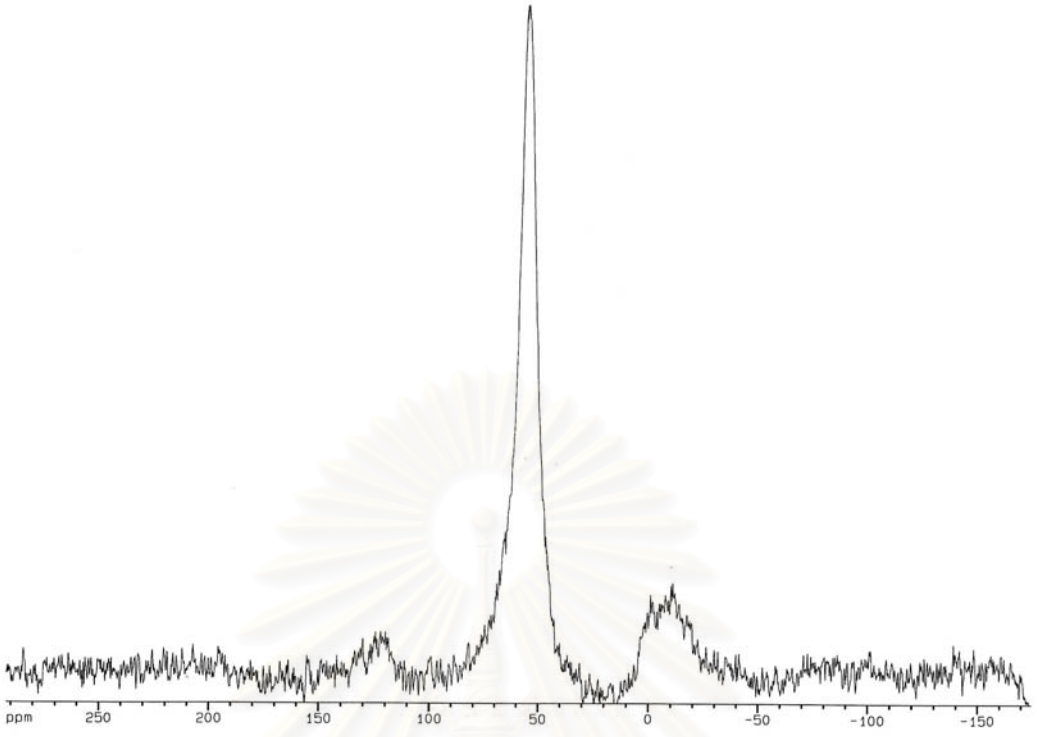

(a)

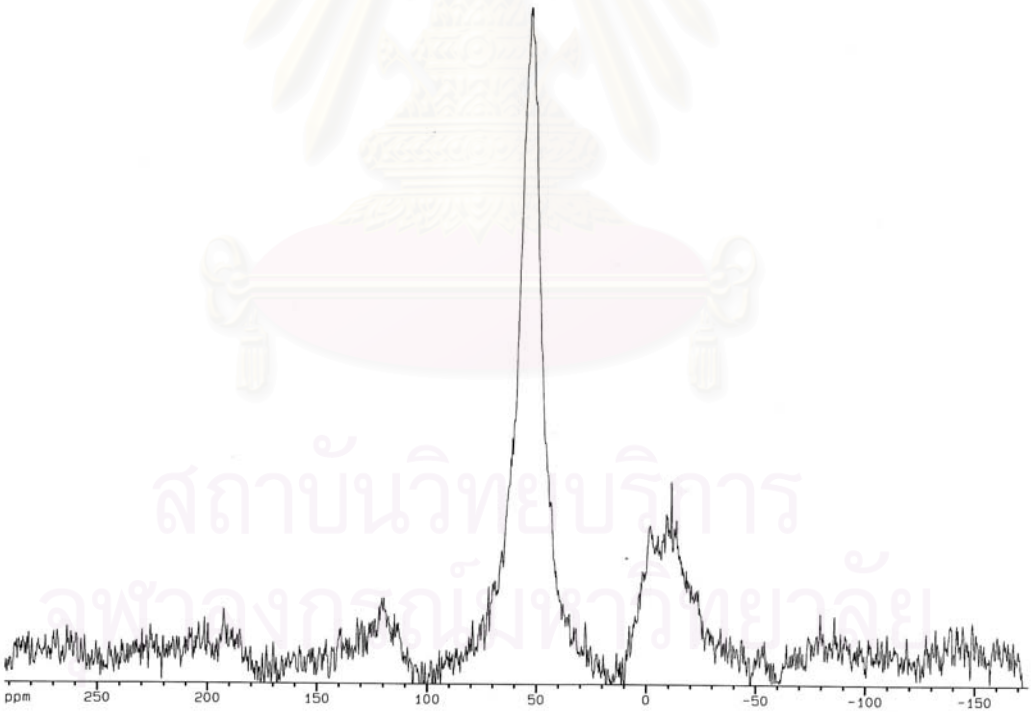

(b)

Figure 5.25 ^{27}Al MAS-NMR spectra of Ce/Co/HZSM-5 (a) fresh catalyst, (b) pretreated catalyst.

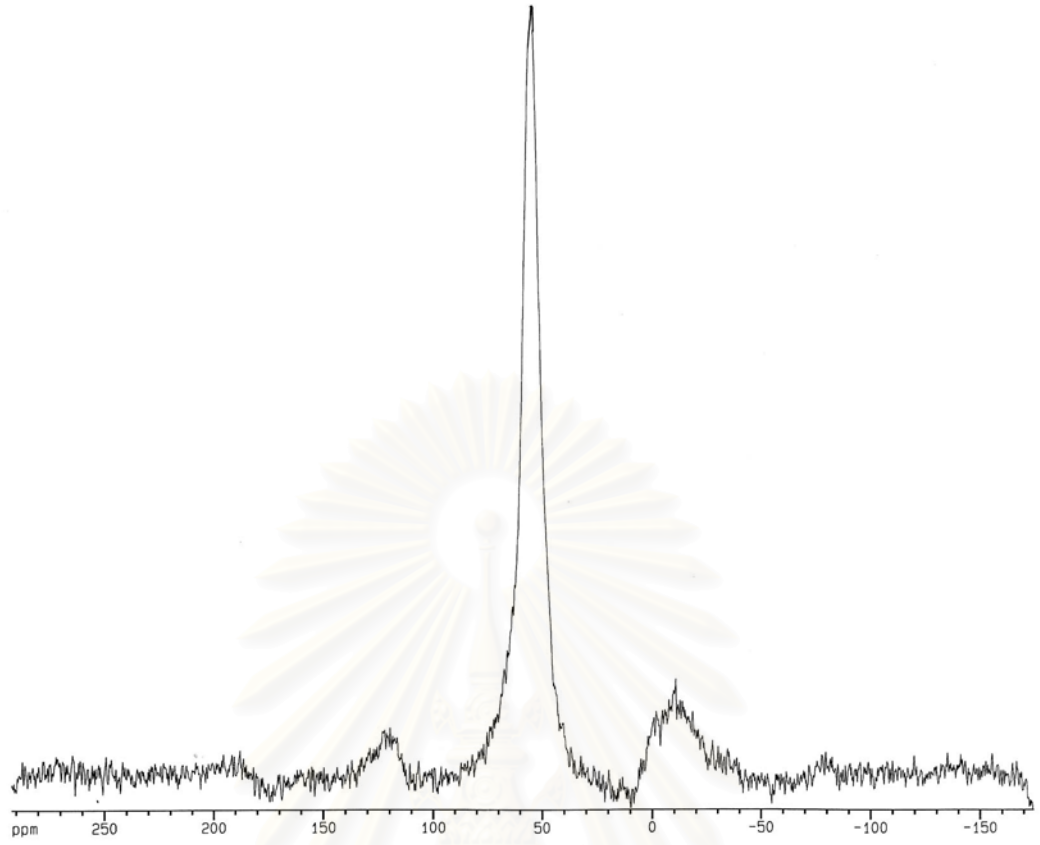

(a)

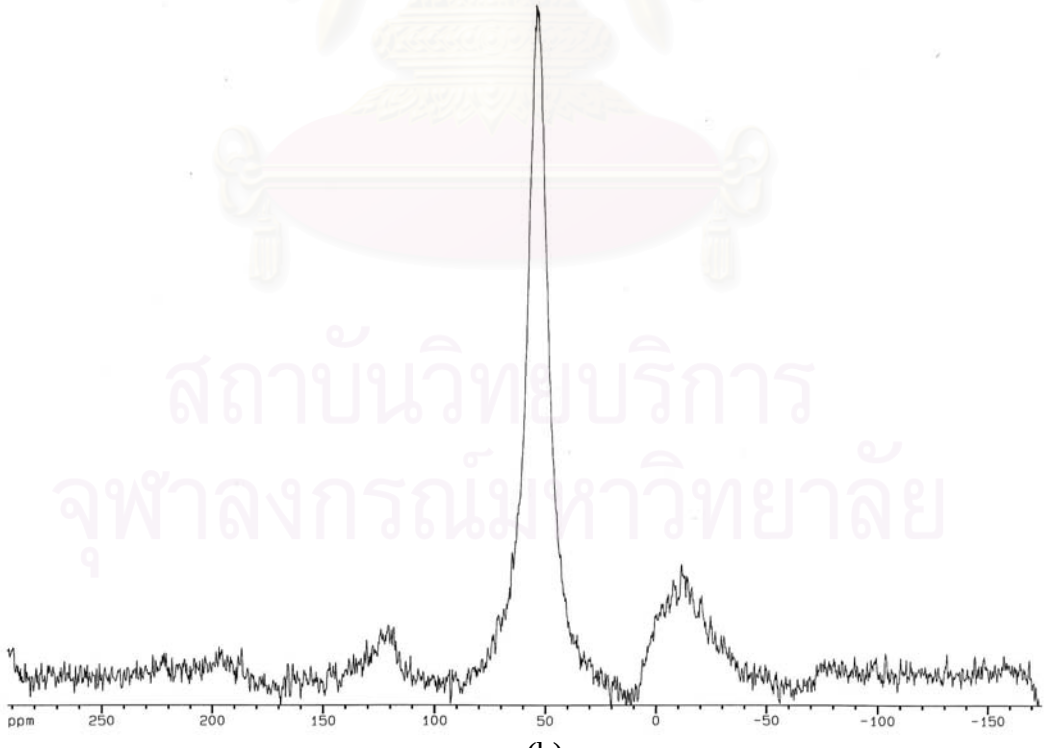

(b)

Figure 5.26 ^{27}Al MAS-NMR spectra of Mn/Co/HZSM-5 (a) fresh catalyst, (b) pretreated catalyst.

5.1.1.5 Electron Spin Resonance

Cobalt-containing microporous had been investigated by using electron spin resonance (ESR) spectroscopy at liquid nitrogen boiling point temperature (-196 ^{o}C) in order to investigate the coordination of high-spin cobalt before and after hydrothermal pretreatment. The ESR spectra at g = 5.4-5.8 is assigned to the high-spin Co(II) [114]. The ESR spectrum of fresh and pretreated Co/HZSM-5 are shown in Figure 5.27. The g value of fresh Co/HZSM-5 is 5.4391. After hydrothermal treatment, the ESR spectra are similar in shape and the g value is 5.4397. Similar ESR spectra were obtained from the sample with different second metal components (.Pd, Cd, Ba, Cu, La, Ni, Zn, Ag, Fe, Ce, and Mn), as shown in Figures 5.28-5.38. The comparison of before and after hydrothermal treatment catalysts shows that all samples have g values in the range of 5.43-5.45, which is assigned to the high-spin Co(II). It means that there is no any change in state of cobalt ion, which was observed in the zeolite.

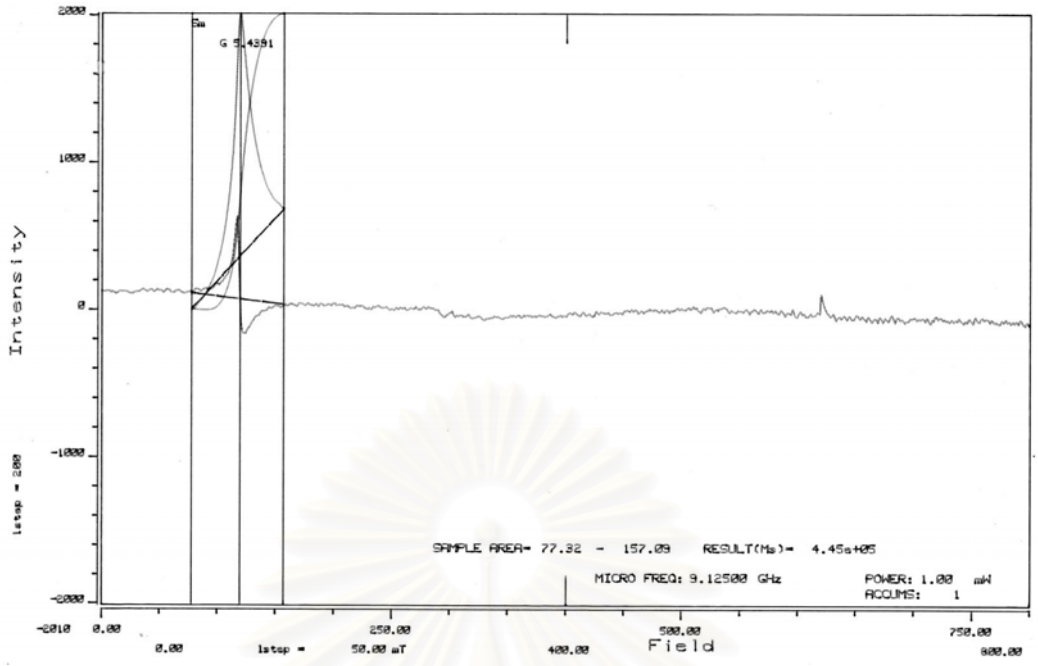

(a)

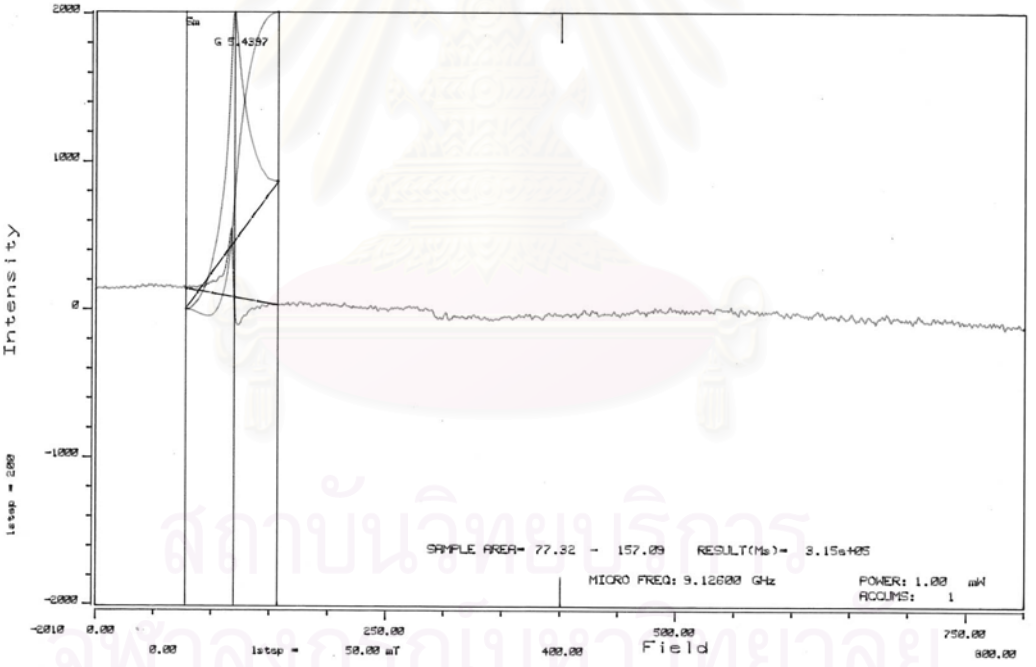

(b)

Figure 5.27 ESR spectra of high spin Co^{2+} of Co/HZSM-5 (a) fresh catalyst, (b) pretreated catalyst

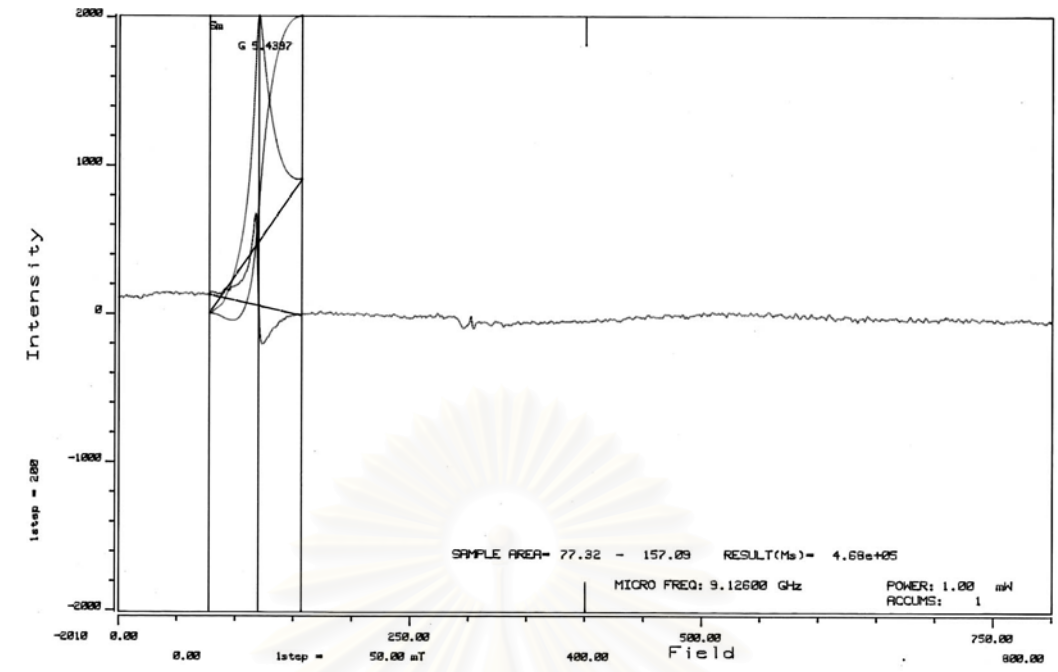

(a)

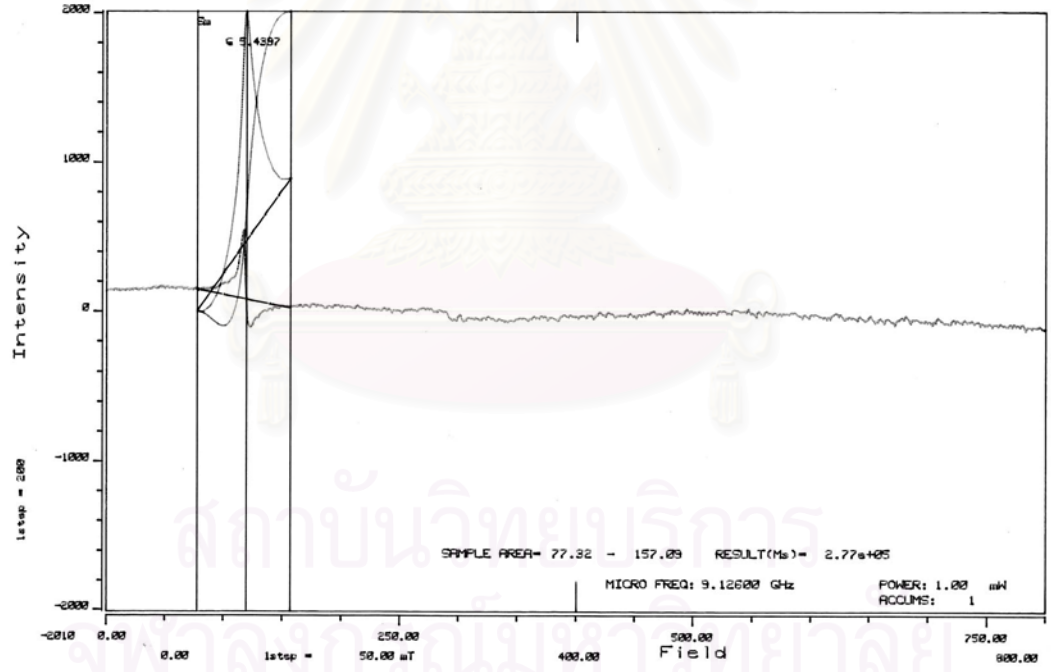

(b)

Figure 5.28 ESR spectra of high spin Co^{2+} of Pd/Co/HZSM-5 (a) fresh catalyst, (b) pretreated catalyst

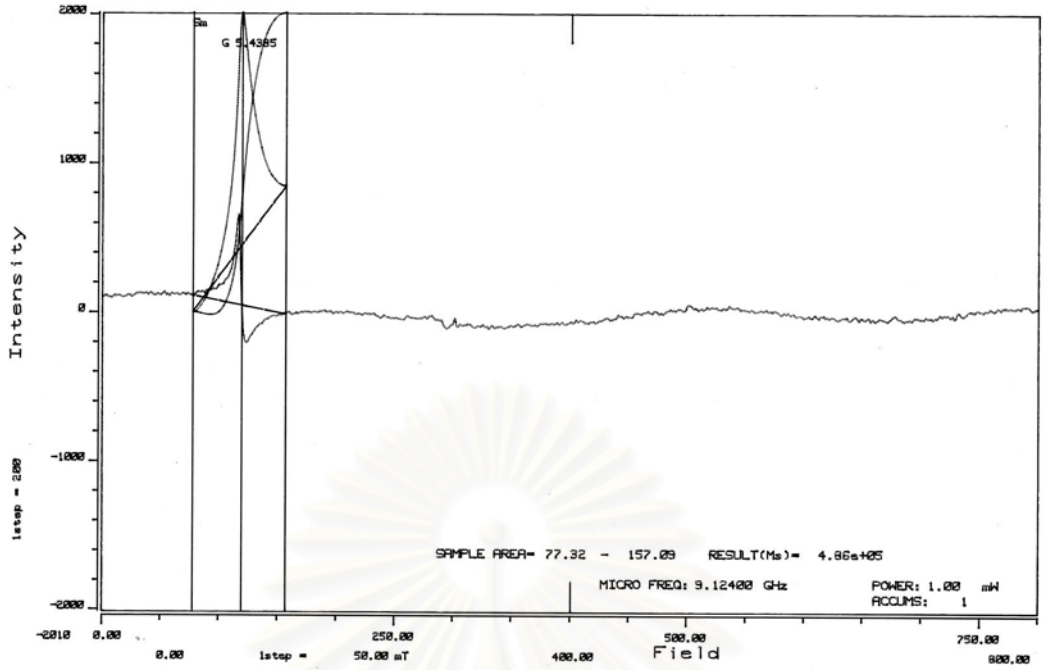

(a)

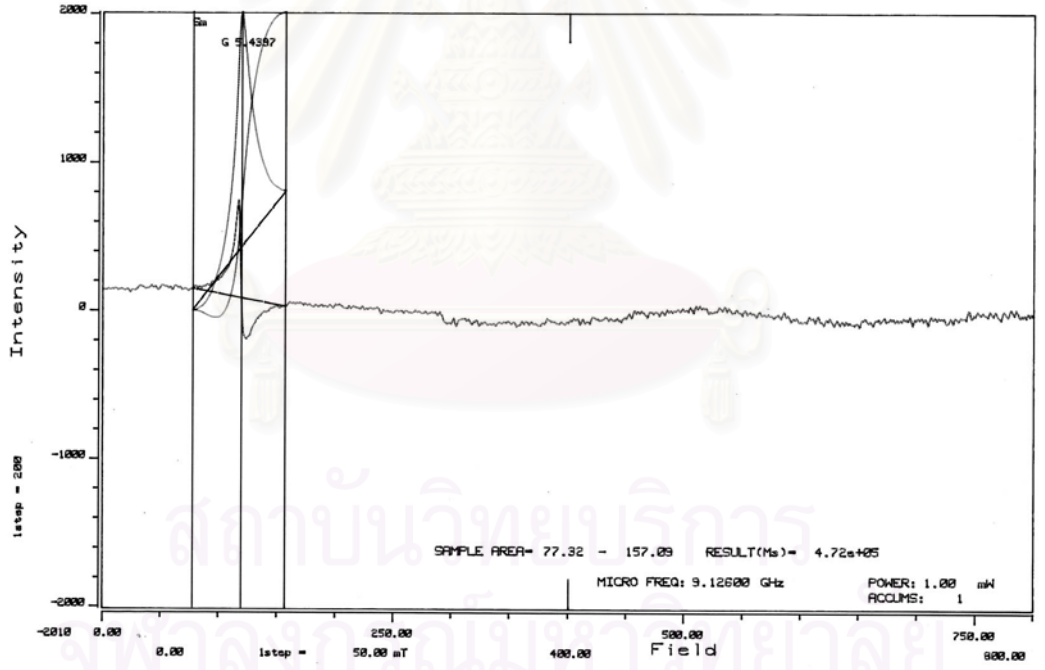

(b)

Figure 5.29 ESR spectra of high spin Co^{2+} of Cd/Co/HZSM-5 (a) fresh catalyst, (b) pretreated catalyst

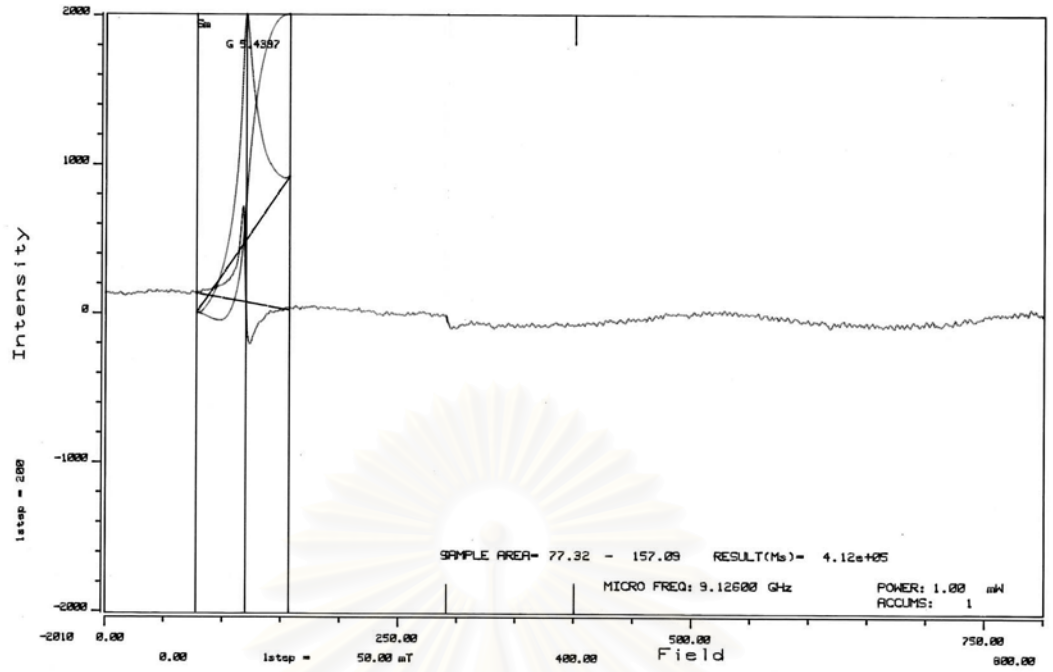

(a)

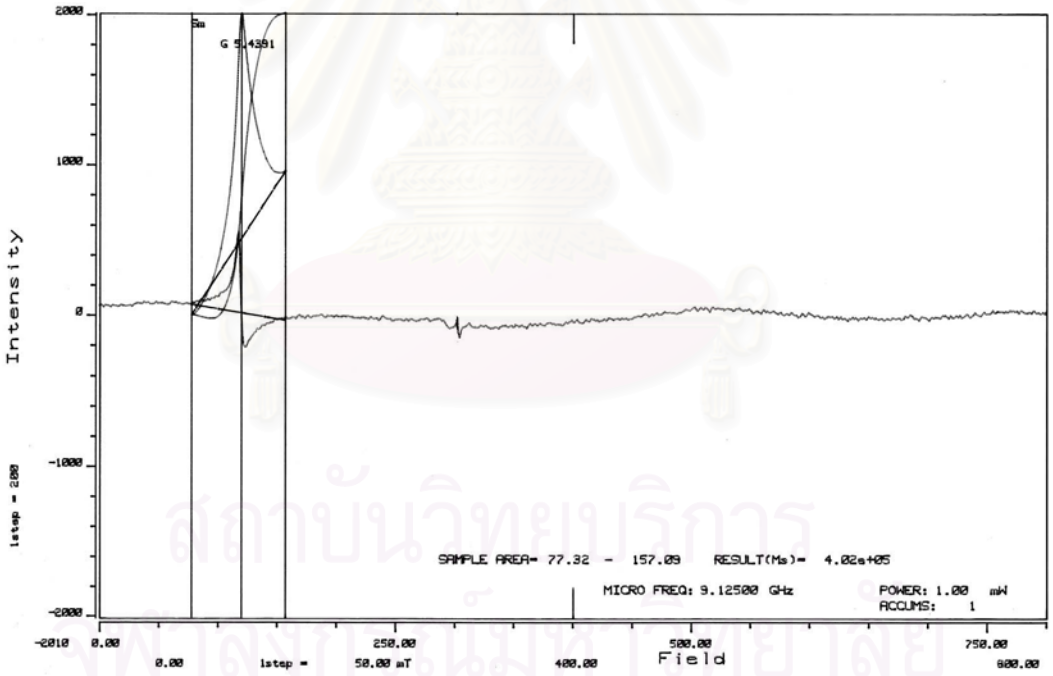

(b)

Figure 5.30 ESR spectra of high spin Co^{2+} of Ba/Co/HZSM-5 (a) fresh catalyst, (b) pretreated catalyst

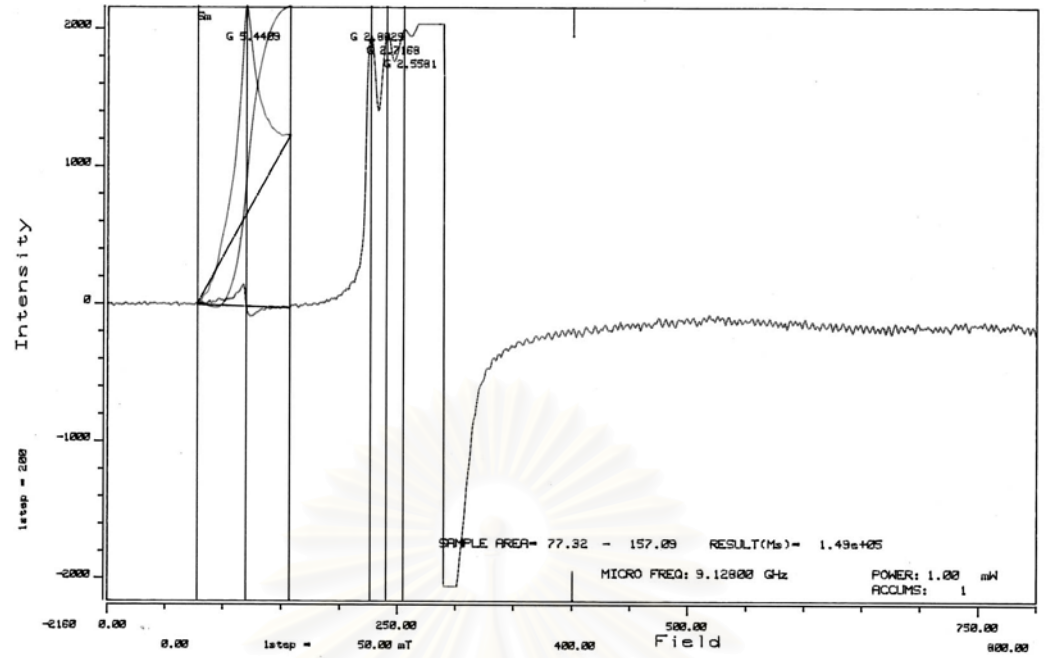

(a)

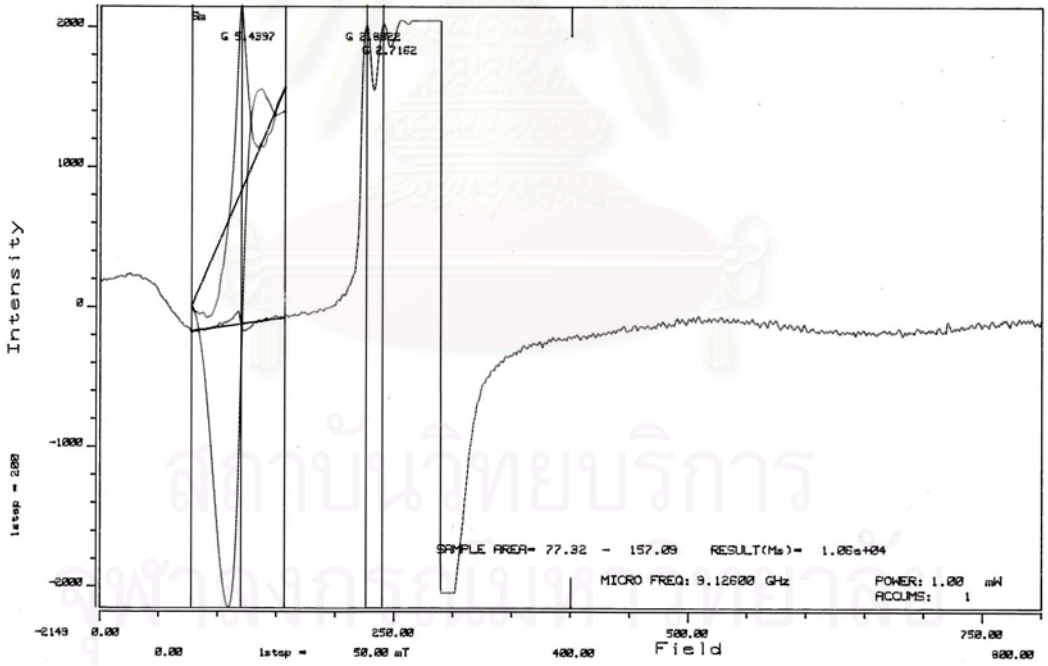

(b)

Figure 5.31 ESR spectra of high spin Co^{2+} of Cu/Co/HZSM-5 (a) fresh catalyst, (b) pretreated catalyst

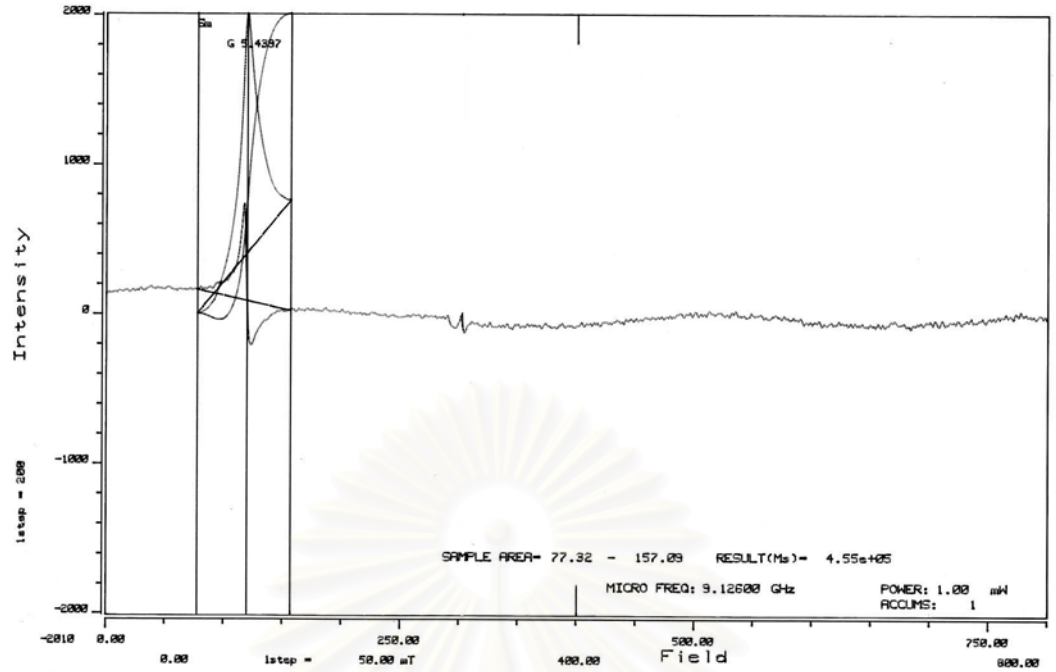

(a)

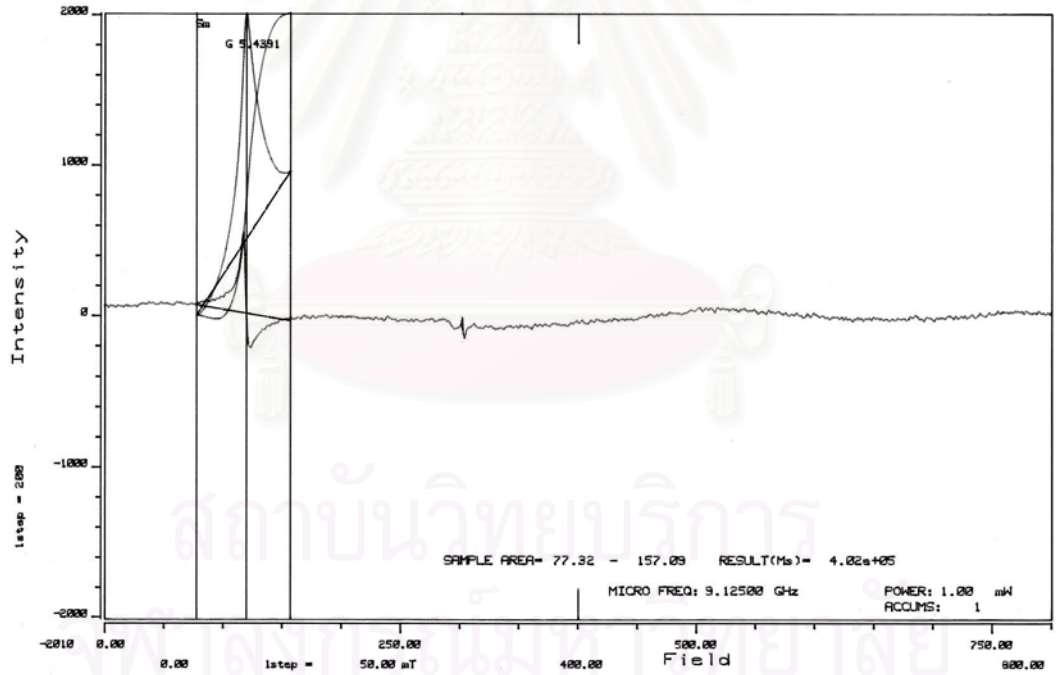

(b)

Figure 5.32 ESR spectra of high spin Co^{2+} of La/Co/HZSM-5 (a) fresh catalyst, (b) pretreated catalyst

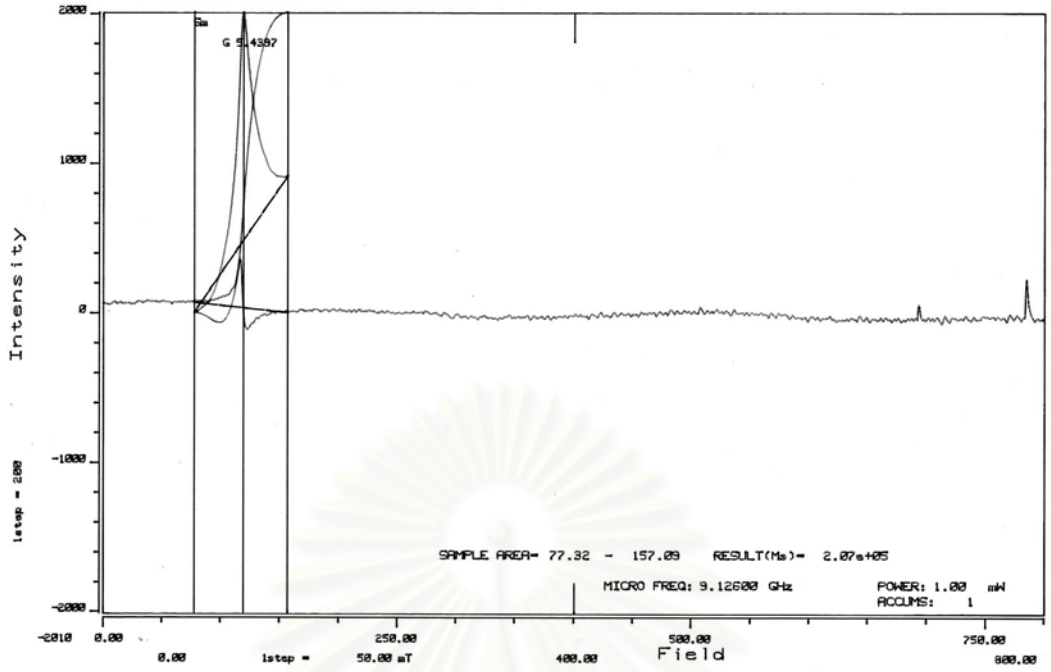

(a)

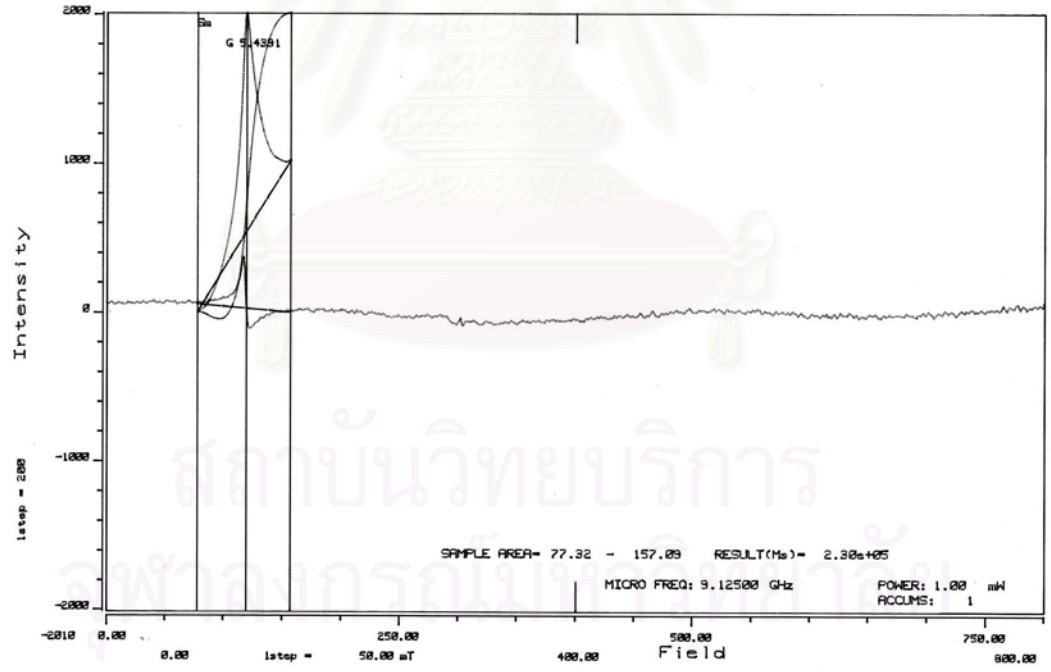

(b)

Figure 5.33 ESR spectra of high spin Co^{2+} of Ni/Co/HZSM-5 (a) fresh catalyst, (b) pretreated catalyst

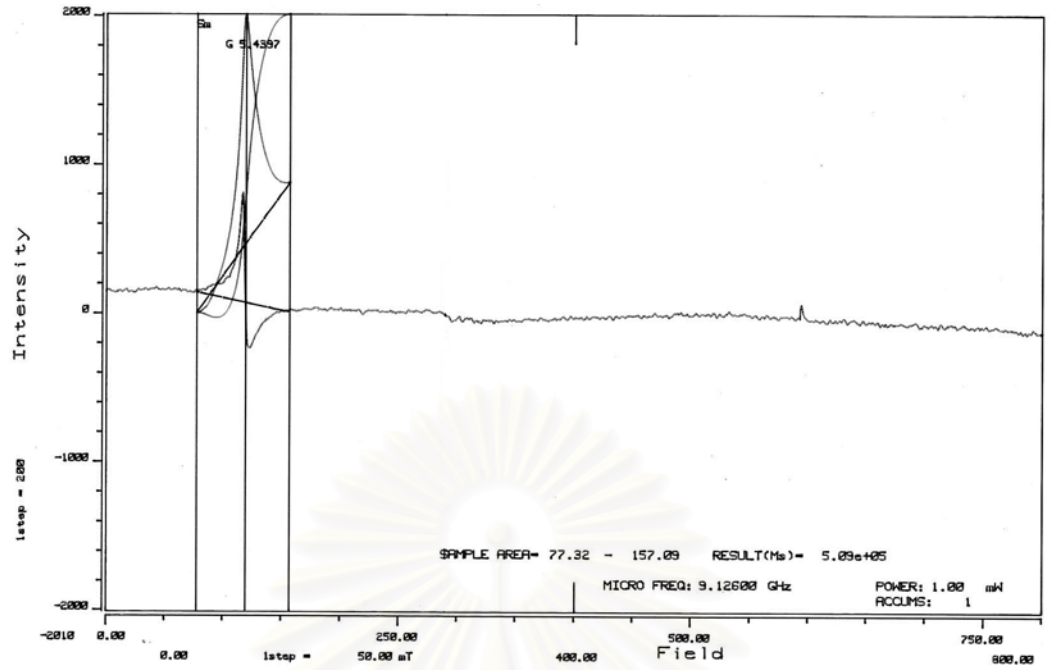

(a)

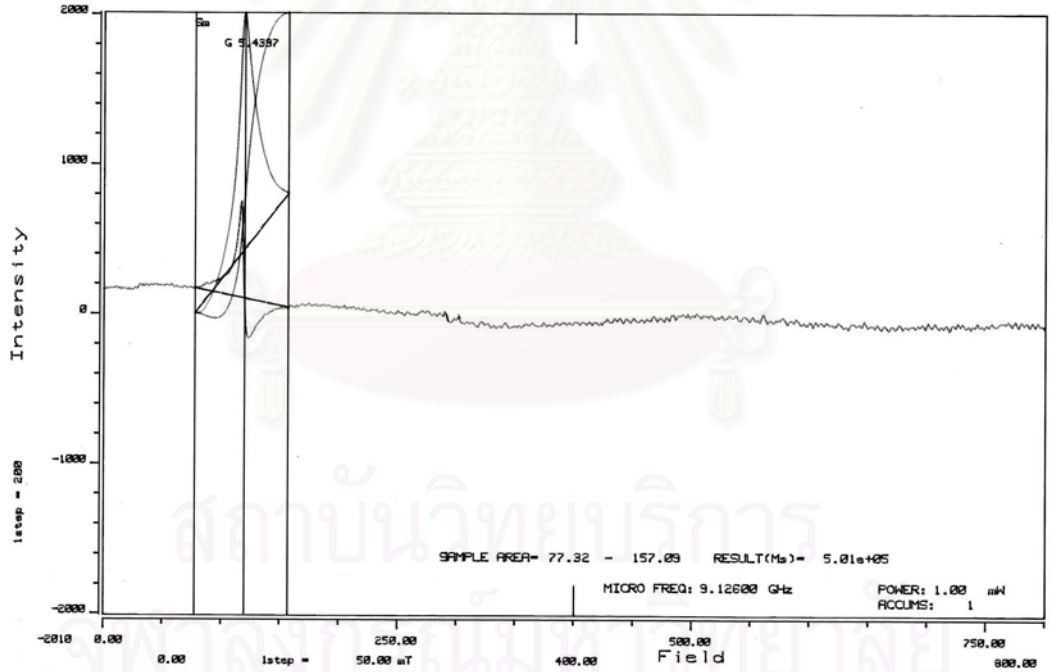

(b)

Figure 5.34 ESR spectra of high spin Co^{2+} of Zn/Co/HZSM-5 (a) fresh catalyst, (b) pretreated catalyst

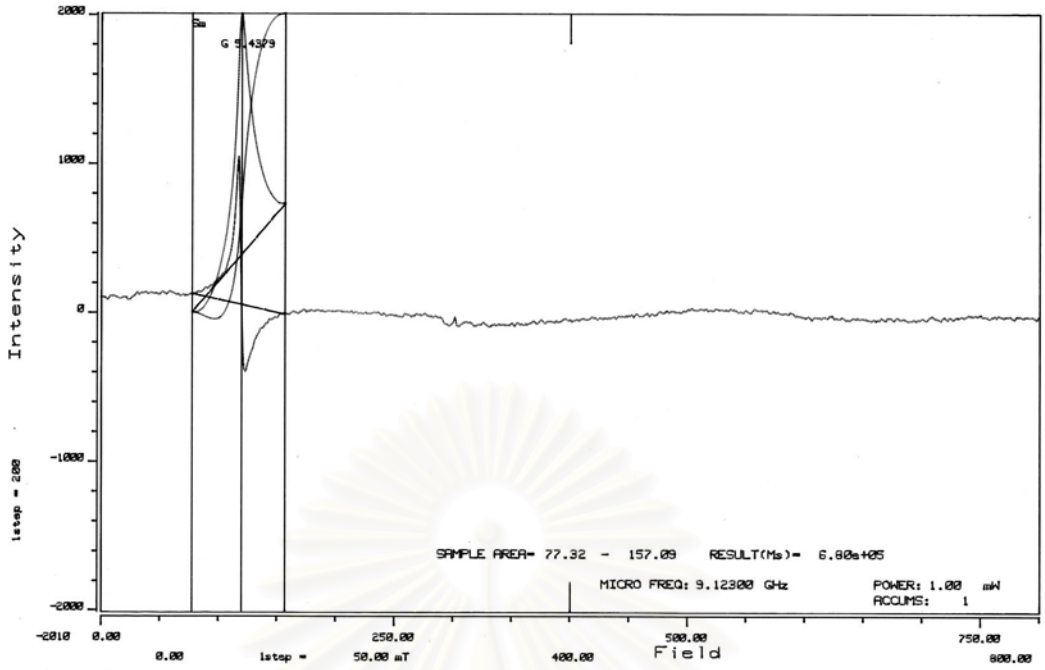

(a)

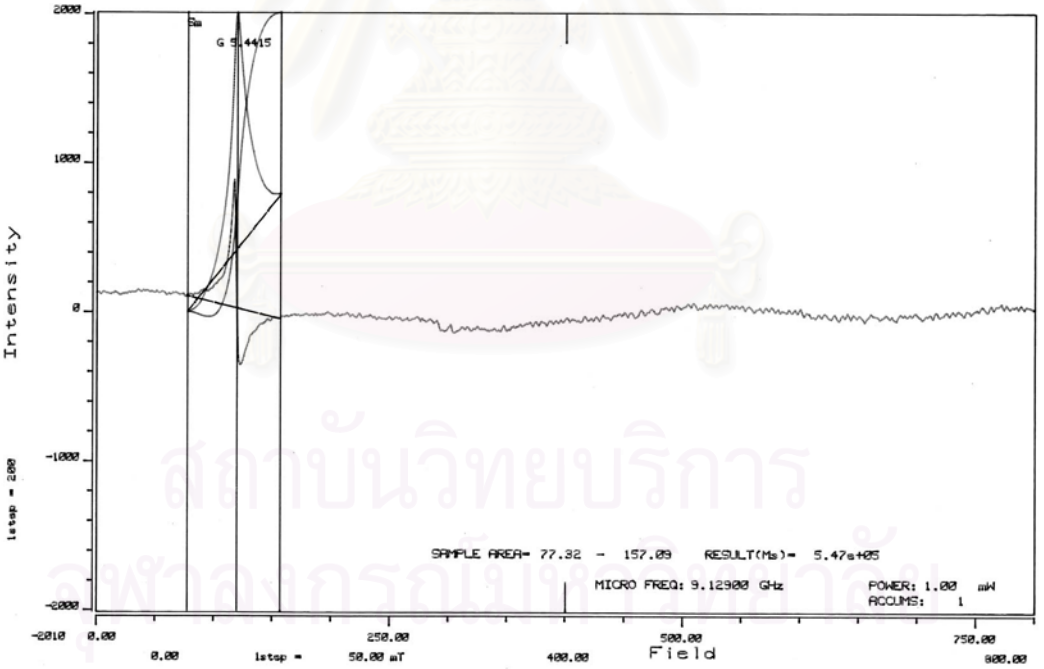

(b)

Figure 5.35 ESR spectra of high spin Co^{2+} of Ag/Co/HZSM-(a) fresh catalyst, (b) pretreated catalyst

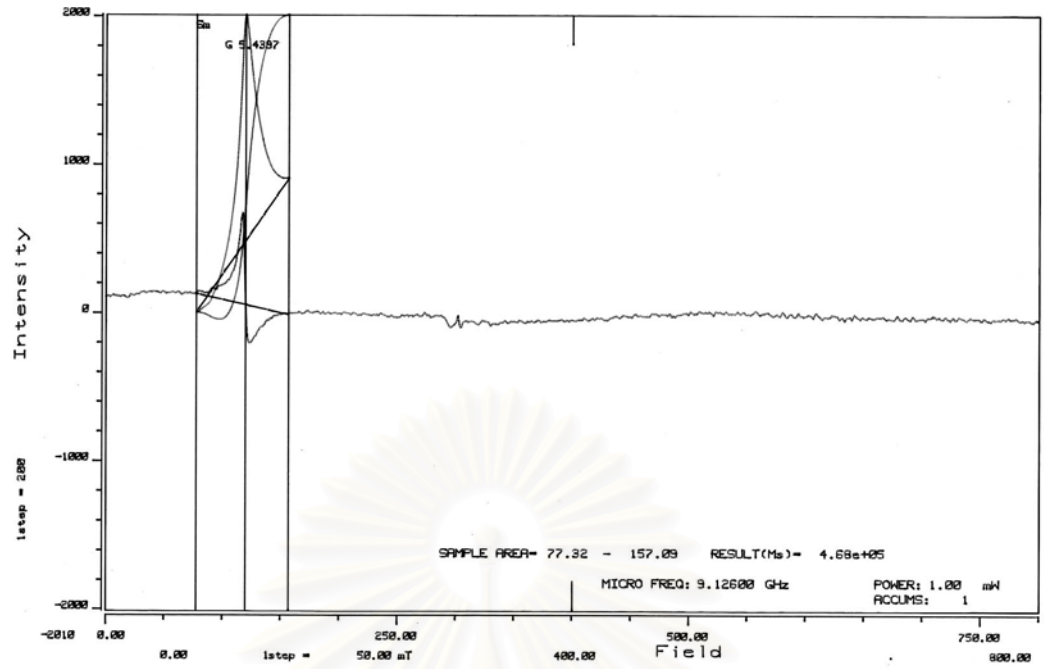

(a)

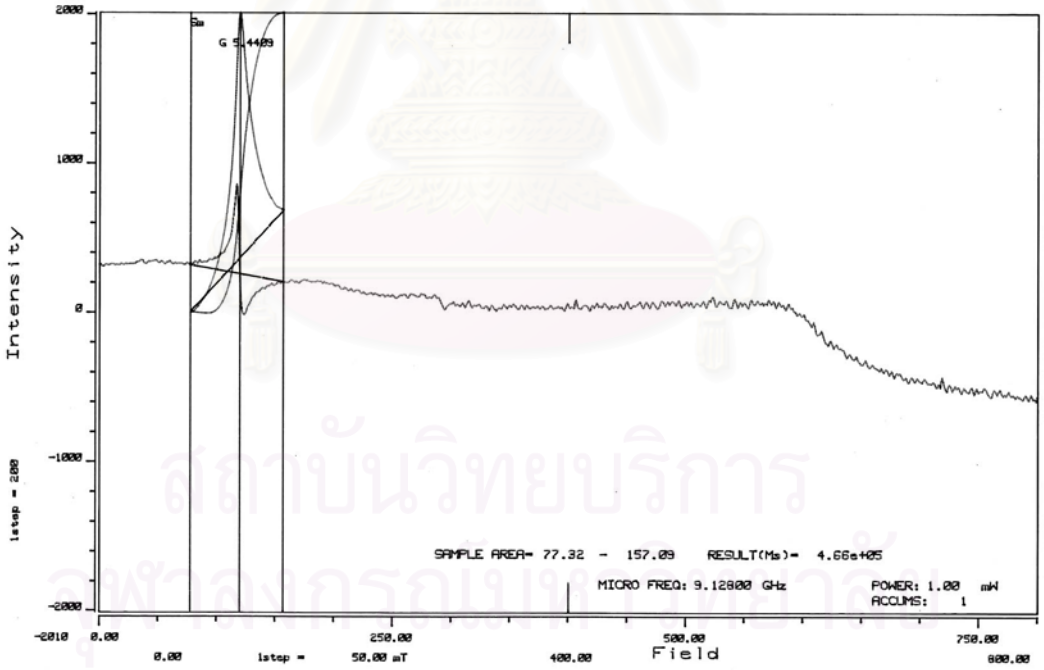

(b)

Figure 5.36 ESR spectra of high spin Co^{2+} of Fe/Co/HZSM-5 (a) fresh catalyst, (b) pretreated catalyst

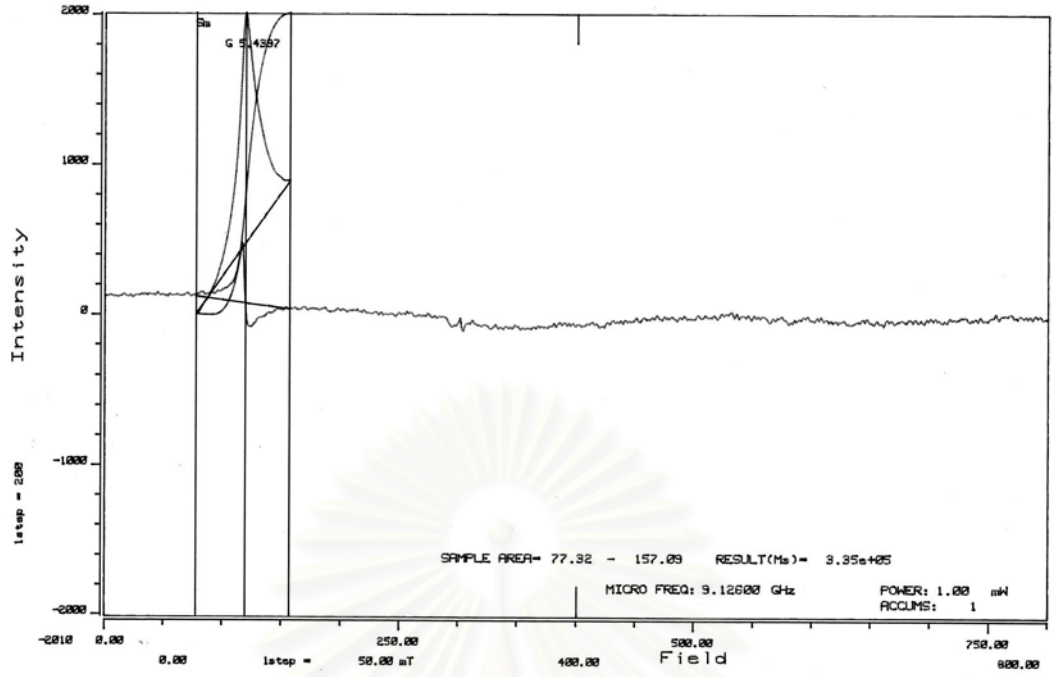

(a)

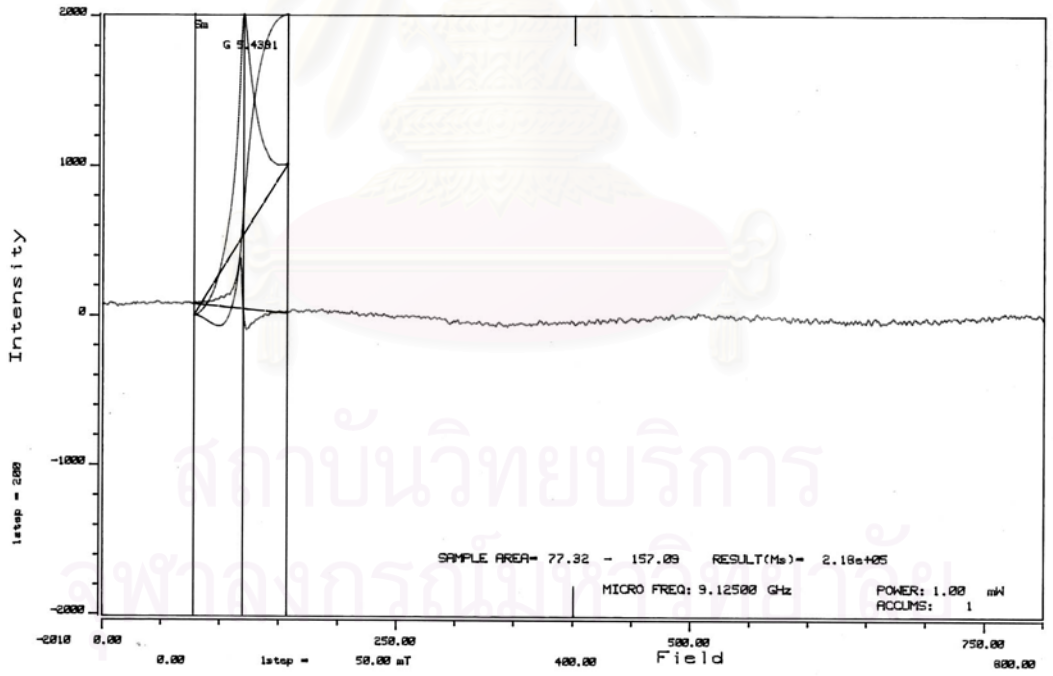

(b)

Figure 5.37 ESR spectra of high spin Co^{2+} of Ce/Co/HZSM-5 (a) fresh catalyst, (b) pretreated catalyst

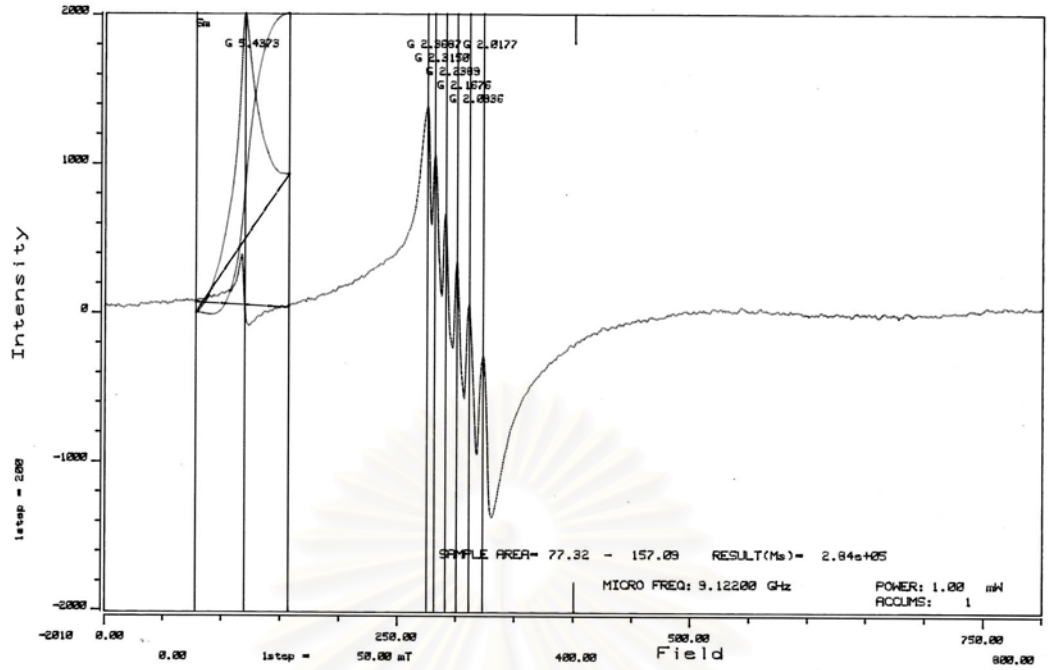

(a)

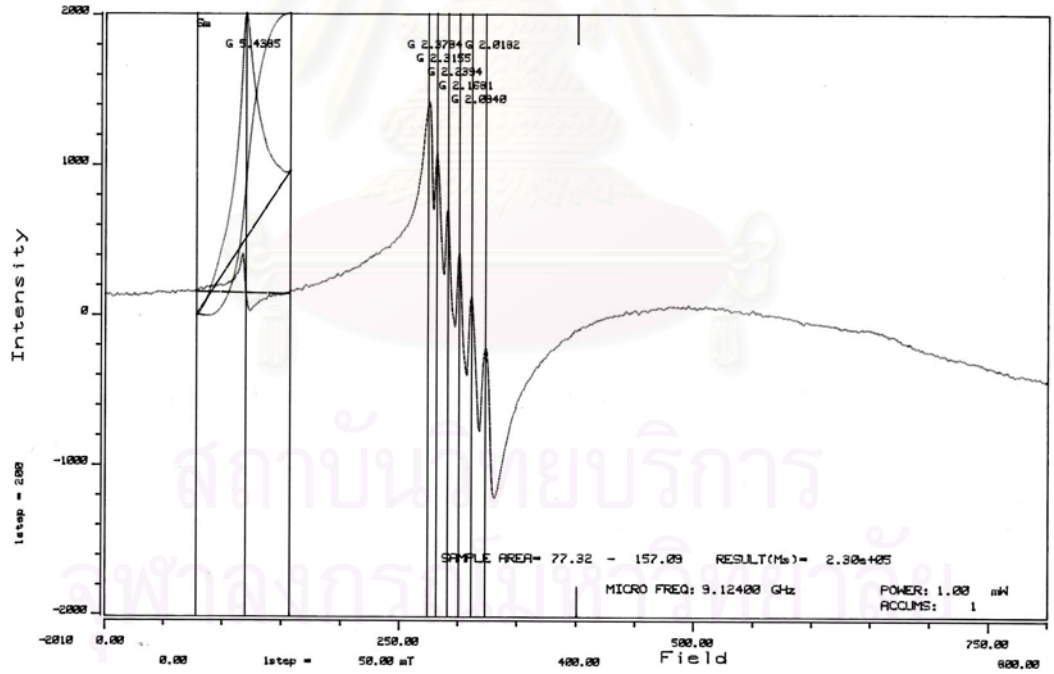

(b)

Figure 5.38 ESR spectra of high spin Co^{2+} of Mn/Co/HZSM-5 (a) fresh catalyst, (b) pretreated catalyst

5.1.2 Catalytic performance

Figures 5.39-5.50 show the percentage of NO conversion and methane conversion of fresh catalysts and pretreated catalysts. For all catalysts, the conversion of NO increases with reaction temperature, but the conversion curve bends down at T > ca 500 ^{o}C while the methane conversion reached almost 100%. The NO conversion of Me/Co/HZSM-5 displays a volcano-shape curve as temperature further increases.

Figure 5.39 represents the NO and methane convesions of fresh and pretreated Co/HZSM-5. The fresh Co/HZSM-5 gave a maximum NO conversion of approx. 45% at a reaction temperature of 500 °C. In comparison, the hydrothermal treatment Co/HZSM-5 showed a dramatically lower conversion of NO at any reaction temperature. The conversion of methane is also demonstrated. The conversion of methane is decreased with hydrothermal pretreatment. The second metal components were ion-exchanged in order to improve the durability of Co/HZSM-5. Figures 5.39-5.50 illustrate that Pd is appropiate for the durability improvement of Co/HZSM-5 and the metal second place is Cd. The fresh Pd/Co/HZSM-5 catalyst shows slightly lower NO conversion than the Pd-free catalyst and the temperature at which maximum activity is observed shifted to 450 ^{o}C. The pretreated Pd/Co/HZSM-5 gives NO conversion rather lower than the fresh catalyst (e.g., 48% conversion at 450 ^{o}C compared with 51% at the same temperature for fresh catalyst). As for the conversion of methane, Pd/Co/HZSM-5 catalyst with hydrothermal pretreatment also exhibited a substantial decrease.

Typical results for the effect of second metal components on the percentage of reaction durability and maximum NO conversion of Co/HZSM-5 are illustrated in Figure 5.51. The percentage of reaction durability, defined as the maximum NO conversion of pretreated catalysts per maximum NO conversion of fresh catalyst, were calculated and shown on the top of each bar. Pd and Cd showed the promotive effects on the catalytic durability of Co/HZSM-5. Also shown in Figure 5.51 are corresponding data for Ba/Co/HZSM-5, Ag/Co/HZSM-5, Zn/Co/HZSM-5 and Ni/Co/HZSM-5 it can be seen that the presence of Ba, Ag, Zn and Ni have a moderate influence only on the durability.

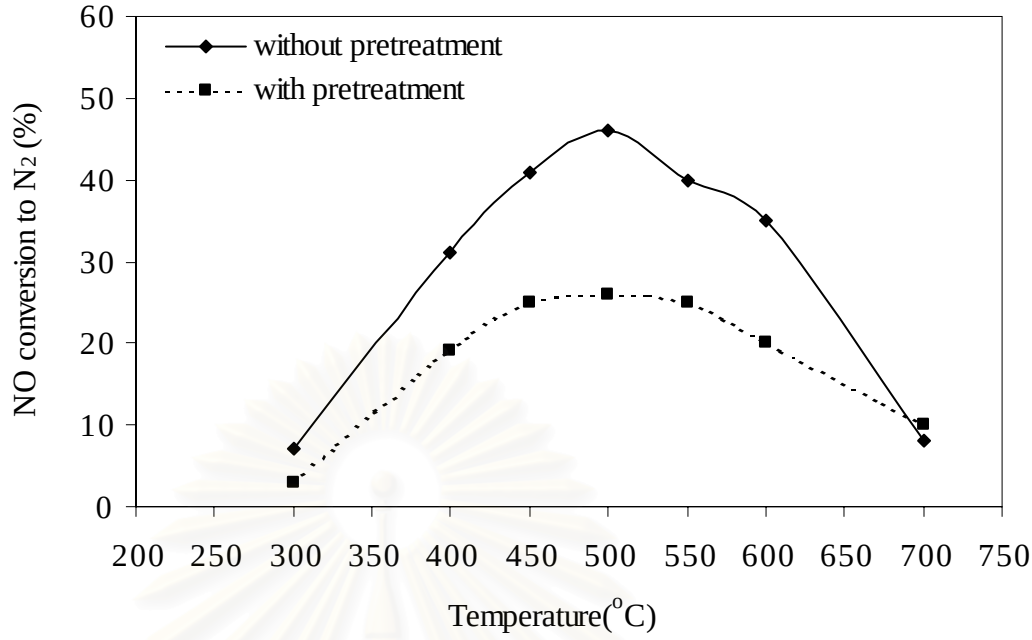

(a)

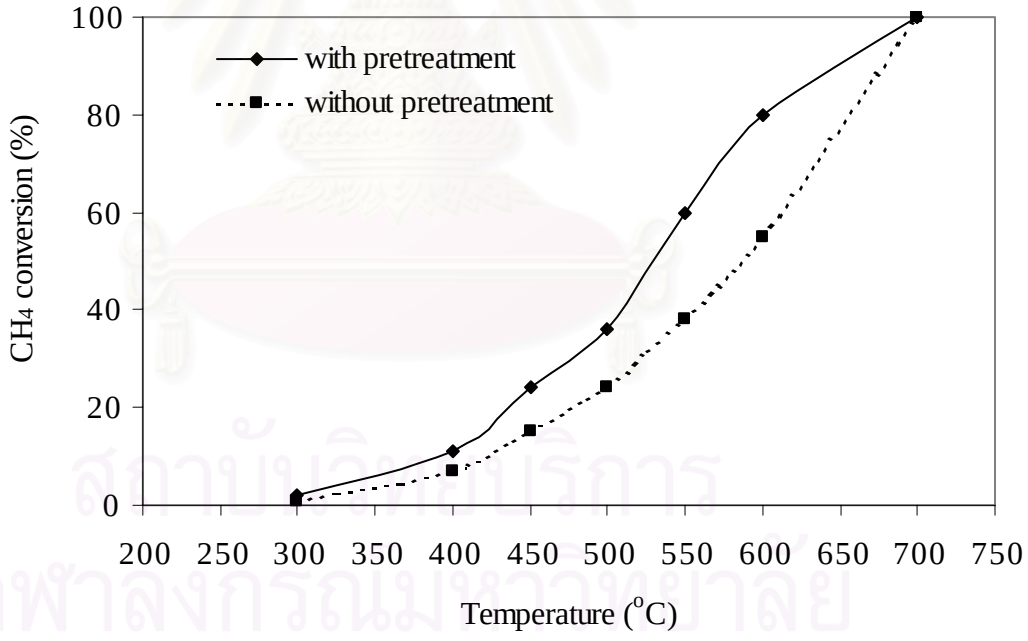

(b)

Figure 5.39 The effect of hydrothermal pretreatment of Co/HZSM-5 on (a) NO conversion(%), (b) CH_4 conversion(%), Feed gas: NO 1000 ppm, methane 1%, O_2 10% He balance, GHSV 10,000 h^{-1}.

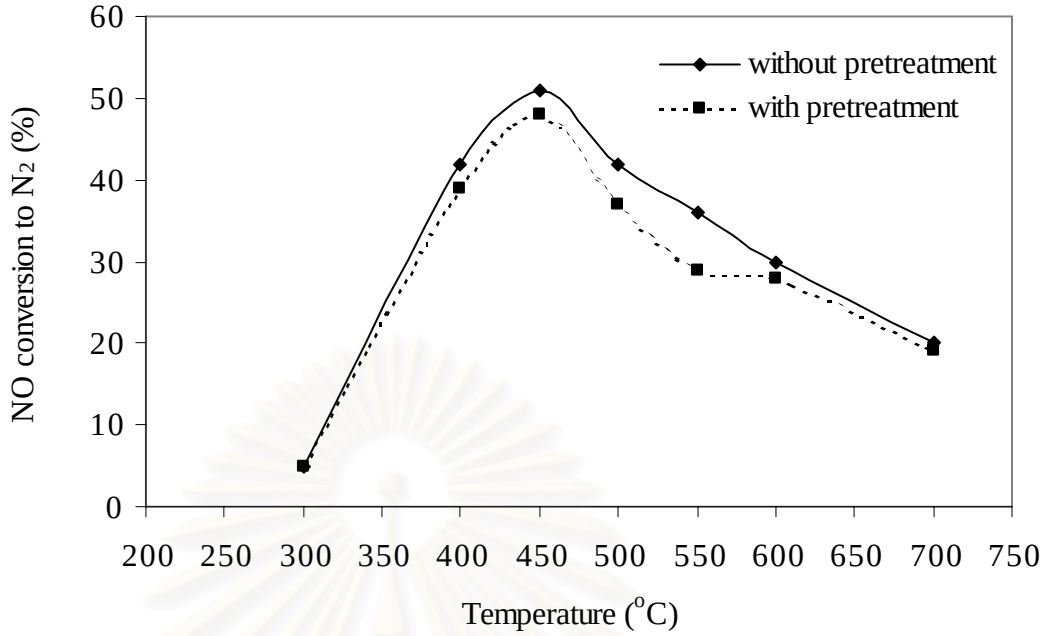

(a)

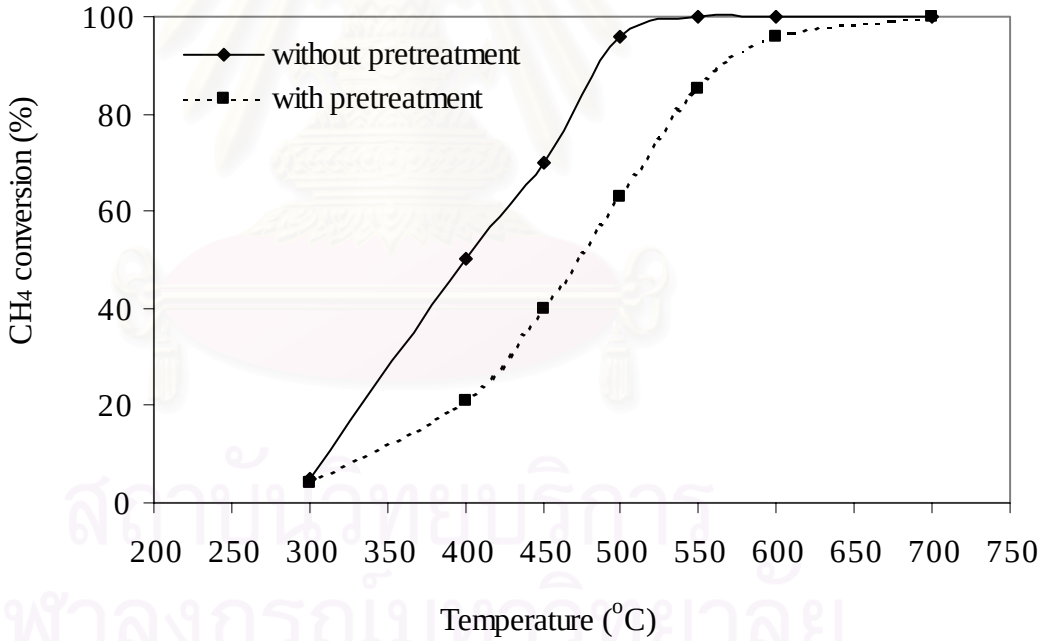

(b)

Figure 5.40 The effect of hydrothermal pretreatment of Pd/Co/HZSM-5 on (a) NO conversion(%), (b) CH_4 conversion(%), Feed gas: NO 1000 ppm, methane 1%, O_2 10% He balance, GHSV 10,000 h^{-1}.

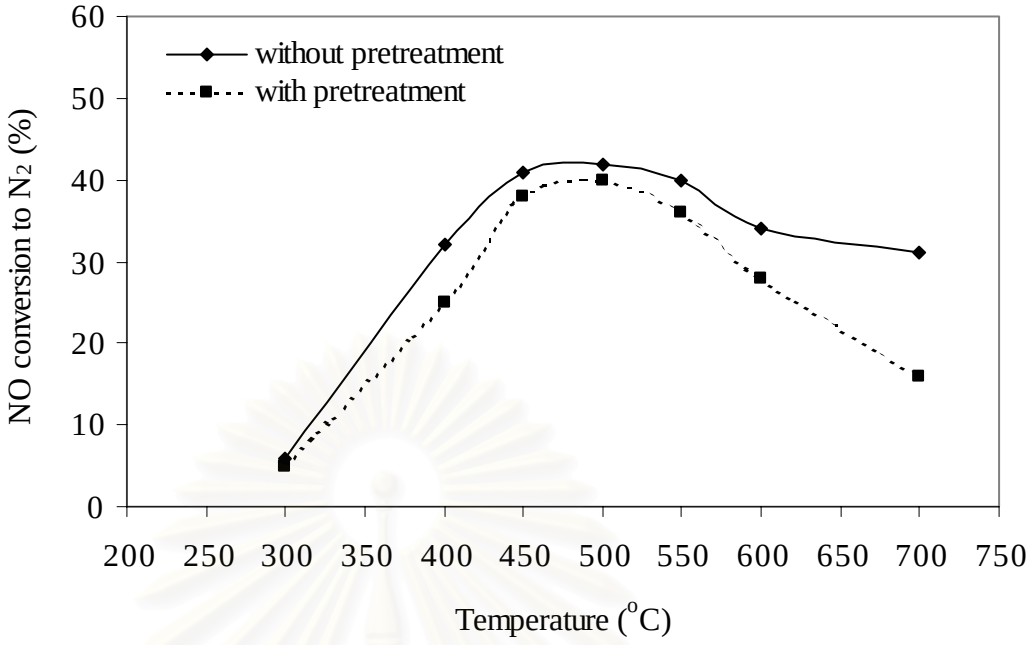

(a)

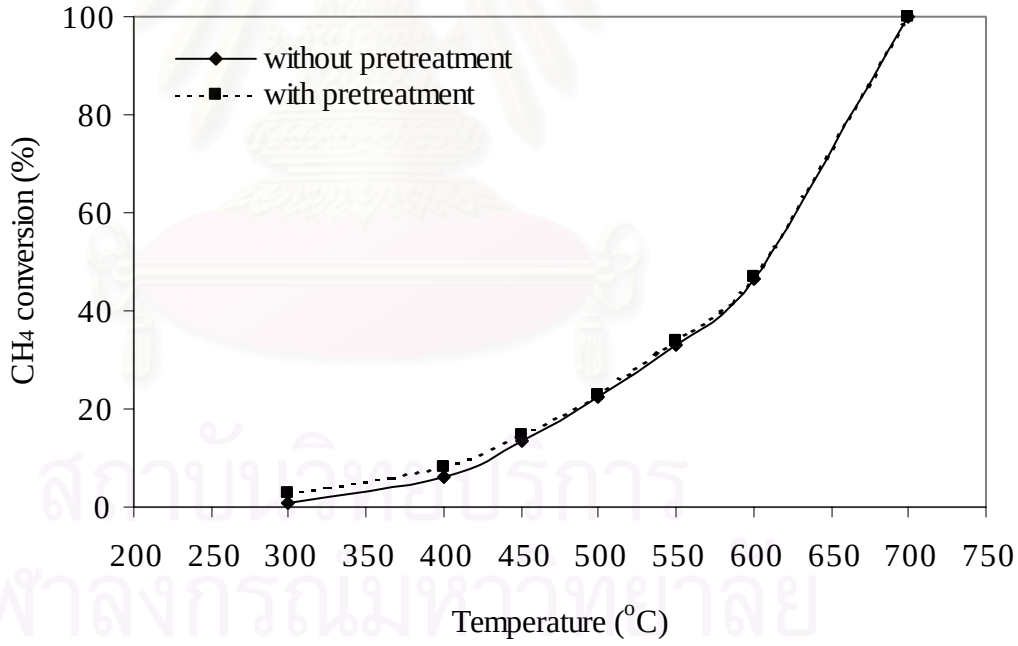

(b)

Figure 5.41 The effect of hydrothermal pretreatment of Cd/Co/HZSM-5 on (a) NO conversion(%), (b) CH_4 conversion(%), Feed gas: NO 1000 ppm, methane 1%, O_2 10% He balance, GHSV 10,000 h^{-1}.

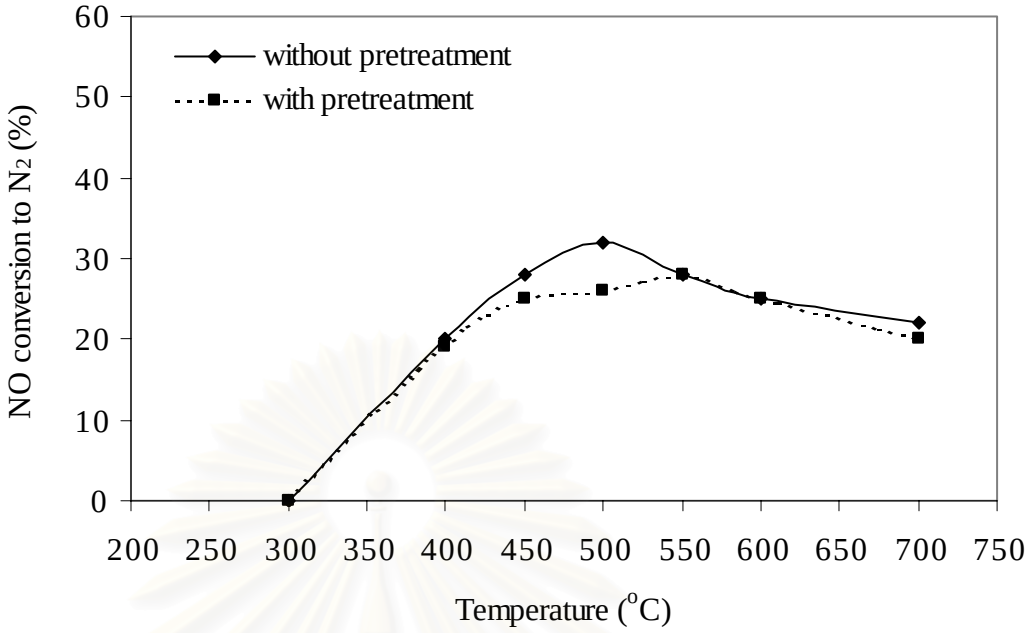

(a)

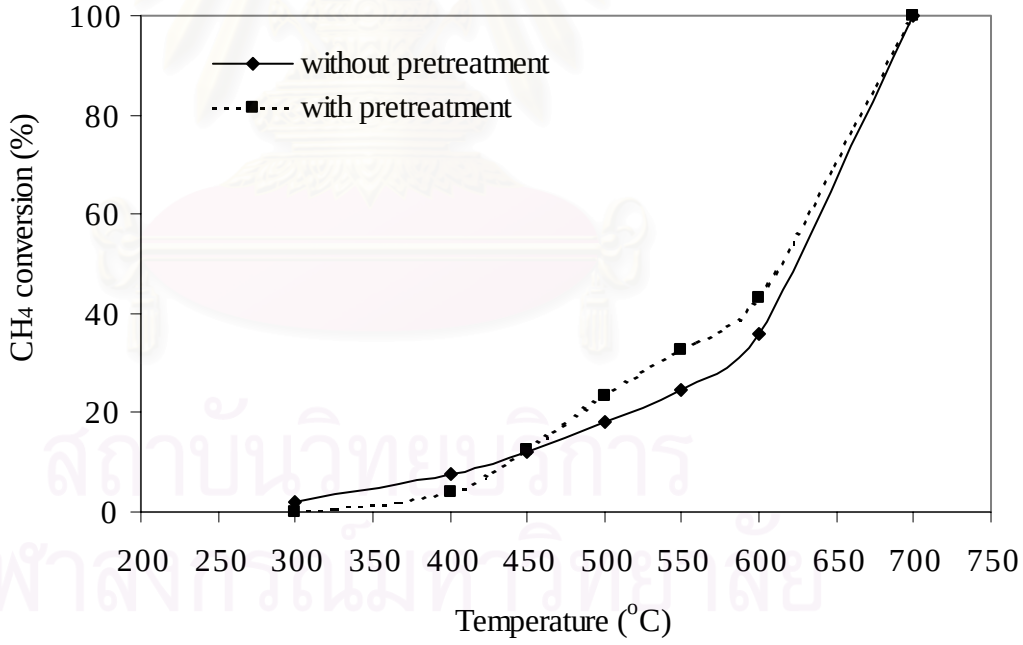

(b)

Figure 5.42 The effect of hydrothermal pretreatment of Ba/Co/HZSM-5 on (a) NO conversion(%), (b) CH_4 conversion(%), Feed gas: NO 1000 ppm, methane 1%, O_2 10% He balance, GHSV 10,000 h^{-1}.

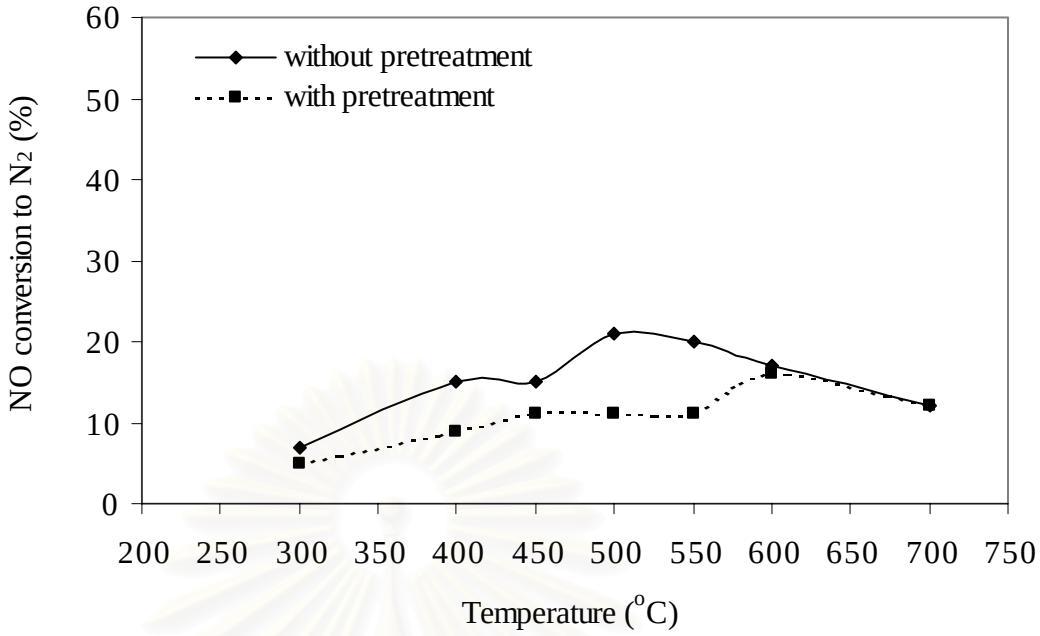

(a)

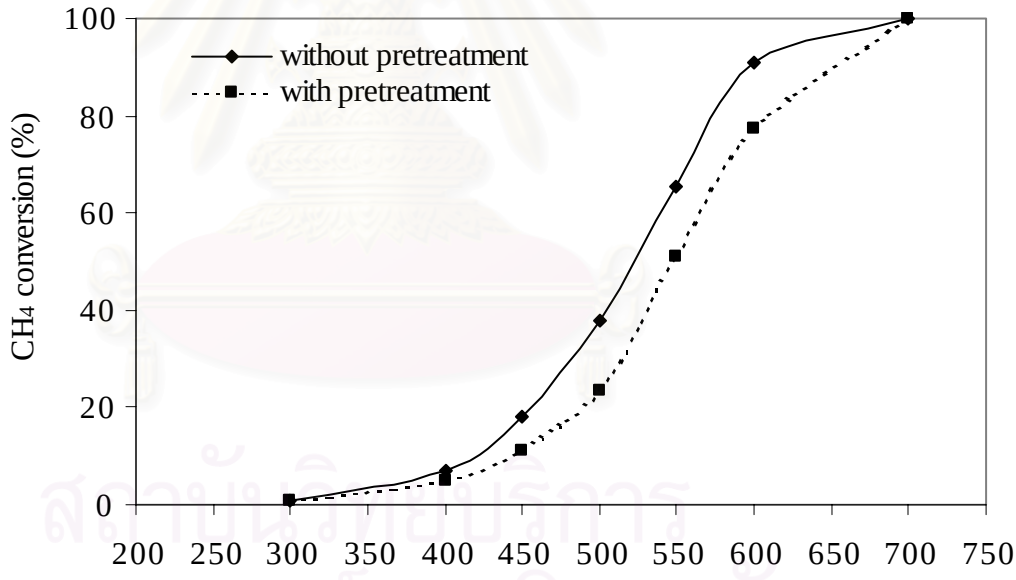

(b)

Figure 5.43 The effect of hydrothermal pretreatment of Cu/Co/HZSM-5 on (a) NO conversion(%), (b) CH_4 conversion(%), Feed gas: NO 1000 ppm, methane 1%, O_2 10% He balance, GHSV 10,000 h^{-1}.

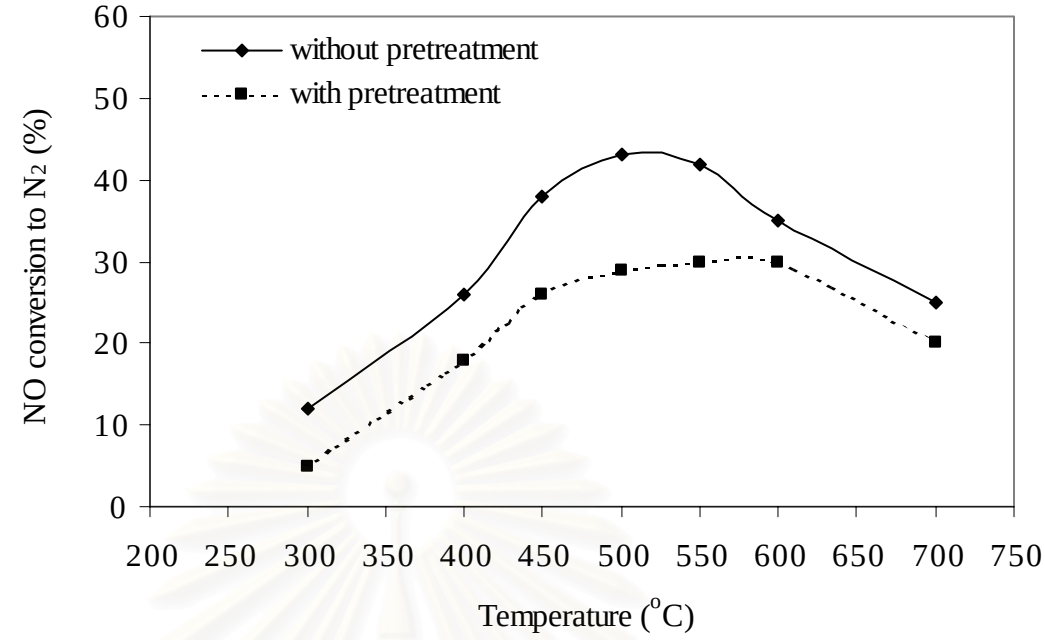

(a)

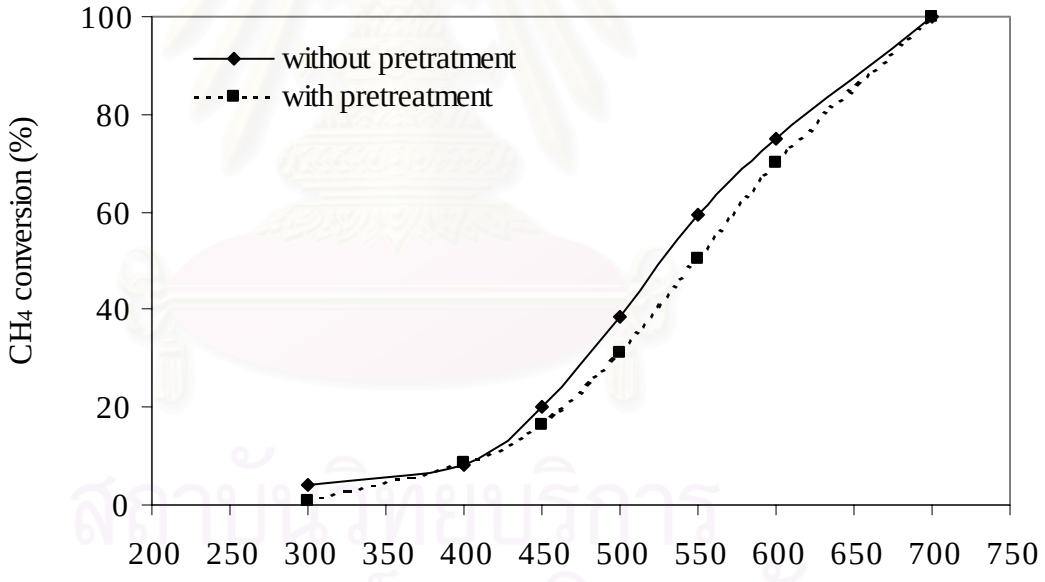

(b)

Figure 5.44 The effect of hydrothermal pretreatment of La/Co/HZSM-5 on (a) NO conversion(%), (b) CH_4 conversion(%), Feed gas: NO 1000 ppm, methane 1%, O_2 10% He balance, GHSV 10,000 h^{-1}.

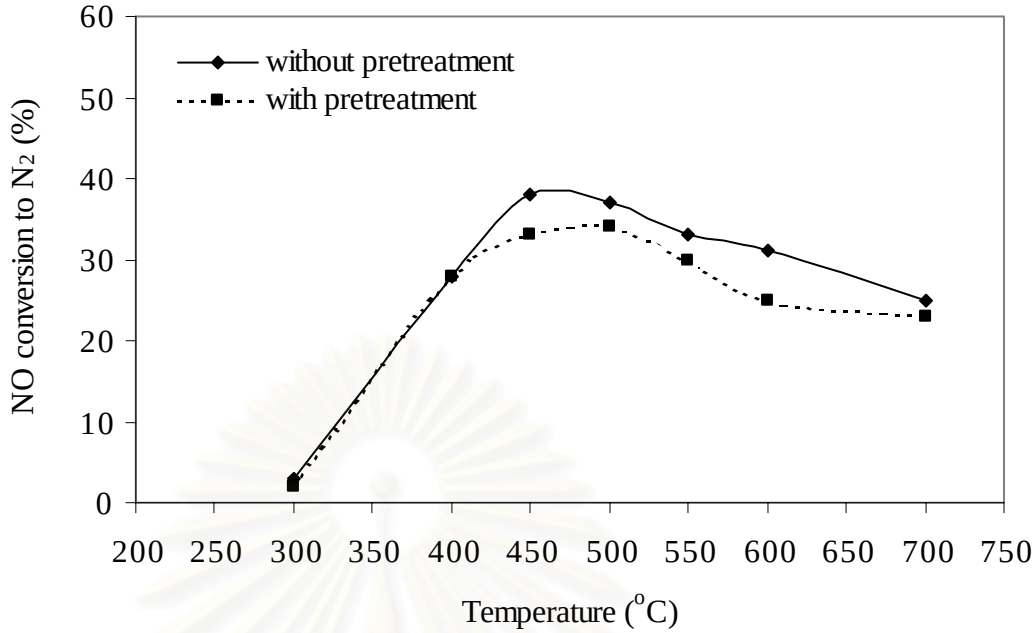

(a)

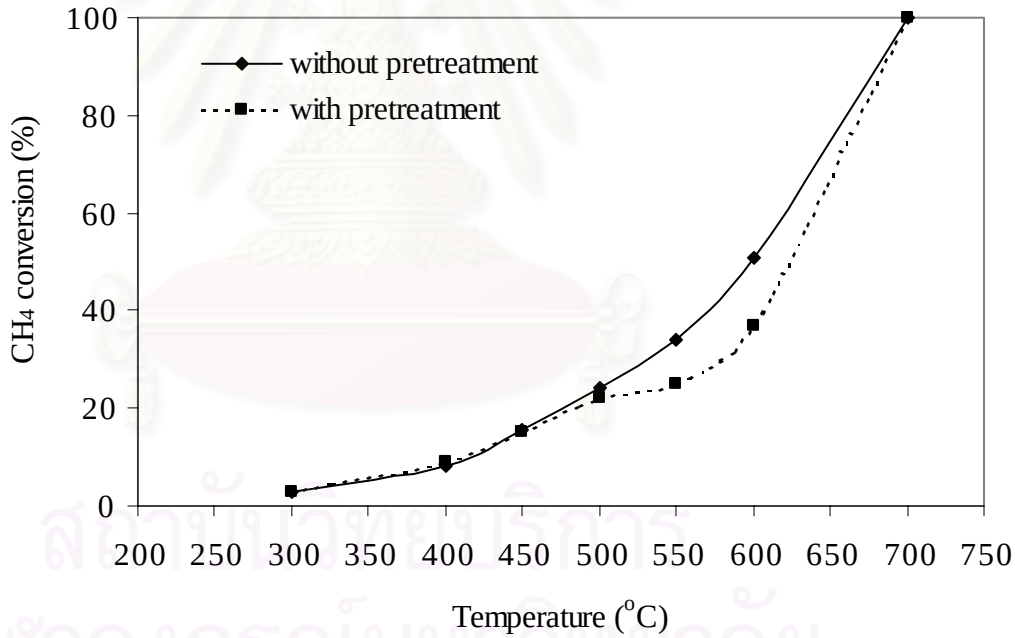

(b)

Figure 5.45 The effect of hydrothermal pretreatment of Ni/Co/HZSM-5 on (a) NO conversion(%), (b) CH_4 conversion(%), Feed gas: NO 1000 ppm, methane 1%, O_2 10% He balance, GHSV 10,000 h^{-1}.

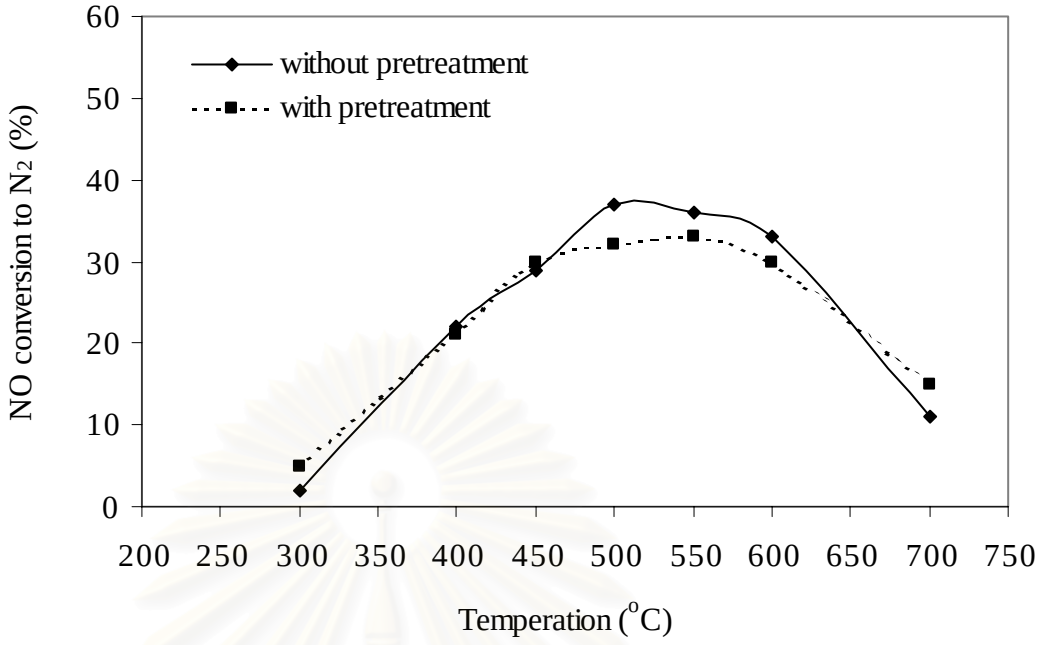

(a)

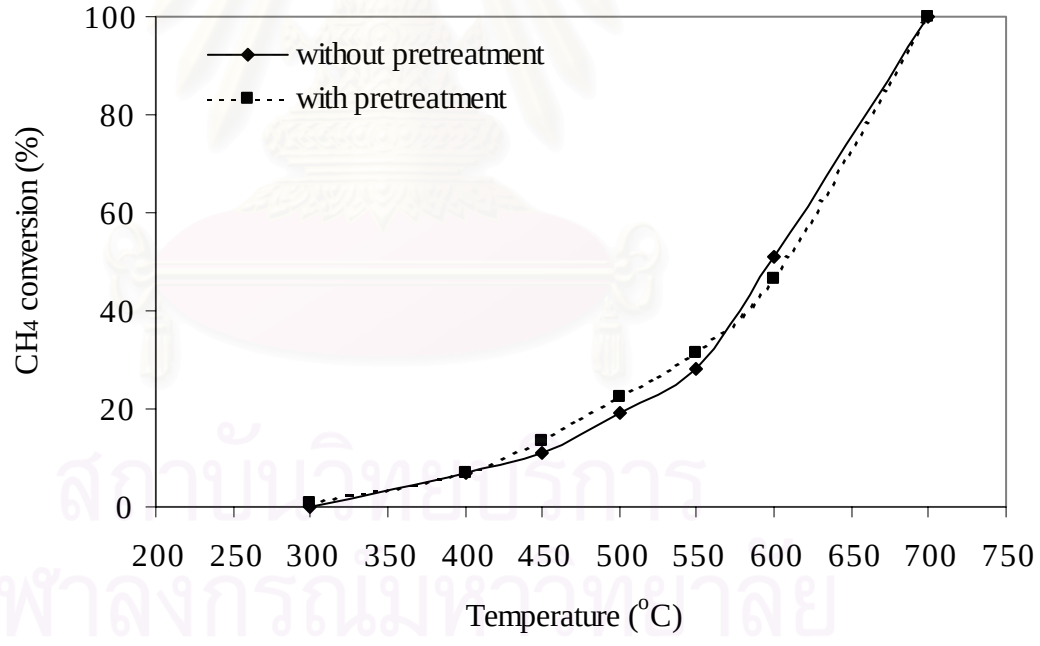

(b)

Figure 5.46 The effect of hydrothermal pretreatment of Zn/Co/HZSM-5 on (a) NO conversion(%), (b) CH_4 conversion(%), Feed gas: NO 1000 ppm, methane 1%, O_2 10% He balance, GHSV 10,000 h^{-1}.

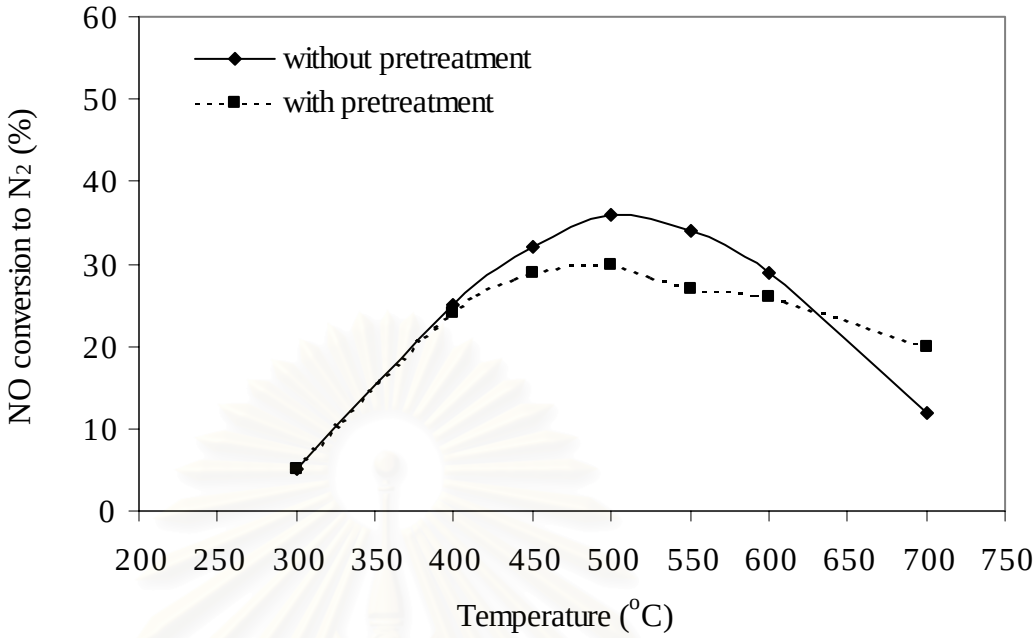

(a)

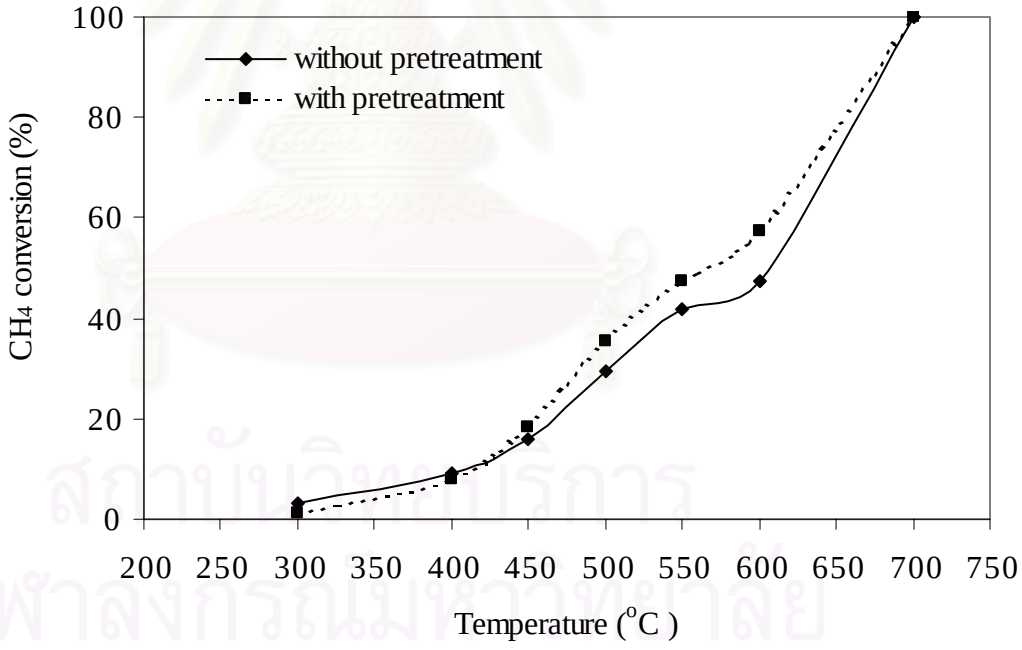

(b)

Figure 5.47 The effect of hydrothermal pretreatment of Ag/Co/HZSM-5 on (a) NO conversion(%), (b) CH_4 conversion(%), Feed gas: NO 1000 ppm, methane 1%, O_2 10% He balance, GHSV 10,000 h^{-1}.

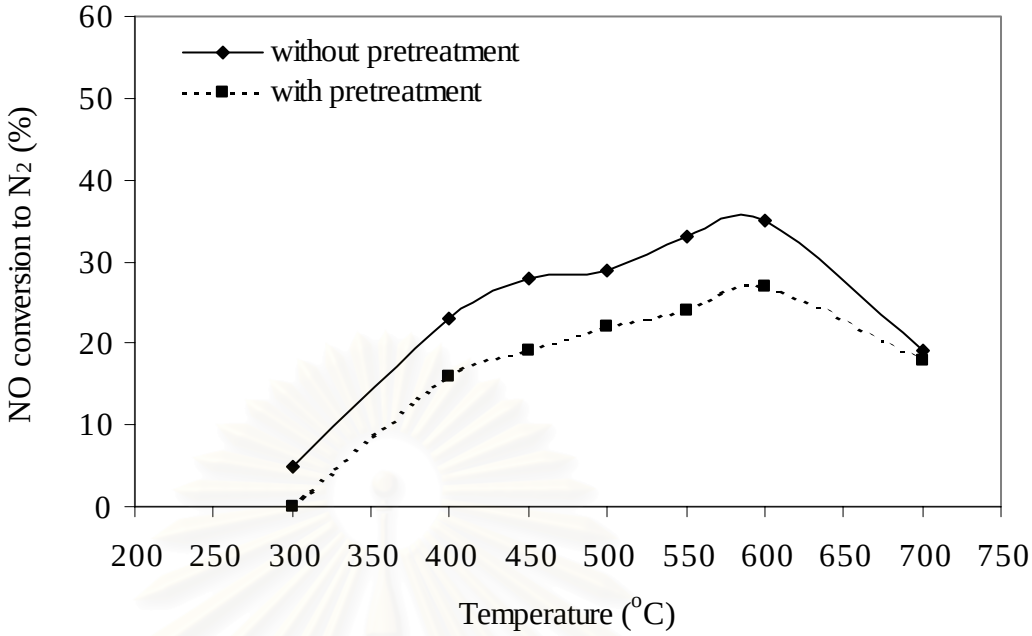

(a)

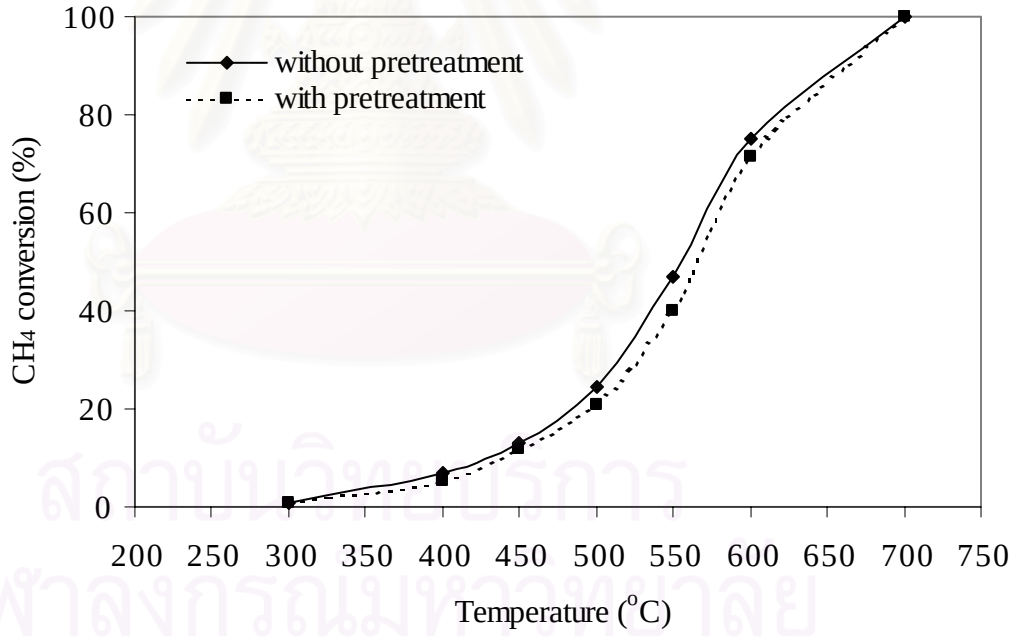

(b)

Figure 5.48 The effect of hydrothermal pretreatment of Fe/Co/HZSM-5 on (a) NO conversion(%), (b) CH_4 conversion(%), Feed gas: NO 1000 ppm, methane 1%, O_2 10% He balance, GHSV 10,000 h^{-1}.

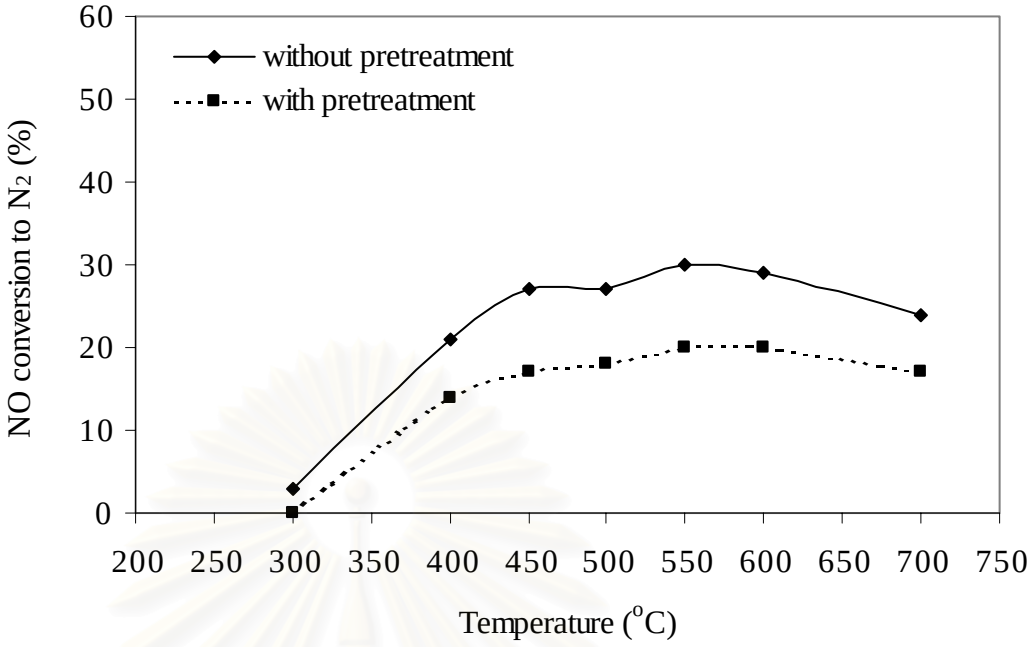

(a)

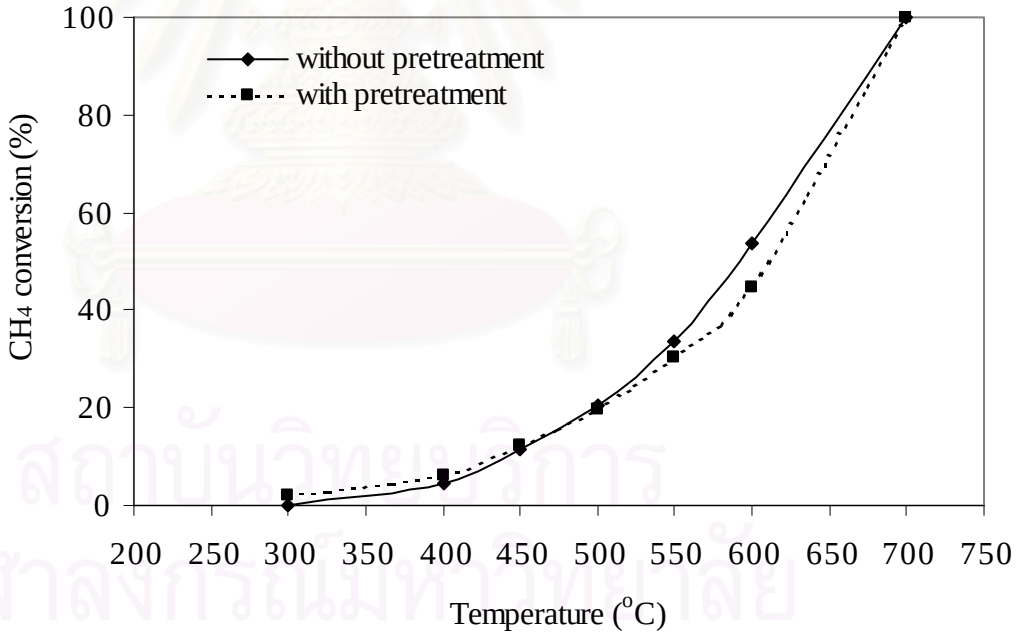

(b)

Figure 5.49 The effect of hydrothermal pretreatment of Ce/Co/HZSM-5 on (a) NO conversion(%), (b) CH_4 conversion(%), Feed gas: NO 1000 ppm, methane 1%, O_2 10% He balance, GHSV 10,000 h^{-1}.

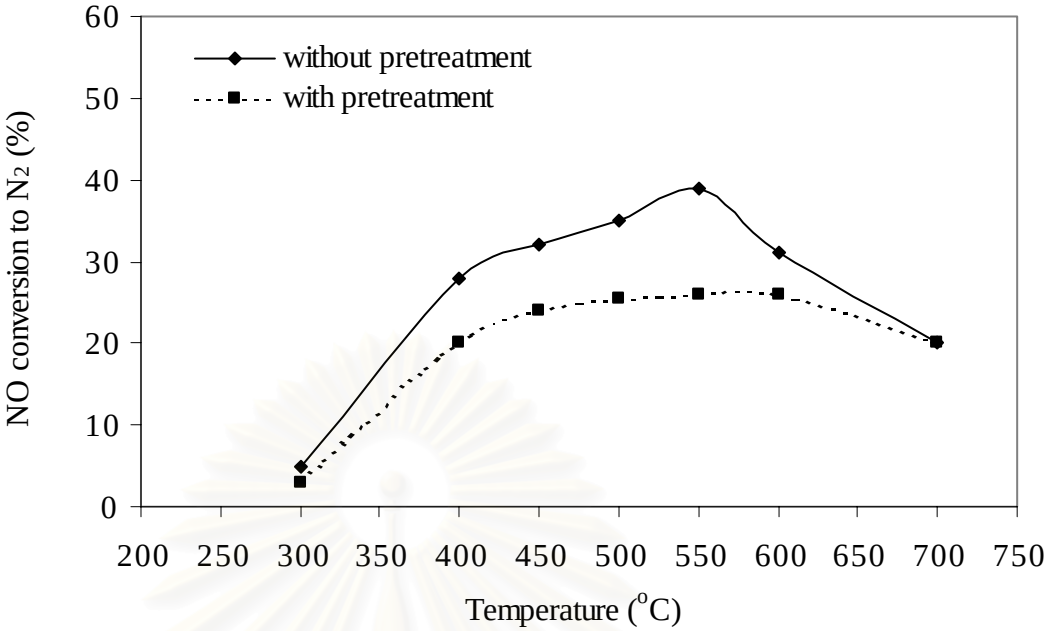

(a)

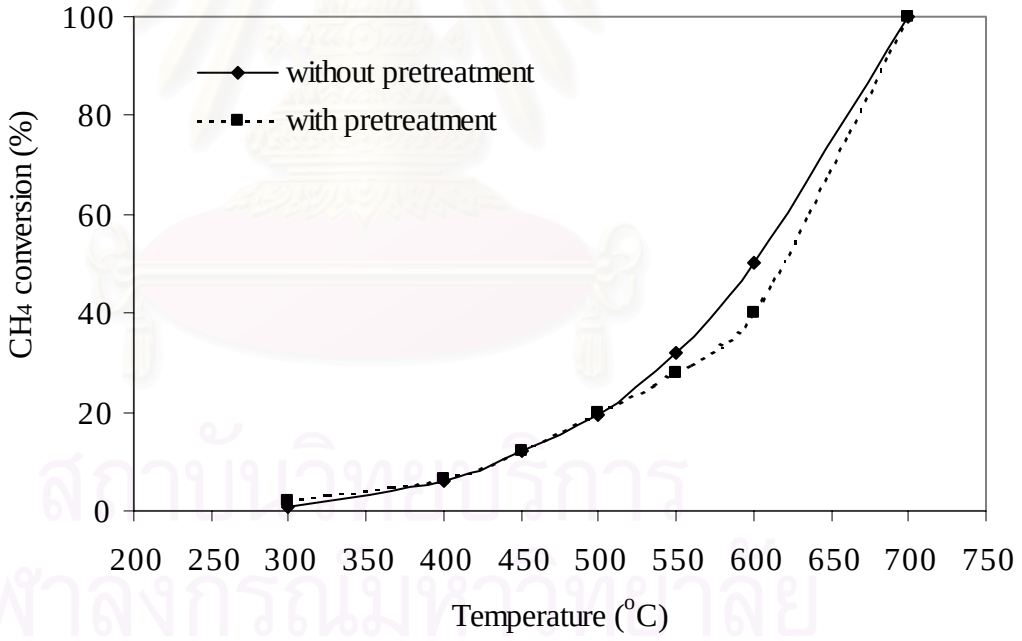

(b)

Figure 5.50 The effect of hydrothermal pretreatment of Mn/Co/HZSM-5 on (a) NO conversion(%), (b) CH_4 conversion(%), Feed gas: NO 1000 ppm, methane 1%, O_2 10% He balance, GHSV 10,000 h^{-1}.

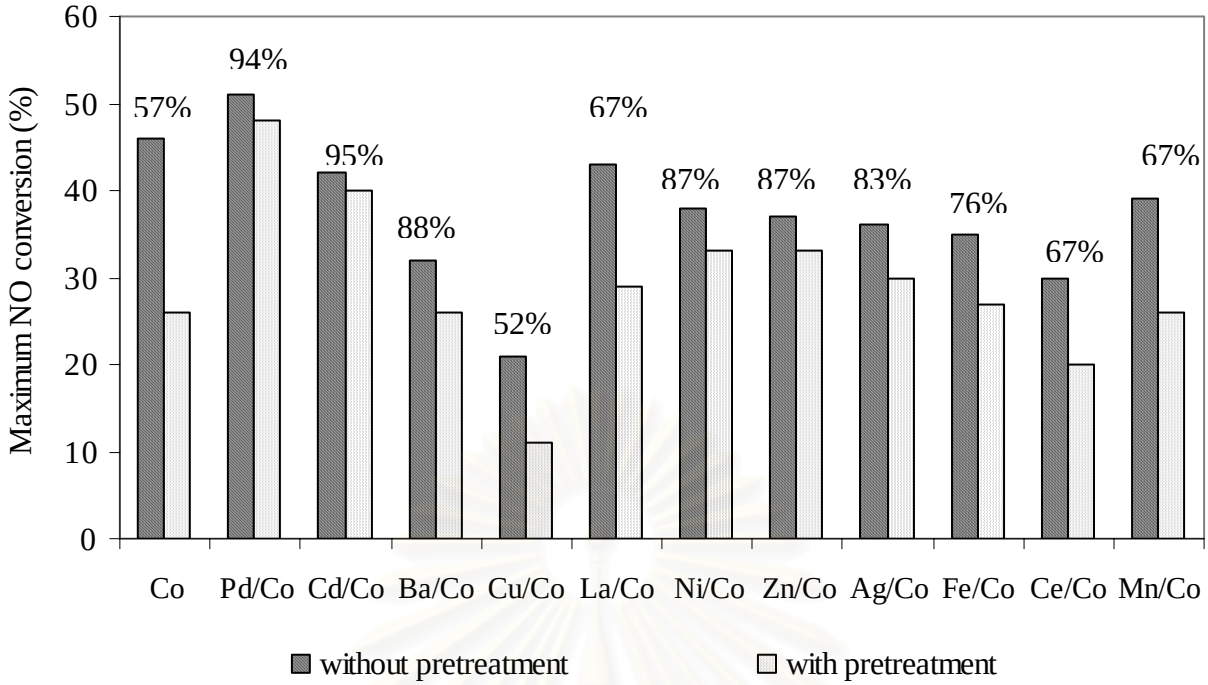

Figure 5.51 The percentage of maximum NO conversion and the values of the percentage of reaction durability on second component loaded Co/HZSM-5.

From these results, it can be observed that some divalent second metals such as Pd^{2+}, Cd^{2+}, improve durability of catalysts however durability of catalysts cannot be improved by some divalent second metal (Cu^{2+}). Therefore, there is no relationship between valency and durability improvement distinctly.

In conclusion, the primary cause of irreversible deactivation of hydrothermal pretreated Co/HZSM-5 was lattice dealumination. The presence of cations improved the Co/HZSM-5 catalyst durability for NO removal under hydrothermal treatment. Cd and Pd showed significant improvement of reaction durability against hydrothermal pretreatment. Besides for Pd, it is not only improved activity but also NO reduction durability.

5.1.3 Effect of Pd loading on the durability improvement of Co/HZSM-5

5.1.3.1 Changes in Physical Properties upon Pretreatment

Table 5.2 shows the physical properties of the catalysts before and after hydrothermal treatment. BET surface area showed some decrease with the pretreatment catalyst. Crystallinity, as determined by XRD profiles, was calculated using the area of the dominant peak, which was compared with that of HZSM-5 as a reference. According to XRD profiles of the fresh catalysts, the crystallinity of HZSM-5 and Co/HZSM-5 lost the considerable degree of their crystallinity after hydrothermal treatment, as shown in Table 5.2. In contrast, for the Pd modified Co/HZSM-5 only a slight decrease upon hydrothermal treatment, especially for the 0.4%Pd/Co/HZSM-5. Consequently, it definitely appears that the 0.4%Pd/Co/HZSM -5 catalyst has higher durability than Co/HZSM-5 on hydrothermal treatment with respect to crystallinity. In addition, the XRD pattern of both fresh and pretreated did not show the formation of detectable cobalt oxide.

Table 5.2 Physical properties of various Pd loadings on Co/HZSM-5 catalysts.

catalysts	Me/Al atomic ratio		BET surface area(m^2/g)		% Crystallinity	
	Co/Al	Pd/Al	fresh	pretreated	fresh	pretreated
HZSM-5	-	-	350	295	100	48
1 %Co/HZSM-5	0.24	-	334	298	99	83
0 .4%Pd/HZSM-5	-	0.042	342	309	100	90
0 .1%Pd/Co/HZSM-5	0.24	0.013	332	320	99	95
0 .4%Pd/Co/HZSM-5	0.25	0.038	331	321	100	98
0 .6%Pd/Co/HZSM-5	0.21	0.073	326	312	98	95

The result of ^{27}Al MAS NMR of the catalysts before and after pretreatment is shown in Figures 5.52-5.54. The spectra confirmed that severe steam treatment caused dealumination. The fresh catalysts exhibited only one signal at approx. 60 ppm, which is assigned, to the tetrahedral aluminum in the zeolite lattice [115]. The Co/HZSM-5 and 0.1%Pd/Co/HZSM-5 catalysts after hydrothermal treatment exhibit two signals approx. 0 ppm attributed to the extra lattice octahedral aluminum in the zeolite lattice and approx. 60 ppm. This is consistent with the report somewhere else of loss in activity and stability after steam pretreatment due to framework dealumination of the zeolite. [82] The extra lattice octahedral aluminum signals were absent in the hydrothermal treatment 0.4%Pd/Co/HZSM-5 and 0.6%Pd/Co/HZSM-5 catalysts. It has been suggested that the presence of a certain amount of Pd, approximately 0.4 wt% loading or higher as observed here, could stabilize the zeolite framework structure by preventing the occurrence of dealumination.

Cobalt-containing microporous had been investigated by using electron spin resonance (ESR) spectroscopy at liquid nitrogen boiling point temperature (-196 ^{o}C) in order to investigate the coordination of high-spin cobalt before and after hydrothermal pretreatment. The ESR spectrum at g = 5.4-5.8 is assigned to high-spin Co^{2+}[114]. The ESR spectrum of fresh and pretreated of Co/HZSM-5 and Pd/Co/HZSM-5 is shown in Figures 5.55-5.57. The g value of fresh Co/HZSM-5 is 5.4391. After hydrothermal treatment, the g value of Co/HZSM-5 is remained at 5.4397. In addition, Pd/Co/HZSM-5 after pretreatment exhibited the same ESR feature and the same g value which is 5.4397, as the fresh one. Nevertheless, there is a significant change in the intensity of the signal obtain from the pretreated Co/HZSM-5 catalyst. This means that there is no any change in state of cobalt ion, which was observed in the zeolite.

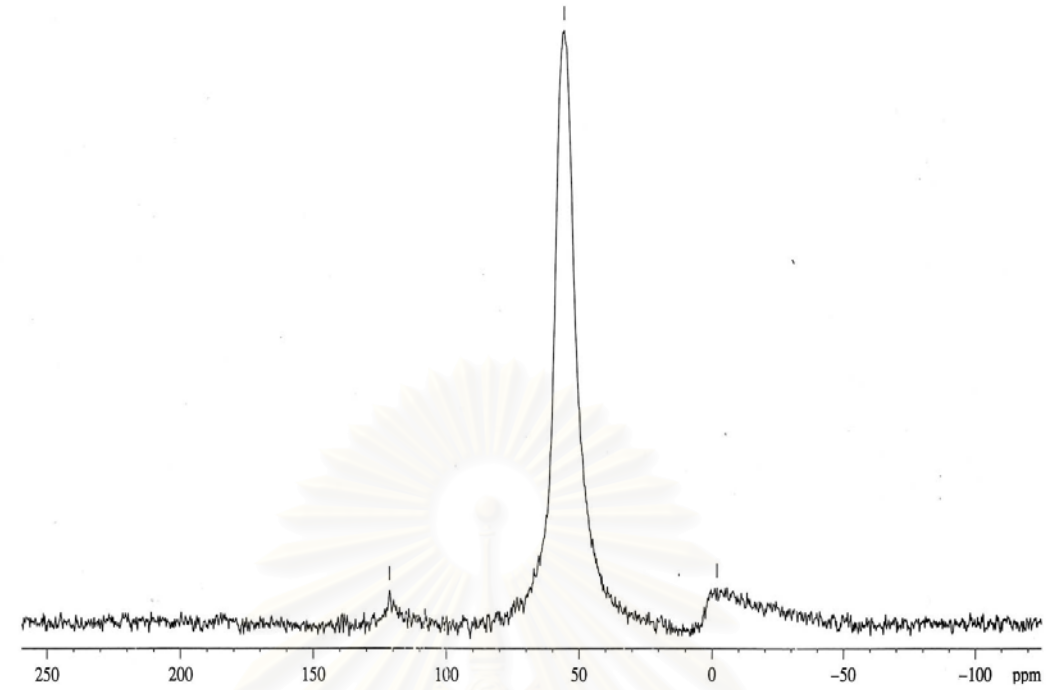

(a)

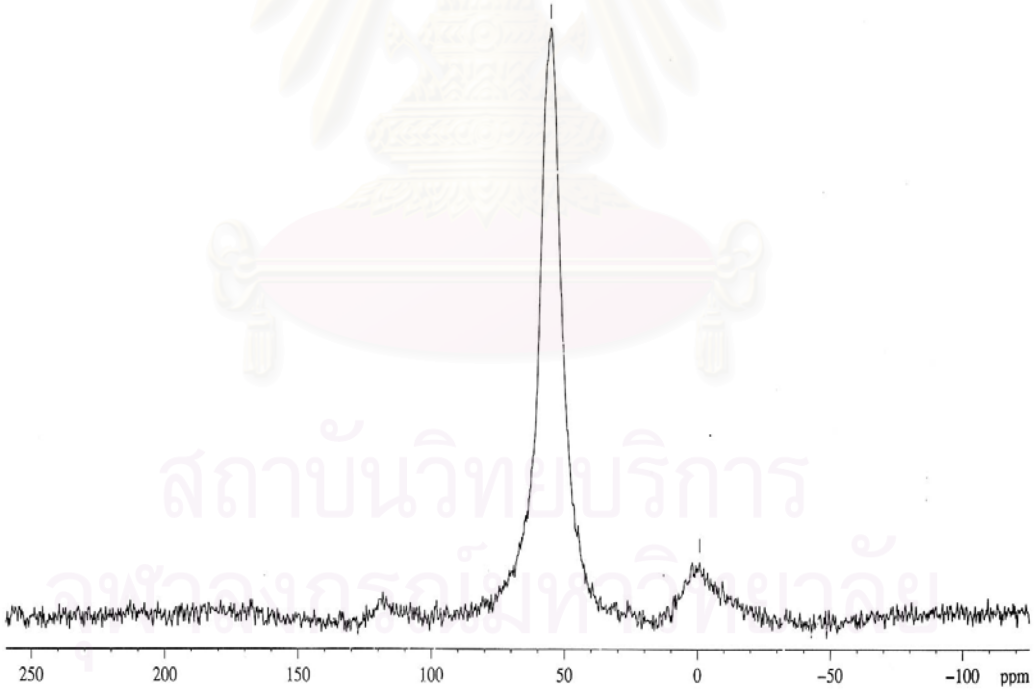

(b)

Figure 5.52 ^{27}Al MAS-NMR spectra of 0.1%Pd/Co/HZSM-5 (a) fresh catalyst, (b) pretreated catalyst.

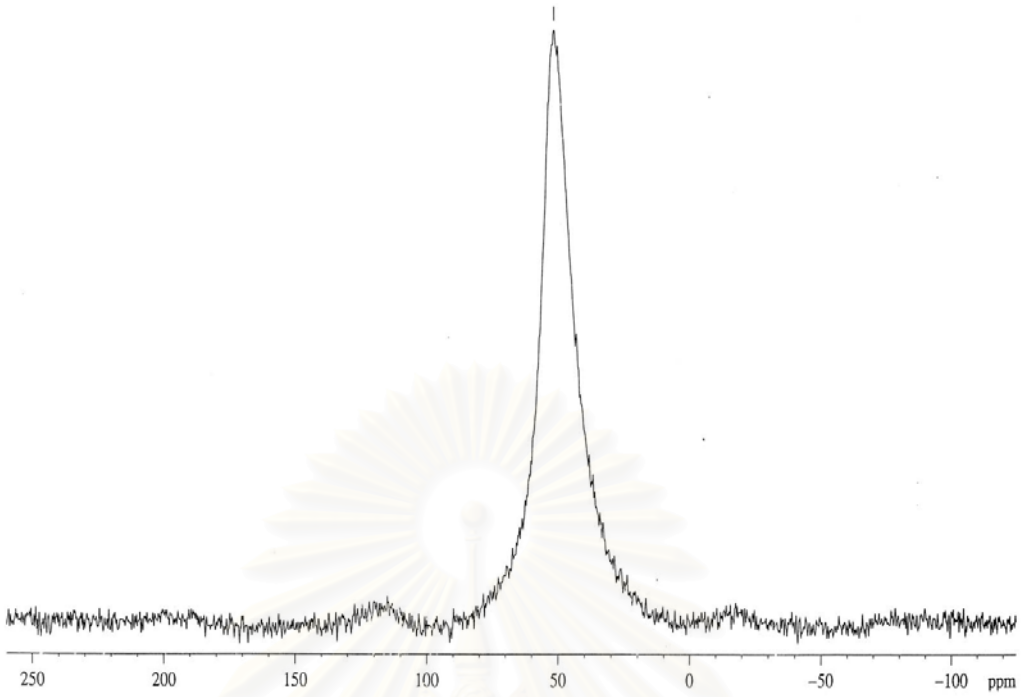

(a)

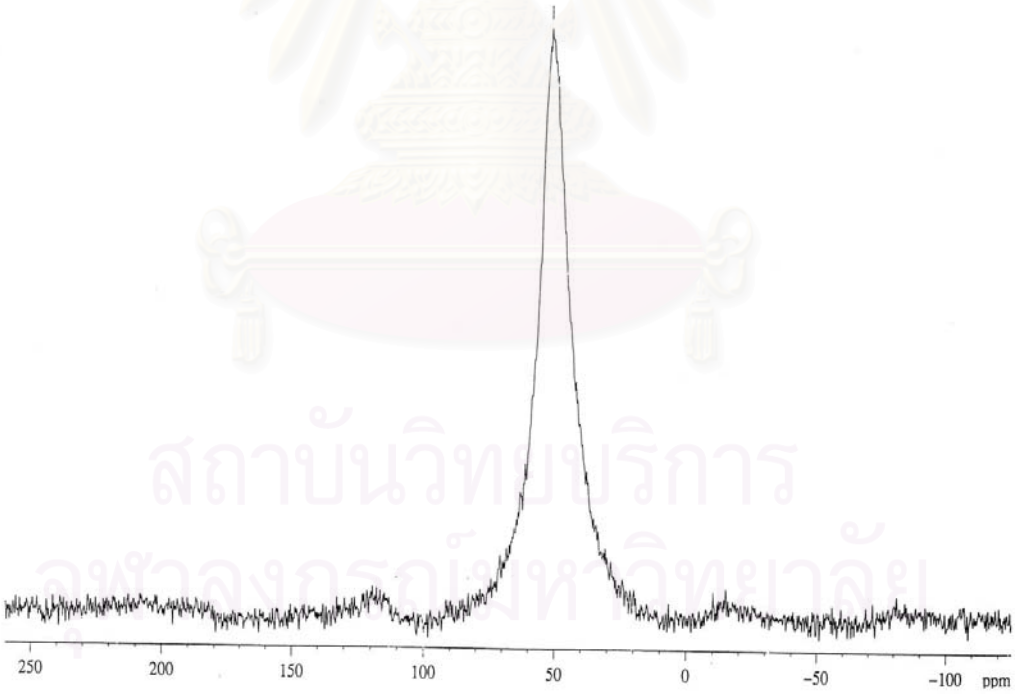

(b)

Figure 5.53 ^{27}Al MAS-NMR spectra of 0.4%Pd/Co/HZSM-5 (a) fresh catalyst, (b) pretreated catalyst.

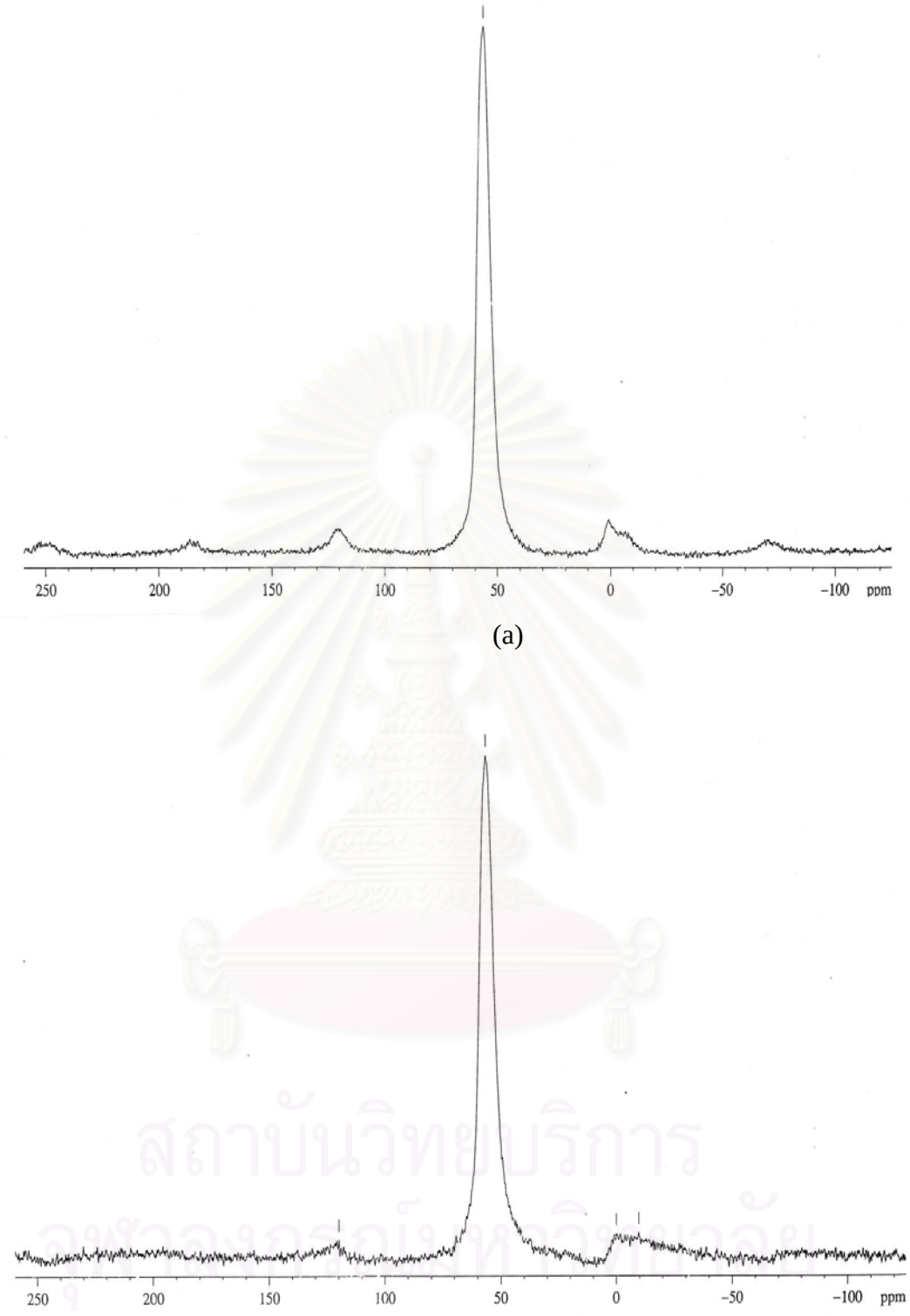

Figure 5.54 ^{27}Al MAS-NMR spectra of 0.6%Pd/Co/HZSM-5 (a) fresh catalyst, (b) pretreated catalyst.

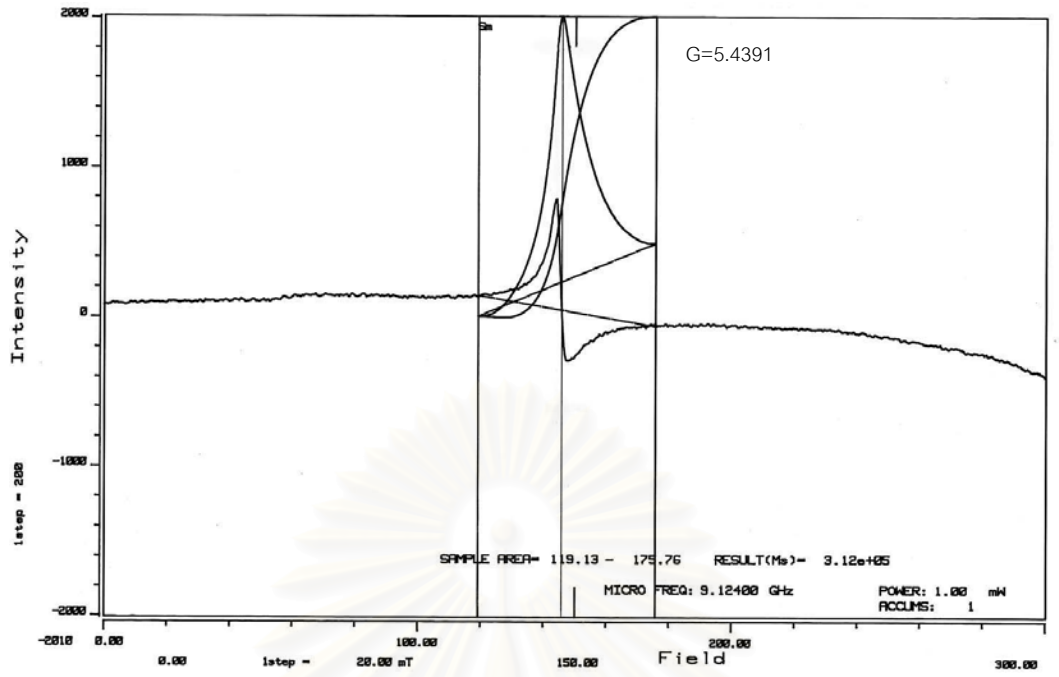

(a)

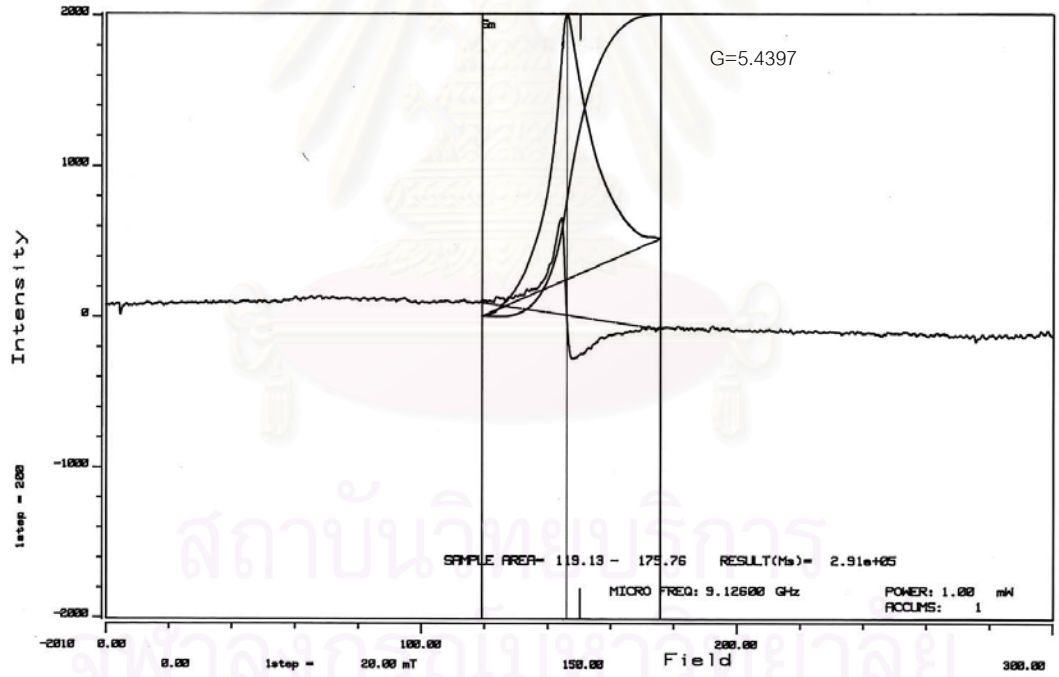

(b)

Figure 5.55 ESR spectra of high spin Co^{2+} of 0.1%Pd/Co/HZSM-5 (a) fresh catalyst, (b) pretreated catalyst.

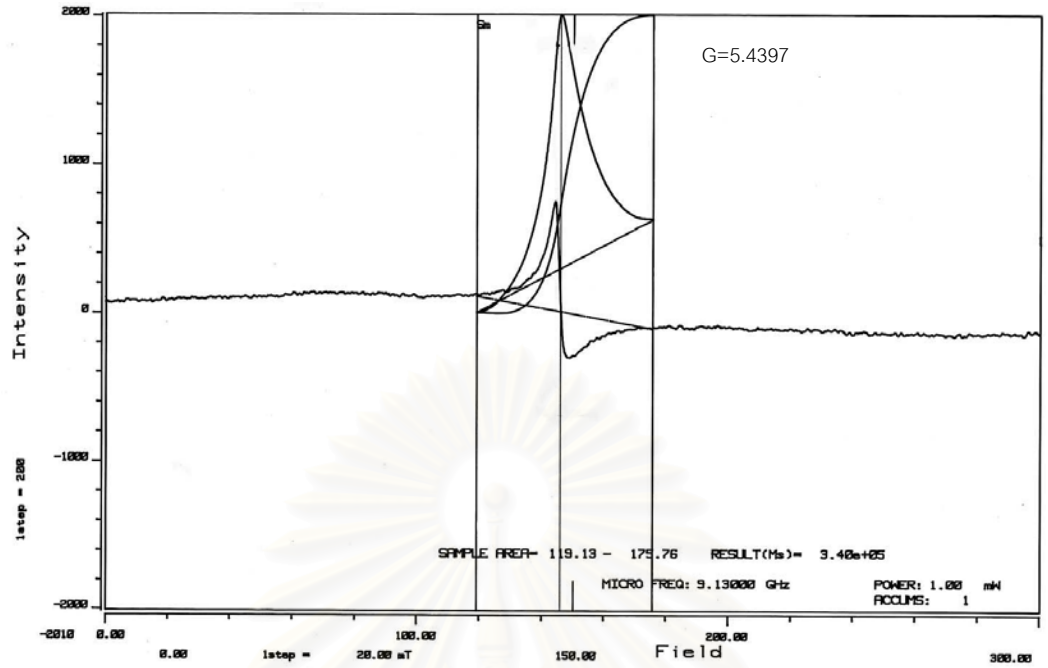

(a)

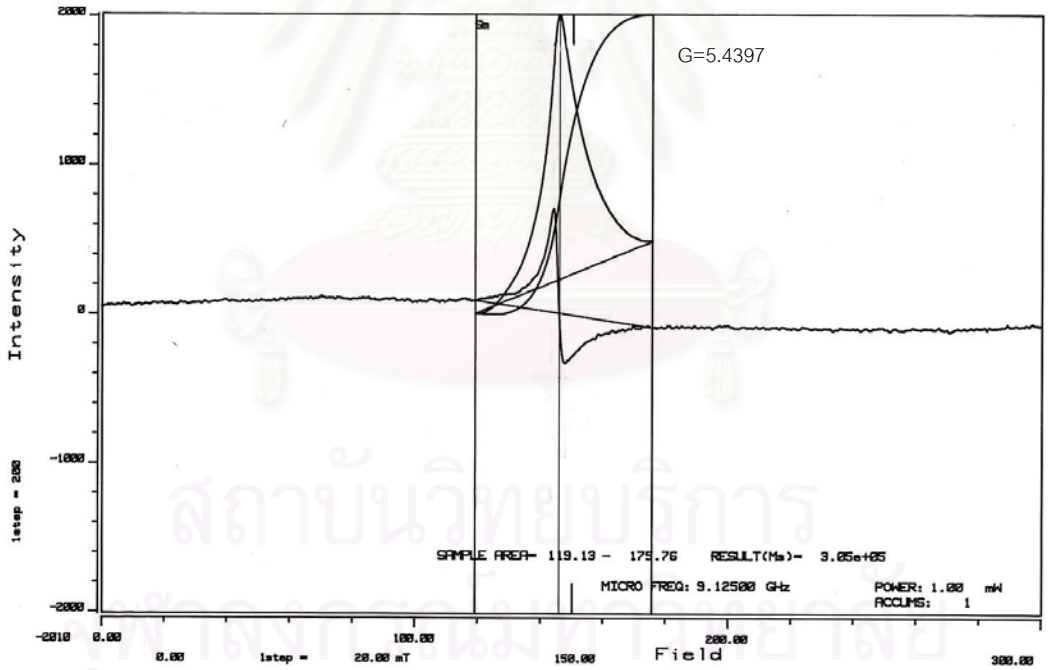

(b)

Figure 5.56 ESR spectra of high spin Co^{2+} of 0.4%Pd/Co/HZSM-5 (a) fresh catalyst, (b) pretreated catalyst.

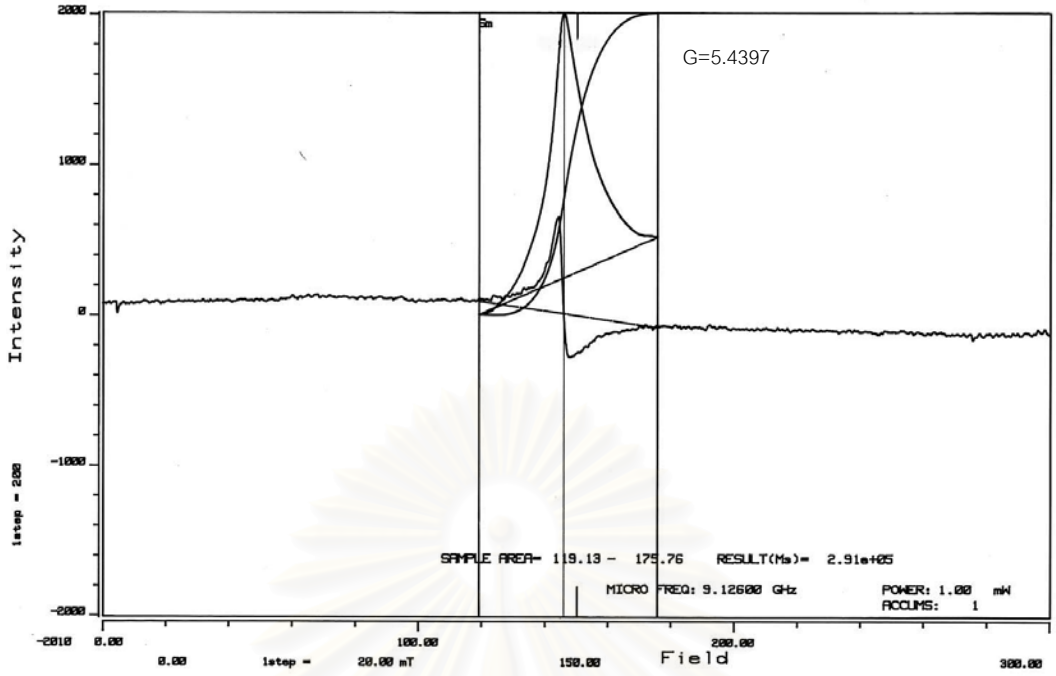

(a)

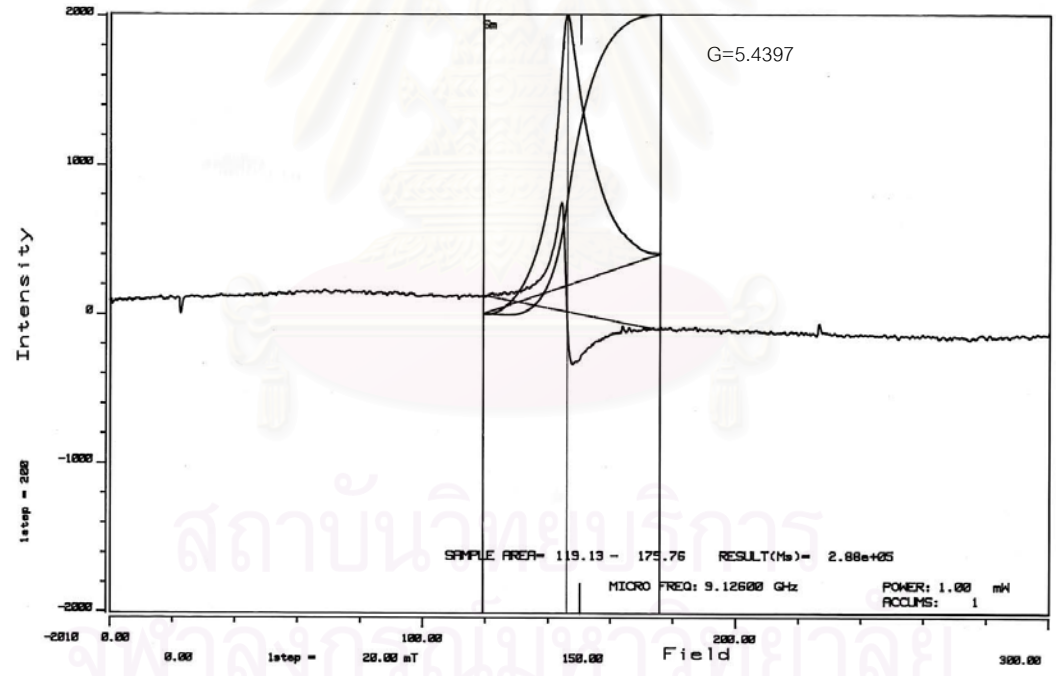

(b)

Figure 5.57 ESR spectra of high spin Co^{2+} of 0.6%Pd/Co/HZSM-5 (a) fresh catalyst, (b) pretreated catalyst.

5.1.3.2 Catalytic Performance

In order to compare the catalytic performance of the catalysts, NO conversion reactions were carried out on the catalysts both with and without pretreatment. The effect of the reaction temperature on NO conversion to N_2 and methane conversion for Co/HZSM-5 and Pd/HZSM-5 with different of Pd is shown in Figures 5.39 and 5.58, respectively. The fresh Co/HZSM-5 and Pd/HZSM-5 gave maximum NO conversions of approx. 45% and 35% at a reaction temperature of 450 °C, respectively. At this temperature the Pd/HZSM-5 reached 100% of methane conversion and 60% in Co/HZSM-5. At higher temperatures, the NO conversion falls in both catalysts. In comparison, the Co/HZSM-5 and Pd/HZSM-5 showed a dramatically lower conversion of NO at 300 to 600°C after hydrothermal treatment. However, the margin difference in catalyst activity before and after pretreatment was alleviated with the presence of a certain amount of Pd (ca. 0.4wt% loading), as shown in Figures 5.59-5.61. When the amount of Pd was raised higher than 0.4wt%, 0.6%Pd/Co/HZSM-5, such beneficial effect on the durability of Co/HZSM-5 was surprisingly lost as shown in Figure 5.62. The percentage of reaction durability, defined as the maximum NO conversion of pretreated catalysts per maximum NO conversion of fresh catalysts, was calculated and is reported above the bar in Figure 5.62. The presence of Pd improved the methane conversion of the pretreated catalyst similar to NO conversion. Nevertheless, while the improvement of NO conversion for the pretreated catalysts was limited with the presence of a certain amount of Pd, the methane conversion was almost continuously improved with the increasing amount of Pd. This indicates that methane would not be effective for use in NO conversion on Pd/Co/H-MFI with high Pd loading. Therefore, this should be one of the reasons for the limitation of NO conversion improvement on Pd/Co/H-MFI after hydrothermal treatment by an optimum amount of Pd. In addition, the possibility of any changes in Pd and Co on H-MFI such as alloying and/or the formation of palladium oxides in case of high Pd loading should not be ruled out.

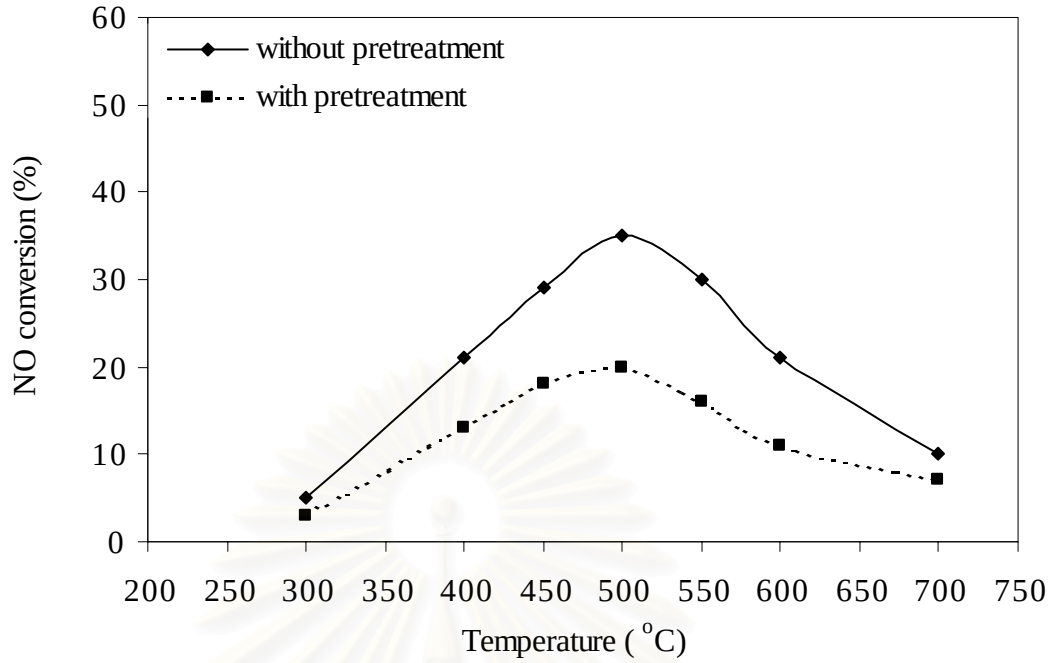

(a)

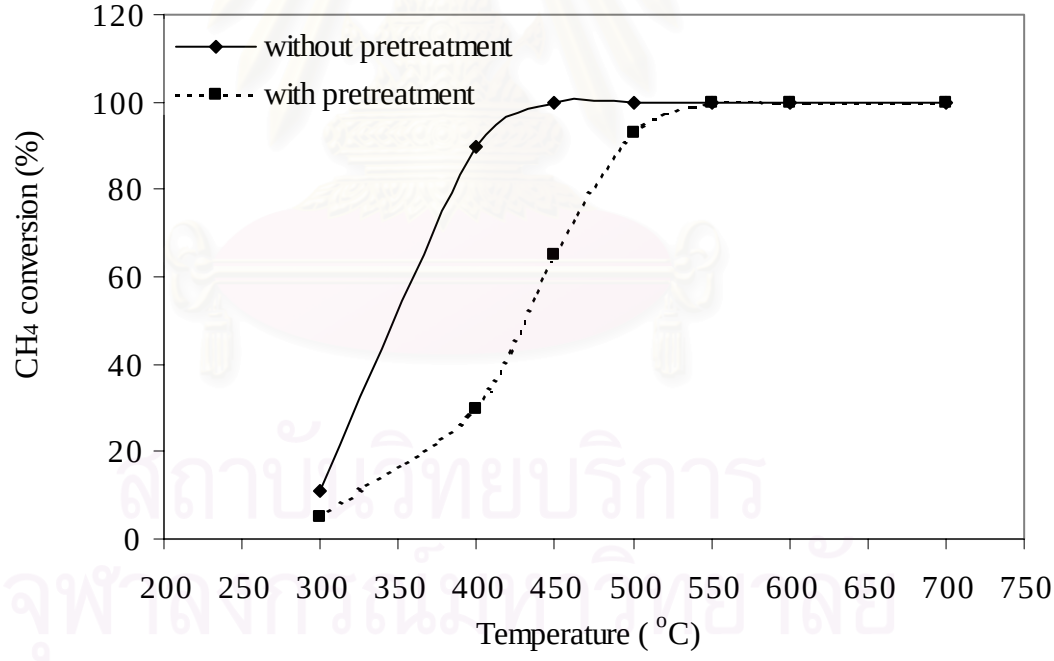

(b)

Figure 5.58 The effect of hydrothermal pretreatment of Pd/HZSM-5 on (a) NO conversion(%), (b) CH_4 conversion(%). Feed gas: NO 1000 ppm, methane 1%, O_2 10% He balance, GHSV 10,000 h^{-1}.

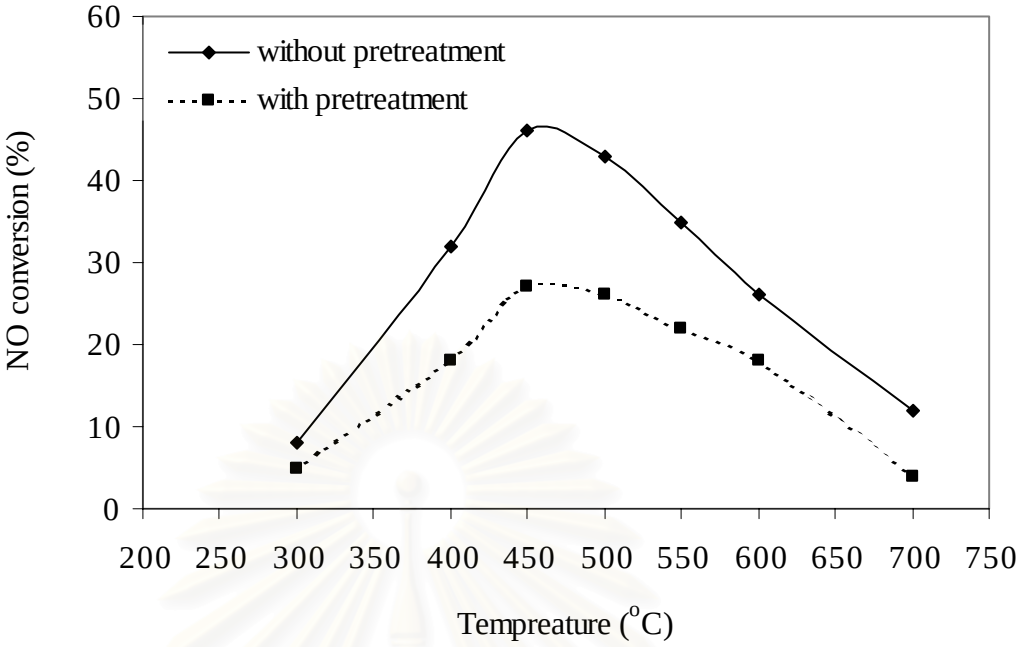

(a)

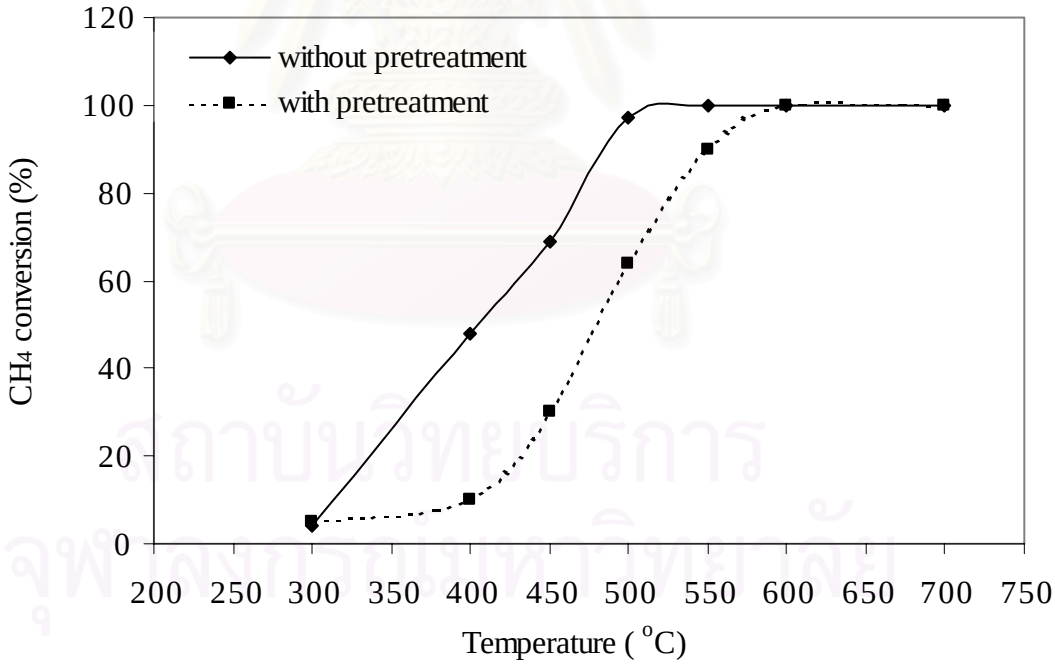

(b)

Figure 5.59 The effect of hydrothermal pretreatment of 0.1%Pd/Co/HZSM-5 on (a) NO conversion(%), (b) CH_4 conversion(%). Feed gas: NO 1000 ppm, methane 1%, O_2 10% He balance, GHSV 10,000 h^{-1}.

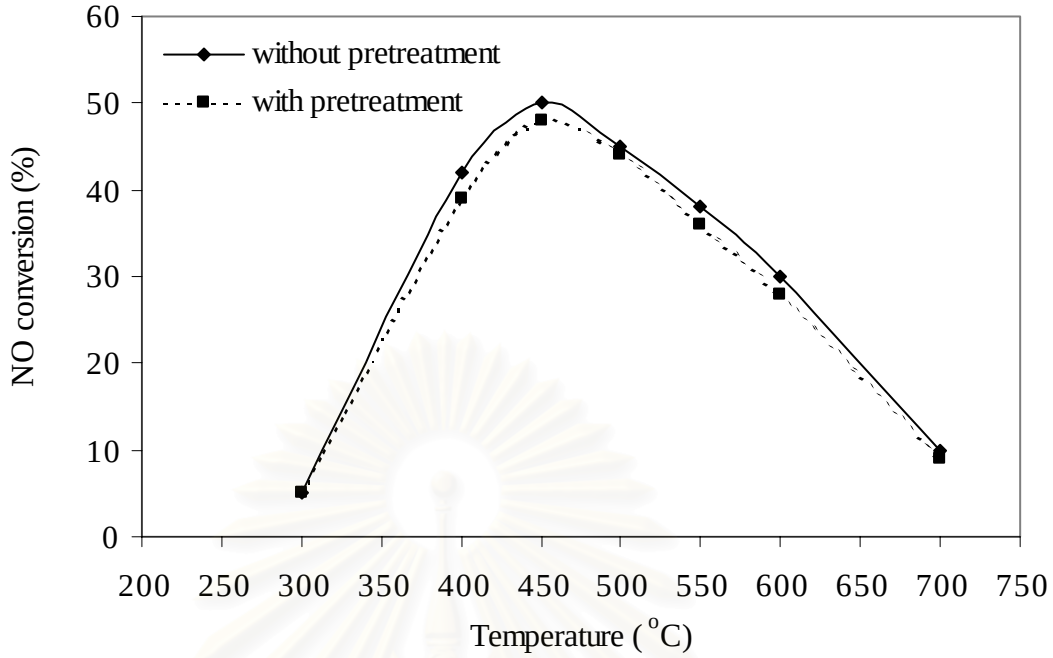

(a)

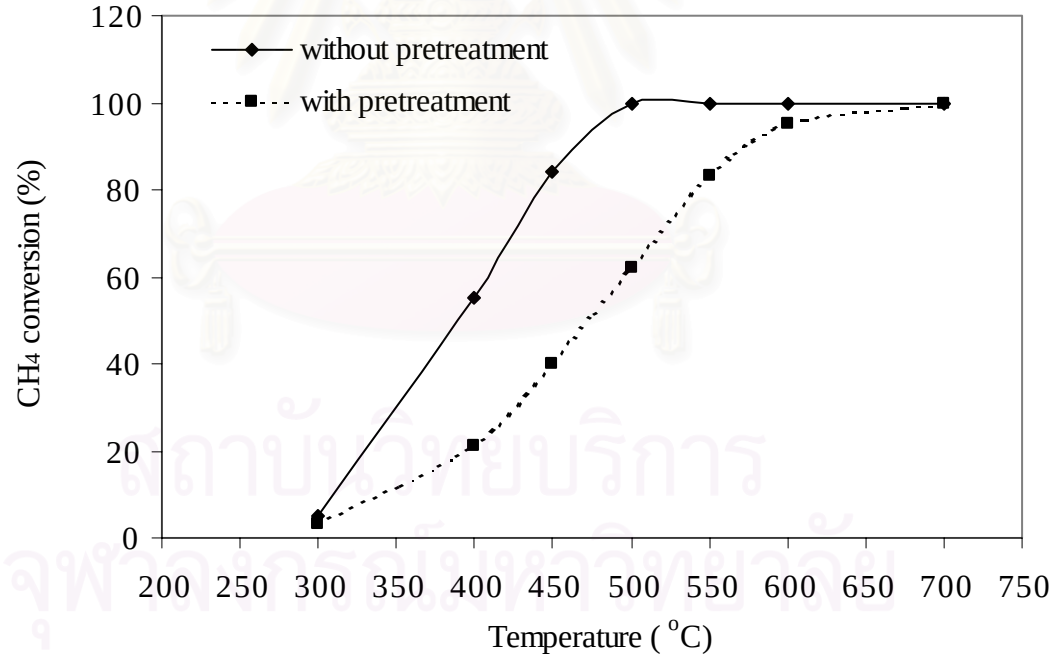

(b)

Figure 5.60 The effect of hydrothermal pretreatment of 0.4%Pd/Co/HZSM-5 on (a) NO conversion(%), (b) CH_4 conversion(%). Feed gas: NO 1000 ppm, methane 1%, O_2 10% He balance, GHSV 10,000 h^{-1}.

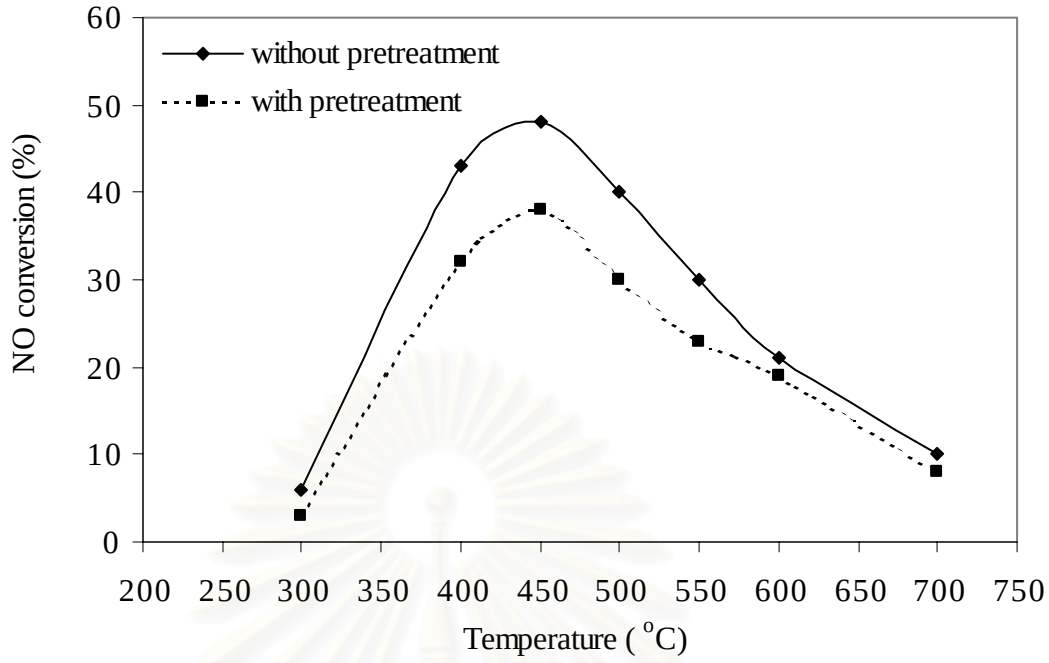

(a)

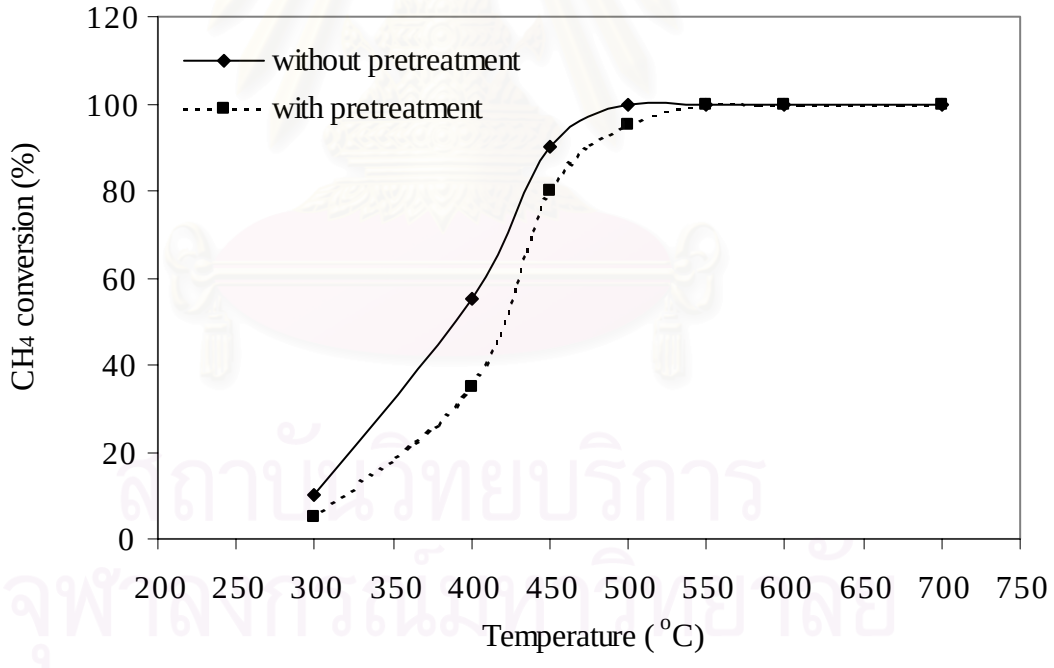

(b)

Figure 5.61 The effect of hydrothermal pretreatment of 0.6%Pd/Co/HZSM-5 on (a) NO conversion(%), (b) CH_4 conversion(%). Feed gas: NO 1000 ppm, methane 1%, O_2 10% He balance, GHSV 10,000 h^{-1}.

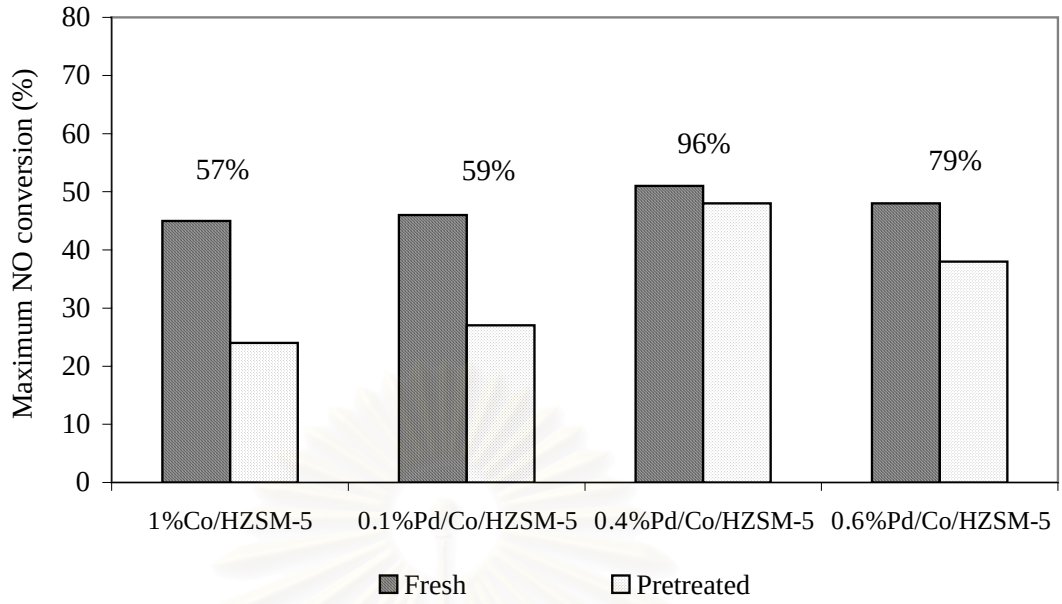

Figure 5.62 The percentage of maximum NO conversion and the values of percentage of reaction durability of catalysts.

In summary, the ZSM-5 framework stability of Co/ZSM-5 was maintained after pretreatment at 600 ^{o}C in a He stream with 10 mol% H_2O for 24 h by the presence of Pd. The dealumination of tetrahedral Al in ZSM-5 framework was completely prevented when the amount of Pd loading was 0.4 wt% or higher. The stabilization effects of Pd are due to the prevention of dealumination. The presence of an optimum amount of Pd in Pd/Co/HZSM-5, approximately 0.4 wt% loading, improved the catalysts durability for NO removal under hydrothermal treatment.

5.2 Effect of crystal size on the durability improvement of Co/HZSM-5 under hydrothermal pretreatment for NO removal by methane

5.2.1 Characterization of the catalysts

The prepared Co ion-exchanged ZSM-5 catalysts were characterized. For the first, the prepared catalysts were performed to confirm the MFI structure and measured the crystallinity by XRD. Second, the crystal size vales estimated for SEM. Next, the metal content were determined by AAS. The spectra characteristics of Co^{2+} were recorded by ESR. Additionally ^{27}Al-MAS-NMR analysis was also performed.

5.2.1.1 X-Ray Diffraction pattern

The X-ray diffraction patterns for the prepared catalysts are shown in Figure 5.63-5.67. All XRD patterns of catalysts correspond well with those report in the literature[116]. This indicates that the prepared MFI catalyst has the same structure as that of the reference.

5.2.1.2 Morphology

Scanning Electron Microscopy (SEM) photographs of the prepared catalysts are shown in Figure 5.68-5.72. As shown, the shape of all catalysts are roughly crystallized spherical particles which are composed of many small regular plates. The crystal sizes of the zeolite samples were measured from scanning electron micrographs by averaging the diameter of a hundred primary particles based on the particle diameter. Crystal size values estimated from SEM images of the catalyst have been reported in many research investigations [95,99,103]. Considerations of the SEM photographs depicted in Figures 5.68-5.72, indicated the diameters of Co/HZSM-5 zeolite samples were 1.0, 1.8, 3.0, 5.6 and 7.6 μm.

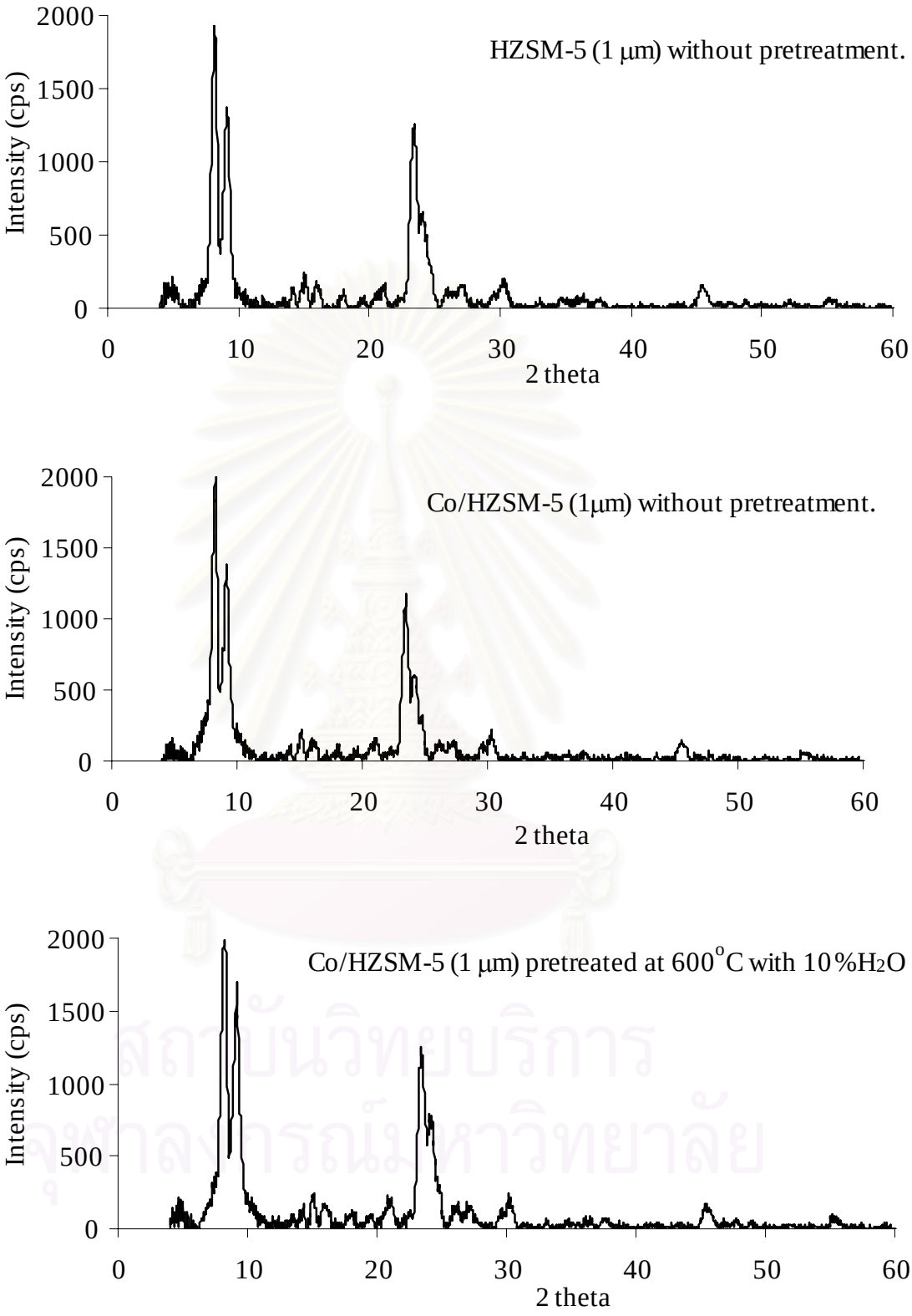

Figure 5.63 XRD patterns of HZSM-5(1μm) and Co/HZSM-5(1μm) catalysts

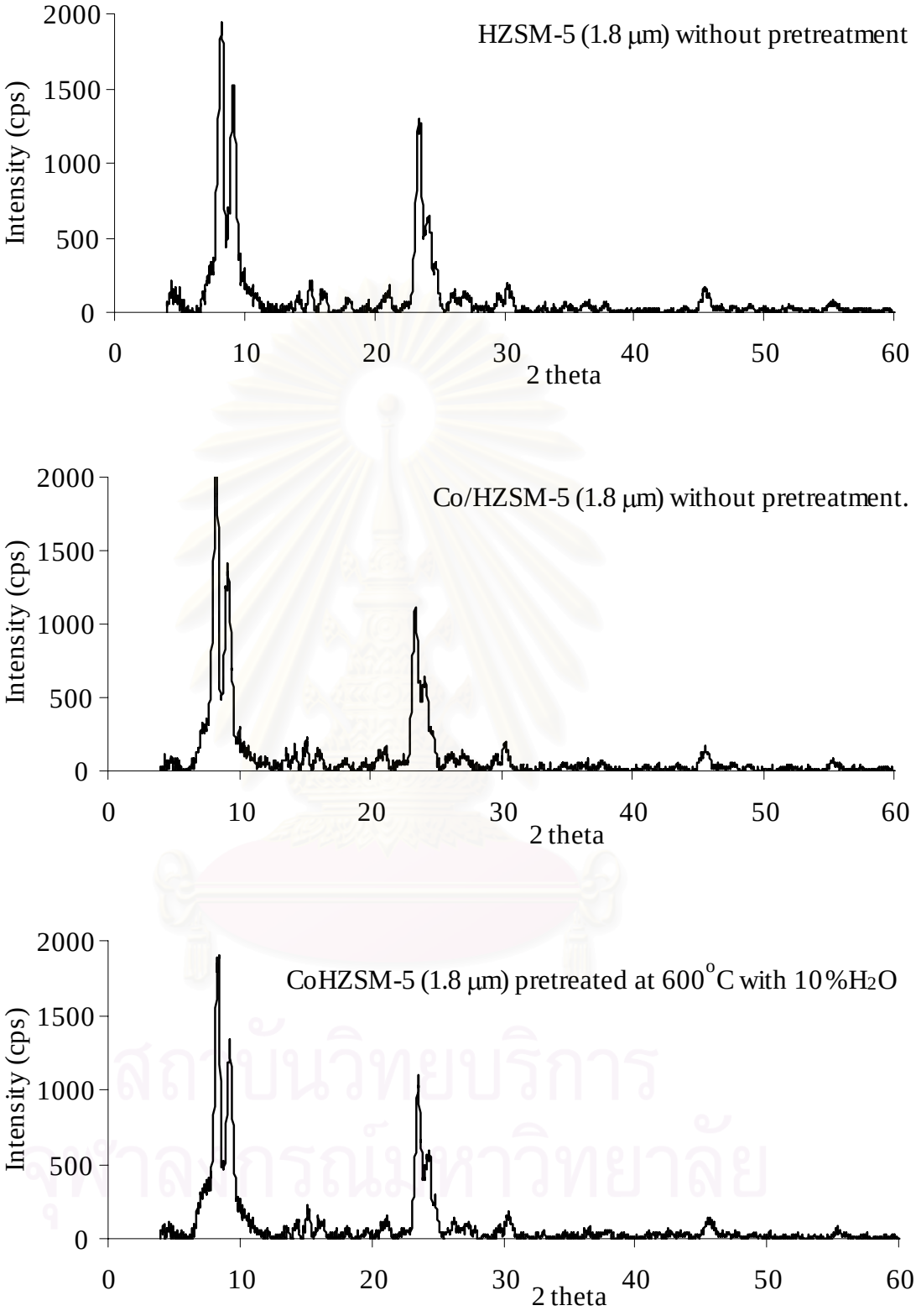

Figure 5.64 XRD patterns of HZSM-5(1.8μm) and Co/HZSM-5(1.8μm) catalysts

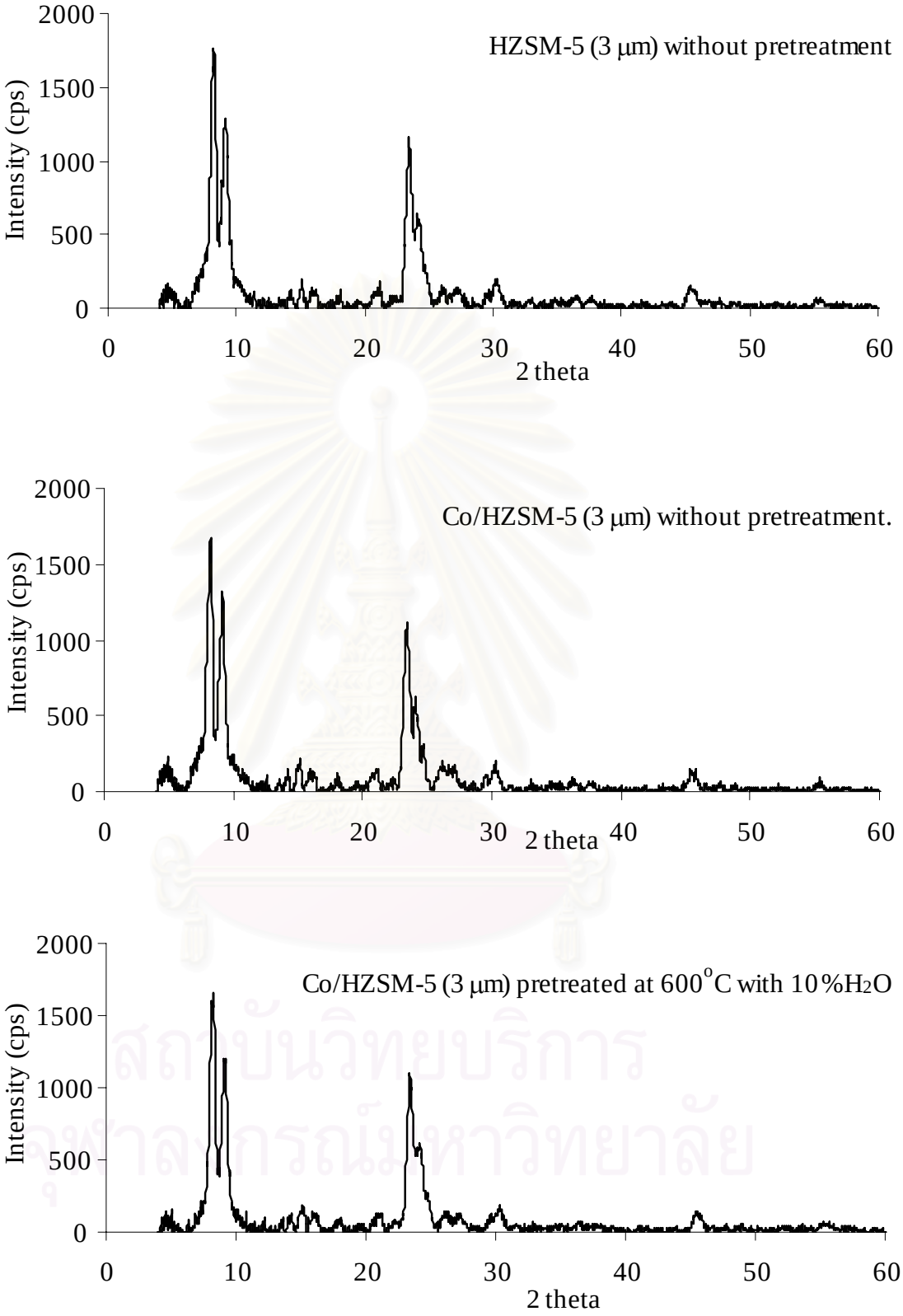

Figure 5.65 XRD patterns of HZSM-5(3μm) and Co/HZSM-5(3μm) catalysts

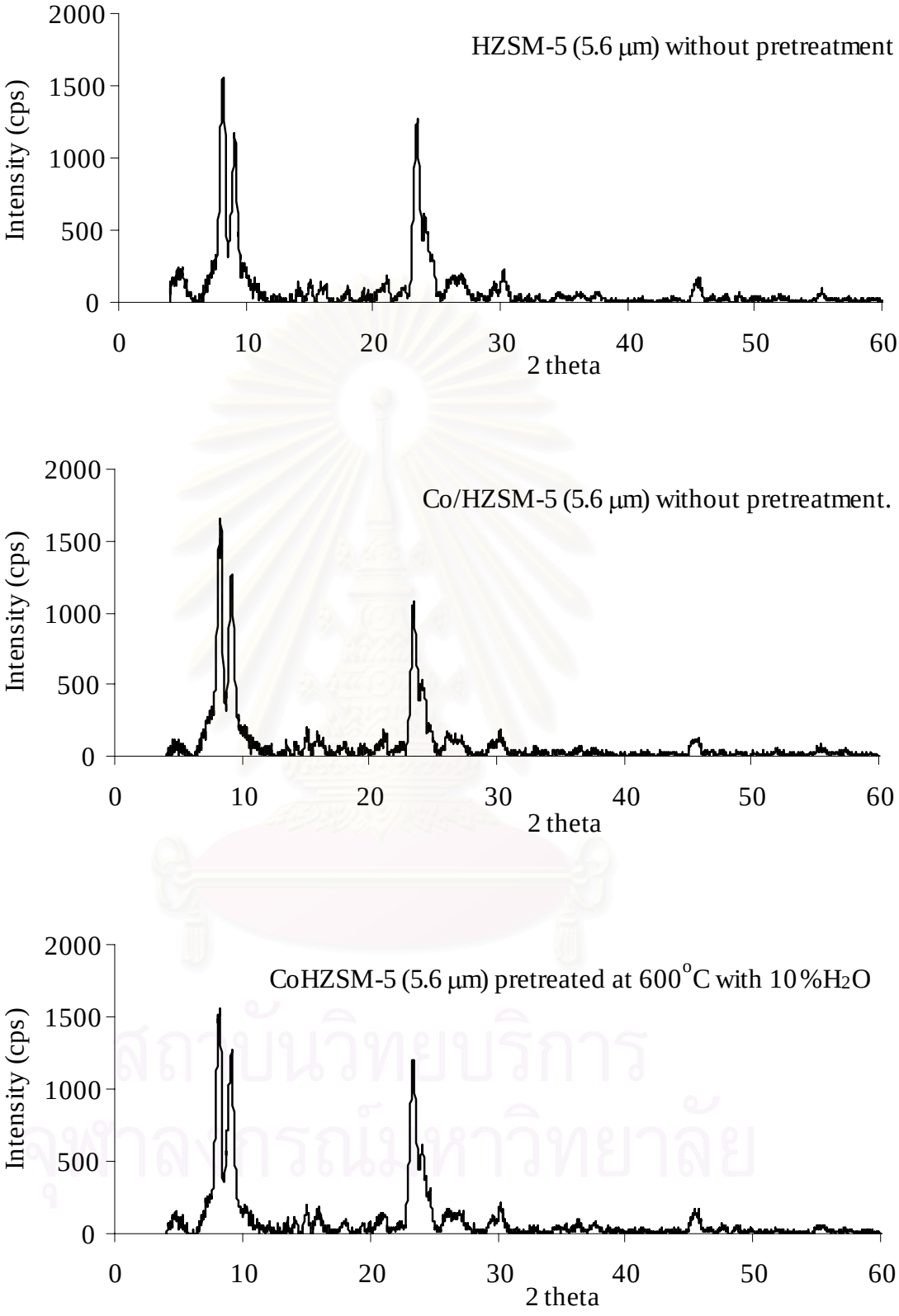

Figure 5.66 XRD patterns of HZSM-5(5.6μm) and Co/HZSM-5(5.6μm) catalysts

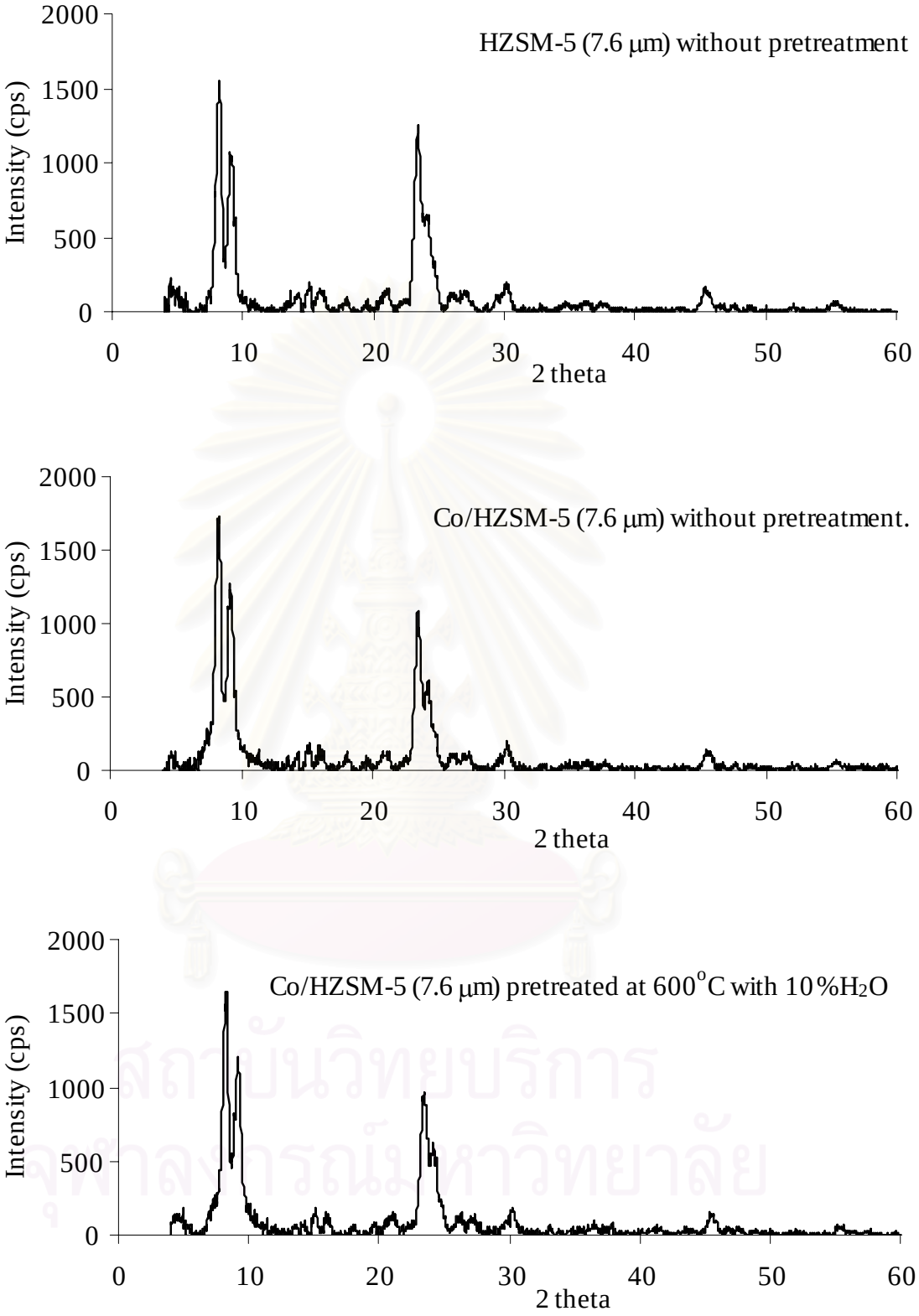

Figure 5.67 XRD patterns of HZSM-5(7.6μm) and Co/HZSM-5(7.6μm) catalysts

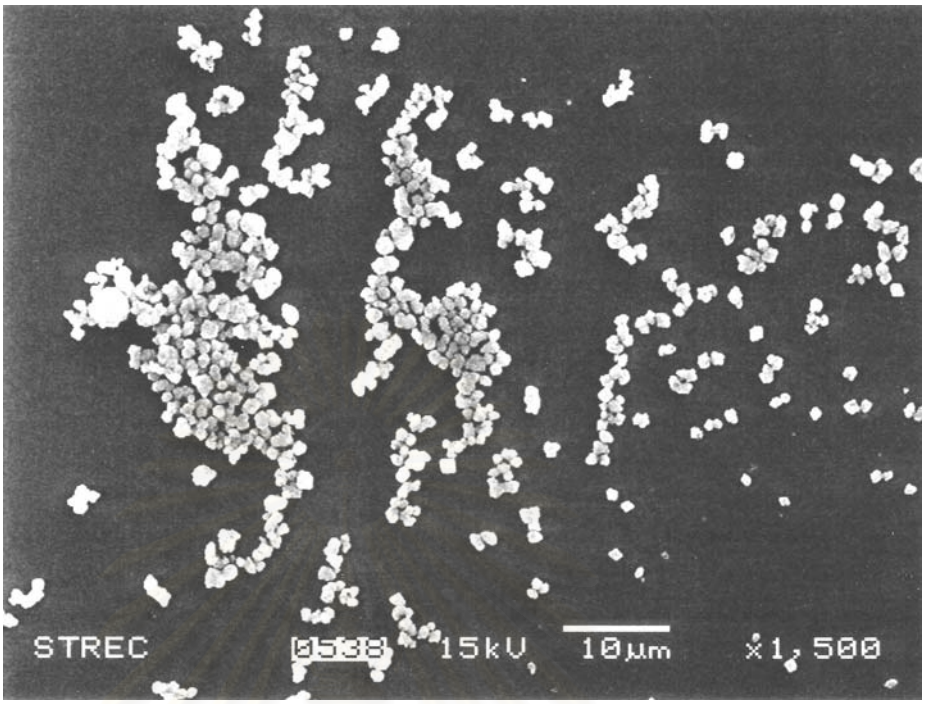

Figure 5.68 Scanning electron micrograph of Co/HZSM-5 (1 µm) catalyst

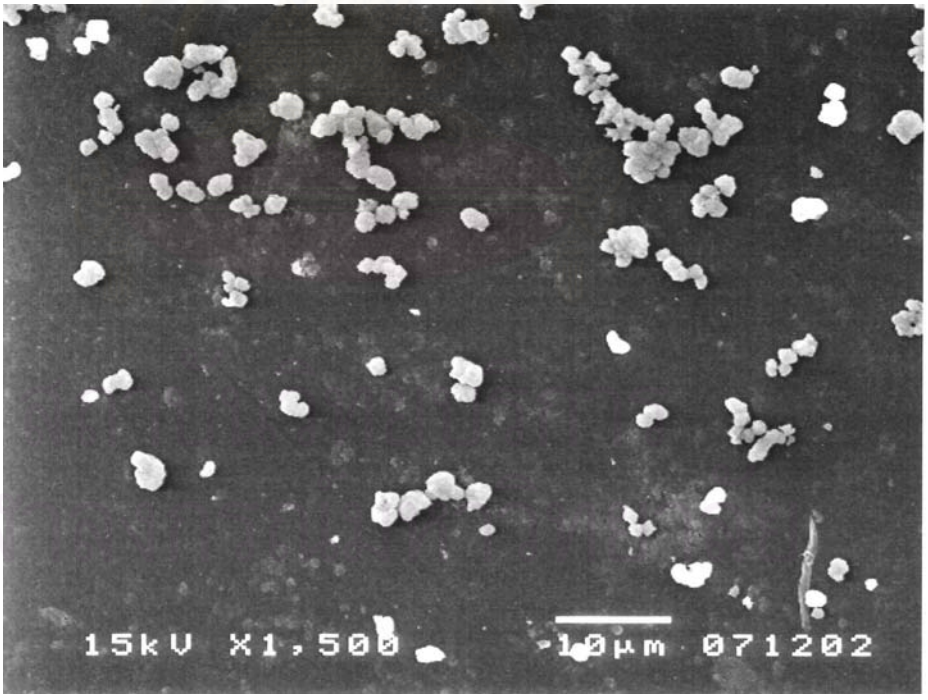

Figure 5.69 Scanning electron micrograph of Co/HZSM-5 (1.8 µm) catalyst

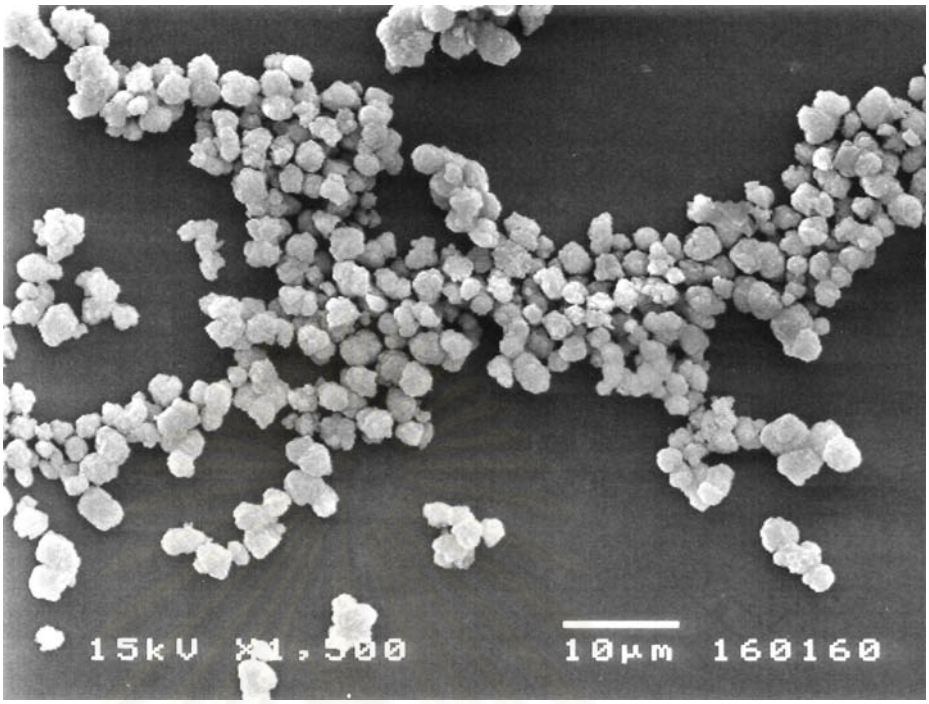

Figure 5.70 Scanning electron micrograph of Co/HZSM-5 (3 µm) catalyst

Figure 5.71 Scanning electron micrograph of Co/HZSM-5 (5.6 µm) catalyst

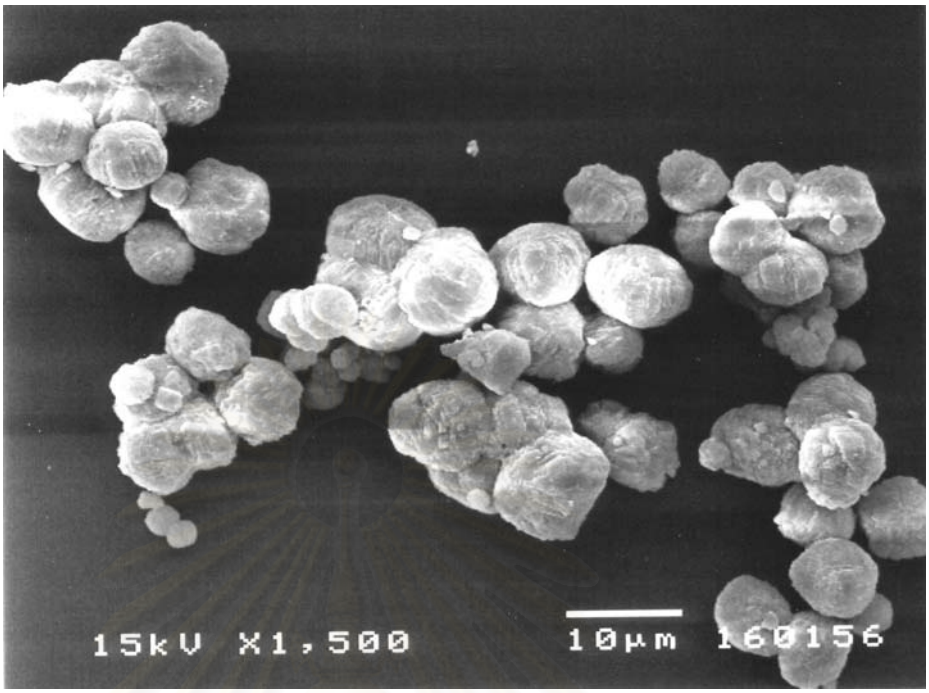

Figure 5.72 Scanning electron micrograph of Co/HZSM-5 (7.6 μm) catalyst

Table 5.3 Physical properties of various crystal sizes of Co/HZSM-5 catalysts

Catalyst	Crystal diameter by SEM(μm)	Si/Al atomic ratio	Co/Al atomic ratio	BET surface area (m^2/g)		%Crystallinity		The relative area of tetrahedral ^{27}Al (%)	
				fresh	pretreated	fresh	pretreated	fresh	pretreated
Co/HZSM-5(1.0μm)	1.0	22.3	0.173	454	443	99	98	85	83
Co/HZSM-5(1.8μm)	1.8	23.1	0.179	434	418	98	96	83	80
Co/HZSM-5(3.0μm)	3.0	23.1	0.175	458	431	99	95	80	73
Co/HZSM-5(5.6μm)	5.6	22.2	0.170	439	401	93	86	77	67
Co/HZSM-5(7.6μm)	7.6	23.0	0.177	447	404	95	87	78	65

5.2.1.3 Physical Properties

The results shown in Table 5.3 indicate that after hydrothermal treatment the BET surface areas of Co/HZSM-5 (5.6μm) and Co/HZSM-5 (7.6μm) were significantly decreased, however for the small crystal size catalysts, Co/HZSM-5 (1.0μm) and Co/HZSM-5 (1.8μm), only a slight decrease in surface area was observed. According to XRD profiles of the fresh catalysts, the crystallinity of Co/HZSM-5 (1.0μm), and Co/HZSM-5 (1.8μm) was found to be higher than that of Co/HZSM-5 (5.6μm) and Co/HZSM-5 (7.6μm). It was also found that, after ion-exchange of Co into HZSM-5, the large crystal size catalyst lost more crystallinity than the small crystal size catalyst. After hydrothermal treatment at 600 ^{o}C in 10% water for 24 h, no significant change in morphology of the samples was observed. As shown in Table 5.3, the large crystal size catalysts lost a considerable degree of their crystallinity after hydrothermal treatment; especially for Co/HZSM-5 (5.6μm) and Co/HZSM-5 (7.6μm). In contrast, for Co/HZSM-5 (1.0μm) and Co/HZSM-5 (1.8μm) only a slight decrease in crystallinity was observed upon hydrothermal treatment. Consequently, it definitely appears that the smaller crystal size Co/HZSM-5 catalysts are higher durability than those with large crystal size on hydrothermal treatment with respect to crystallinity.

5.2.1.4 Dealumination

Figures 5.73-5.77 show the ^{27}Al MAS NMR spectra of fresh Co/HZSM-5 and pretreated Co/HZSM-5 for various crystal sizes. The observed spectra confirmed that severe steam treatment causes dealumination. The catalysts exhibited two signals at approx. 60 ppm, which is assigned to the tetrahedral aluminum, and at approx. 0 ppm, which is attributed to the extra lattice octahedral aluminum in the zeolite lattice [82]. For the small crystal size, samples Co/HZSM-5 (1.0μm) and Co/HZSM-5 (1.8μm), there are no significant changes in the ^{27}Al-MASNMR spectra for both the fresh and pretreated catalysts. On the other hand, the large crystal size catalysts, Co/HZSM-5 (5.6μm) and Co/HZSM-5 (7.6μm), showed a loss of tetrahedral aluminum but an increase in octahedral aluminum after hydrothermal treatment. This is consistent with a previous report that a loss in activity and durability results after steam pretreatment was due to framework dealumination of the zeolite [82]. Based on ^{27}Al-MASNMR signals, the results obtained for the stabilization of the tetrahedral aluminum by different crystal sizes are summarized in Table 5.3. After hydrothermal treatment of the catalysts, the relative area of tetrahedral ^{27}Al is decreased similarly in accord with the BET surface area and crystallinity. It can be concluded that for the small crystal size catalysts, Co/HZSM-5 (1.0μm) and Co/HZSM-5 (1.8μm), the zeolite framework structure is stabilized, preventing the occurrence of dealumination.

A similar dependence for the relative loss of crystallinity and the relative loss of tetrahedral aluminum on crystal size are shown in Figures 5.78 and 5.79, respectively. The relative loss of crystallinity and tetrahedral aluminum are defined as the difference between fresh and pretreated catalysts per fresh catalyst. After hydrothermal treatment, the small crystal size catalyst showed a slight decrease in crystallinity and moderate loss of tetrahedral aluminum while the large crystal size catalysts lost a considerable amount of their crystallinity and their tetrahedral aluminum, which resulted in lower durability in the case of large crystal size catalysts. However, the reason for less dealumination for the smaller crystal size catalysts is still unclear. It might be expected that the large crystal size catalyst may have many defect points compared with the small size catalyst. Consequently, further studies which aim at clearly describing the influence of crystal size effects on durability are warranted.

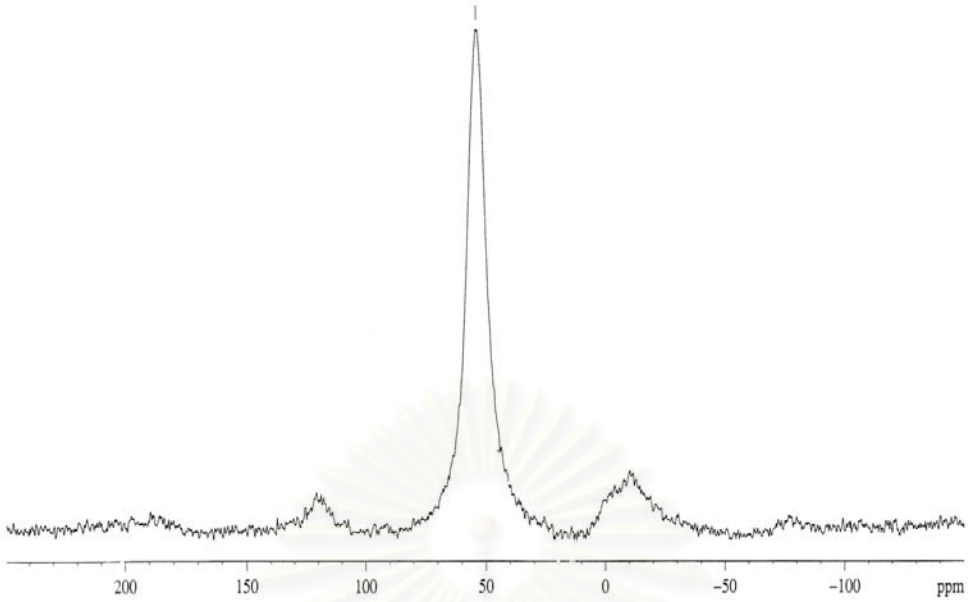

(a)

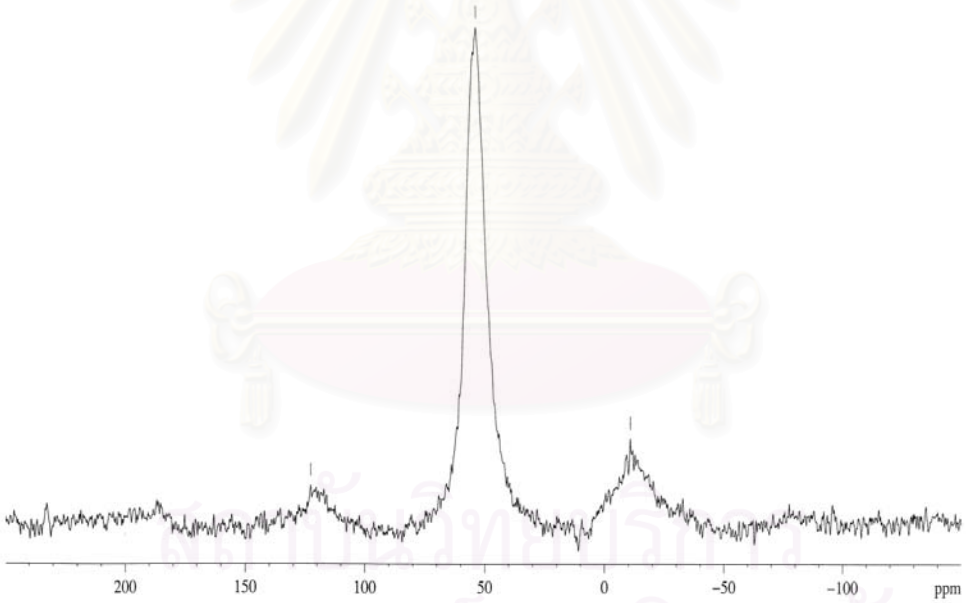

(b)

Figure 5.73 ^{27}Al MAS-NMR spectra of Co/HZSM-5(1 μm) (a) fresh catalyst, (b) pretreated catalyst.

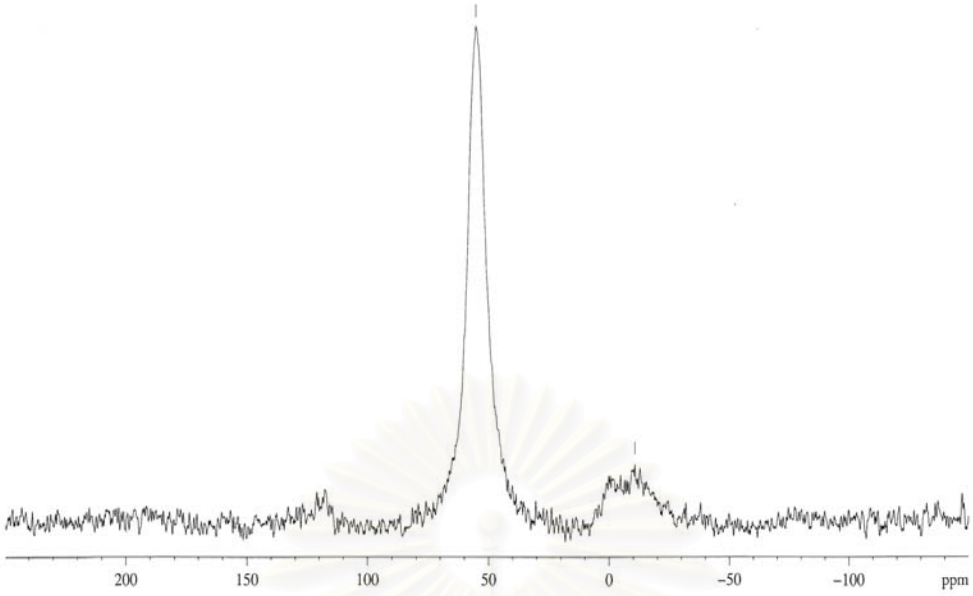

(b)

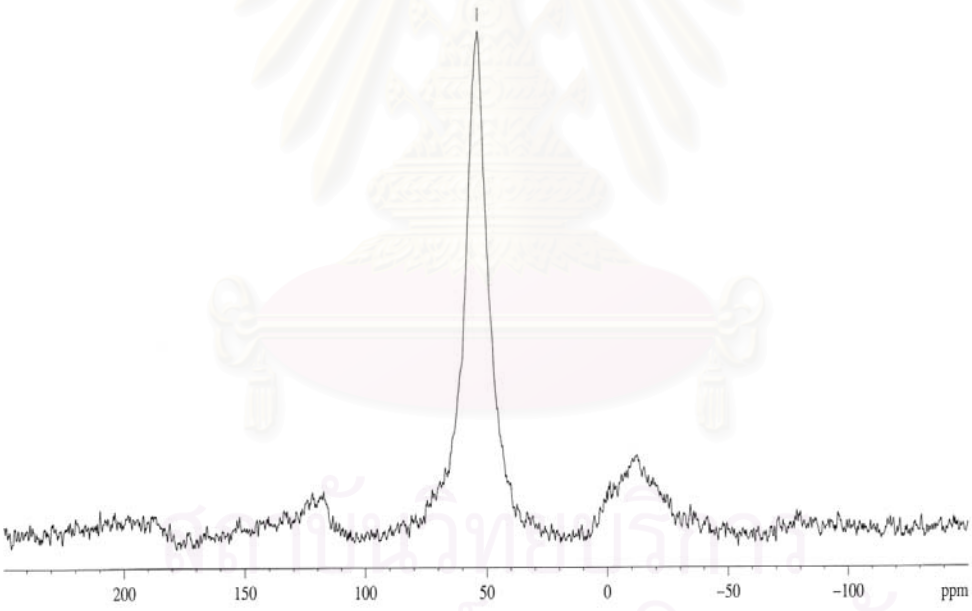

(b)

Figure 5.74 ^{27}Al MAS-NMR spectra of Co/HZSM-5(1.8 μm) (a) fresh catalyst, (b) pretreated catalyst.

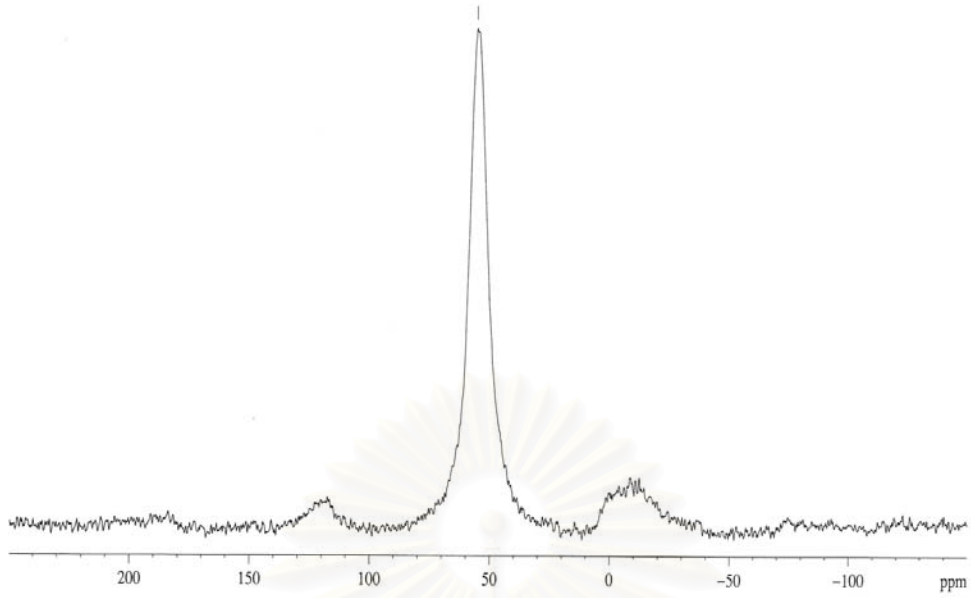

(a)

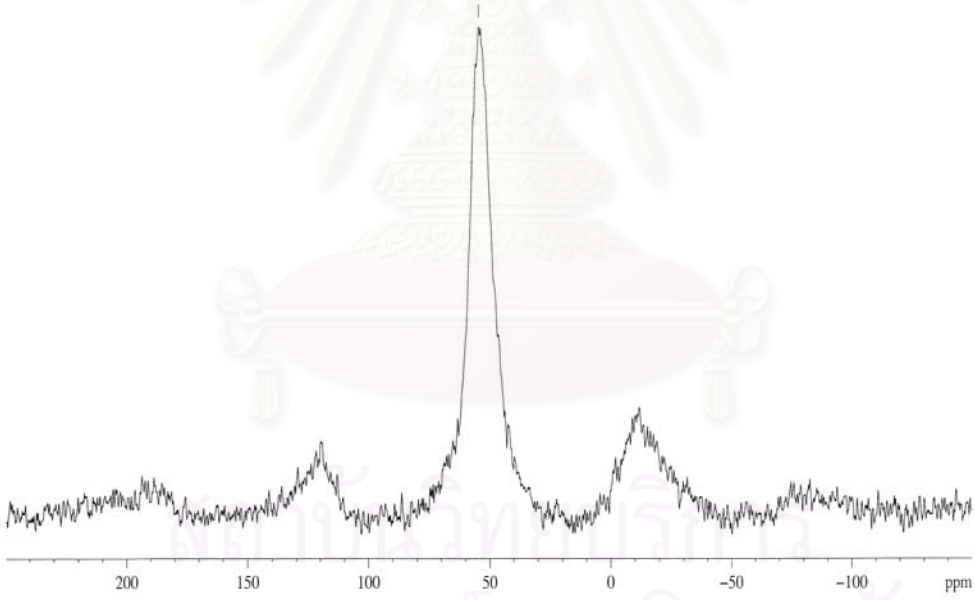

(b)

Figure 5.75 ^{27}Al MAS-NMR spectra of Co/HZSM-5(3 μm) (a) fresh catalyst, (b) pretreated catalyst.

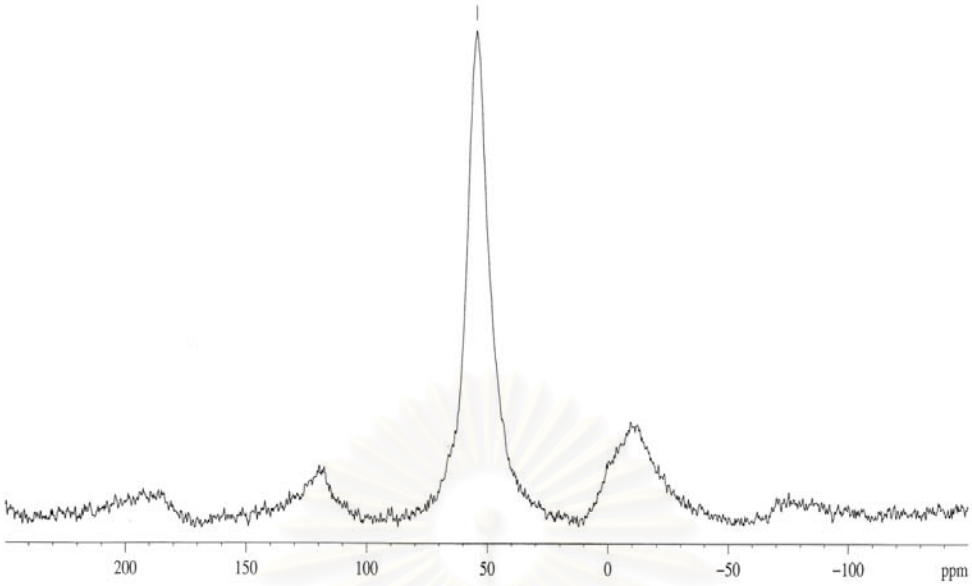

(a)

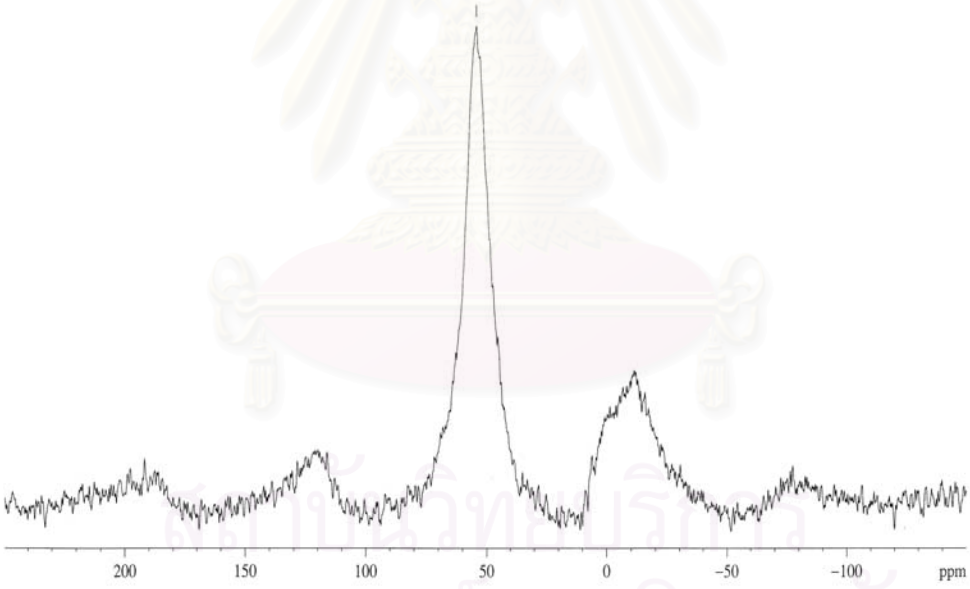

(b)

Figure 5.76 ^{27}Al MAS-NMR spectra of Co/HZSM-5(5.6 μm) (a) fresh catalyst, (b) pretreated catalyst.

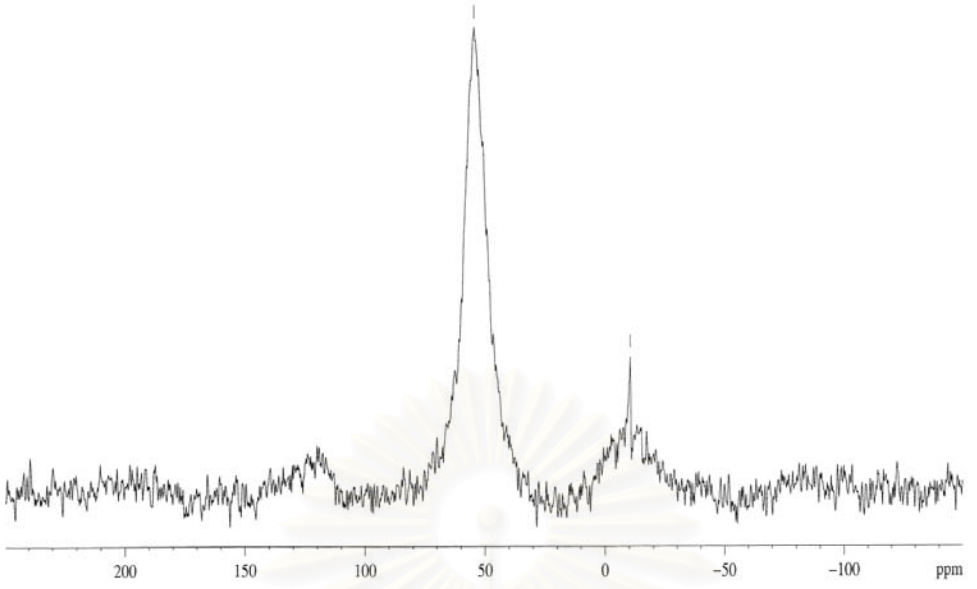

(a)

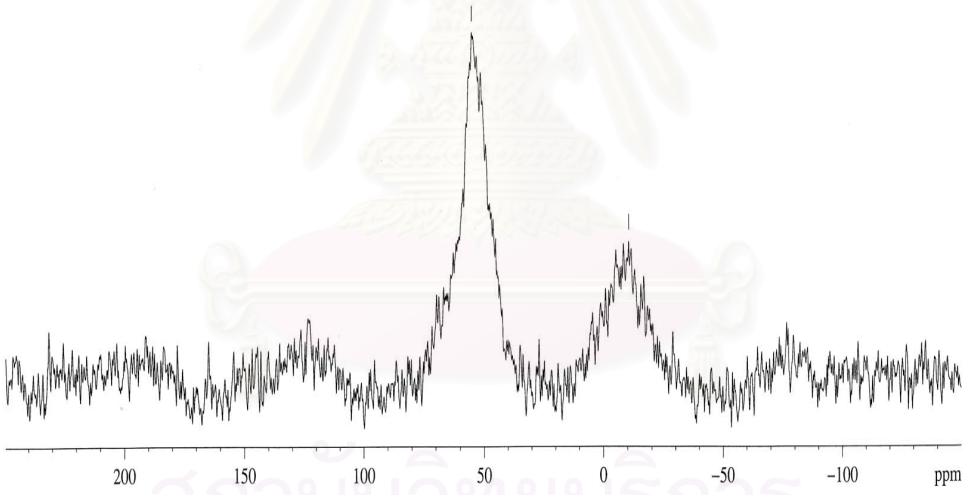

(b)

Figure 5.77 ^{27}Al MAS-NMR spectra of Co/HZSM-5(7.6 μm) (a) fresh catalyst, (b) pretreated catalyst.

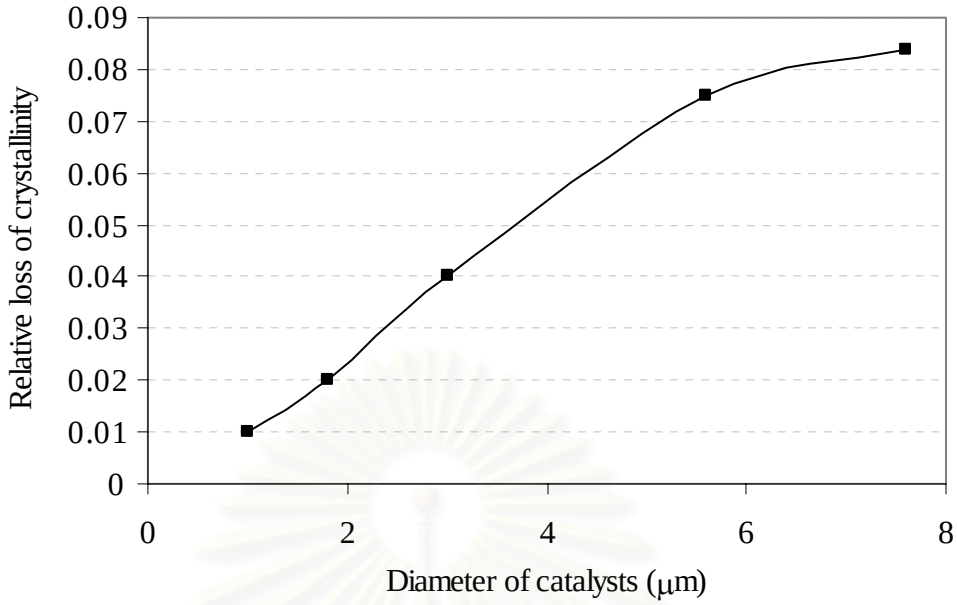

Figure 5.78 The effect of crystal size on the relative loss of crystallinity(ν)

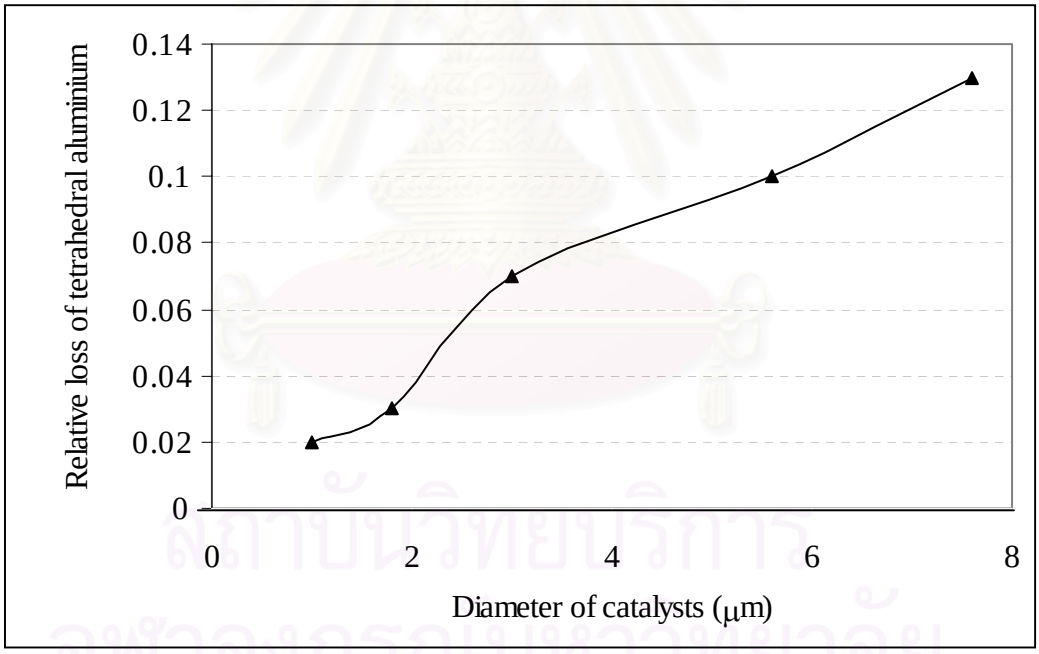

Figure 5.79 The effect of crystal size on the relative loss of tetrahedral aluminium(σ)

5.2.1.5 Electron Spin Resonance

The ESR spectra of fresh and pretreated catalyst of Co/HZSM-5 are shown in Figures 5.80-5.86. The spectra of all Co/HZSM-5 catalysts are similar. The same type of Co^{2+} coordination present the g values in the range of 5.4391-5.4409. It indicate that there is no any change in state of cobalt ion, which was observed in the zeolite.

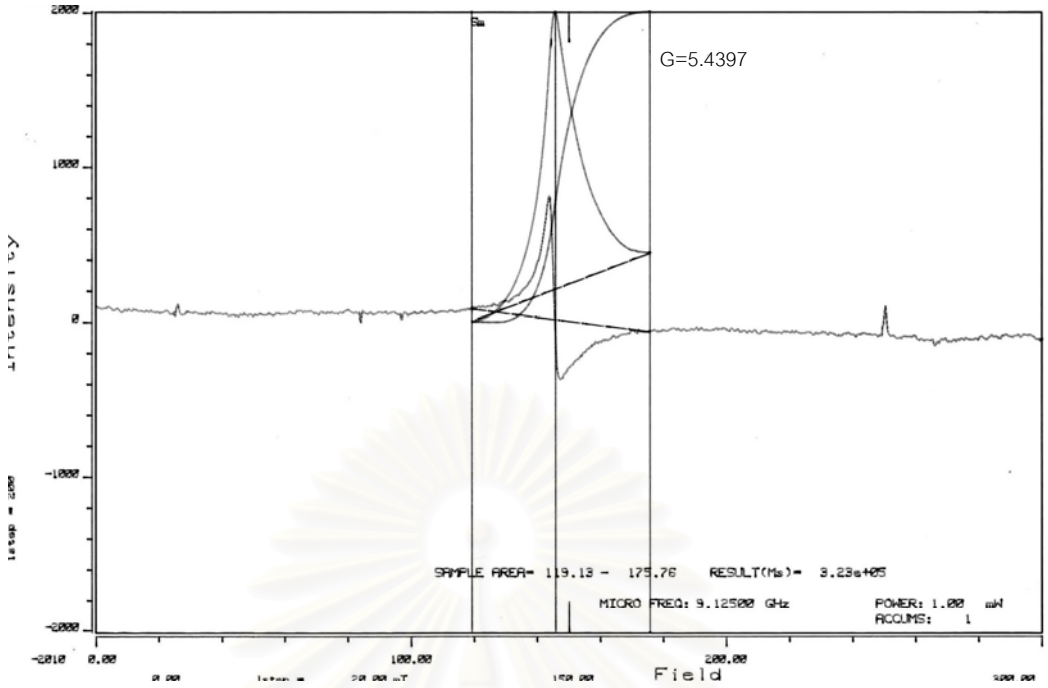

(a)

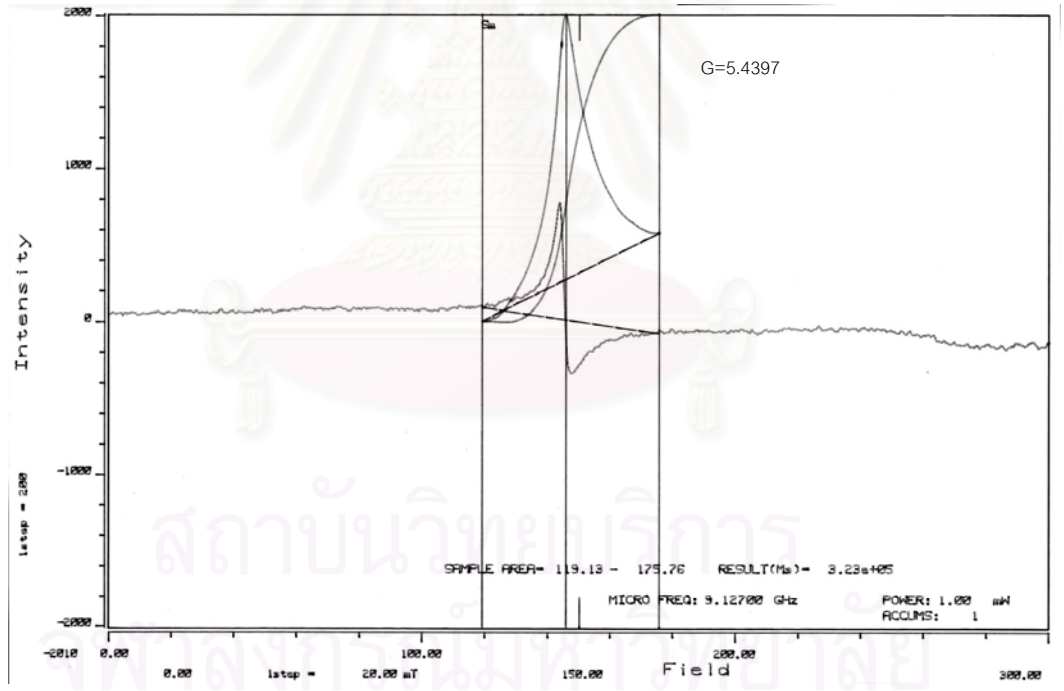

(b)

Figure 5.80 ESR spectra of high spin Co^{2+} of Co/HZSM-5 (1μm)(a) fresh catalyst, (b) pretreated catalyst.

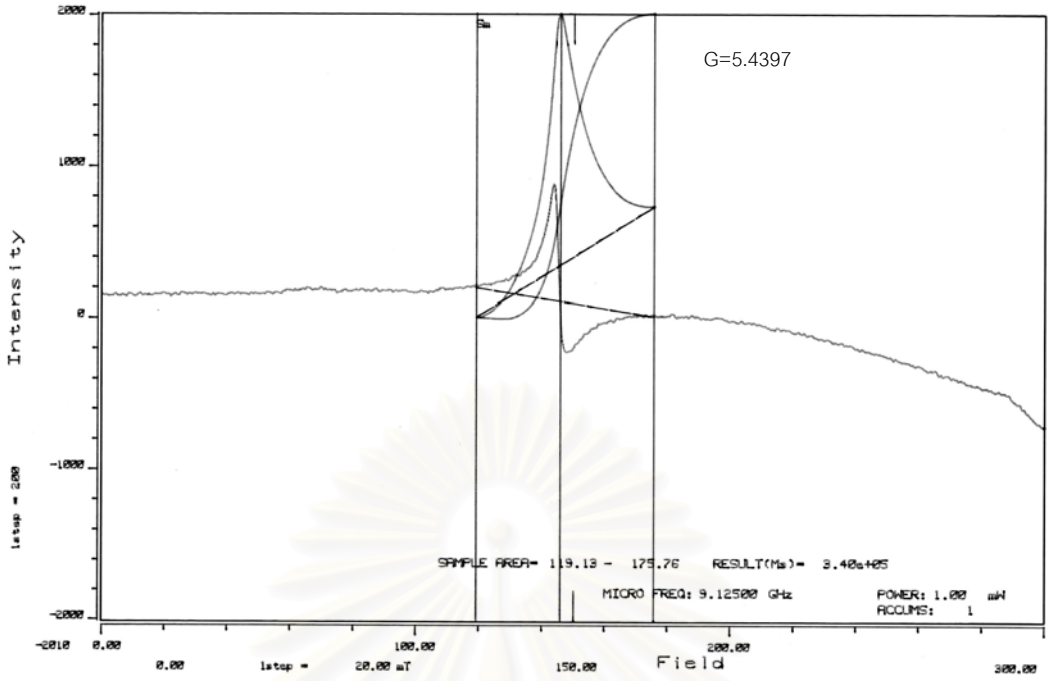

(a)

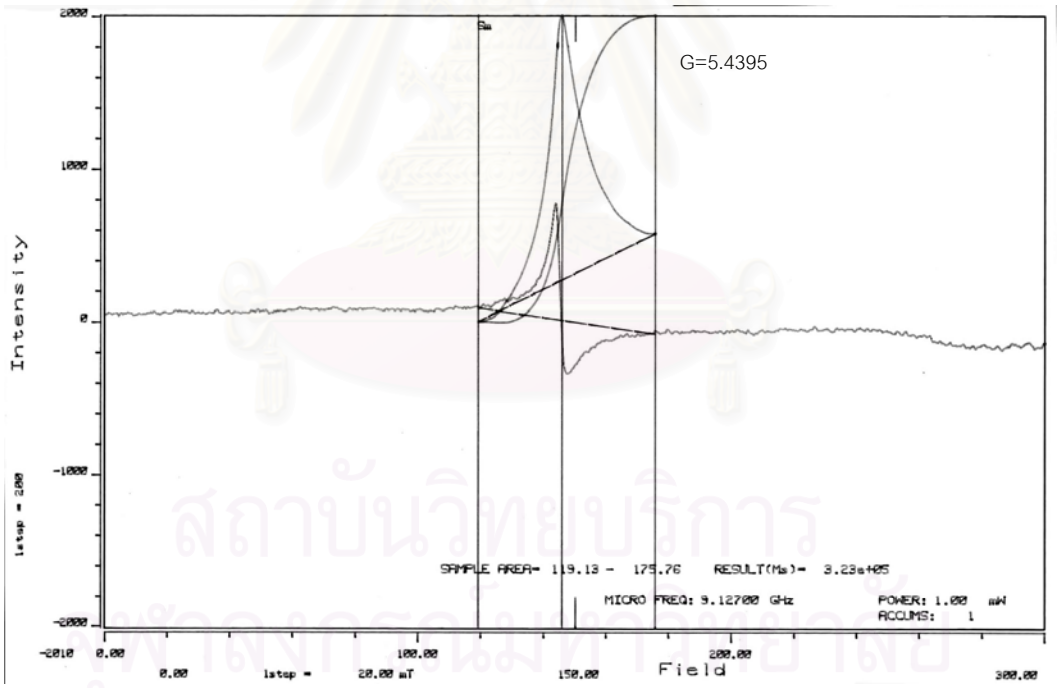

(b)

Figure 5.81 ESR spectra of high spin Co^{2+} of Co/HZSM-5 (1.8 μm)(a) fresh catalyst, (b) pretreated catalyst.

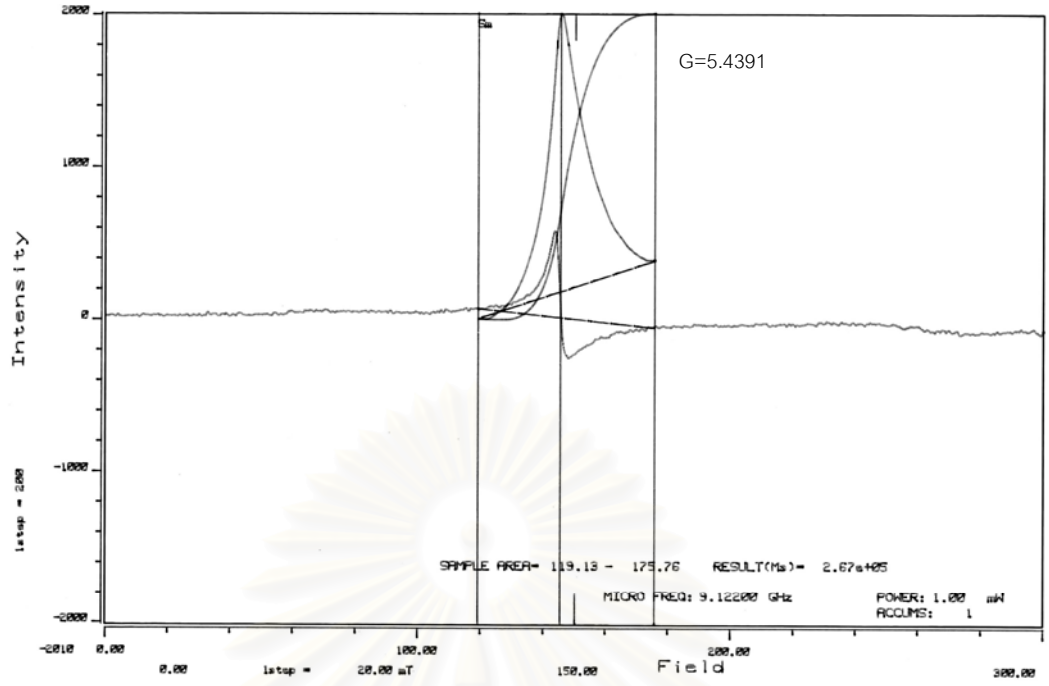

(a)

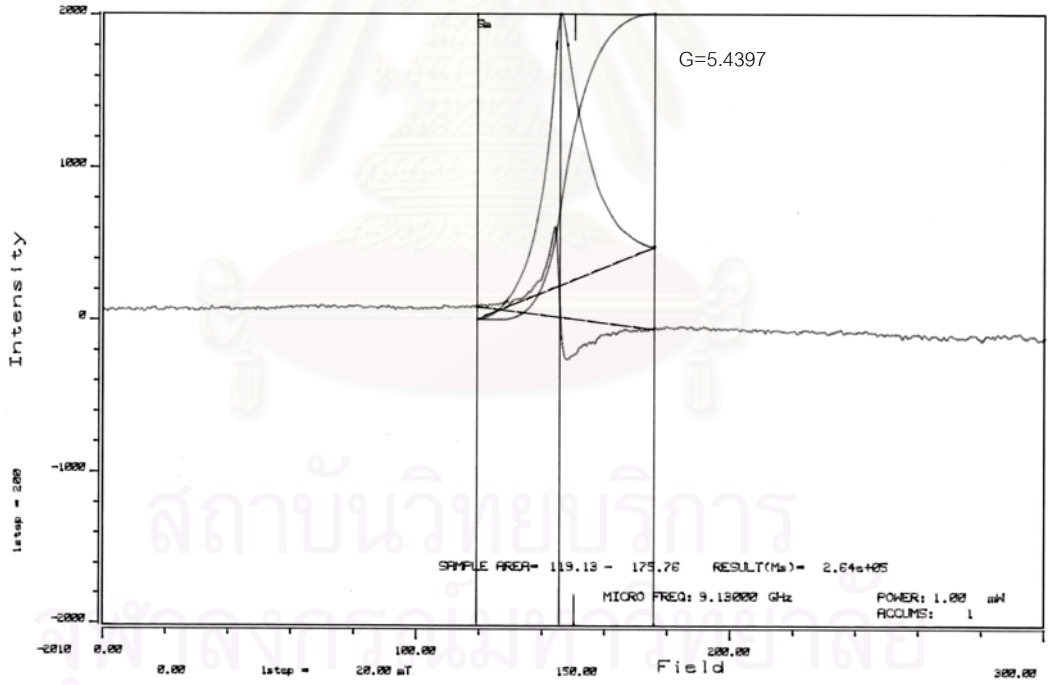

(b)

Figure 5.82 ESR spectra of high spin Co^{2+} of Co/HZSM-5 (3 μm)(a) fresh catalyst, (b) pretreated catalyst.

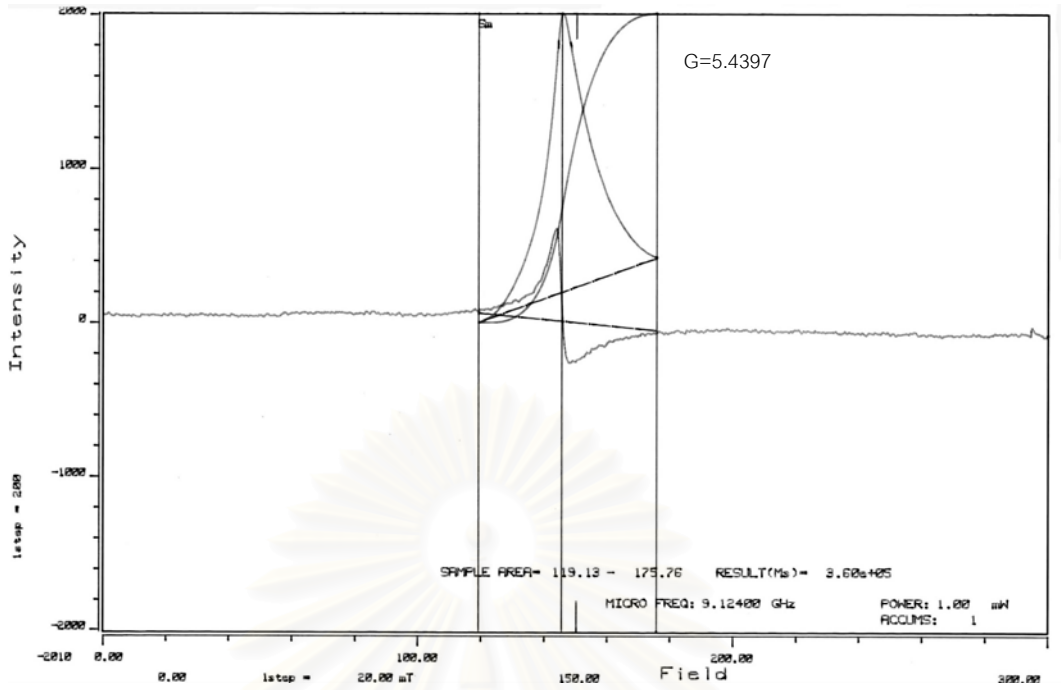

(a)

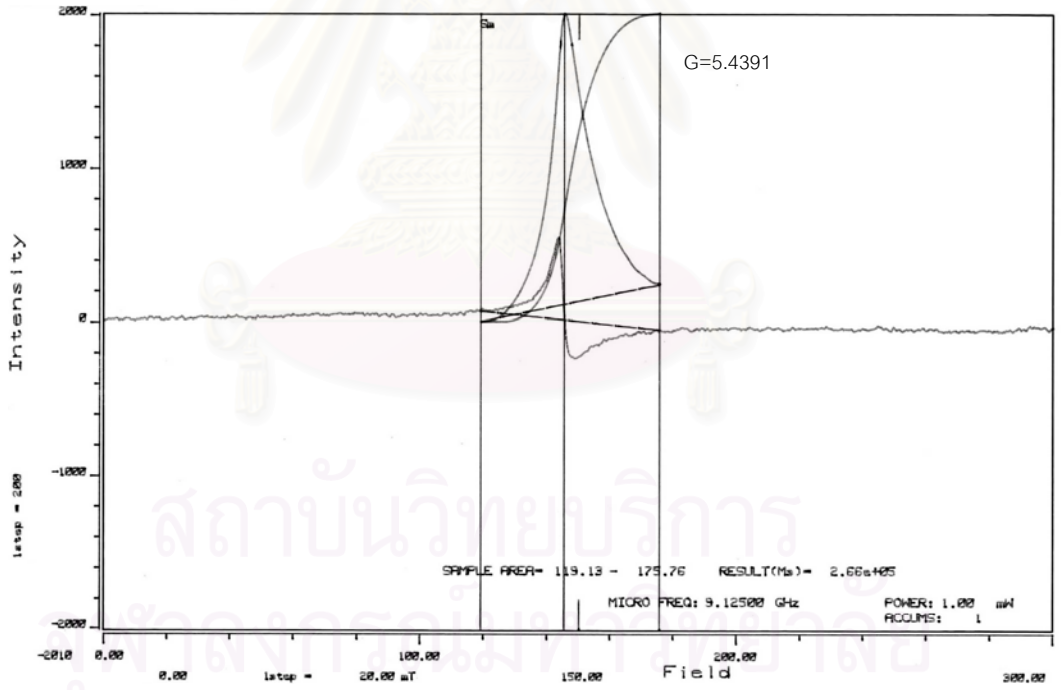

(b)

Figure 5.83 ESR spectra of high spin Co^{2+} of Co/HZSM-5 (5.6μm)(a) fresh catalyst, (b) pretreated catalyst.

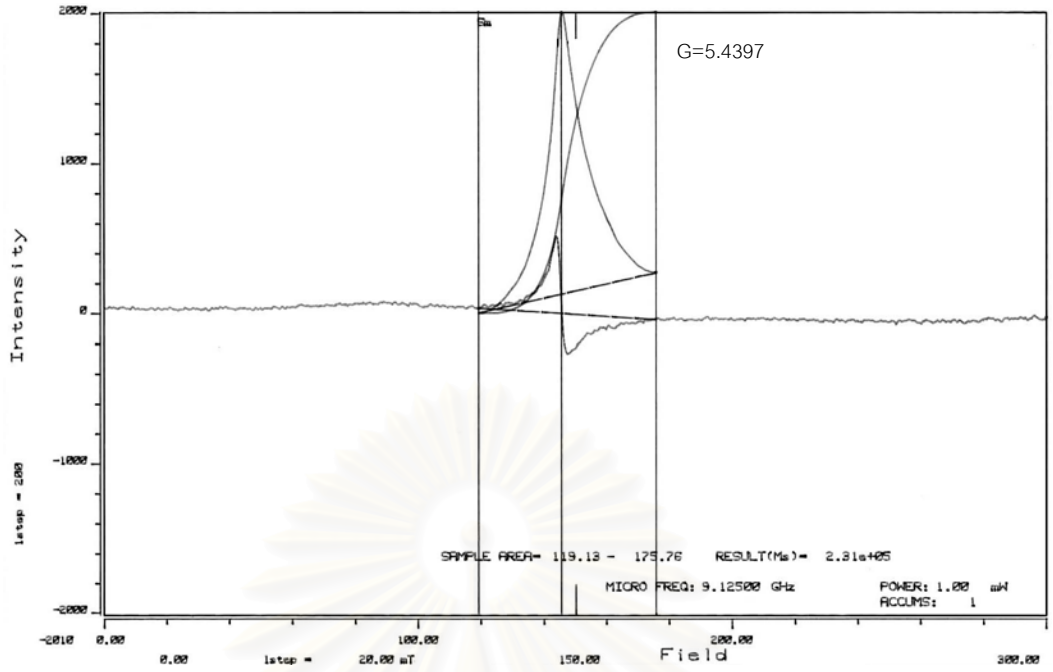

(a)

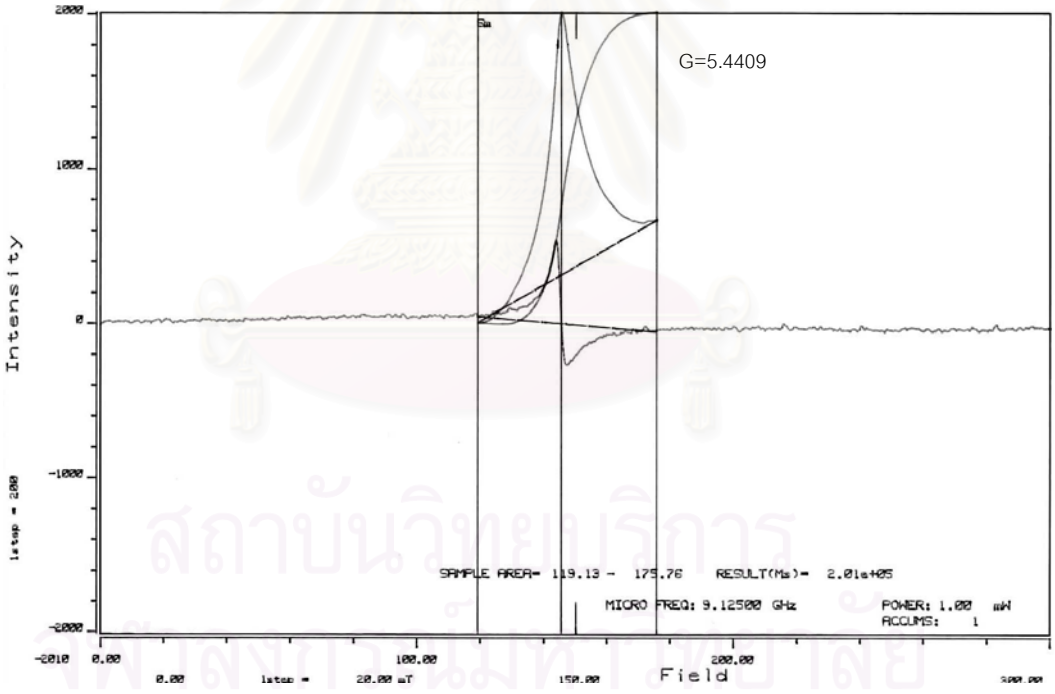

(b)

Figure 5.84 ESR spectra of high spin Co^{2+} of Co/HZSM-5 (7.6 μm)(a) fresh catalyst, (b) pretreated catalyst.

5.2.2 Catalytic performance

SCR of NO by methane was investigated for various crystal size catalysts both with and without pretreatment. The effect of reaction temperature on NO conversion to N_2 for Co/HZSM-5 with different crystal size is shown in Figure 5.80(a) whereas conversion of methane is shown in Figure 5.80(b). The conversion of NO into N_2 over these catalysts was enhanced with reaction temperature up to about 500^{o}C, however the conversion curve bent down beyond 500 ^{o}C while the methane conversion reached almost 100%. This phenomenon is typical for NO reduction by methane over Co/HZSM-5 [12,13].

It was found that NO conversion was dependent on the zeolite crystal size. The NO conversion over large crystal catalyst was less than that over the small crystal catalyst. These results indicate that intracrystalline diffusion has influence on the SCR of NO by methane over Co/HZSM-5 catalysts which corresponds to work of Shichi et al. on Cu/ZSM-5 catalysts [103]. After hydrothermal treatment of catalysts, the conversion of NO significantly decreased at any reaction temperature. NO conversions on large crystal size catalysts were found to decline to a greater extent after the hydrothermal pretreatment than those on a catalyst having a smaller crystal size. However, the difference in methane conversion changed only slightly since the conversion came from both combustion and reduction.

The percentage of reaction durability, defined as the maximum NO conversion of pretreated catalysts per maximum NO conversion of fresh catalysts, was calculated and is reported in Figure 5.81. Small crystal size Co/HZSM-5 had a higher reaction durability than the large crystal size zeolites. This suggests that the small crystal size exhibited a more steady and stable activity for conversion of NO to N_2. It should be noted that the durability is limited by crystal sizes up to about 2 μm. In other words, a Co/HZSM-5 crystal size of 2 μm is the critical diameter for enhanced durability after hydrothemal treatment.

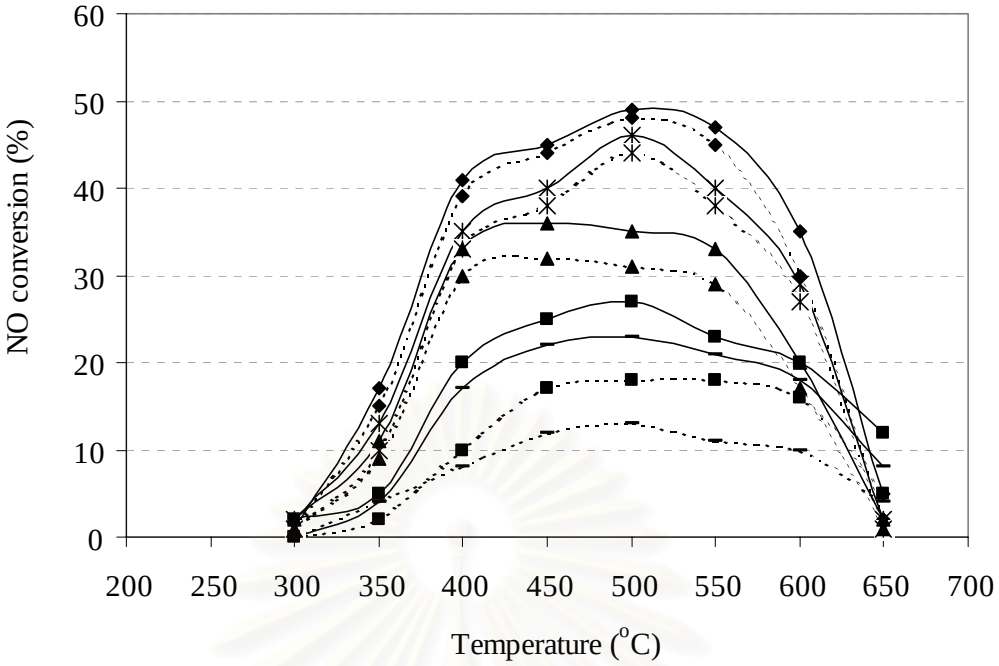

(a)

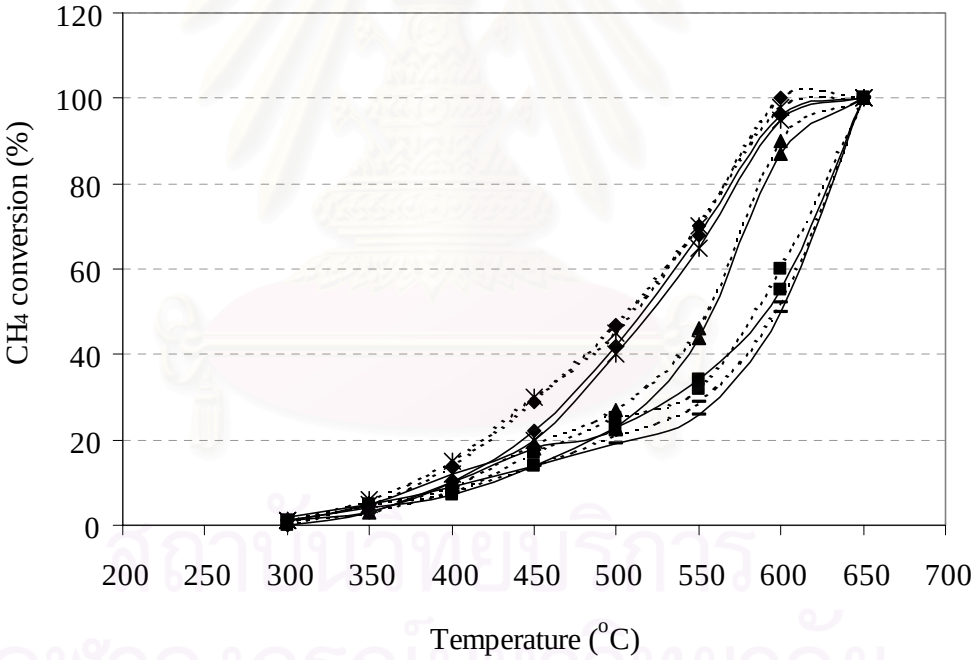

(b)

Figure 5.85 The effect of pretreatment of Co/HZSM-5 on (a) % NO conversion, (b) % CH_4 conversion solid line: fresh catalyst, broken line: pretreated catalyst; (υ)Co/HZSM-5(1.0 μm),(δ)Co/HZSM-5(1.8 μm), (σ)Co/HZSM-5(3.0 μm), (ν)Co/HZSM-5(5.6 μm) and (-)Co/HZSM-5(7.6 μm)

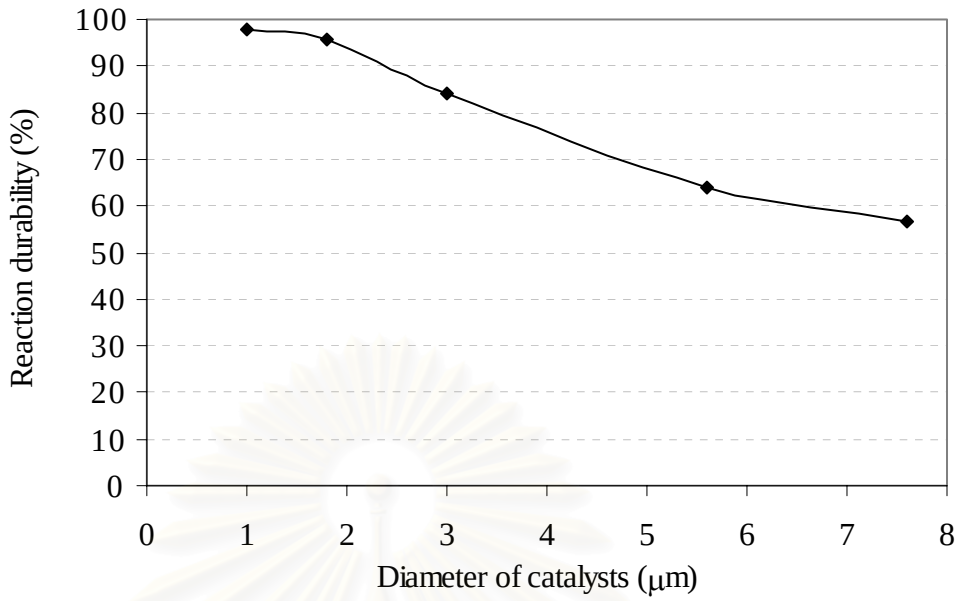

Figure 5.86 The effect of crystal size on the percentage of the reaction durability (υ)

In conclusion, the smaller crystal size Co/HZSM-5 zeolite showed the greater durability for conversion of NO to N_2. The small crystal size catalysts showed a slight decrease in crystallinity and moderate dealumination of tetrahedral aluminum while the large crystal size catalysts lost considerable crystallinity and were extensively dealuminated. Durability is retained by crystal sizes up to 2 μm so that this is a critical diameter for this reaction conditions. It is suggested that, commercial catalysts should be kept below the critical diameter in order to sustain the durability of the zeolite.

CHAPTER VI

CONCLUSIONS AND RECOMMENDATIONS

6.1 CONCLUSIONS

This dissertation has described studies of the effect of hydrothermal pretreatment on catalytic durability both various types of metal on Co/HZSM-5 zeolite and various crystal sizes of zeolite. The conclusions of this research were summarized as follows:

1. The presence of cations improved the Co/HZSM-5 catalyst durability for NO removal under hydrothermal treatment. Cd and Pd showed significant improvement of reaction durability against hydrothermal pretreatment. In addition, no significant relation between the valency of second metal and durability improvement of Co/HZSM-5 was observed.

2. From ^{27}Al MAS-NMR results, it suggests that Pd/Co/HZSM-5 with 0.4 wt.% Pd loading or higher can stabilize the tetrahedral aluminum in zeolite lattice even after being pretreated at 600^{o}C with 10 mol%H_2O for 24 h. In our study, 0.4%Pd/Co/ZSM-5 catalyst is the most effective catalyst durability for NO removal under hydrothermal treatment.

3. The smaller crystal size Co/HZSM-5 zeolite showed the greater durability for conversion of NO to N_2. The small crystal size catalysts showed a slight decrease in crystallinity and moderate dealumination of tetrahedral aluminum while the large crystal size catalysts lost considerable crystallinity and were extensively dealuminated. Durability is retained by crystal sizes up to 2 μm so that this is a critical diameter for this reaction conditions. It is suggested that, commercial catalysts should be kept below the critical diameter in order to sustain the durability of the zeolite.

6.2 RECOMMENDATIONS

From this research, the recommendations for further study are as follows:

1. The role of the second metal on the thermal durability of zeolite, in which they prevent the dealumination should be studied.

2. Further studies which aim at clearly describing the influence of crystal size effects on durability should be investigated.

REFERENCES

1. Shelef, M., Otto, K., Gandhi, H.S., *Atmos. Environ*. 3 (1969): 107.
2. Bosch, H. and Janssen, F.J.J.G., *Catal. Today* 2 (1988): 369.
3. Iwamoto, M. and Hamada, H., *Catal. Today* 10 (1991): 57.
4. Held, W., Kohig, A., *German Patent DE 3642018 A1* (1987).
5. Fujitani, Y., Muraki, H., Kondo, S., Fukui, M., *Japanese Patent JP 631009190A* (1988).
6. Held, W., Kohig, A., Richter, T., Puppe, L., *SAE Technical Paper, No.900496* (1990).
7. Iwamoto, M., Yahiro, H., Yu-u, Y., Shundo, S., Mizuno, N., *Shokbai(Catalyst)* 32 (1990): 430.
8. Iwamoto, M., Yahiro, H., Shundo, S., Yu-u, Y., Mizuno, N., *Appl. Catal*. 69 (1991): L15.
9. Hamada, H., Kintaichi, Y., Sasaki, M., Ito, T., Tabata, M., *Appl. Catal* (1990): L1
10. Kintaichi, Y., Hamada, H., Tabata, M., Sasaki, M., Ito, T., *Catal. Lett.* 6 (1990): 239.
11. Li, Y., and Armor, J.N., *US Patent 5149512* (1992).
12. Li, Y., and Armor, J.N., *Appl. Catal*. B 1 (1995): L31.
13. Tabata, T., Kokitsu, M., Okada, O., Nakayama, T., Yasumatsu, T., Sakane, H., *Stud. Surf. Sci. Catal*. 88 (1994): 409.
14. Yu-u, Y., Torikai, Y., Sato, Y., Hososе, H., Yahiro, H., Mizuno, N., Iwamoto, M., *Shokubai (Catalyst)* 33 (1991): 61.
15. Armor, J.N., *Catal Today* 26 (1995): 147.
16. Li, Y., Battavio, P.J., Armor, J.N., *J. Catal.* 142 (1993): 561.
17. Budi, P., Curry-Hyde, E., Howe, R.F., in Chon, H., Ihm, S.K., Uh (Editors), Y.S., Progress in Zeolite and Microporous Materials, *Studies in Surface Science and Catalysis*, Vol. 105, Part B, Elsvier, Amsterdam (1997): 1549.
18. Kikuchi, E., Ogura, M., Terasaki, I., Goto, Y., *J. Catal*. 161 (1996): 465.
19. Descrome, C., Gelin, P., Lecuyer, C. and Primet, M., *Appl. Catal*. B 13 (1997):185-195.

20. Iwamoto, M. *Proceeding of meeting of Catalyst Technology for removal of nitrogen monoxide*, Tokyo, Jan (1990) 17.
21. Held, W., Konig, A., Richter, T., and Puppe, L., *SAE 900496* (1990): 13.
22. Hamada, H., Sasaki, M., Kintaichi, Y., and Ito, T. Catal. Lett 15 (1992): 17.
23. Shelef, M., Montreuil, C. N. and Jen, H. W. *Catal. Lett.* 26 (1994): 277-284
24. Petunchi, J. O. and Hall, W. K. *Appl. Catal. B.* 2 (1993): L17-L26.
25. Beutel, T., Adelman, B. J., Lei, G-D. and Sachtler, W. M. H. *Catal. Lett.* 32 (1993): 83 - 92.
26. Chajar, Z., Primet, M., Praliaud, H., Cherrier, M., Gauthier G. and Mathis, F. *Catal. Lett.* 28 (1994): 33-40.
27. Yokkoyama, C. and Misono, M. *J. Catal.* 150 (1994): 9- 17.
28. Guyon, M., Chanu, V. L., Gilot, P., Kessler, H. and Prade, G., *Appl. Catal. B* 8 (1996): 183 - 196.
29. Iwamoto, M., Yahiro, H., and Mizuno, N., Proc.9th Int. zeolite conference, Montreal (1992) 170.
30. Montreuil, C.N., and Shelef, M *Appl. Catal. B* 1 (1992): L1-L8.
31. Bennett, C.J., Bennett, P.S., Golunski, S.E., Hayes, J.W., and Walker, A.P., *Appl. Catal. B.* 6 (1992): L1 - L6.
32. Kharas, K. C. C., *Appl. Catal. B.* 2 (1993): 207 - 224.
33. Ansell, G.P., Diwell, A.F., Golunski, S.E., Hayes, J.W., Rajaram, Truex, T.J., and Walker, A. P., *Appl. Catal. B* 2 (1993): 81 - 100.
34. Burch, R. and Millington, P. J. *Appl. Catal. B.* 2 (1993): 101-116.
35. Cho, B K.J. *J. Catal.* 155 (1995): 184-195.
36. Li, Y., Armor, J.N., *J. Catal.* 150 (1994): 376.
37. Li, Y., Armor, J.N., *Appl. Catal. B* 3 (1993): 55.
38. Burch, R., Seire, S., *Appl. Catal. B* 3 (1994): 295
39. Li, Y., Armor, J.N., *Appl. Catal. B* 2 (1993): 239.
40. Li, Y., Armor, J.N. in Curry-Hyde, H.E., Howe(Editors), R.F., Natural Gas Conversion II, *Studies in Surface Science and Catalysis*, Vol. 81, Elsevier, Amsterdam (1994): 103
41. Li, Y., Armor, J.N., *Appl. Catal. B* 3 (1993): L.l.
42. Hansel, J.G., Raman, S.V., Stolz, J.L., Armor, J.N., Li Y., *US Patent 5451385* (1994).
43. Lukyanov, D.B., Sill, G., d'Itri,J.L., Hall, W.K., *J. Catal*. 153 (1995): 265.

44. Lukyanov, D.B., d'Itri, J.L., Sill, G., Hall, W.K., in Hightower, J.W., Delgass, W.N., Iglesia, E., Bell(Editors), A.T., 11th Int. Catalysis – 40th Anniversary, *Studies in Surface Science and Catalysis*, Vol. 101, Part A, (1996): 651.
45. Cowan, A.D., Dumpelmann, R., Cant, N.W., *J. Catal*. 151 (1995): 356.
46. Sun, T., Fokema, M.D., Ying, J.Y., *Catal. Today* 33 (1997): 251.
47. Hall, W.K., Lombardo, E.A., d'Itri, J.L., Sill, G.A., *Prepr. Am. Chem. Soc. Div. Pet. Chem.* 42 (1997): 841.
48. Lombardo, E.A., Sill, G.A., d'Itri, J.L., Hal, W.K., *J. Catal.* 173 (1998): 440.
49. Cant, N.W., Cowan, A.D., Doughty, A., Haynes, B.S., Nelson, P.F., *Catal. Lett.* 46(1997): 207.
50. Cowan, A.D., Cant, N.W., Haynes, B.S., Nelson P.F., *J. Catal.* 176 (1998): 329.
51. Yan, J-L., Kung, H.H., Sachtler, W.M.H., Kung, M.C., *J. Catal.* 175 (1998): 294.
52. Stakheev, A.Y., Lee, C.W., Park, S.J., Chong, P.J., *Appl. Catal. B* 9 (1996): 65.
53. Stakheev, A.Y., Lee, C.W., Park, S.J., Chong, P.J., *Catal. Lett.* 38 (1996): 271.
54. Stakheev, A.Y., Lee, C.W., Park, S.J., Chong, P.J., in Zeolite and Microporous Materials, *Studies in Surface Science and Catalysis*, Vol. 105, Part B, (1997): 1579.
55. LEE, C.W., Chong, P.J., Lee, Chin, C.S., Kevan, L. *Catal. Lett*. 48 (1997): 129.
56. Kawai, Y., Sekizawa, K., *European Patent Application 499087* (1992).
57. Bellussi, G., Sabatino,L.M.F., Ohtsuka, H. T., Tabata, O.Okada, *European Application 766992* (1997).
58. Ohtsuka, H., Tabata, Okada, O., *Prepr. Am. Chem. Soc. Div. Pet. Chem*. 42 (1997): 855.
59. Ohtsuka, H., Tabata, Okada, O., Ssabatino, L.M.F., Bellussi, G., *Catal. Lett.* 44 (1997): 265.
60. Ohtsuka H., Tabata. Okada, O., Ssabatino, L.M.F., Bellussi, G., *Catal. Today* 12 (1998): 45.
61. Campa, M.C., De Rossi, S., Ferraris, G., Indovina, V., *Appl. Catal. B* 8 (1996): 15.
62. Miller, J.T., Glusker, E., Peddi, R., Zheng, T., Regal-buto, J.R., *Catal. Lett.* 51 (1998): 15.
63. Momtes de Correa, C., Luz Villa de P. A., *Catal. Lett.* 53 (1998): 205.

64. Zhang, W., Yahiro, .H., Mizuno, N., Izumi, J., Iwamoto, M., *Chem. Lett.* (1992): 851.

65. Iwamoto, M., *Trans. Mater. Res. Soc. Jpn. A* 15 (1994): 117.

66. Zhang, W., Yahiro, H., Iwamoto, M., Izumi, *J., Chem. Soc, J., Faraday Trans.* 91 (1995): 767.

67. Iwamoto, M., Hoshino, Y., *Chem. Lett.* (1995): 729.

68. Li, Y., Slager, T.L., Armor, J.N., *J. Catal*. 150 (1994): 388.

69. Zhu, C.Y., Lee, C.W., Chong, P.J., *Zeolite* 17 (1996): 483.

70. Bell, A.T., Lobree, L.J., Aylor, A.W., Reimer, J.A., *Prepr. Am. Chem. Soc. Div. Pet. Chem.* 42 (1997): 815.

71. Aylor, A.W., Lobree, L.J., Riemer, J.A., Bell, A.T., in Hightower, J.W., Degess, W.N., Iglesia, E., Bell (Editors), A.T., 11th Int. Congress on Catalyst-40th Anniversary, *Studies in Surface Science and Catalysis*, Vol. 101, Part A, (1996): 661.

72. Lobree, L.J., Aylor, A.W., Riemer, J.A., Bell, A.T., *J Catal.* 169 (1997) 188.

73. Betutel, T., Adlman, B., G-D. Lei, Sachtler, W.M.H., *Prepr. Am. Chem. Soc. Div. Fuel Chem*. 40 (1995): 1063.

74. Adelman, B.J., Beutel, T., G-D. Lei, Sachtler, W.M.H., *J. Catal*. 158 (1996): 327.

75. Betutel, T., Adlman, B., G-D. Lei, Sachtler, W.M.H., *Appl. Catal*. B 9 (1996): L1.

76. T. Sun, M.L. Trudeau, J.Y. Ying, *J. Phys. Chem*. 100 (1996): 13662.

77. Vassallo, J., Lezcano, M., Miro, E., Petunchi, J., in Frennet, A., Bastin (Editors), J.N., Catalysis and Automotive Pollution Control III, *Studies in surface Science and Catalysis*, Vol. 96, (1995): 697.

78. Vassallo, J., Miro,E., Petunchi, J., *Appl. Catal. B* 7 (1995): 65.

79. Gutierrez, L., Ribotta, A., Boix, A., Petunchi, J., in. Hightower, J.W., Degess, E., Iglesia, W.N., Bell (Editors), A.T., 11th Int. Congress on Catalyst-40th Anniversary, *Studies in Surface Science and Catalysis*, Vol. 101, Part A, (1996).

80. Li. Y., Armor, J.N., *Prepr. Am. Chem. Soc. Div. Fuel Chem*. 40 (1995): 1082.

81. Li, Y., Armor, J.N., *Appl. Catal. B* 5 (1993): L257.

82. Budi, P., Howe, R.F., *Catal. Today* 38 (1997): 175.

83. Park, S-E, React. Kinet. *Catal. Lett.* 57 (1996): 339.

84. Kasahara, S., Okazaki, S., Sekizawa, K., *European Patent Application 462598* (1991).

85. Ogura, M., Sgiura,Y., Hayashi, M., Kikuchi, E., *Catal. Lett*. 42 (1996): 185.

86. Eshita, A., Kasahara, S., Matsumoto, S., Ishibashi, K., Yokota, K., Kondoh, S., *European Patent Application 434063* (1991).

87. Ciambelli, P., Corbo, P., Gambino M., Migliardini F., Minelle, G., Morretti, G., Porta, P., in L. Bonneviot L., Kaliaguine (Editors), S., Zeolite: A Refined Tool for Designing Catalytic Sites, *Studies in Surface Science and Catalysis*, Vol. 97, Part B (1995):.295.

88. Ohtsuka, H., Tabata, T., Kokisu, M., Okada, O., Sabatino, L.M.F., Bellussi, G., *Int. Gas Res. Conf*. (1996): 2803.

89. Takeshima, S., Tanaka, T., Oishi, K., Inoue, T., European Patent Application 463626 (1992).

90. Miyoshi, N., *Trans. Mater. Res. Soc. Jpn. A* 15 (1994): 123.

91. Rak, Z.S., Veringa, H.J., *React. Catal. Lett*. 60 (1997): 303.

92. Chen, N.Y., Degnan, T.F., Jr., Smith, C.M., *Molecular Transport and Reaction in zeolites*, VCH, New York, 1994.

93. Post, M.F.M., *Stud. Surf. Sci. Catal*. 58 (1991): 391.

94. Weisz, P.B., *Chemtech* 3 (1973): 498.

95. Tabata, T., Ohtsuka, H., *Catal. Lett*. 48 (1997): 203.

96. Tabata, T., Kokitsu, M., Ohtsuka, H., Okada, O., Sabatino, L.M.F., Bellussi, G., *Catal. Today* 27 (1996): 91.

97. Tabata, T., Ohtsuka, H., Sabatino, L.M.F., Bellussi,G., *Micropor. Mesopor. 21* (1998): 517.

98. Okada, O., Tabata, T., Kokitsu, M., Ohtsuka, H., Sabatino, L.M.F., Bellussi, G., *Appl. Surf. Sci.* 121/122 (1997): 267.

99. Shichi, A., Satsuma, A., Iwase, M., Shimizu, K., Komai, S., Hattori, T., *Appl. Catal. B* 179 (1998): 107.

100. Witzel, F., Sill, G.A., Hall, W.K., *J. Catal*. 149(1994) 229.

101. Witzel, F., Sill, G.A., Hall, WK., in Weitkamp, J., Karge, H.G., Pfeifer, H., Holderich(Editors), W., Zeolites and Related Materials: State of the Art 1994, *Studies in Surface Science and Catalysis*, Vol. 84, Part C (1994):.1531.

102. Satsuma, A., Iwase, M., Shichi, A., Hattori, T., and Murakami, Y., *Stud. SurfSci. Catal.* 105 (1997): 1533.

103. Shichi, A., Katagi, K., Satsuma, A., and Hattori, T., *Appl, Catal. B* 24 (2000): 97.

104. Olson, D.H.; Haag WO; Borghard WS *Microporous and Mesoporous Materials* 35-6 (2000): 435-446

105. Shichi A; Satsuma A; Hattori T *Appl. Catal. A* 207 (2001) 315.

106. Wark, K., Wanner, C.F., *Air Pollution*, Harper&Row , 1981.

107. Armor, J.N., *Environmental Catalyst*, ACS Symposium Series, 1994.

108. Heck, R.M. and Farrauto, R.J., *Catalytic Air Pollution Control*, New York, Van Nostrand Reinhold. (1995).

109. Farrauto, R.J and Bartholomew, *Fundamentals of industrial catalytic processes* , London, Blackie academic & Professional 1997.

110. Vaughan, D.E.W., *Chem. Eng. Progr*. 84 (1988): 25.

111. Ward, J.W., *Applied. Industrial Catalysis Acadeemic Press*, 3 (1984): 272

112. McDaniel, C.V. and Maher, P.K. *American Chemical Society, ACS Monograph* 171 (1976): 285.

113. Wang, X., Chen, H.Y. and Sachtler, W.M.H., *Appl. Catal., B* 26 (2000): L227.

114. Weckhuysen, B.M., Verberckmores, A.A., Uytterhoeven, M.G., Mabbs, F.E. and Schoonheydt, R.A., *J. Phys. Chem. B* 104 (2000): 37.

115. Budi, P., Hyde, E.C. and. Howe, R.F., *Catal. Lett*., 41 (1996): 47.

116. Treacy, M.M.J., Higgins, J.B. and Ballmoos, R. *Zeolite*. 16 (1996): 525.

117. Gmehling, J., Onken, U., *Vapor-Liquid Equilibrium Data Collection. Chemistry Data Series.* Frankfurt: DECHEMA, 1977.

118. Hirata, M., Ohe, S., Nagama, K., *Computer Aided Data Book of Vapor-Liquid Equilibria*. Amsterdam: Elsevier, 1975.

APPENDICES

APPENDIX A

SAMPLE OF CALCULATIONS

A-1 Calculation of Si/Al Atomic Ratio for ZSM-5

The calculation is based on weight of Sodium Silicate ($Na_2O{\cdot}SiO_2{\cdot}H_2O$) in B1 and B2 solutions (Topic 4.1.1).

M.W. of Si = 28.0855

M.W. of SiO_2 = 60.0843

Weight percent of SiO_2 in Sodium Silicate = 28.5

M.W. of Al = 26.9815

M.W. of $AlCl_3$ = 133.3405

Weight percent purity of $AlCl_3$ = 97

For example, to prepare ZSM-5 at Si/Al atomic ratio of 25.

Using Sodium Silicate 69 g with 45 g of water as B1 solution.

$$\text{mole of Si used} = \frac{\text{wt. (\%)}}{100} \times \frac{\text{(M.W. of Si)}}{\text{(M.W. of } SiO_2\text{)}} \times \frac{\text{(1 mole)}}{\text{(M.W. of Si)}}$$

$$= 69 \times (28.5/100) \times (1/60.0843)$$

$$= 0.3273$$

Si/Al atomic ratio = 25

mole of $AlCl_3$ required = 0.3273/25

$$= 1.309 \times 10^{-2} \text{ mole}$$

amount of $AlCl_3$ $= 1.309 \times 10^{-2} \times 133.34\ (100/97)$

$= 1.799$ g

which used in A1 and A2 solutions.

A-2 Calculation of the amount of metal ion-exchanged ZSM-5

For example: Determine the amount of Co into catalyst = 1 wt.%

The catalyst use = x g

so that Co/(x+Co) = 1/100

100×Co = 1× (x+Co)

(100-1) ×Co = x

thus Co = x/(100-1) g

use $Co(CH_3COO)_2.4H_2O$ (M.W. 249, purity 99.5%)

weight of $Co(CH_3COO)_2.4H_2O$ = $[x/(100-1)] \times [(249/59) \times (99.5/100)]$

A-3 Calculation of percent weight of cobalt in catalysts

Since the total cobalt content in catalysts used in this study were determined by AAS analysis, and the obtained results are always show as concentration of cobalt in prepared solution, it would better convert to the conventional value (% wt./ g. cat.)

Weight of catalyst used for digestion = w g.

Volume of solution obtained from digestion = 50 ml.

From the result of AAS analysis

Concentration of cobalt in digested solution = C ppm

Thus,

Amount of cobalt in solution (50 ml.)

= Amount of copper in digested solution(w g.)

= $(C \times 50)/(1 \times 10^6)$ g.

Amount of Co in 1g. catalyst = $(C \times 50)/(1 \times 10^6 \times w)$ g.

Thus,

Cobalt content in catalyst = $(C \times 50 \times 100)/(1 \times 10^6 \times w)$ wt.%

= $0.005 \times C/w$ wt.%

A-4 Calculation of gas velocity

The catalyst used = 0.20 g.

packed catalyst into quartz reactor (diameter = 0.6 cm)

determine the average high of catalyst bed = x cm

So that, volume of catalyst bed = $p \times (0.3)^2 \times x$ ml-catalyst

used GHSV (Gas Hourly Space Velocity) = 10,000 h^{-1}

$$GHSV = \frac{\text{Volumetric flow rate}}{\text{Volume of Catalyst}} = 10{,}000 \ h^{-1}$$

Volumetric flow rate = 10,000 × Volume of catalyst

= $10{,}000 \times p\,(0.3)^2 \times x$ ml/h

= $10{,}000 \times p\,(0.3)^2 \times x / 60$ ml/ min

at STP : Volumetric flow rate = $\frac{\text{Volume flow rate} \times (273.15+t)}{273.15}$

where : t = room temperature, ^oC

A-5 Calculation of CH_4 and NO and conversion

The CH_4 oxidation activity was evaluated in terms of the conversion of CH_4 into CO and CO_2.

$$CH_4 \text{ Conversion (\%)} = \frac{([CH_4]_{in} - [CH_4]_{out}) \times 100}{[CH_4]_{in}}$$

The effluent gas was analyzed by gas chromatography, the NO reduction activity was evaluated in terms of the conversion of NO into N_2.

$$2NO \longrightarrow N_2 + O_2$$

$$\text{NO Conversion (\%)} = 2 \times ([N_2]_{out} - [N_2]_{ref})/[NO]_{in} \times 100$$

Where $[NO]_{in}$ = 1000 ppm

$[N_2]$: analyzed by gas chromatograph from calibration curve

Calibration curve of N_2

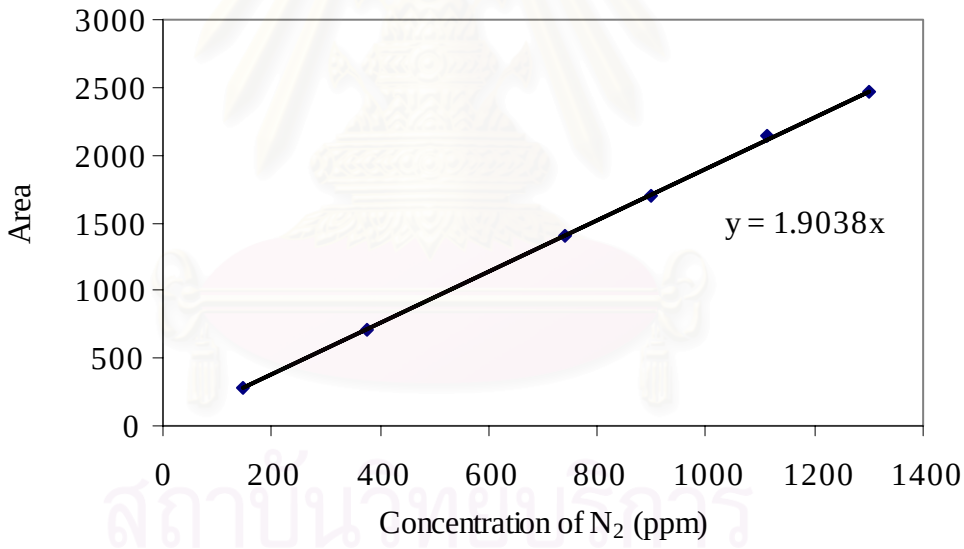

Area = 1.9038× conc. of N_2 (ppm)

Thus, $[N_2]$ = Area/1.9038

A-6 Calculation of vapor pressure of water

Set the partial vapor pressure of the reactants to the requirement by adjusting the temperature of saturator according to the antoine equation [117,118];

$$\log P = A - \frac{B}{(T+C)}$$

When P = vapor pressure of water, mbar

T = temperature, ^{o}C

A, B and C is constants

Range of temperature that applied ability –20 – 126 ^{o}C

The values of constants.

Reactant	A	B	C
Water	8.19625	1730.630	233.426

A-7 Calculation of %Crystallinity

$$\% \text{ Crystallinity} = \frac{\text{Area under XRD pattern of sample} \times 100}{\text{Area under XRD pattern of reference}}$$

Reference is the fresh commercial HZSM-5.

A-8 Calculation of the relative area of tetrahedral aluminum (%)

$$\text{The relative area of tetrahedral Aluminum (\%)} = \frac{\text{Area of tetrahedral Al} \times 100}{\text{Total Area}}$$

Area of tetrahedral Aluminum is a peak at a chemical shift of around 60 ppm.
Total area is summation area of tetrahedral and octahedral aluminum (0 ppm).

A-9 Calculation of % Reaction Durability

$$\% \text{ Reaction Durability} = \left(1 - \frac{NO_{fresh} - NO_{pretreated}}{NO_{fresh}} \right) \times 100$$

NO_{fresh} is the maximum NO conversion of fresh catalyst.
$NO_{pretreated}$ is the maximum NO conversion of pretreated catalyst.

APPENDIX B

PROPERTIES OF NO

B-1 Nitric oxides

Physical properites of NO

Property	Value
mol. wt.	30.1
m.p., ^{o}C	-161
b.p., ^{o}C	-151.18
heat of fusion, kJ/mole	2.3023
heat of vaporization, kJ/mole	13.78
heat of formation, kJ/mole	90.00
density [0 ^{o}C, 1 atm], g/L	1.2536
sp. gr., gas, [0 ^{o}C, 1 atm], (air = 1)	1.018
critical temperature, ^{o}C	-93
critical pressure, atm at -94.8 ^{o}C	64
color	colorless gas, blue liquid and solid
odor	ordorless
flash point	non - flamable
threshold limit value	25 ppm , 30 mg/m^3

Hazard and noxious effect.

Nitric oxide is converted in air to nitrogen dioxide, but at concentration below 50 ppm this conversion is slow

Animal experiments indicate Nitric oxide about 1/5 as toxic as nitrogen dioxide

Nitric oxide's cheif toxic effect has been attributed to the formation of methemoglobin followed by central nervous system effects

In mixed exposure with either carbon monoxide or nitrogen dioxide, additive effects should be assumed.

60 to 150 ppm, cause immediate nose & throat irritation with coughing and burning in the chest and throat.

100 to 150 ppm are dangerous for short exposures (30 to 60 minutes)

It is able to reach all parts of the respiratory system because of its low solubility in water. It diffuses through the Alveolar-cells and the adjacent capillary vessels of the lungs and damages the Alvolar-structures and their function throughout the lungs.

Chronic exposure may cause respiratory tract irritation, cough headache, appetite loss, teeth corrosion and dyspepsia.

It also plays a major role in the photochemistry of the troposphere and the stratosphere. NO is rapidly oxidized by atmospheric oxidants such as ozone. NO_2 itself is a precursor for nitric acid, which contributes substantially to so-called acid rain. NO_2 is formed through oxidation of NO with ozone or through photochemically-generated peroxy radicals.

APPENDIX C

LIST OF PUBLICATIONS

1. Piyasan Praserthdam and Pornsawan kanchanawanichkun,“ Effect of Crystal Size on the Durability of Co/HZSM-5 in Selective Catalytic Reduction of NO by Methane”, Catalysis Communications, in press.

2.Piyasan Praserthdam, Nakarin Mongkolsiri and Pornsawan Kanchanawanichkun, “Effect of Pd on the Durability Improvement of Co/HZSM-5 for NO Removal under Hydrothermal Pretreatment”, Journal of the Chinese Institute of Chemical Engineerings, under review.

3. Piyasan Praserthdam, Choowong Chaisuk and Pornsawan kanchanawanichkun, “Comparative Study of Coke Deposition on Catalysts in Reactions with and without Oxygen”, Ressearch on Chemical Intermediates, vol.24, No. 5 (1998) 605.

4. Piyasan Praserthdam and Pornsawan kanchanawanichkun,“Realationship between Coke Formation, Hydrocarbon and NO Conversion on Selective Catalytic Reduction of NO by Propene on Cu/Na/ZSM-5 with Excess Oxygen”2nd World Congress on Environmental Catalysis, Miami, USA, November 15-20, 1998.

5. Piyasan Praserthdam and Pornsawan kanchanawanichkun,“ Effect of NO on Coke Formation for Propane and Propene Conversion via Cu/Na-ZSM-5 Catalysts**”,** 15th Candian Symposium on Catalysis 1998, Qubec, Canada, May 17-20, 1998.

CATCOM 105
DISK / 18/4/02
ARTICLE IN PRESS
No. of pages: 7
DTD 4.3.1/ SPS-N

ELSEVIER

00 April 2002

Catalysis Communications xxx (2002) xxx–xxx

CATALYSIS COMMUNICATIONS

www.elsevier.com/locate/catcom

Effect of crystal size on the durability of Co/HZSM-5 in selective catalytic reduction of NO by methane

Piyasan Praserthdam [a,*], Nakarin Mongkolsiri [b], Pornsawan Kanchanawanichkun [a]

[a] *Department of Chemical Engineering, Research Center on Catalysis and Catalytic Reaction Engineering, Chulalongkorn University, Payatai Rd., Bangkok 10330, Thailand*

[b] *Research and Technology Institute, Petroleum Authority of Thailand, Ayuthaya, Thailand*

Received 1 February 2002; received in revised form 27 February 2002; accepted 27 February 2002

Abstract

The effect of crystal size on the durability of Co/HZSM-5 in the selective catalytic reduction (SCR) of NO with methane was studied. The durability of the catalysts subjected to hydrothermal treatment with a He stream containing 10% steam at 600 °C for 24 h. was investigated. After hydrothermal treatment, the decrease of catalytic activity for small crystal sizes of Co/HZSM-5(1.0 and 1.8 μm) was less than for large crystal sizes of Co/HZSM-5(5.6 and 7.6 μm). This infers that the durability of Co/HZSM-5 increased with a decrease in crystal size. Small crystal size catalyst showed a slight decrease in crystallinity and tetrahedral aluminum while the large crystal size catalyst lost crystallinity and tetrahedral aluminum. This indicated that the occurrence of framework dealumination was higher in the large crystal size catalyst. © 2002 Published by Elsevier Science B.V.

Keywords: Co/HZSM-5; Hydrothermal treatment; NO removal and durability

1. Introduction

The selective catalytic reduction (SCR) of NO with hydrocarbons in the presence of excess oxygen has received much attention recently because of its potential application to mobile lean-burn engines [1–3]. Reports by Iwamoto et al. [4] and Held et al. [5], which have shown that Cu-ZSM-5 was capable of catalysing the reduction of nitric oxide by hydrocarbons in the presence of oxygen, has generated a considerable amount of research work on related systems. The sintering of Cu ion into Cu oxide under wet conditions leads to a deterioration in the activity in Cu/ZSM-5 [6]. Furthermore, Cu-ZSM-5 is ineffective in catalyzing the reduction when methane is employed as the reductant. In 1992, Li and Armor [7–11] reported that Co/ZSM-5, unlike Cu/ZSM-5, shows good activity for reduction of NO_x with methane in the presence of oxygen. Co/ZSM-5 also possesses much better hydrothermal stability than Cu/ZSM-5 [12–15]. A key issue of metal zeolite catalysts for

* Corresponding author. Tel.:+66-2-2186711; fax: +66-2-218-6769.
E-mail address: piyasan.p@chula.ac.th (P. Praserthdam).

1566-7367/02/S - see front matter
PII: S1566-7367(02)00090-0

CATCOM 105 DISK / 18/4/02 ARTICLE IN PRESS No. of pages: 7 DTD 4.3.1/ SPS-N

NO_x reduction is catalyst durability. In particular steam, which is unavoidably present in combustion gases, will irreversibly deactivate catalysts above a certain temperature [16,17]. The effect of water on the activity of SCR of NO by methane over Co/ZSM-5 was investigated by Armor and co-workers [14]. They concluded that Co/ZSM-5 is more stable than Cu/ZSM-5 under wet conditions at high temperature. However, Howe and co-workers [18] reported that Co/ZSM-5 catalysts are also not durable under long steam aging at severe conditions. Although, many researchers have tried to find a catalyst that can handle severe conditions for NO removal, it is also well know that a small crystal size zeolite may provide high conversion because of the diffusion influence on the SCR of NO over zeolite catalysts [19–21]. However these studies have not been concerned with the durability of such catalysts. Thus, this work aims to investigate the effect of crystal zeolite size on the durability of Co/HZSM-5 under hydrothermal treatment.

2. Experimental

2.1. Catalyst preparation

Five ZSM-5 zeolite catalysts, having different crystal size, but of the same Si/Al ratio (Si/Al = 20) and Co loading, were used in this investigation. The ZSM-5 zeolites were prepared according to the rapid crystallization method [22] using various rates of crystallization. In order to transform the Na form of zeolite crystals into NH_4 form all samples were ion-exchanged with ammonium nitrate solution and then washed and dried, and calcined at 540 °C for 3.5 h in air. Co/HZSM-5 was prepared by using an aqueous solution of $Co(CH_3COO)_2$ for ion-exchange with HZSM-5 at 80 °C for 24 h. The Co exchanged catalyst was then washed, dried and calcined at 540 °C for 3.5 h in air.

In order to investigate the durability of the catalysts, the catalysts were heated under He, while elevating the temperature from ambient temperature to 600 °C with a heating rate 10 °C/min. The catalyst samples were then kept at 600 °C for 24 h. while adding 10% mol of steam whereafter they were cooled down to ambient temperature under a He stream.

2.2. Characterization

Specific surface areas of the catalysts were measured by physical adsorption based on BET assumption, with N_2 as the adsorbent using a Micromeritics model ASAP 2000. The crystallinity of the catalysts was determined using a X-ray diffractometer (SEIMEN D5000) with Cu Kα radiation. %Crystallinity, as determined by XRD profiles, was calculated based on the area of the main peak compared with that of HZSM-5 as a reference. The elemental composition of the catalysts were determined by Atomic Absorption Spectroscopy (AAS, Shimazu atomic absorption/flame emission spectrometer AA-640-01). The morphology of the catalysts was observed using a Scanning Electron Microscope (SEM, JEOL, JSM-35). Quantitative analysis of tetrahedral aluminum in zeolites was conducted by Al magnetic angle spinning nuclear magnetic resonance (^{27}Al MAS NMR, BRUKER DPX-300 spectroscopy operating at 78.2 MHz). The relative area of tetrahedral ^{27}Al is calculated from the area of tetrahedral aluminum per summation area of tetrahedral and octahedral aluminum.

2.3. Reaction method and analysis

Catalysts were tabletted, crushed and sieved to 8–16 mesh for reaction testing. A 0.2 g portion of the catalyst was packed into a quartz tube reactor. It was heated from room temperature to 500 °C under a He flow at a constant heating rate of 10 °C/min, and maintained at 500 °C for 1 h. The reactor was then cooled down to 300 °C and then the reaction mixture comprising NO (1000 ppm), CH_4 (1 vol%), O_2 (10 vol%) balance He, was flowed over catalyst at GHSV 10,000 h^{-1}. The effluent gas composition was analyzed by using gas chromatographs (SHIMADSU GC-8ATP, and SHIMADSU GC-8AIT with Molecular Sieve-5A and ParapakQ column, respectively). The catalytic activity was evaluated based on the conversion of NO to N_2.

CATCOM 105
DISK / 18/4/02
ARTICLE IN PRESS
No. of pages: 7
DTD 4.3.1/ SPS-N

Table 1
Physical properties of Co/HZSM-5

Catalyst	Crystal diameter by SEM (μm)	Si/Al atomic ratio	Co/Al atomic ratio	BET surface area (m^2/g)		%Crystallinity[a]		The relative area of tetrahedral ^{27}Al[b]	
				Fresh	Pretreated	Fresh	Pretreated	Fresh	Pretreated
Co/HZSM-5(1.0 μm)	1.0	22.3	0.173	454	443	99	98	85	83
Co/HZSM-5(1.8 μm)	1.8	23.1	0.179	434	418	98	96	83	80
Co/HZSM-5(3.0 μm)	3.0	23.1	0.175	458	431	99	95	80	73
Co/HZSM-5(5.6 μm)	5.6	22.2	0.170	439	401	95	88	77	67
Co/HZSM-5(7.6 μm)	7.6	23.0	0.177	447	404	93	85	78	65

[a] %Crystallinity was calculated using the area of the dominant peak, which was compared with HZSM-5 as a reference.
[b] The relative area of tetrahedral ^{27}Al was calculated from the area of tetrahedral aluminium per summation area of tetrahedral and octahedral aluminium

3. Results and discussion

3.1. Changes in physical properties upon pretreatment

Table 1 shows the physical properties of the catalysts before and after pretreatment. Five ZSM-5 samples were selected as the parent ZSM-5 as they have similar Si/Al and Co/Al ratio but different crystal size from each other. The crystal sizes of the zeolite samples were measured from scanning electron micrographs by averaging the diameter of a hundred primary particles based on the particle diameter. Crystal size values estimated from SEM images of the catalyst have been reported in many research investigations [18,20,21]. Considerations of the SEM photographs depicted in Fig. 1, indicated the diameters of Co/HZSM-5 zeolite samples were 1.0, 1.8, 3.0, 5.6 and 7.6 μm.

The results shown in Table 1, indicate that after hydrothermal treatment the BET surface area of Co/HZSM-5(5.6 μm) and Co/HZSM-5(7.6 μm) were significantly decreased, however for the small crystal size catalysts, Co/HZSM-5(1.0 μm) and Co/HZSM-5(1.8 μm), only a slight decrease in surface area was observed. For the fresh catalyst, the %crystallinity of Co/HZSM-5(1.0 μm), and Co/HZSM-5(1.8 μm) was found to be higher than that of Co/HZSM-5(5.6 μm) and Co/HZSM-5(7.6 μm). It was also found that, after ion-exchange of Co into HZSM-5, the large crystal size catalyst lost more crystallinity than the small crystal size catalyst. After hydrothermal treatment at 600 °C in 10% water in 24 h, no significant change in morphology of the samples was observed. As shown in Table 1, the large crystal size catalysts lost a considerable degree of their crystallinity after hydrothermal treatment; especially for Co/HZSM-5(5.6 μm) and Co/HZSM-5(7.6 μm). In contrast, for Co/HZSM-5(1.0 μm) and Co/HZSM-5(1.8 μm) only a slight decrease in crystallinity was observed upon hydrothermal treatment. Consequently, it definitely appears that the smaller crystal size Co/HZSM-5 catalysts are more durable than the large ones on hydrothermal treatment with respect to crystallinity.

Figs. 2(a) and (b) show the ^{27}Al MAS NMR spectra of fresh Co/HZSM-5 and pretreated Co/

CATCOM 105
DISK / 18/4/02
ARTICLE IN PRESS
No. of pages: 7
DTD 4.3.1/ SPS-N

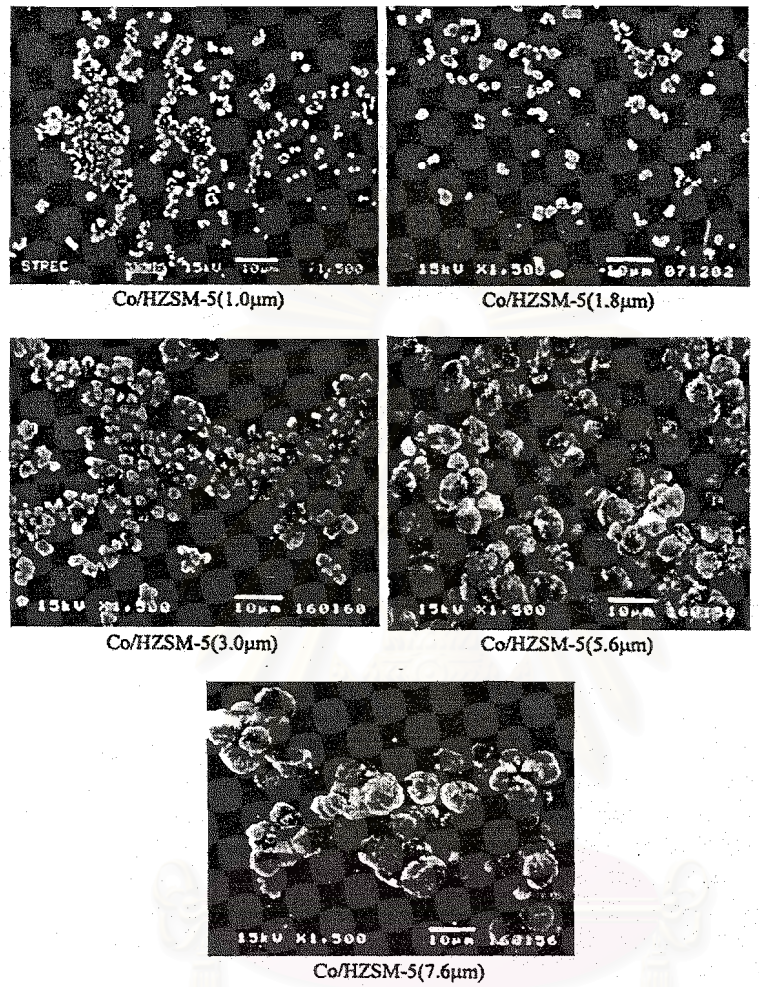

Fig. 1. Scanning electron micrograph of Co/HZSM-5.

HZSM-5, respectively, for various crystal sizes. The observed spectra confirmed that severe steam treatment causes dealumination. The catalysts exhibited two signals at approximately 50 ppm, which is assigned to the tetrahedral aluminum, and at approximately 0 ppm, which is attributed to the extra lattice octahedral aluminum in the zeolite lattice [23]. For the small crystal size, Co/HZSM-5(1.0 μm) and Co/HZSM-5(1.8 μm), there are no significant changes in the ^{27}Al-MASNMR spectra for both the fresh and pretreated catalysts. On the other hand, the large crystal size catalysts, Co/HZSM-5(5.6 μm) and Co/HZSM-5(7.6 μm) catalysts showed a drop in tetrahedral aluminum but an increase in octahedral aluminum after hydrothermal treatment. This is consistent with a previous report that loss in activity and durability after steam pretreatment was due to framework dealumination of the zeolite [23]. Based on ^{27}Al-MASNMR signals, the results obtained for the stabilization of the tetrahedral ^{27}Al by different crystal sizes are summarized in Table 1. After hydrothermal treatment of the catalysts, the relative area of tetrahedral ^{27}Al is decreased similarly in accord with the BET surface area and crystallinity. It can be concluded that for the small crystal size catalysts, Co/HZSM-5(1.0 μm) and Co/HZSM-5(1.8 μm), the zeolite framework structure is sta-

CATCOM 105 DISK / 18/4/02 ARTICLE IN PRESS No. of pages: 7 DTD 4.3.1/ SPS-N

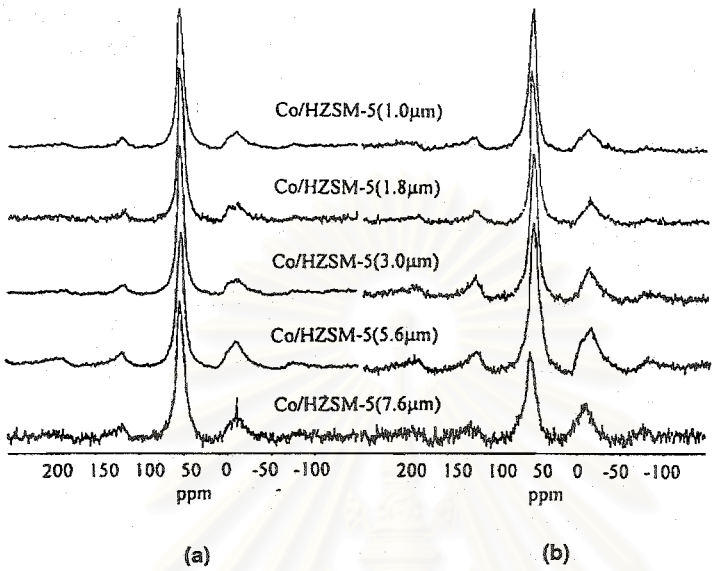

Fig. 2. ^{27}AIMAS-NMR spectra of Co/HZSM-5 (a) fresh and (b) pretreated catalysts.

bilized, preventing the occurrence of dealumination.

Similar results for the crystallinity ratio and the tetrahedral aluminum ratio on crystal size are shown in Fig. 3. The ratio of crystallinity and tetrahedral aluminum are defined as the difference between fresh and pretreated catalysts per fresh catalyst. After hydrothermal treatment, the small crystal size catalyst showed a slight decrease in crystallinity and tetrahedral aluminum while the large crystal size catalysts lost a considerable amount of their crystallinity and their tetrahedral aluminum, which resulted in lower durability in the case of large crystal size catalysts. However, the reason for less dealumination for the smaller crystal size catalysts is still unclear. It might be expected that the large crystal size catalyst may have many defect points compared with the small

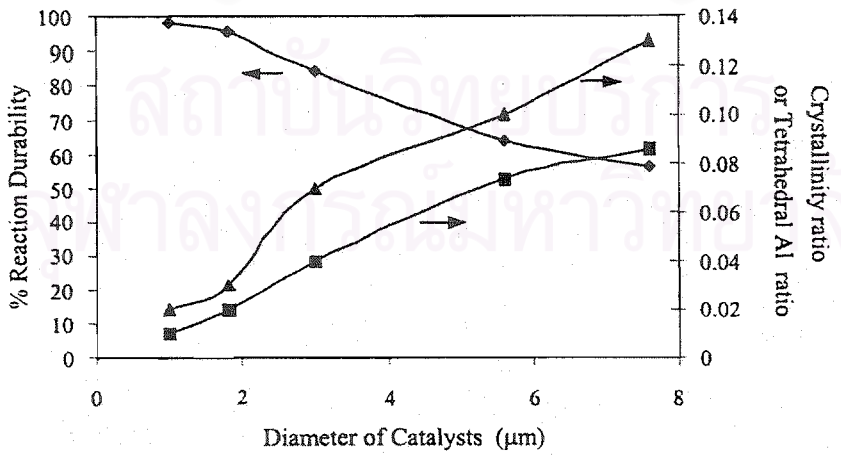

Fig. 3. The effect of crystal size on the durability (◆) crystallinity (■) and relative areas of ^{27}AI-MAS-NMR (▲) of Co/HZSM-5.

CATCOM 105
DISK / 18/4/02
ARTICLE IN PRESS
No. of pages: 7
DTD 4.3.1/ SPS-N

size catalyst. Consequently, further studies which aim at clearly describing the cause of crystal size effects on durability are warranted.

3.2. Catalytic performance

SCR of NO by methane was investigated for various crystal size catalysts both with and without pretreatment. The effect of reaction temperature on NO conversion to N_2 for Co/HZSM-5 with different crystal size is shown in Fig. 4(a) whereas conversion of methane is shown in Fig. 4(b). The conversion of NO into N_2 over these catalysts was enhanced with reaction temperature upto about 500 °C, however the conversion curve bent down beyond 500 °C while the methane conversion reached almost 100%. This phenomenon is typical for NO reduction by methane over Co/HZSM-5 [6,7,23].

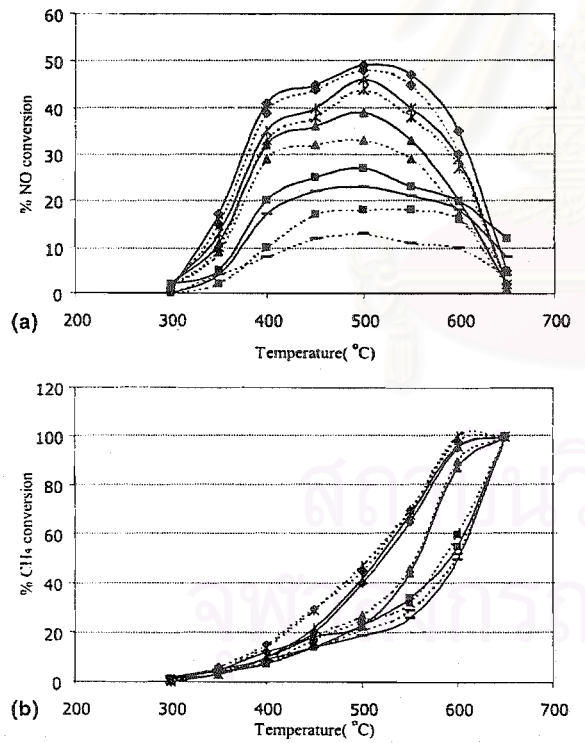

Fig. 4. The effect of pretreatment of Co/HZSM-5 on (a) NO conversion (b) CH_4 conversion solid line: fresh catalyst: broken line: pretreated catalyst, (◆) Co/HZSM-5(1.0 μm), (×) Co/HZSM-5(1.8 μm), (▲) Co/HZSM-5(3.0 μm), (■) Co/HZSM-5(5.6 μm) and (−) Co/HZSM-5(7.6 μm).

It was found that NO conversion was dependent on the zeolite crystal size. The NO conversion over large crystal catalyst was less than that over the small crystal catalyst. These results indicate that intracrystalline diffusion has influence on the SCR of NO by methane over Co/HZSM-5 catalyst which is in accord with the work of Shichi et al. [21] on Cu/ZSM-5 catalysts. After hydrothermal treatment of catalysts, the conversion of NO significantly decreased at any reaction temperature. NO conversions on large crystal size catalysts were found to decline to a greater extent after the hydrothermal pretreatment than those on a catalyst having a smaller crystal size. However, the difference in methane conversion changed only slightly since the conversion came from both combustion and reduction.

The %reaction durability, defined as the maximum NO conversion of pretreated catalysts per maximum NO conversion of fresh catalyst, were calculated and are reported in Fig. 3. Small crystal size Co/HZSM-5 had a higher reaction durability than the large crystal size zeolites. This suggests that the small crystal size exhibited a more steady and stable activity for conversion of NO to N_2. It should be noted that the durability is limited by crystal size up to about 2 μm. In other words, for Co/HZSM-5, 2 μm is the critical diameter for more durability after hydrothemal treatment.

4. Conclusions

The smaller crystal size Co/HZSM-5 zeolite showed the greater durability for conversion of NO to N_2. The small crystal size catalysts showed a slight decrease in crystallinity and dealumination of tetrahedral aluminum while the large crystal size catalyst lost considerable crystallinity and were extensively dealuminated. Durability is retained by crystal size up to 2 μm so that this is a critical diameter for this reaction condition. It is suggested that, the diameter of a commercial catalyst should be kept below the critical diameter in order to sustain the durability of zeolite.

CATCOM 105
DISK / 18/4/02
ARTICLE IN PRESS
No. of pages: 7
DTD 4.3.1/ SPS-N

Acknowledgements

The author would like to acknowledge Prof. Garry Rempel for help and suggestion in preparation of this manuscript. This study was financial supported by National Science and Technology Development Agency (NSTDA) and The Thailand Research Fund (TRF).

References

[1] M. Shelef, Chem. Rev. 95 (1995) 209.
[2] F. Witzel, G.A. Sill, W.K. Hall, J. Catal. 149 (1994) 229.
[3] E. Kikuchi, K. Yoko, Catal. Today 22 (1994) 73.
[4] M. Iwamoto, H. Yahiro, S. Shundo, N. Mizono, Appl. Catal. 69 (1994) L15.
[5] W. Held, A. Konig, T. Richter, L. Puppe, SAE Tech. 900496.
[6] T. Tabata, M. Kokisu, O. Okada, T. Nakayama, T. Yasumasu, H. Ssakane, Stud. Surf. Sci. Catal. 88 (1994) 409.
[7] Y. Li, J.N. Amor, Appl. Catal. B 1 (1992) L31.
[8] Y. Li, J.N. Amor, Appl. Catal. B 2 (1993) 239.
[9] Y. Li, J.N. Amor, Appl. Catal. B 3 (1993) L1.
[10] Y. Li, J.N. Amor, Appl. Catal. B 5 (1992) L257.
[11] J.N. Amor, Catal. Today 26 (1995) 147.
[12] A.P. Walker, Catal. Today 26 (1995) 107.
[13] V.I. Parvulescu, P. Grange, B. Delmon, Catal. Today 46 (1998) 233.
[14] Y. Li, P.J. Battavio, J.N. Armor, J. Catal. 142 (1993) 561.
[15] J.N. Armor, T.S. Farris, Appl. Catal. B 4 (1994) L11.
[16] K.C. Kharas, H.J. Robota, D.J. Liu, Appl. Catal. B 2 (1993) 225.
[17] V.A. Bell, J.S. Feeley, M. Deeba, R.J. Farauto, Catal. Lett. 29 (1994) 15.
[18] P. Budi, E. Curry-Hyde, R.F. Howe, Stud. Surf. Sci. Catal. 105 (1997) 1549.
[19] A. Shichi, A. Satsuma, M. Iwase, K. Shimizo, S. Komi, T. Hattori, Appl. Catal. B 17 (1998) 107.
[20] T. Tabata, h. Ohtsuka, Catal. Lett. 48 (1997) 203.
[21] A. Shichi, K. Katagi, A. Satsuma, T. Hattori, Appl. Catal. B 24 (2000) 97.
[22] T. Inui, ACS Symp. Ser. 389 (1989) 492.
[23] P. Budi, R.F. Howe, Catal. Today 38 (1997) 175.

VITA

Miss Pornsawan Kanchanawanichkun was born in Singburi, Thailand, on February 9, 1974. She received her Bachelor degree of Science from Chulalongkorn University in 1996. She continued in Doctoral degree of Engineering from the department of Chemical Engineering, Chulalongkorn University in June, 1996.